Universidade de Aveiro Departamento de Química
2013

Carla Isabel Madeira dos Santos

Corróis: síntese, funcionalização e aplicação como quimiossensores

Corroles: synthesis, functionalization and application as chemosensors

Universidade de Aveiro Departamento de Química
2013

Carla Isabel Madeira dos Santos

Corróis: síntese, funcionalização e aplicação como quimiossensores

Corroles: synthesis, functionalization and application as chemosensors

Tese apresentada à Universidade de Aveiro para cumprimento dos requisitos necessários à obtenção do grau de Doutor em Química, realizada sob a orientação científica da Doutora Maria da Graça de Pinho Morgado Silva Neves, Professora Associada com Agregação do Departamento de Química da Universidade de Aveiro,da Doutora Maria do Amparo Ferreira Faustino, Professora Auxiliar do Departamento de Química da Universidade de Aveiro e do Doutor Carlos Lodeiro Espiño, Professor Auxiliar do Departamento de Química da Faculdade de Ciências e Tecnologias da Universidade Nova de Lisboa

Apoio financeiro do POPH - QREN.

PROGRAMA OPERACIONAL POTENCIAL HUMANO

Apoio financeiro da FCT e do FSE no âmbito do III Quadro Comunitário de Apoio.

Fundação para a Ciência e a Tecnologia
MINISTÉRIO DA CIÊNCIA, TECNOLOGIA E ENSINO SUPERIOR

União Europeia
Fundo Social Europeu

Dedico esta dissertação aos meus pais e à minha irmã Paula…

o júri

Presidente

Prof. Doutor José Rodrigues Ferreira da Rocha
Professor catedrático da Universidade de Aveiro

Prof. Doutora Rufina Bastida
Professora Catedrática da Universidade de Santiago de Compostela

Prof. Doutora Maria da Graça de Pinho Morgado da Silva Neves
Professora Associada com Agregação do Departamento de Química da Universidade de Aveiro

Prof. Doutor Augusto Costa Tomé
Professor Associado com Agregação do Departamento de Química da Universidade de Aveiro

Prof. Doutor José Luis Capelo
Professor Auxiliar do Departamento de Química da Faculdade de Ciências e Tecnologias da Universidade Nova de Lisboa

Prof. Doutora Francesca Giuntini
Liverpool John Moores University

Doutora Elisabete de Jesus Oliveira Marques

Doutora Joana Filipa Brites Barata

Agradecimentos

Desejo expressar o meu mais sincero agradecimento a todos os que de alguma forma permitiram a realização deste trabalho.

À Professora Doutora Maria da Graça P. M. S. Neves e à Professora Doutora Maria do Amparo Ferreira Faustino, orientadoras desta dissertação, o meu sincero reconhecimento pelos preciosos ensinamentos que me transmitiram e pela constante disponibilidade e amizade que me dedicaram ao longo destes anos. Obrigada por todas as palavras de incentivo transmitidas quando tudo parecia demasiado complicado.

Ao Professor Doutor Carlos Lodeiro Espiño, orientador desta dissertação, desejo expressar a minha gratidão por todo o apoio científico concedido, e pelos seus muitos e bons conselhos. O seu espírito sempre optimista e motivador tornou as estadias em Lisboa e em Ourense muito enriquecedoras.

Ao Professor Doutor Artur Silva e ao Professor Doutor José Luís Capelo agradeço a forma como me receberam nos grupos de investigação QOPNA e BIOSCOPE, bem como a disponibilidade imediata para o esclarecimento de qualquer dúvida.

Ao Professor Doutor José Cavaleiro, responsável pela Unidade de Investigação QOPNA, agradeço todo o apoio prestado ao longo da realização deste trabalho.

À Doutora Elisabete Oliveira e à Doutora Joana Barata agradeço os valiosos ensinamentos, os conselhos, os incentivos, a paciência, a amizade e acima de tudo a vossa total disponibilidade. A partilha de ideias, experiências e sugestões fez-me crescer. Obrigada.

Ao Doutor José Menezes agradeço o apoio concedido durante o trabalho desenvolvido com as porfirinas, a disponibilidade, a energia positiva transmitida e o companheirismo.

Ao Dr. Hilário Tavares, agradeço a disponibilidade e o contributo prestados na obtenção dos espectros de RMN.

À Universidade de Aveiro, ao Departamento de Química e a todos os seus funcionários pela disponibilização dos meios necessários à execução experimental deste trabalho

À Fundação para a Ciência e Tecnologia, pela concessão de uma Bolsa de Doutoramento (SFRH/64155/2009) que permitiu a realização deste trabalho e ao FSE pelo apoio financeiro no âmbito do III Quadro Comunitário de Apoio.

.

À Sónia, à Cláudia e à Joana Ferreira agradeço a amizade, compreensão
e ajuda principalmente nos momentos mais difíceis.

Cristina, Daniela, Javier, Hugo, Eduardo y Júlio muchas gracias por las risas
que hemos compartido juntos.

À Vânia F. Pais, amiga de sempre, agradeço os bons momentos que passamos
juntas em Aveiro. Sempre que vinhas de estadia sentia-me mais perto de casa,
mais perto do nosso Alentejo.

Por fim, aos meus pais e à minha irmã um agradecimento muito especial pelo
apoio, pela energia positiva e incentivo que sempre me transmitiram na realização
deste trabalho, mas também por tudo o que me ensinaram ao longo da vida.

Paula obrigada por seres o meu Porto de Abrigo!!!

Palavras-chave

Corróis, dienos, dienófilos, reacções de cicloadição, sensores colorimétricos, nanopartículas quimiossensores, aniões, iões metálicos

Resumo

O trabalho de investigação apresentado nesta dissertação foi desenvolvido tendo como objectivo a síntese e funcionalização de *meso*-triarilcorróis para utilização como quimiossensores.

Este trabalho encontra-se apresentado ao longo de cinco capítulos. No primeiro capítulo são apresentadas as características gerais, as metodologias de síntese e de funcionalização de macrociclos de tipo corrólico, e descrevem-se algumas aplicações em que têm sido utilizados. São ainda abordadas algumas das propriedades e características dos quimiossensores e os mecanismos de deteção de diversos analítos.

No segundo capítulo, após uma pequena introdução às reações de Wittig e de Diels-Alder, escolhidas para a funcionalização do macrociclo corrólico, descreve-se o estudo efectuado para a obtenção do complexo de gálio(III) do 3- vinil-5,10,15-tris(pentafluorofenil)corrol e o seu comportamento como dieno, em reações de Diels-Alder na presença dos dienófilos 1,4-benzoquinona e 1,4-naftoquinona. Desses estudos resultaram dois aductos cuja habilidade sensorial, bem como a dos seus precursores, foi estudada, em solução, na presença de aniões esféricos (F^-, Br^-, Cl^-), lineares (CN^-) e volumosos (CH_3COO^-, $H_2PO_4^-$). Dos macrociclos estudados verificou-se que o corrol base-livre 5,10,15-tris(pentafluorofenil)corrol apresenta uma elevada sensibilidade para o anião fluoreto (F^-), e que a coordenação do núcleo corrólico com gálio(III) diminui a afinidade para este anião. Em geral, todos os compostos mostraram afinidade para o anião cianeto (CN^-) mesmo quando em suportes poliméricos. O gel de poliacrilamida revelou-se muito promissor na determinação de CN^- em amostras de água.

No terceiro capítulo é avaliada a reatividade do complexo de gálio(III) do 3-vinil-5,10,15-tris(pentafluorofenil)corrol ainda como dieno mas agora na presença de um dienófilo linear, o acetilenodicarboxilato de dimetilo. Desse estudo resultaram dois novos derivados corrólicos. A habilidade sensorial dos mesmos perante os aniões fluoreto, cianeto, acetato, e fosfato foi avaliada por espectroscopia de absorção e emissão tendo um dos aductos mostrado ser colorimétrico para o anião cianeto.

No quarto capítulo descreve-se a síntese e caracterização de dois conjugados do tipo corrol-cumarina, resultantes de reações de Hetero-Diels-Alder entre o 3-vinil-5,10,15-tris(pentafluorofenil)corrolatogálio(III)(piridina) e *orto*-quinonas-metídeos gerados *in situ* a partir de reacções de Knoevenagel entre cumarinas e paraformaldeído. Realizaram-se estudos de afinidade sensorial para aniões e catiões com estes macrociclos, bem como com conjugados porfirina-cumarina análogos. A inserção de uma unidade cumarina conferiu uma excepcional solubilidade tendo os novos derivados apresentado solubilidade em etanol.

No quinto e último capítulo desta dissertação é avaliada a capacidade sensorial do 5,10,15-tris(pentafluorofenil)corrol e da sua espécie monoaniónica, para os catiões metálicos Na^+, Ca^{2+}, Cu^{2+}, Cd^{2+}, Pb^{2+}, Hg^{2+}, Ag^+, Al^{3+}, Zn^{2+}, Ni^{2+}, Cr^{3+}, Ga^{3+}, Fe^{3+} em tolueno e acetonitrilo. Os macrociclos corrólicos mostraram ser selectivos e colorimétricos para o catião Hg^{2+}. Neste trabalho descreve-se ainda a síntese do derivado *β*-iminocorrol, que após funcionalização com o 3-isocianatopropiltrimetoxisilano originou um derivado do tipo alcoxisilano, que foi, posteriormente, ancorado a nanopartículas comerciais de sílica. As novas nanopartículas ancoradas com o alcoxisilano corrol foram estudadas na presença de Cu^{2+}, Hg^{2+} e Ag^+. Na presença do catião Ag^+ assistiu-se a uma mudança de cor, de verde para amarelo.

Keywords Corroles, dienes, dienophlies, cycloaddition reactions, imines, nanoparticles, chemosensors

Abstract

The work described in this dissertation was focused on the synthesis of *meso*-triarylcorroles and their functionalization for later use as chemosensors.

This work is divided in five chapters. In the first chapter it is described the general features of corroles, synthetic methodologies, the functionalization procedures and the applications of this kind of macrocycles. Additionally, some considerations about chemosensors and the importance of analytes that will be evaluated is also discussed. In the second chapter the Wittig and Diels- Alder reactions were chosen as post-functionalization procedures to apply to corroles. In this way, by the use of a Wittig reaction, the derivative 3–vinil-5,10,15-tris(pentafluorophenyl)corrolatogallium(III) was synthetized, from the corresponding 3-formy-5,10,15-tris(pentafluorophenyl)corrolatogallium(III), and its behavior as diene in Diels–Alder reactions, in the presence of the dienophiles 1,4-benzoquinone and 1,4-naphthoquinone was evaluated. These studies afforded two Diels-Alder adducts whose sensorial ability, as well as of their precursors, was studied in solution in the presence of spherical(F^-, Br^-, Cl^-), linear (CN^-) and bulky (CH_3COO^-, $H_2PO_4^-$) anions. The 5,10,15-tris(pentafluorophenyl)corrole showed to be the most sensitive macrocycle to the fluoride anion (F^-). Although all derivatives have interacted with this anion the coordination of the corrole core with gallium(III) decreased their affinity for this anion. In general, all compounds showed interaction with cyanide (CN^-) anions. By these results two low cost polymers based on polymethylmethacrylate and polyacrylamide were prepared and used in the detection of CN^- in water. The polyacrylamide gel proved to be very promising.

In the third chapter the reactivity of the gallium(III) (pyridine) complex of 3-vinyl-5,10,15-tris(pentafluorophenyl)corrole as a diene was extended to dimethyl acetylenedicarboxylate as dienophile. This study afforded two new corrole derivatives. The sensorial ability of the new macrocycles towards fluoride, cyanide, acetate and phosphate anions was carried out by absorption and emission spectroscopy. One of the derivatives showed to be colorimetric to cyanide, where a change of colour from *green* to *colourless* was visualized.

In the fourth chapter is described the synthesis and characterization of two new derivatives resulting from hetero-Diels-Alder reactions between the gallium(III) (pyridine) complex of 3-vinyl-5,10,15-tris(pentafluorophenyl)corrole and *o*-quinone methides (*o*-QM) generated *in situ* from Knoevenagel reactions of coumarins with paraformaldehyde. The sensing ability of the resulting compounds was studied in the presence of different anions and cations. These sensorial studies were extended to porphyrin-coumarin analogues. The insertion of a coumarin moiety conferred an unusual solubility to these conjugates in ethanol.

In the last chapter is shown the sensorial ability of 5,10,15-tris(pentafluorophenyl)corrole and of its monoanionic species towards Na^+, Ca^{2+}, Cu^{2+}, Cd^{2+}, Pb^{2+}, Hg^{2+}, Ag^+, Al^{3+}, Zn^{2+}, Ni^{2+}, Cr^{3+}, Ga^{3+}, Fe^{3+} metal ions in toluene and acetonitrile. The photophysical studies towards metal ions were carried out by absorption and emission spectroscopy. These corroles showed to be selective and colorimetric for Hg^{2+}. In addition a new *β*- imine corrole was successful synthetized and further functionalized with 3-isocyanatopropyl-trimethoxysilane resulting an alkoxysilane derivative. The grafting of alkoxysilane derivative, with optically transparent silica nanoparticles (SiNPs) was also performed. The new-coated silica nanoparticles with corrole were studied in the presence of Cu^{2+}, Hg^{2+} and Ag^+ as metal ion probes. In the presence of Ag^+ was observed a change of colour from green to yellow.

INDEX

Chapter I- Introduction

Chapter II- Exploiting the fluorescence behaviour of a new corrole family as anions chemosensors: From solution to solids-supported devices

Abbreviatures

δ	chemical shift
ε	molar extinction coefficient
η	yield reaction
λ	wavelenght
ϕ_f	fluorescent quantum yield
2D	two dimensional
CHEF	chelation enhancement of fluorescence emission
CHEQ	chelation enhancement of quenching emission
Conc.	concentrated
COSY	^{1}H-^{1}H Correlation spectroscopy
d	doublet
dd	double doublet
ddd	double doublet of doublet
DDQ	2,3-dichloro-5,6-dicyano-1,4-benzoquinone
DLS	dynamic light scattering
DMF	*N, N*-dimethylformamide
DMSO	dimethyl sulfoxide
equiv.	Equivalent
ESI	electrospray ionization
EtOH	ethanol
FAB-HRMS	fast atom bombardment high resolution mass spectroscopy
HMBC	heteronuclear multiple bond correlation
HSQC	heteronuclear single quantum coherence
HRMS	high resolution mass spectroscopy
IUPAC	International Union of Pure and Applied Chemistry
J	coupling constant (Hz)
m	multiplet
$M^{+\cdot}$	molecular ion
m/z	mass charge ratio
MALDI-TOF	matrix-assisted laser desorption/ ionization-time of flight
MS	mass spectrometry
NMR	nuclear magnetic resonance
Ph	phenyl
PMMA	polymethylmethacrylate
t	triplet
TEM	transmission electron microscopy
TFA	trifluoroacetic acid
TLC	thin layer chromatography
THF	tetrahydrofuran
TMS	tetramethylsilane
TPFFC	5,10,15-tris(pentafluorophenyl)corrole
UV-Vis	ultraviolet-visible

Chapter I

Introduction

INDEX

1- Introduction

Preamble

Corroles are tetrapyrrolic macrocycles which exhibit unique properties to be used in different fields namely as chemosensors. In this introduction a brief overview related with the structure, reactivity, synthesis and applications of corroles is present. In the final part, some concepts related with optical chemosensors and their importance in the detection and quantification of anions and metal ions is describe.

1 Corroles

1.1 The Origin of Corroles

The development of a new drug is a complex and risky process, since just one of many molecules tested is able to reach the final stage and to be materialized as a new medicinal product. However, in such development other products can sometimes produce new knowledge and to be used in new applications. This is the situation of corroles that were discovered by chance, during the development of a synthetic model of vitamin B_{12} for studies on pernicious anaemia.

In the beginning of twentieth century, pernicious anaemia (hematologic perturbation resulting from lack of vitamin B_{12} in the body) was one of the main causes of death in Northern Europe and different researchers tried to understand this disease and to find new methods to combat it. In this context the scientist George Whipple decided to study in 1920 the influence of different foods intake in the regeneration of hemoglobin in dogs with anaemia. Through blood tests, he verified that the raw liver was the food that allowed the greatest regeneration of red blood cells.[4] Based on the previous results, Minot and Murphy decided to extend the studies to patients with pernicious anemia and verified that they were cured after ingestion of considerable amounts of raw liver. The researchers concluded that the disease under study was caused by the absence of a supplement present in raw liver, and the approach was labeled as "Liver Therapy. The three scientists, Whipple, Minot and Murphy were awarded with the Nobel Prize for medicine for their work in the treatment of pernicious anaemia in 1934.[1]

After the success of "Liver Therapy", some researchers using liver concentrates, tried to isolate the complex responsible by the "anti-pernicious anaemia effect". This objective was attained by Folkers *et al*[2] in the late forties when he was able to isolate a crystalline pigment from liver and named it vitamin B_{12}. Soon after, Pierce *et al*[3] isolated two crystalline forms of vitamin B_{12} equally effective in combating pernicious anaemia; one of the forms contained in its structure a cyanide group and it was therefore called cyanocobalamin (Figure 1), while the other known as hydroxocobalamin is produced when cyanocobalamin is exposed to light.[4]

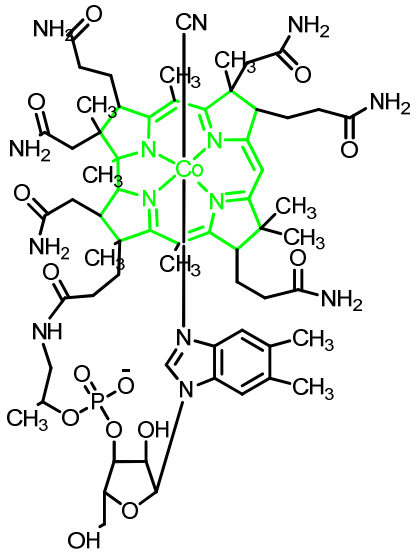

Figure 1- Cyanocobalamin structure

Some years later, in 1956, Hodgkin and co-workers[5] determined the molecular structure of cyanocobalamin by X-ray crystallography. This study allowed them to identify the new tetrapyrrolic macrocycle corrin. The macrocycle complexed with cobalt possess a direct linkage between two pyrrolidine units and is less symmetric than the porphyrinic macrocycle.

Once determined the structure of vitamin B_{12}, the scientists tried to develop synthetic methods, in order to prepare the corrin precursor. In 1960, Johnson and Price[6] during one of those attempts discovered a method that allowed to obtain a new metallic macrocycle with eleven double bonds. The process was complicated and involved the treatment of 5,5'-dibromo-3,3'-diethyl-4,4'-dimethyldipyrromethane with palladium-strontium carbonate and formaldehyde. The editor of the journal where the authors published these results suggested that the macrocycle synthesized was called corrole. Four years later, Johnson and Kay[7] developed a second approach to prepare corroles that involved the photocyclization of biladienes (Scheme 1). The biladienes were prepared by condensation of dipyrromethane-5,5´-dicarboxylic acids with two equivalents of a 3,4-dialkyl-2-formylpyrrole, or by condensation of 5,5´-di-formyldipyrromethanes with two equivalents of a 3,4-dialkylpyrrole-2-carboxilic acid. The cyclization of corrole occurred when methanolic suspensions of bilane **1** were treated with a slight excess of sodium acetate or ammonium hydroxide and the resulting solutions irradiated with light.

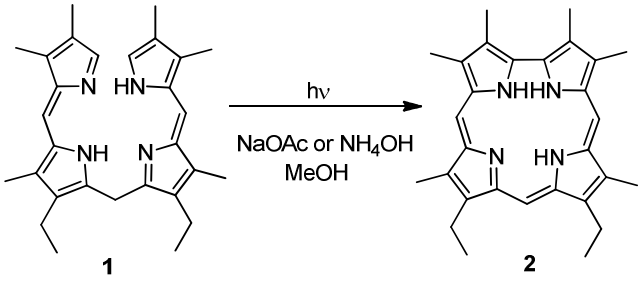

Scheme 1

Throughout the process they found that corrole contains only ten double bonds and that the first structure published by Johnson and Price[6] was incorrect. The structure of corrole **2** (8,12-diethyl-2,3,7,13,17,18-hexamethylcorrole) was confirmed in 1971 by Harrison, Hodder and Crowfoot-Hodgkin[8] by X-ray diffraction.

Nevertheless, the methods above described didn't attract the interest of different research groups, since the total synthesis involved multi-steps and the preparation of biladienes was difficult. In 1999, this situation changed with the discovery of much easier one-pot procedures to synthetize *meso*-substituted corroles.[9,10] Having this type of macrocycles more accessible a new and exciting era started and the academic interest on the synthesis, functionalization and potential applications of corroles increased exponentially. A quick search on the SCOPUS using the word "corrole" showed that in December of 2013 there are about 420 articles available concerning this topic.

1.2 Structure and General Properties of Corroles

Corroles are tetrapyrrolic macrocycles that maintain the skeletal structure of corrins, and the aromaticity of porphyrins (Figure 2). In porphyrins the four units of pyrrole type are linked through four *meso*-carbon bridges, whereas in corroles two of those units present a direct pyrrole–pyrrole linkage. Like in porphyrins, corroles aromaticity is attained by a delocalized 18 π-electron system.

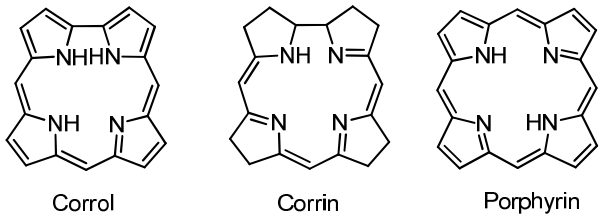

Figure 2- Structures of corrole, corrin and porphyrin core.

The IUPAC numbering scheme of corroles is derived from the one of porphyrins and the only difference between the two macrocycles is the elimination in corrole of the carbon designated with number 20 in porphyrins. All the other carbons are assigned from 1 to 19 (Figure 3). It should be noted that positions 2, 3, 7, 8, 12, 13, 17 and 18 can also be designated by β-pyrrolic positions and positions 5, 10 and 15 as *meso* positions. In the interior of the corrole macrocycle there are three nitrogen atoms of amine type and one of imine type. These nitrogen atoms are numbered from 21 to 24, retaining the same numbering scheme as that of porphyrin.

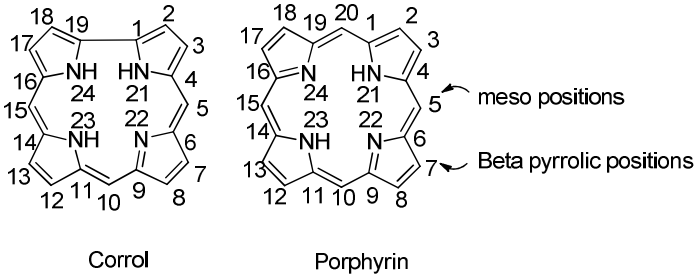

Figure 3- IUPAC numbering scheme of corrole and porphyrin.

According to an article published by Dyke and co-workers[11] in 1971, the double bond, of the imine group, would be established preferentially with the nitrogen atom 22. However, Ghosh and Jynge[12] in 1997 suggested the existence of two tautomers (Scheme 2) and determined through a theoretical study that there are no significant energetic differences between them. In 2005 Ding *et al*[13] presented the high resolution X-ray single crystal structures for 5,10,15-triphenylcorrole and 5,10,15-tris(pentafluorophenyl)corrole, and concluded that these two free-base structures exhibited different proton tautomerizations in their cores.

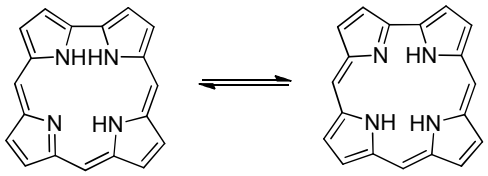

Scheme 2

The missing of the *meso* carbon-20 in corrole, originates a core with a smaller central cavity than the one in the porphyrin system, and the D_{4h} porphyrin symmetry is reduced to C_{2v} in corroles. The reduction in the symmetry imparts to the corrole macrocycle unique properties.

A significant property of corroles is their acid/base character (scheme 3). Corroles are more acidic than porphyrins, affording in diluted basic solutions the corresponding monoanion (structure **D** in scheme 3). In the presence of a dilute acid occurs the monoprotonation (structure **B** in scheme 3); these monocationc species present a strong absorption in the visible range, indicating that the addition of the proton occurs at the inner core nitrogen atom. A different situation is observed under strong acidic conditions with the disappearance of the Soret band (typical of a conjugated π system, vide infra); the spectroscopic analysis suggests that the interruption of the conjugated π system is due to the protonation at carbon 5 or 15 affording dicationic species of type **C**.

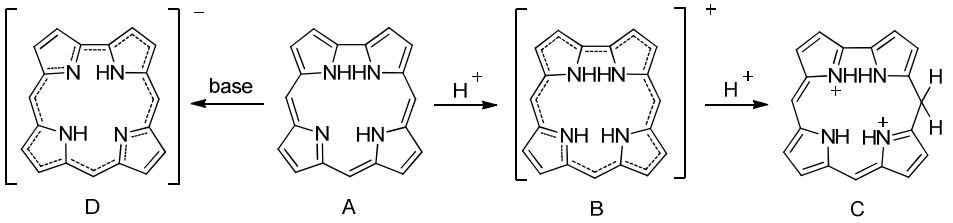

Scheme 3

Another important feature of corroles is their ability to stabilize higher oxidation states of metals, due to the existence of three NH protons in the inner core. Corroles can act as trianionic ligands, as opposed to corrins, which are monoanionic ligands, and porphyrins, which are dianionic ligands.[14] Typically, the more stable oxidation state in metallocorroles is three. Actually are known thirty corrole chelates, that may be divided into five main groups: (a) Early and late transition metals: Ti, V, Ni, Cu, Ag; (b) Group 6–9 transition metals: Cr, Mo, Mn, Re, Fe, Ru, Co, Rh, Ir; (c) Lanthanides: La, Gd, Tb, (d) Actinides: U, Th and (e) the other groups: Zn, Ga, Al, Ge, Sn, Sb, P, B.[15]

Corroles exhibit very strong colors and apparently their absorption spectra, which are dominated by π-π* transitions, are very similar to those of porphyrins. The spectra of corrole macrocycles show an intense and broadband near 400 nm like porphyrins, which is commonly known as Soret band and also several weaker bands in the 500-650 nm region known as Q bands (Figure 4). However, there are two key differences between both macrocycles. First, the effect of substituents on the optical properties of corroles is significantly larger than in normal porphyrins, leading to a diversity of absorption differences upon simple substitution. For example, in the absorption spectra of 5,10,15-triphenylcorrole and 5,10,15-tris(pentafluorophenyl)-corrole the Soret bands arise at 414 and 407 respectively.[16] Second, corroles exhibit very significant solvent-dependent absorptions, in contrast to the small shifts typically seen in porphyrins. It is believed that in polar solvents, such dependence is justified by the occurrence of interactions by hydrogen bonding between the internal groups NH and the solvent.[17]

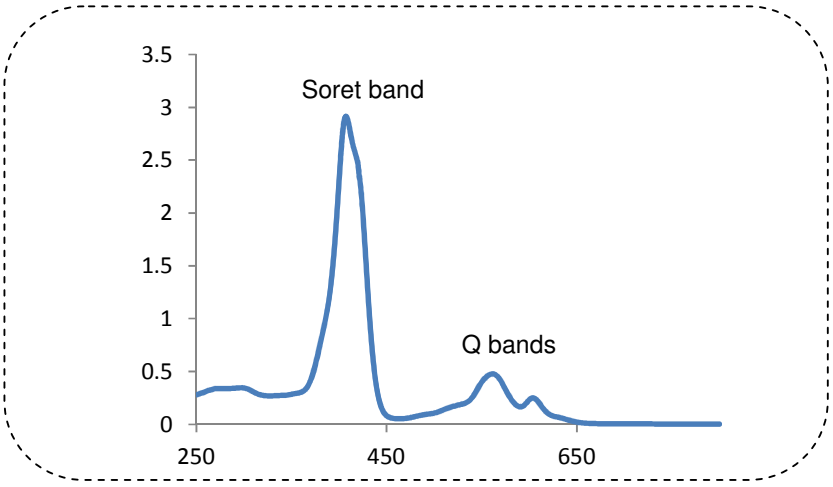

Figure 4-UV-Visible spectrum of 5,10,15-tris(pentafluorophenyl)corrole in dichloromethane.

Corroles can also be very emissive, with high quantum yields of fluorescence. Their fluorescence intensity is much larger than that of analogue porphyrins and other related macrocycles. For example the fluorescence quantum yield (ϕf) in DMF of 5,10,15,20-tetraphenylporphyrin is 0.11 and it is 0.27 for 5,10,15-tris(pentafluorophenyl)-corrole.[18]

In terms of chemical stability, corroles are less robust than porphyrins, principally the free bases in the presence of O_2 and light. The oxidative decomposition of corroles can afford different type of products: biliverdins,[19] isocorroles[20] and *β –β* linked dimers and

trimers.[21] The first example describing the photoinstability of corroles was reported for 2,3,17,18-tetraethyl-7,8,12,13-tetramethyl-10-phenylcorrole **3** (scheme 4). This corrole, when dissolved in dichloromethane and in the presence of air and light is slowly transformed into an open-chain biliverdin derivative. This transformation involves the cleavage of the pyrrole–pyrrole bond by dioxygen (Scheme 4).[19]

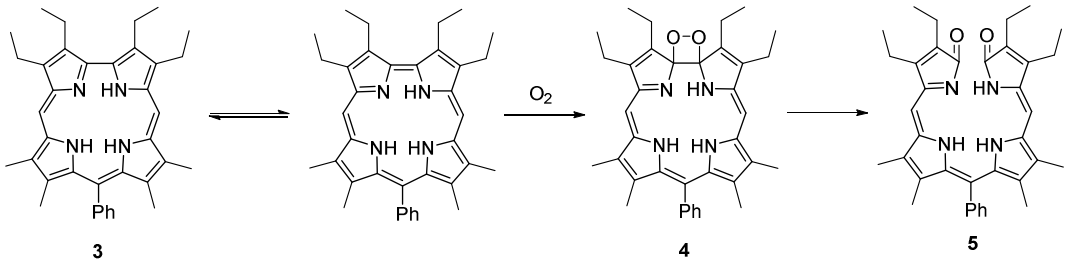

Scheme 4

Recently Cavaleiro and co-workers[21] showed that even the 5,10,15-tris(pentafluorophenyl)corrole **6** considered one of the most stable corroles, is slowly converted at room temperature and in the presence of air and light, into a 3,3´-corrole dimer **7** and a 3,3´,17',3´´-corrole trimer **8** (Scheme 5). Posteriorly, the same type of oligomers were obtained via oxidation of **6** with *p*-chloranil and *p*-fluoranil by Osuka and co-workers.[22]

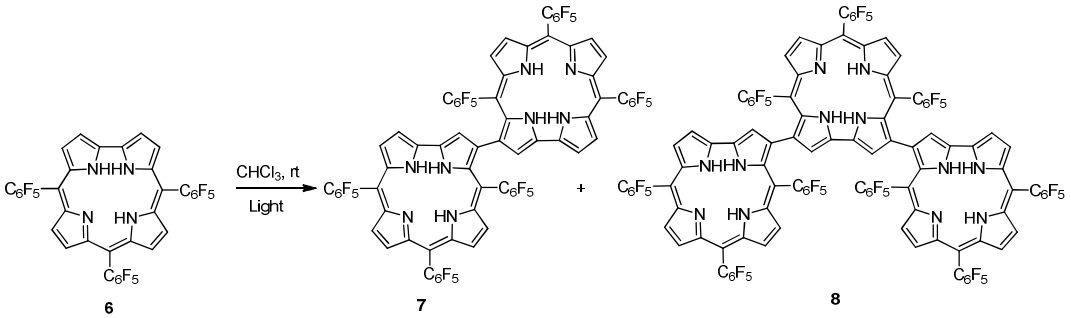

Scheme 5

Another consideration that merits being referred is related with corroles NMR spectra. Theses macrocycles exhibit a diamagnetic ring current effect similar to that observed in porphyrins, which is responsible by the shifting of the peripheral protons to lower fields (δ between 7 and 9 ppm) and by the appearance of the ressonances due the inner nitrogen protons at *ca.* δ -2.9 ppm. [23]

1.3 Syntheses of Corroles

Free-bases

As it was already referred, in the nineties the access to corroles required the use of precursors that were not commercially available and the existent synthetic routes usually involved several steps. This fact was responsible by the limited studies concerning corroles that were published, until 1999. In this year, two research groups, one led by Gross[9] and another by Paolesse[24] reported two different methods to synthesize corrole derivatives bearing aryl groups on the three *meso* positions, from commercial available reagents (pyrrole and aldehydes).

The procedure proposed by Gross and co-workers[9] was based on the condensation of pyrrole and aldehydes in the absence of solvent (Scheme 6). The method involved the heating at 100 °C for 4 h, of a mixture of pyrrole and aldehyde in equimolar quantities, on a solid support (silica or basic alumina), followed by oxidation with 2,3-dichloro-5,6-diciano-1,4-benzoquinone (DDQ). When it was used as aldehyde, the pentafluorobenzaldehyde, the corrole 5,10,15-tris(pentafluorophenyl)corrole **6** was obtained with a yield of 11%. On the other hand, when the aldehyde selected was the benzaldehyde, it was only obtained the corresponding porphyrin. The method described allowed to synthesize, for the first time, *meso*-aryl free-base corroles, with three identical substituents (*meso*-A_3-substituted corroles). The authors referred that this approach it was only suitable for the synthesis of corroles from aldehydes with strong electron-withdrawing substituents.

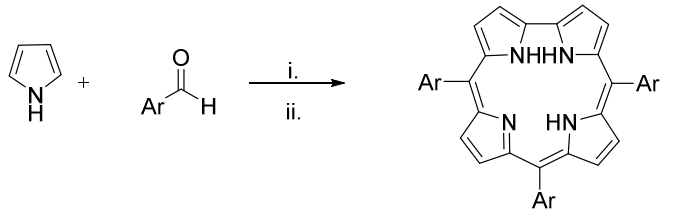

Scheme 6

The route developed by Paolesse *et al*[24] was based on the Rothemund method developed by Alder *et al*[25] for the synthesis of *meso*-tetraarylporphyrins. The researchers changed the ratio of pyrrole and aldehyde from 1:1 used for porphyrins to 3:1, and the reagents were refluxed in acetic acid during 4 h. Under these conditions, were obtained as

the main reaction products, the 5,10,15-triphenylcorrole **11** and the corresponding 5,10,15,20-tetraphenylporphyrin **12**, both with yields of 6% (Scheme 7).

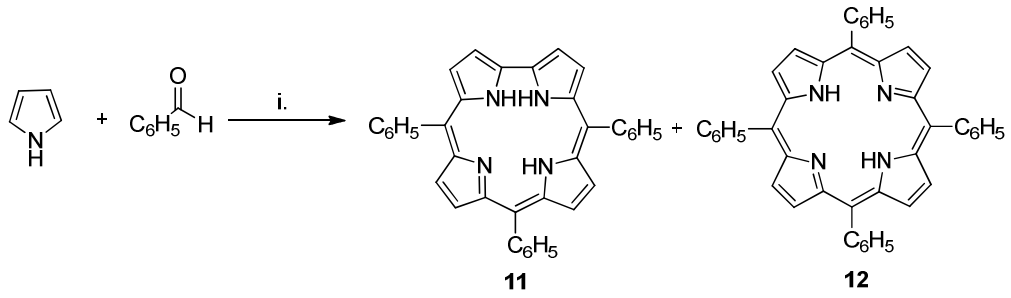

i. CH_3COOH, reflux

Scheme 7

This work was extended, in 2001, to other aromatic aldehydes. Of the sixteen aldehydes studied stands out the reaction with 4-nitrobenzaldehyde which originated the corresponding corrole with a yield of 22%.[26]

These two landmark approaches were followed by other publications, considering new improvements in the experimental conditions. For instance, in 2001 the researchers Daniel Gryko and Jadach[27] published a paper on the synthesis of *meso*-substituted *trans*-A_2B corroles (corroles with equal substituents on the 5 and 15-position and a different substituent on the 10-position). They prepared twenty one corroles of this type with the following functionalities: ester, nitrile, ether, fluoro, hydroxy, iodo, nitro, thioacetate, methylsulfoxy. The synthetic pathway involved the acid-catalyzed condensation of a dipyrromethane and an aldehyde followed by oxidation with DDQ (Scheme 8). Optimal conditions for the condensation were identified after examining various reaction parameters (solvent, acid, concentration, time). The conditions identified (CH_2Cl_2, [DPM] = 33 mM, [aldehyde] = 17 mM, [TF\ A] = 1.3 mM, 1 eq. DDQ) resulted in the formation of corroles in 3-25% yield. Through this work the authors concluded that high concentrations of substrates and small amounts of TFA favor the formation of corroles and minimize the formation of porphyrins.

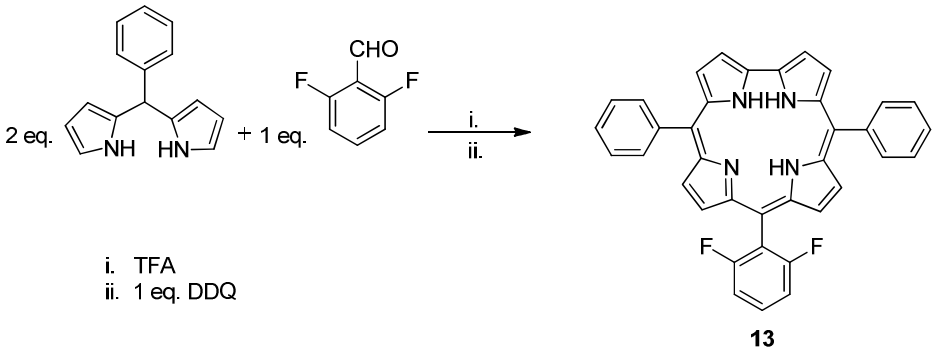

Scheme 8

A novel methodology for the synthesis of corroles that uses microwave (MW) irradiation was proposed in 2003 by Collman and Decréau.[28] The authors reported the synthesis of free base tris-aryl- and tris-pyrimidyl-corroles using solvent-free conditions and MW irradiation. Compared to conventional heating, the MW technique afforded an increase in corrole yields of 30% and led to noticeably cleaner reaction mixtures. Across this method it was demonstrated that short reaction times and high temperatures are required to afford optimum yields.

At the same year Gryko *et al*[29] refined the methods for the synthesis of *meso*-substituted A_3- and *trans*-A_2B-corroles. After thorough examination of various reaction parameters (reactivity of the aldehyde, catalyst, solvent, concentration, time *etc*.), the authors elaborated three different sets of conditions for diverse types of aromatic aldehydes—highly reactive, moderately reactive and sterically hindered. The conditions referred consisted in the variation of reaction time (10 min for the reactive aldehydes and 16 h for sterically hindered aldehydes), ratio of pyrrole and aldehydes (1.5:1 to 5:1 for aldehyde reactive and sterically hindered aldehydes) and equivalents numbers of TFA. Through this work it was observed that small amounts of TFA promoted the bilane (tetrapyrromethane) formation, the direct precursor of corrole. Moreover, it was verified that the amount of pyrrole used in obtaining the corrole depends on the reactivity of the aldehyde.

In 2006, the same research group developed new and efficient conditions for the synthesis of *meso*-substituted corroles.[30] The condensation between the aldehyde and the pyrrole was performed in a water-methanol mixture in the presence of HCl. The optimization of various reaction parameters, such as co-solvent, reagent, and acid concentration, allowed to obtain high yields of bilanes that were isolated and subsequently

oxidized. The 5,10,15-triphenylcorrole **11** (scheme 7) was obtained, through this method, in the highest yield (32%) reported to date.

Chauhan and Kumari,[31] in 2008, reported a new method for the synthesis of *meso*-triarylcorroles. They performed the condensation of aryl aldehydes with pyrrole, in the presence of Amberlyst 15 (an ion exchange resin composed by polystyrene and molecules of sulfonic acid) and under solvent-free conditions. According to the authors the absence of solvent is ideal for the formation of the tetrapyrromethanes and therefore the synthesis of corroles is favored. When the same reaction was carried out in solvent, it is observed the formation of porphyrinogens and consequently of the porphyrinic macrocycle. With this method it was possible to isolate the 5,10,15-triphenylcorrole with a yield of 15% and the 5,10,15-tris(pentafluorophenyl)corrole with a yield of 30%. Recently Nocera and co-workers[39] carried out the synthesis of the 5,10,15-tris(pentafluorophenyl)corrole in large scale. This was performed by condensation of commercially available pyrrole, pentafluorobenzaldehyde and paraformaldehyde under Lindsey conditions. The synthetic strategy that it was used is shown in Scheme 9. The role of paraformaldehyde in the corrole forming reaction, though not delineated, is likely to tune the acid concentration for the formation of the bilane that delivers corrole rather than the corresponding porphyrin.

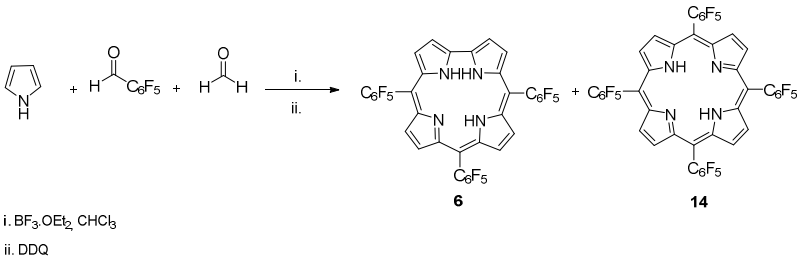

Scheme 9

More recently, the researcher Hai-Ying Zhan presented a new and simple method for the preparation of *meso*-substituted *trans*-A_2B-corroles in ionic liquids[32]. 1-Butyl-3-methylimidazolium tetrafluoroborate [Bmim][BF_4] was found a suitable reaction medium (Scheme 10), and the principal advantage of the protocol is the reduction of the amount of organic solvents in response to the demand of green chemistry.

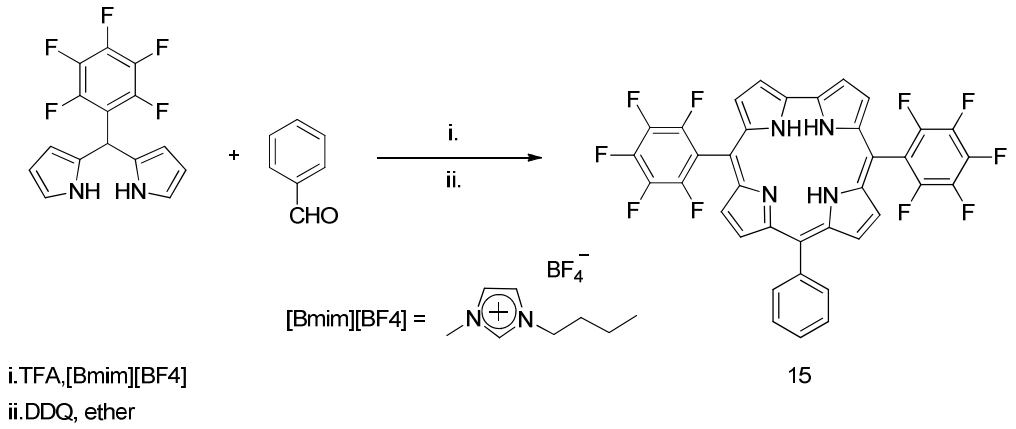

Scheme 10

All these studies allow the research community to have access not only to corroles of type A_3, but also to ABC and *trans*-A_2B corrole types. Although there are no experimental data to confirm the mechanism of formation of *meso*-triarylcorroles, it is considered that it involves two independent reactional steps (Scheme 11). In the first step occurs the formation of the ring-opening corrole precursor, the bilane and in the second one the oxidative macrocyclization. The most used oxidizing agent in these syntheses is DDQ. It should be noted that the efficiency of this step depends on the concentration of the bilane and on the solvent in which the oxidation occurs.[33]

All the work performed in this dissertation was based on 5,10,15-tris (pentafluorophenyl)corrole **6** and the Gryko method[29] was considered the most adequate for its synthesis, when compared with other methodologies also tested.

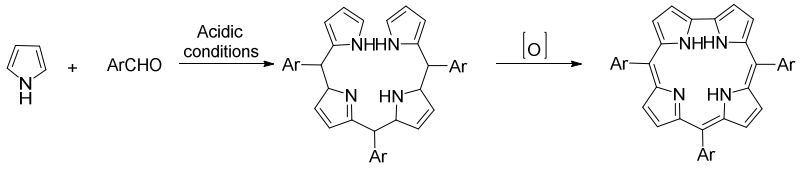

Scheme 11

Metallocorroles

As mentioned above corroles have been shown to possess excellent chelating properties and at least thirty metal ions have so far been introduced into the macrocycle. Although the coordination chemistry of corroles is far from being as developed as that of porphyrins, it is not unreasonable to believe that the number of metals coordinated to corroles can be greatly expanded in the future. Having three amino and one imino like nitrogen atoms in the inner core, the fully deprotonated form of the corrole acts as a trianionic ligand, different from both corrins and porphyrins, which are, respectively, monoanionic and dianionic ligands as it was also already referred. Furthermore, the ability of corroles to stabilize higher metal oxidation states when compared to porphyrins makes its coordination chemistry particularly interesting. For example, iron(IV) porphyrins exist only as unstable intermediates while a large number of stable iron(IV) corroles are known.[34] Thus, metallocorroles are of great interest as stable model compounds of high-valence active intermediates of various heme proteins as well as for general investigations of the electronic structures of high-valence transition metal complexes.

The procedures for metal insertion into corroles are very simple and normally all *N*-pyrrole atoms participate in the metal binding providing a trianionic equatorial coordination sphere. Pyridine appears to be the most general solvent, similar to the role of DMF for insertion of metal ions into porphyrins (Scheme 12) and the most commonly used metal sources are metal chlorides or acetates. In general, square pyramidal is the most commonly adopted coordination geometry of corroles. The affinity of corrole-chelated metal ions for a sixth ligand to form 6-coordinated complexes is quite low and most of the reported complexes of this type contain pyridine as axial ligands. As examples of the quite rare situation where all the *N* atoms do not participate in the coordination sphere are the rhodium(I), (oxo)vanadium(IV) and (oxo)titanium(IV) complexes of corroles.[35]

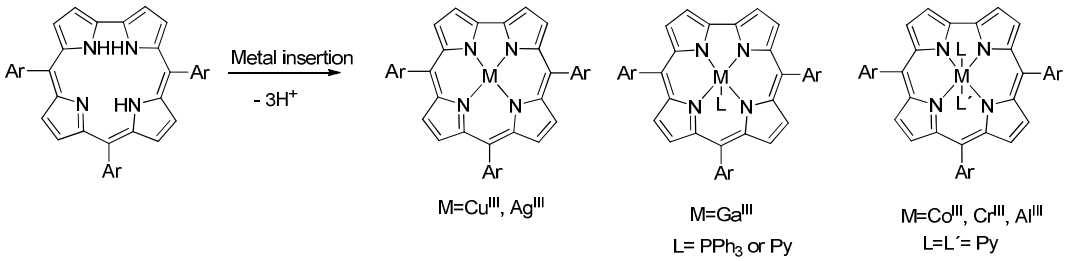

Scheme 12

Based on density functional theory (DFT) calculations it is possible to affirm that gallium(III) is the metal that fits perfectly in the coordination core of corroles.[36]
The synthesis of corrole lanthanide complexes (La, Gd, and Tb) was reported only this year by Arnold *et al*,[37] which combined the free base 10-(4-methoxyphenyl)-5,15-dimesitylcorrole with 1.1 equivalents of lanthanide silylamides at room temperature in THF. Efforts are underway to extend this methodology across the lanthanide series and to explore the use of these materials as fluorescence imaging agents.[37]

1.4 Functionalization of Corrole Macrocycle

The post-functionalization of corroles was a quite unexplored field until the appearance of efficient methodologies to prepare *meso*-triarylcorroles. In fact, these macrocycles showed to be convenient starting platform for the construction of more elaborated molecular architectures. A corrole macrocycle is susceptible to react at the inner nitrogen atoms, at the *β*-pyrrolic positions (2,3,7,8,12,13,17,18), at the *meso*-positions (5,10,15) and at its aryl substituents. In this section will be highlighted some of synthetic methodologies available for the functionalization of corrole macrocycles giving a special attention to the ones that were important for the development of this work.

Considering the inner core of corroles besides the protonation and deprotonation and the formation of complexes already mentioned, other reactions like the alkylation of the inner nitrogens can occur.[38] In fact, thinking on further functionalization on the corrole periphery the protection of the inner core by metallation is an important issue, to prevent the occurrence of those types of reactions in the inner nitrogens (vide infra).

Considering the 5,10,15-tris(pentafluorophenyl)corrole **6**, the selected corrole in this study, an important approach of post-functionalization involves the nucleophilic aromatic substitution reaction of the *para*-F atoms in pentafluorophenyl groups, like it is frequently used for the modification of porphyrins.[39] For instance, Osuka and co-workers[40] explored the approach to introduce several amines into corrole **6**, while Cavaleiro and co-workers[41] used it to link galactose residues or to functionalize it with silica particles.[42]

Looking at the the *β*-pyrrolic positions several procedures based on electrophilic aromatic substitutions, cycloaddition reactions and involving reagents or catalysts based on transition metals were developed to modify the corrole core.[38] In fact, efficient procedures were established for the insertion of different halogen atoms (Cl, Br, I) into the *β*-pyrrolic positions of the corrole macrocycle.[43-49] Also, conventional procedures, such as sulfonation

and chlorosulfonation, afforded the expected derivatives in excellent yields. In particular, the 2,17-bisulfonated corrole **16** (Figure 5) has been extensively used as a versatile precursor of corroles with sulfonamide groups to be used for advanced applications and materials.[50-57] The introduction of nitro and amino groups at the β-pyrrolic positions of corroles were also explored for further modifications of these compounds.[58-64]

Considering that the functionalization of corroles via formylation, carboxylation and cycloadditions reactions have a special role in the development of this work a special attention will be given now to this type of transformations.

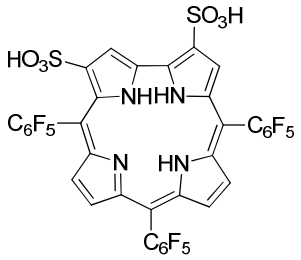

16

Figure 5- Structure of 2,17-bis-sulfonated corrole **16**

Formylation

The introduction of a formyl group in a corrole core is based on the use of Vilsmeier-Haack conditions. Currently the efficiency of the Vilsmeier-Haack reaction is well established giving access to β-formylcorroles in excellent yields. In 2002 Gross and co-workers[65] described the Vilsmeier formylation of gallium(III) complex of 5,10,15-tris(pentafluorophenyl)corrole. Depending on the corrole:Vilsmeier reagent molar ratio, the 3-formyl derivative **18** or the 2,17-diformyl derivative **19** were obtained as main products (Scheme 13).

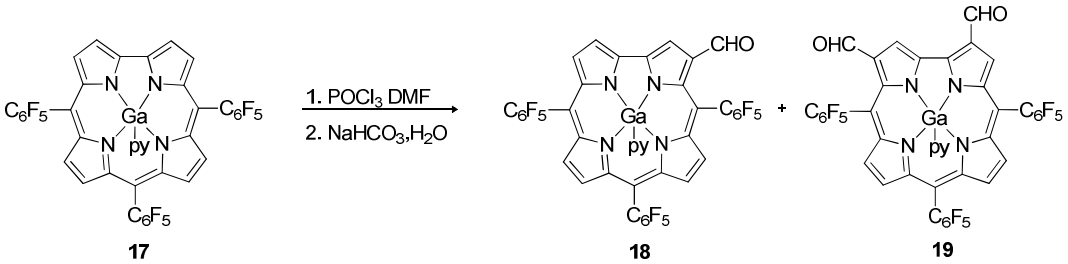

Scheme 13

Some years later, Cavaleiro and co-workers[66] repeated the previous procedure and isolated a mono-formyl derivative in position 2, with a yield of 17%. This compound showed a slightly higher R_f in silica than corrole **18**, and their structure was confirmed by X-ray studies.

A peculiar behavior was observed by Paolesse and co-workers when the formylation reaction was carried out on the free-base 5,10,15-triphenylcorrole.[67] The expected 3-formyl derivative was obtained along with a polar compound that became the major product in the presence of an excess of DMF. The X-ray crystallographic characterization of this product allowed identifying this compound as an inner core ethane bridged derivative **20** (Figure 6). This compound is unprecedented in the case of porphyrins and it is probably obtained from the attack of the Vilsmeier reagent to the inner core nitrogen atoms, followed by a complex series of reactions. Also in this case this peculiar reactivity can be probably inferred to its higher acidity with respect to that of porphyrins, biasing the formation of the corrole anion, which can drive the attack of the Vilsmeier reagent to the macrocyclic core.

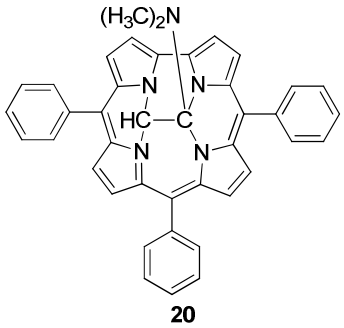

Figure 6 -Product of the formylation reaction carried out on the free-base corrole.

Carboxylation reaction

The carboxylation was the methodology used to introduce carboxylic groups in the corrole periphery. During the first attempt Gross and co-workers[68] used phosgene and corrole free-base **6** (Scheme 14). Also in this case the preferred reaction site was the corrole inner core, affording the *N*-substituted corrole **22** or the bridged carbamide **23**, depending on the solvent used.

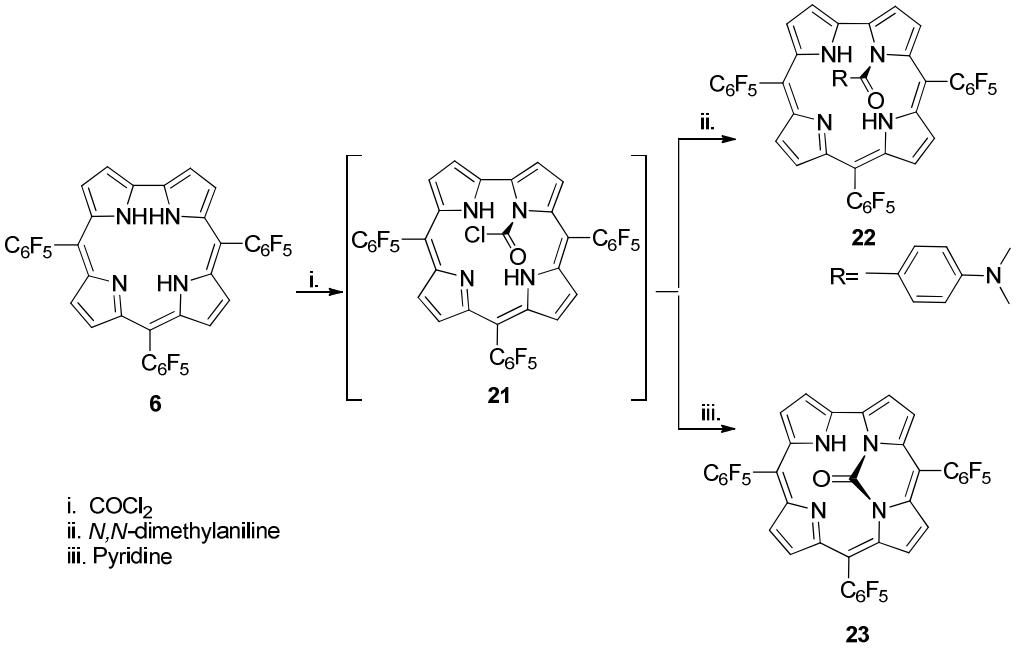

Scheme 14

The authors also performed the reaction with the corresponding gallium(III) complex **17**. In this case, the reaction was successful and the monocarboxylated derivative C-3 was obtained in 58% yield (Figure 7).

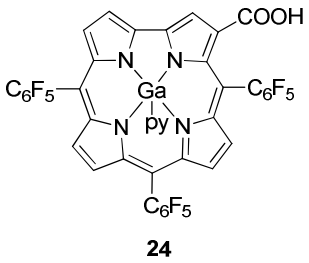

Figure 7- Product of the carboxylation reaction carried out on the gallium(III) complex **24**.

More recently, Girababu and co-workers[69] described an efficient one-pot conversion of 3-formyl-5,10,15-triarylcorroles Cu(III) complexes **25** and **26** to the corresponding carboxylic acid corroles **27-28**, using hydroxylamine hydrochloride and phthalic anhydride (Scheme 15). The products were obtained in yields ranging from 70 to 80%.

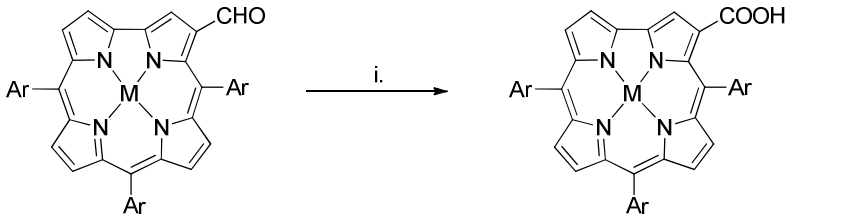

25, M = Cu(III), Ar = C_6H_5
26, M = Cu(III), Ar = 4-$CH_3(C_6H_4)$

27, M = Cu(III), Ar = C_6H_5
28, M = Cu(III), Ar = 4-$CH_3(C_6H_4)$

i. $NH_2OH.HCl$; $N(C_2H_5)_3$, phthalic anhydride

Scheme 15

Cycloaddition reactions

The possibility that cycloaddition reactions can be explored in the functionalization of corrole *β*-pyrrolic positions was reported for the first time by Cavaleiro and co-workers.[70] The studies started in 2004 with the reaction of 5,10,15-tris(pentafluorophenyl)corrole **6** with pentacene. This reaction was carried out at 200 ºC for 6 h in 1,2,4-trichlorobenzene and afforded the expected dehydrogenated Diels-Alder cycloadducts **29** and **30** in moderate yields and a surprising third compound resulting from the cycloaddition reaction [4+4], which was identified as the cycloadduct **31** (scheme 16). Under these conditions it was verified that corrole **6** can act either as a 2π or as a 4π component. These studies were extended to other polycyclic aromatic dienes, such as anthracene, tetracene, 9,10-dimethylanthracene, and naphtho[2,3-*a*]pirene.[71]

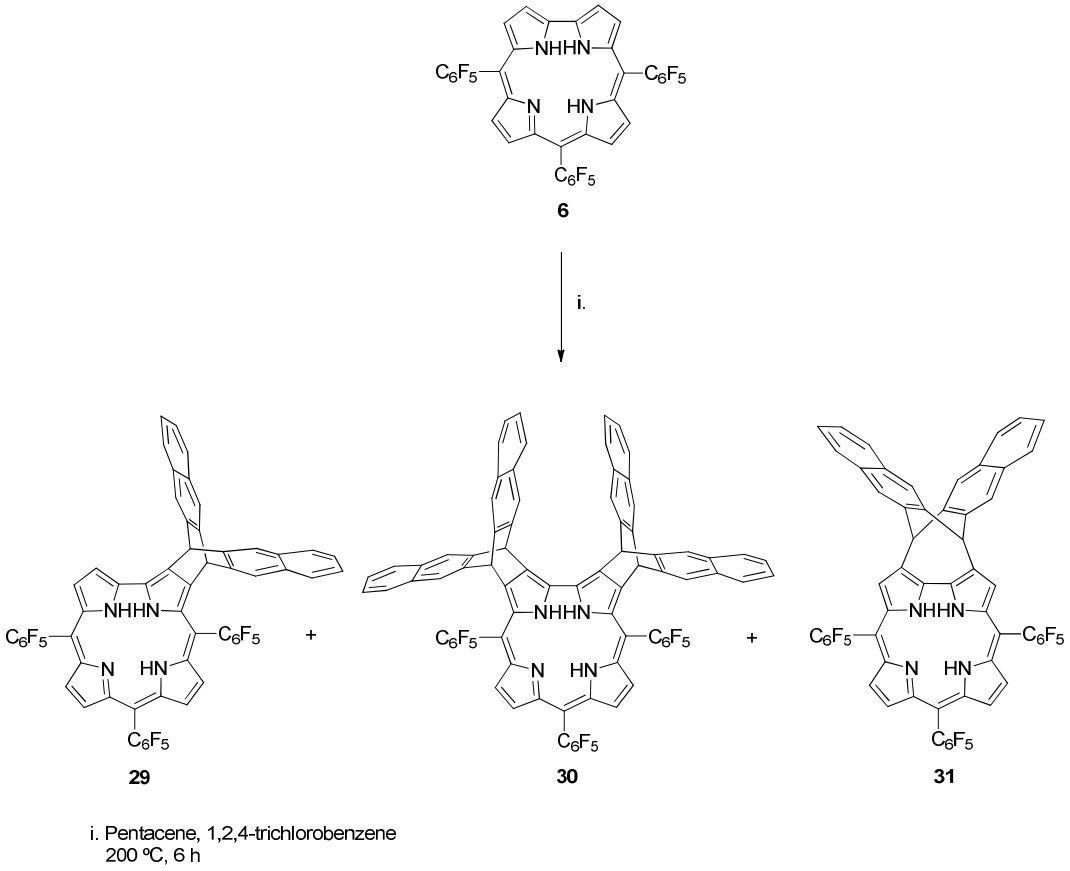

Scheme 16

In 2007 the gallium(III)(pyridine) complex 17 bearing a formyl group was used with *N*-methylglycine to generate a azomethine ylide **32** which was trapped *in situ* with several dipolarophiles (1,4-benzoquinone, 1,4-naphthoquinone, 1,4-anthraquinone, C_{60}, dimethylfumarate and dimethyl acetylenedicarboxilate) in 1,3-dipolar cycloaddition reactions (Scheme 17). The new derivatives **33**-**41** have been obtained in yields ranging from 29 to 62%.[72]

In the reactions with 1,4-naphthoquinone and 1,4-anthraquinone, besides the expected dehydrogenated cycloadducts **35** and **39** , two novel π -extended chromophores (**36** and **38**) were also formed in moderate yields (18% and 46%) (Scheme 17).[72]

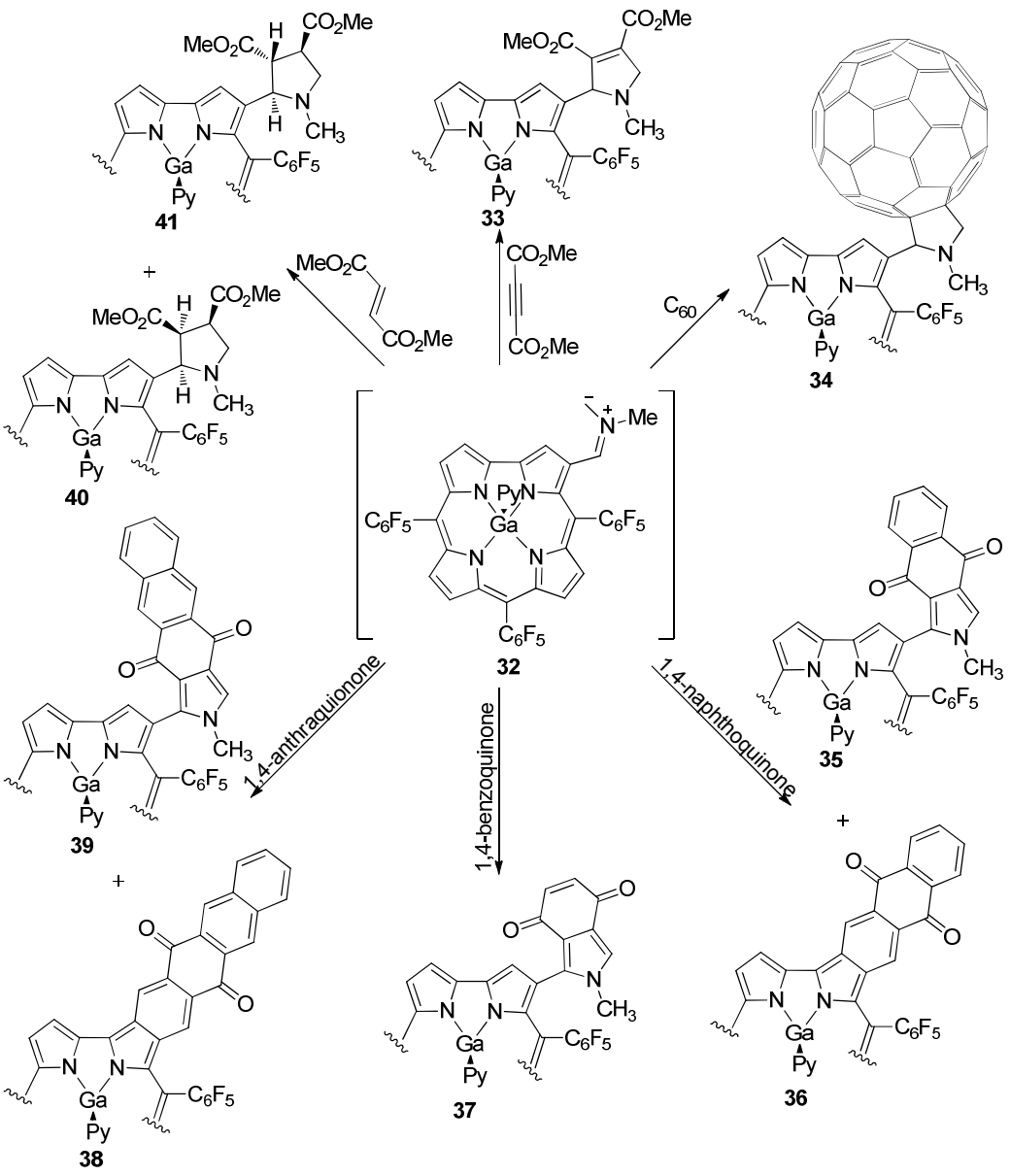
41
33
40
34
32
39
35
37
38
36
1,4-anthraquionone
1,4-benzoquinone
1,4-naphthoquinone
C60

Scheme 17

1.5 Applications

The discovery of facile and efficient methodologies to synthetize and functionalize corroles, allowed that studies concerning their potentiality in different scientific fields were performed. In fact, due to their unique structural, spectroscopic, and photophysical properties these macrocycles are currently being studied in catalysis,[73,65-70] dye sensitized solar cells,[74] medicine,[75] as pH optical sensors, electrodes,[76] and chemosensors.[77]

Catalysis

In the first article that reported the utilization of corroles as catalysts, Gross group[73] decided to compare the efficiency of iron(IV) complex of 5,10,15-tris(pentafluorophenyl)corrole **42** with the efficiency of iron(III) complex of 5,10,15,20-tetrakis(pentafluorophenyl)porphyrin **43** (Figure 8) in the epoxidation of olefins and in the hydroxylation of alkanes by iodosylbenzene, and in the cyclopropanation of alkenes by carbenoids (Scheme 18).

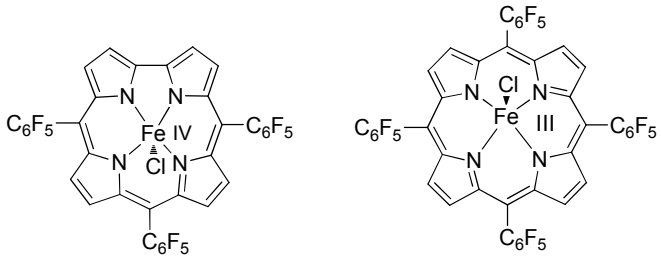

42 **43**

Figure 8- Product of the carboxylation reaction carried out on the gallium(III) complex **24**.

The studies showed that the corrole complex **42** was a good catalyst in all three reactions but less effective than porphyrin complex **43** for the epoxidation and hydroxylation of hydrocarbons (Scheme 18). However, in the cyclopropanation of styrene with ethyl diazoacetate complex **42** showed to be more efficient than **43**.

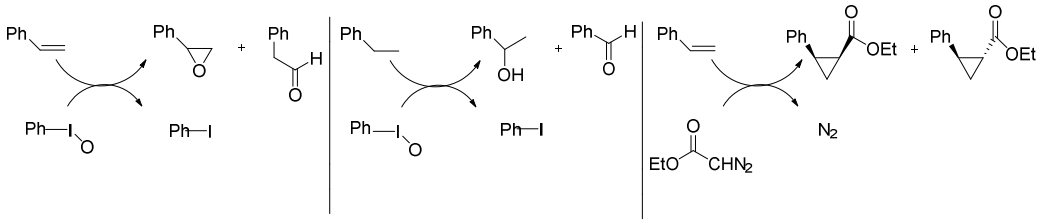

Scheme 18

These results prompted the authors to extend the cyclopropanations studies to Co(III) and Rh(III) complexes of 5,10,15-tris(pentafluorophenyl)corrole. The results obtained revealed that the catalytic efficiency of the complexes increased in the following order Co(III) << Fe(III) < Rh(III). After the divulgation of the results above described, corrole metal complexes began to be extensively used as catalysts in the formation of C-C, C-N, and C-S bonds reactions.

Thereby, in 2006 the same group of investigation used iron(III) complex of different corroles to catalyze the insertion of ethyl diazoacetate and ethyl diazopropionate into the N-H bonds of primary and secondary amines (Scheme 19).[73b] These complexes showed to be more efficient catalyst than all the other previously reported catalysts, affording in a few minutes the corresponding *N*-substituted glycine ethyl esters in very high yields.

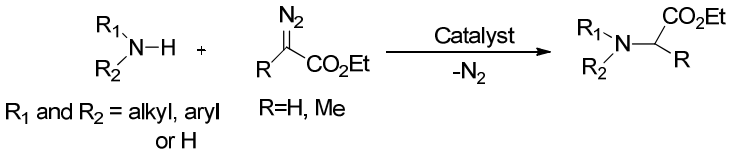

Scheme 19

In 2008 iron(III) corrole complexes were also used as efficient catalysts for insertion reactions involving α-diazoesteres (ethyl diazoacetate and ethyl diazopropionate), thiols and sulfides (Scheme 20).[73c]

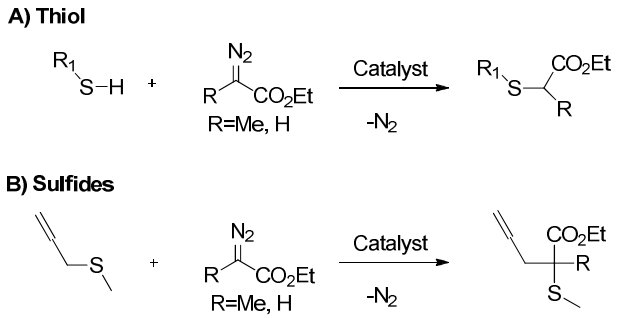

Scheme 20

The possibility of using corrole complexes to oxidize prochiral sulfides by hydrogen peroxide in the presence of five albumin sources (HAS, BSA, PSA, RSA, and SSA) was also evaluated by Gross group.[73d] The authors selected the gallium, iron, and manganese complexes of the amphiphilic bis-sulfonated corrole **44-46** for the catalytic oxidation studies (Scheme 21). The experiments showed clearly that catalysis relied on the corrole complexes and the enantiomeric excesses on the chiral environment provided by the albumin. The examinations included ten different arylmethyl sulfides and in general the best results were obtained with the BSA-conjugated manganese corrole.

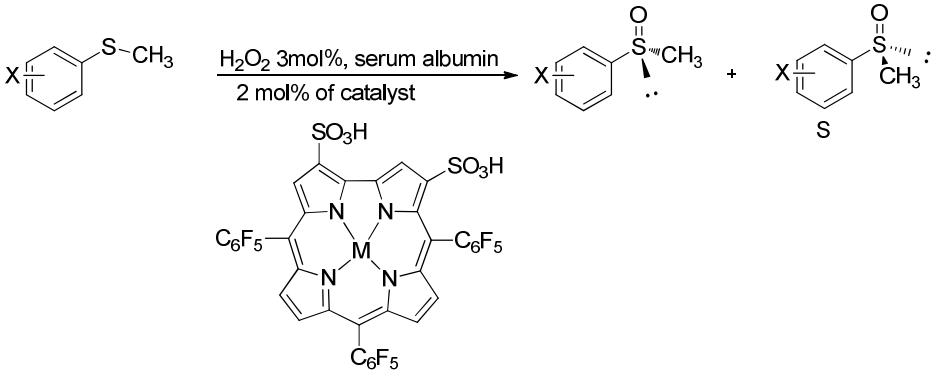

44 M=Mn
45 M=Fe
46 M=Ga

Scheme 21

Another interesting catalytic study with metallocorroles involved the decomposition of peroxynitrite (HOONO).[73e] This is a damaging toxin which decomposes spontaneously in radical species ($^{\bullet}OH$ and $^{\bullet}NO_2$), that can cause irreversible damages in cells. In 2006 Gross and co-workers[73e] proved that it is possible to decompose peroxynitrile without the formation of the above referred species. The group used the bis-sulfonated manganese(III) complex **44** in the disproportionation process, and obtained as final product HNO_2 without the intervention of radical species (Scheme 22).

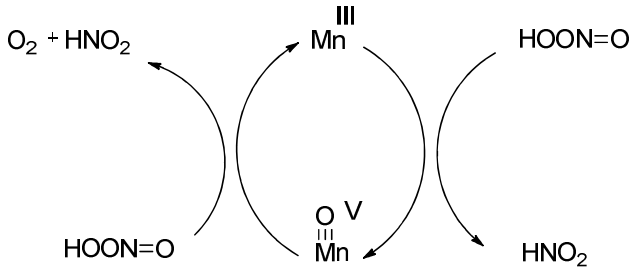

Scheme 22

Dye sensitized solar cells

The possibility of using corroles as dyes in dye-sensitized solar cells (DSSCs) also known as Gratzel cells was considered by Walker *et al*[74] in 2006. These devices, that in general can efficiently convert solar energy into electricity comprise a nanocrystalline titanium dioxide (TiO_2) electrode modified with a photosensitive dye fabricated on a transparent conducting oxide (TCO), a platinum (Pt) counter electrode, and an electrolyte solution usually containing iodide ion/triiodide ion as the redox couple. The authors selected the bis-sulfonated 5,10,15-tris(pentaflourophenyl)corrole **16** and the corresponding gallium(III) **46** and (chloro)tin(IV) **47** complexes to be used as the photosensitive materials for solar cells due to their structural similarity to the best performing dyes (Figure 9).

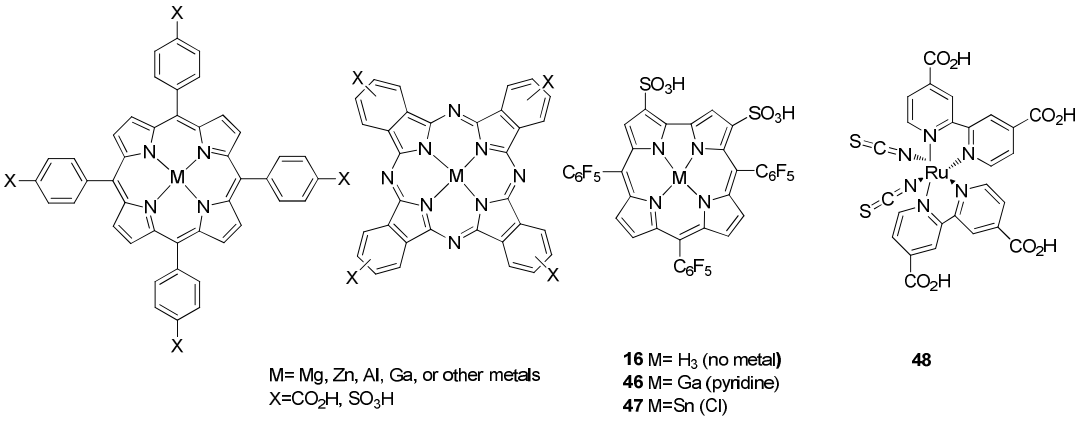

Figure 9 - Corrole complexes and other dyes used as photosensitive materials for solar cells.

All the new complexes were found to bind to nanoporous TiO_2 electrodes and the incident photon to current efficiency (IPCE) spectra of the corroles on nanoporous TiO_2 revealed substantial differences in the efficiencies of the dyes.

Complex **47** showed to be much less efficient than the others complexes namely the standard *cis*-bis(4,4'-dicarboxy-2,2'-bipyridine)dithiocyanatoruthenium(II) **48**; the authors considered that its low efficiency is a consequence of the inability of the excited state to inject electrons into the TiO_2 film. Corroles **16** and **46** showed very similar efficiencies.

Medicinal applications

Currently there are also some studies concerning the use of corroles in medicine. For example, in 2009 Gross *et al*[75] coupled the sulphonated derivates **16**, **46** and **47** with carrier proteins of viral origin (HerPBK10). The corrole - protein aggregates were injected in mice with implanted human breast cancer tumors. The results revealed that the tumors could be detected by fluorescence-based imaging and that their growth can be completely suppressed by this combination. The mechanism of action regarding tumor cell destruction by the Ga(III) complex **46** is not clear yet, but the advantage of being able to follow the biodistribution of an active drug in live animals is enormous.

Another contribution of corroles to pharmaceutical applications was recently reported by Cavaleiro and co-workers,[41] which evaluated the photodynamic potentialities of compounds **49** and **50** in Jurkat cells (Figure 10). The authors found that the presence of the sugar moieties increase the uptake by the cells.

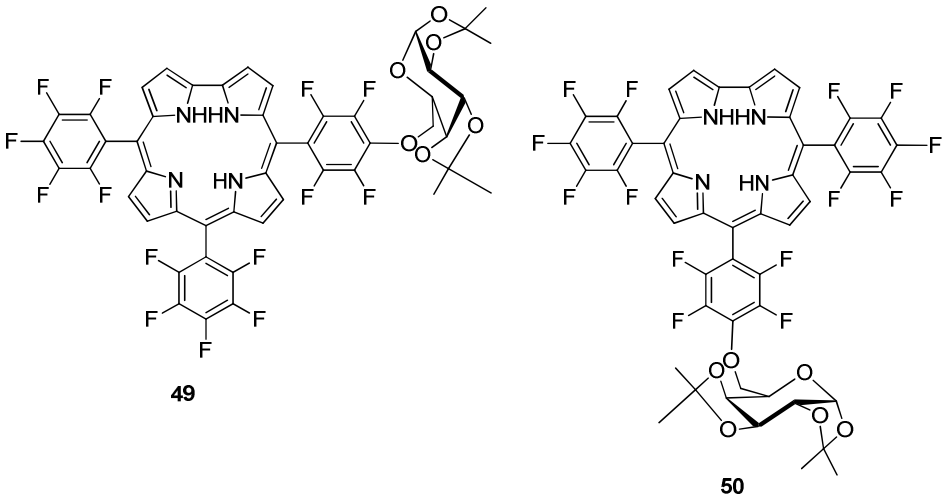

Figure 10- Corrole-galactose conjugates tested in Jurkat cells.

Chemosensors

Corroles have also useful properties to be used as fluorescent chemosensors for molecular recognition. They absorb and emit light in the visible region, and show high excitation coefficients, fluorescent quantum yields and photostability.[15] Corroles also display inner nitrogen donor atoms available for metal recognition.[78] However, in contrast to porphyrins, the sensorial ability of corroles has been under study. In the beginning of 2012 it was published the first study about the use of corroles as optical chemosensors. The sensorial ability of a new family of substituted nitrophenyl free-base A_2B-corroles (where A = nitrophenyl, and B = *N*,*N*-dimethylaminophenyl, thienyl, naphthyl and tridecyloxyphenyl group) towards Hg(II) was evaluated.[79] The corrole with a tridecyloxy long chain moiety exhibited the highest Hg(II) sensing ability. The detection was based on the fluorescence quenching of the corroles, arising from the combined effect of static factors (coordination).

Another study showed that corroles have also useful properties to be used as optical pH sensors, since they exist in three protonation states at different aqueous pH values ($[H_4(cor)]^+$, $[H_3(cor)]$, $[H_2(cor)]^-$, that differ very much in fluorescence intensity. This behavior was demonstrated for the first time by Li *et al*,[80] using the new 10-(4-aminophenyl)-5,15-dimesitylcorrole **51** (Figure 11) immobilized in a sol–gel glass matrix and characterized upon exposure to aqueous buffer solutions. The response of the sensor was based on the corrole fluorescence intensity changing owing to the multiple steps of protonation and deprotonation.

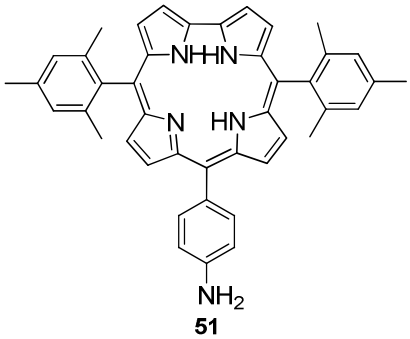

51

Figure 11-Structure of 10-(4-aminophenyl)-5,15-dimesitylcorrole **51** sensing compound.

The corrole based electrode showed a superior pH range response (between 2.17–10.30) than the ones of 5,10,15,20-tetraphenylporphyrin **12** and 5,10,15-tris(pentafluorophenyl)corrole **6**. The same group used also a PVC [high molecular weight poly(vinyl chloride)] membrane with 5,10,15-tris(pentafluorophenyl)corrole **6** as the electroactive material for the construction of a silver(I) electrode.[81] The corrole-based material displayed better response characteristics than the one based on 5,10,15,20-tetraphenylporphyrin **12**, with a working pH range from 4.0 to 8.0, and fast response time of < 30 s.

2 Chemosensors and Sensing Targets

2.1 General Considerations

Currently a vast number of molecules of different sizes and structures ranging from a simple hydrogen molecule (H_2) to a more complex biological protein are known. Although the first attempt is to believe that the structures and properties of more complex systems are directly related to those of the individual molecules, this notion is far from reality. In fact, it is known that the structures, functions and properties of materials and molecular assemblies resulting from the organization of individual molecules, cannot be explained based only on the knowledge of individual molecules nature. The discipline that provides us the tools to understand how simple molecules organize themselves to build-up more complex units is known as "*Supramolecular Chemistry"*.

Supramolecular chemistry is a relatively new area that seeks to understand how discrete molecules can cooperate through non-covalent interactions as hydrogen bonding, metal coordination, hydrophobic forces, van der Waals forces, interactions and electrostatic effects, to easily generate unique nanostructured supermolecules that present different properties (often better) than the sum of the properties of each individual component. In general, the goal of supramolecular chemistry is the design and synthesis of 'supermolecules' that are assembled by a series of molecular recognition events involving intermolecular interactions between the constituent components, a host and a guest (Figure 12).

To obtain entities of higher complexity than the discrete molecules two main criteria should be met: (i) molecules should contain complementary functionalities –

appropriate geometrical and electronic structure and (ii) necessary reaction conditions should be provided. The reversibility of non-covalent bonds allows the system to equilibrate, thereby to generate single or diverse structural entities.[82]

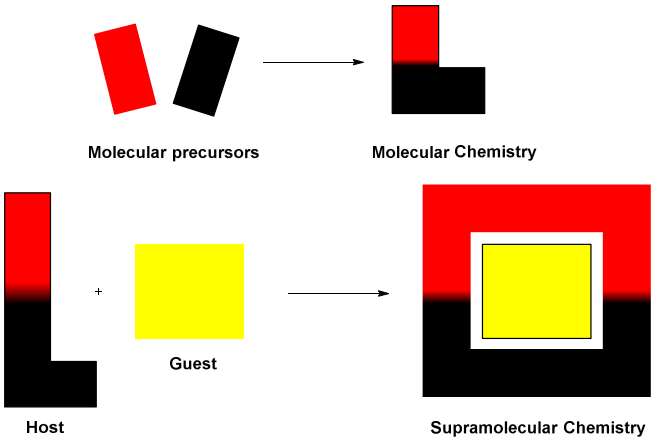

Figure 12- Schematic representation of a molecular recognition event.

One of the most exciting features of the supramolecular structures is their ability to include neutral and charged molecules as guests in the void space. For instance, the crown ethers, discovered by Pedersen[83] in 1967, have the ability to serve as hosts for binding inorganic and organic guests, especially cationic ones. The synthesis of host-guest inclusion compounds has attracted much attention and currently numerous different host frameworks are known.

2.2 Chemosensor Concept

The word sensor is usually referred to devices that can receive information and turn it into a form which is compatible with human perception, knowledge and understanding. The development of sensors is related with the need that man has to control his surroundings. Among the great variety of sensors available to man, there are those which allow the detection of chemical species. This particular type of device is called a chemical sensor, and is defined by IUPAC as "a device that transforms chemical information, ranging from the concentration of a specific sample component to total composition analysis, into an analytically useful signal".[84] This type of device can be either macroscopic (e.g. a pH measuring electrode) or microscopic.

Currently are known molecular devices that are able to act as chemical sensors; these devices are usually designed as chemosensors and are defined as "molecules of abiotic

origin that signal the presence of matter or energy" or as "molecular systems that exhibit changes in their properties after interaction with an analyte".[85] In a strict sense, a chemosensor is a molecule (or an assembled supra-molecular unit) that can bind selectively a target (analyte), and furnish information through a measurable change in its properties about the binding. Due to the two different processes that take place in chemical sensing through analyte detection, *i.e.* molecular recognition and signal transduction, there are usually three parts that constitute a chemosensor (Figure 13): a receptor (which is responsible for the selective analyte binding), an active unit (whose properties should change upon the aforementioned binding) and, in some cases, a spacer that is able to modify the geometry of the system and tune the electronic interaction between the two other components.[86]

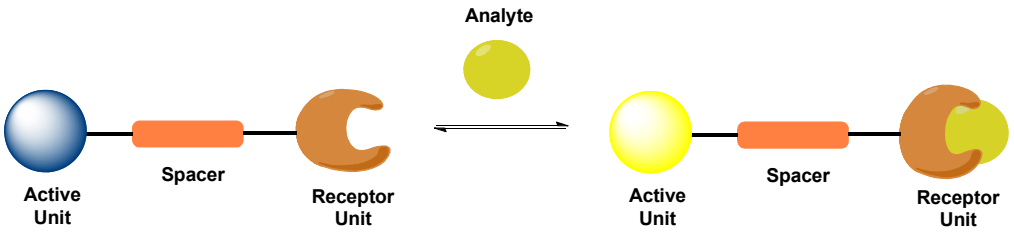

Figure 13-Schematic representation of a chemosensor

Chemosensors can be classified according to the nature of the signal emitted by the active unit. They can be categorized as colorimetric or fluorescent chemosensors (Figure 14).[87]

In the colorimetric chemosensors when the coordination site interacts with the analyte a change of colour is shown by the signaling unit. In fluorescent chemosensors the modification resulting from the analyte-receptor binding generally leads to a change in fluorescence intensity.[88] The development of colorimetric chemosensors is increasingly appreciated, since naked eye detection can offer qualitative and quantitative information without resort to any spectroscopic instrumentation. The fluorescent chemosensors on the other hand are usually very sensitive, versatile and selective. These molecular devices can be conveniently used as tool to analyze and measure the amount of guest species as well as sense biologically important species in vitro an in vivo to clarify their function in living systems. Currently fluorescent chemosensors are applied in food analysis, process control, environmental monitoring and medical diagnosis.[89]

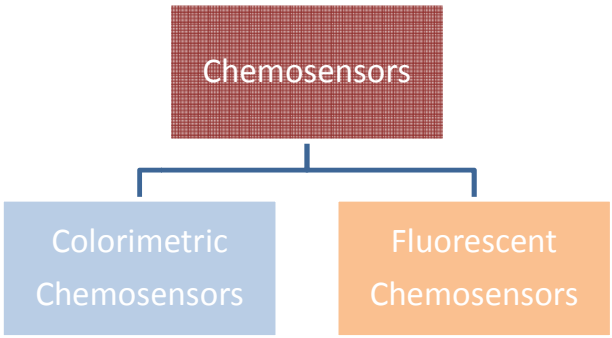

Figure 14- Chemosensors classification.

2.3 Fluorescent Chemosensors and Recognition Mechanisms

In fluorescent chemosensors the active unit is a molecule capable of exhibiting fluorescence (a fluorophore). This radiative transition can be easily explained by the modified Jablonski diagram (Figure 15). The absorption of a quantum light by a molecule results in the promotion of an electron from the molecule's ground electronic state (S0) to one of the several vibrational levels in the excited state. In solution, the excited state molecule rapidly relaxes to the lowest vibrational level of the electronic state S1 via internal conversion. Therefore, the energy stored in the excited state may be released in several ways: fluorescence, intersystem crossing, and phosphorescence. After relaxing to the lowest vibrational level of the S1 state, the electron may return to the S0 state with light emission (fluorescence). If the molecule is sufficiently long-lived in the S1 state, it may cross into a lower energy triplet state (intersystem crossing). Relaxation from the T1 to S0 state can also occur with light emission in solids (phosphorescence), and is generally shifted to longer wavelengths (lower energy) relative to the fluorescence.[90] Molecules containing heavy atoms such as bromine and iodine are frequently phosphorescent. The heavy atoms facilitate intersystem crossing and thus enhance phosphorescence quantum yields.

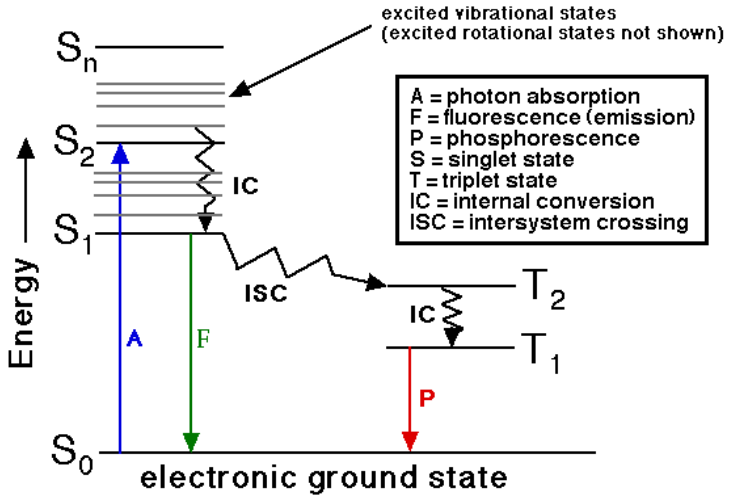

Figure 15- One form of a Jablonski diagram.[90]

In recent years, the success of fluorescent chemosensors between the scientific community, can be explained by the several characteristics that distinguish fluorescence spectroscopy from all other methods used in chemical sensing.[91] This technique is a simple, rapid and non-destructive one, which allows its accomplishment in solid, liquid and gaseous media. According to literature a good fluorescent chemosensor must have a strong affinity and selectivity for the analyte, must be photostable and the environmental interferences should not disturb the fluorescence signal. [92]

From the structural point of view the fluorescent chemosensors can be classified as intrinsic or conjugated. In the intrinsic chemosensors both functions (binding and signaling) are performed by the fluorophore. In the conjugated chemosensors the binding/recognizing and signaling units are separated by a spacer (Figure 16).[93] Corroles can be considered intrinsic chemosensors.[79]

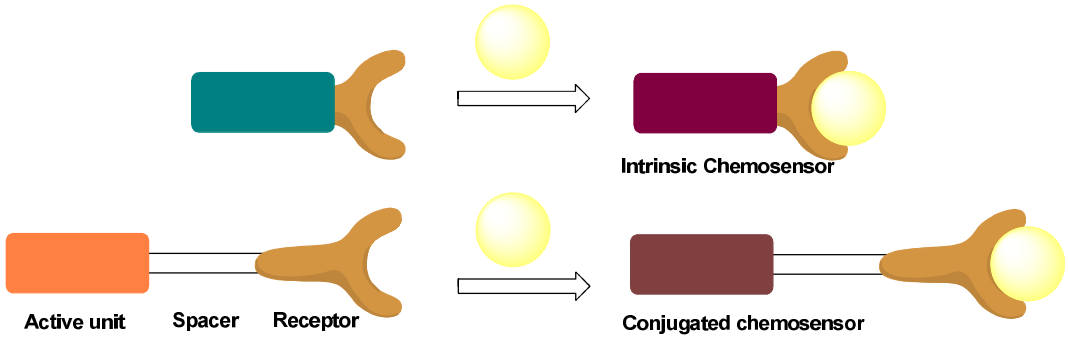

Figure 16- Schematic representation of intrinsic and conjugated chemosensors.

In fluorescent chemosensors the recognition of the analyte causes changes in the optical signal of the fluorophore. These changes may be reflected in an increase or decrease in fluorescence emission intensity of the fluorophore. Two processes can be observed upon analyte binding: Chelation Enhancement of Quenching (CHEQ), which means that the fluorescence emission is quenched, and Chelation Enhancement of Fluorescence (CHEF), where an increase in the emission intensity is observed. It is also possible to perceive the formation of new emission bands.[94]

The transformations above described are the result of the occurrence of a photophysical reaction, which is based on the following signal mechanisms: electron transfer, charge transfer, energy transfer, excimer or exciplex formation. [95]

Based on some revisions that appeared in the last years some considerations about those mechanisms will be now outlined. In fluorescent chemosensors the electron transfer (ET), namely the photo-induced electron transfer (PET) is considered one of the most important mechanisms. PET is a fluorescence quenching process which generally involves two components: an electron donor and an electron acceptor. Its principle is based on the fact that, in the excited state, the oxidative and reductive properties of molecules are enhanced and therefore, electron transfer processes may take place. This process only occurs in conjugated chemosensors. The receptor unit is an electron donor group such as amino group and the fluorophore plays the role of an acceptor. Figure 17 shows how PET mechanism generally occurs. An electron of the highest occupied molecular orbital (HOMO) is promoted to the lowest unoccupied molecular orbital (LUMO) upon excitation of the fluorophore. Therefore, this enables PET from the HOMO of the donor (which belongs to the free receptor) to that of the fluorophore. As a result, the fluorescence is quenched. On the other hand, upon analyte binding the redox potential of the donor is

altered and the relevant HOMO becomes lower in energy than that of fluorophore; as a consequence a fluorescence enhancement occurs.[96]

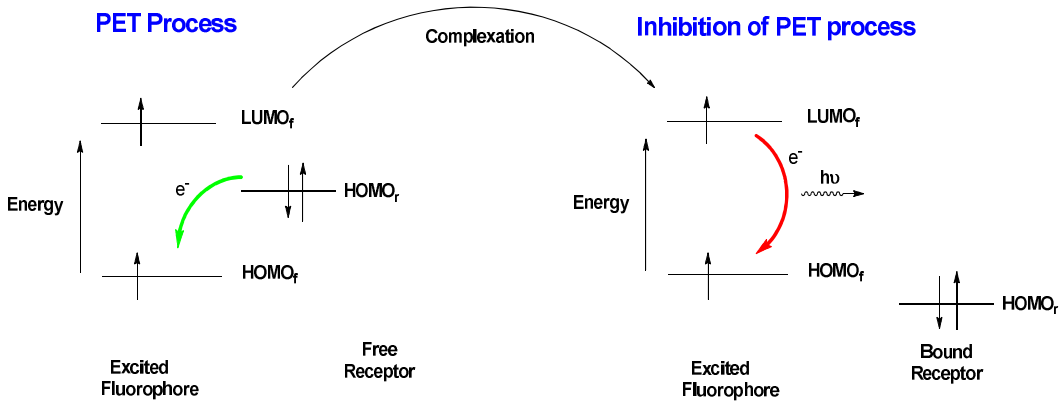

Figure 17- Schematic representation of an excited-state photoinduced electron transfer (PET) process and its inhibition.

Charge transfer processes include intramolecular charge transfer (ICT) and ligand-metal charge transfer (LMCT). In contrast to PET, the charge transfer processes occur in intrinsic chemosensors and are based on charge dipole interactions, which can lead to a red or blue shift in the absorption and emission spectra. For example, in intramolecular charge transfer process the fluorophore, that is directly integrated with the receptor, should contain in their structure a donor and an electron acceptor group, so that during the excitation occurs the formation of a dipole, arising from a redistribution of electronic density. Posteriorly, when a target species, especially a charged one, binds into the receptor, an interaction with this excited state dipole occurs. This energetic interaction will be responsible by a Stokes shift. In practical terms, when for example an amino group playing the role of an electron donor in the fluorophore interacts with a cation, there is a reduction on its electron-donating character; this fact is responsible by a reduction on the conjugation of the system. Therefore, a blue shift of the absorption spectrum is expected. On the other hand, if a cation interacts with the acceptor group (like a carbonyl group), there is a raise in its electron-withdrawing character. Consequently, the absorption spectrum is red shifted. The fluorescence spectra are shifted in the same direction as those of the absorption spectra.[97]

Energy transfer can be classified as electronic energy transfer (EET) or fluorescence resonance energy transfer (FRET) according to the interaction distance

between the energy donor and the energy acceptor. EET is also called Dexter electron transfer, which requires a distance between donor and acceptor of within 10 A° to be efficient, while FRET requires a certain degree of spectral overlap between the emission spectrum of the donor and the absorption spectrum of the acceptor.[98]

Finally, an excimer can be defined as a complex formed by the interaction of a fluorophore in the excited state with a fluorophore of the same structure in the ground state. If the fluorophore in the excited state is different from the fluorophore in the ground state, the resulting complex is called an exciplex.[99]

2.4 Fluorescent Organic-Inorganic Hybrid Materials

Currently one of the key tasks of supramolecular chemistry is to seek new and effective chemosensors that show enhanced performance with respect to selectivity and sensitivity, for example, by signal amplication and reduction in the limit detection. The advent of nanotechnology has opened up a number of new possibilities to reach these goals and overcoming many of the typical limitations of conventional molecular systems. In the last few years have been described several detection systems based on hybrids materials which combine inorganic solid supports (e.g. silica or gold nanoparticles) with organic dyes. These nanoparticle-based chemosensors were able to detect biologically as well as environmentally relevant target species with high precision and accuracy.[100] In this context, some examples were selected in order to demonstrate the advantages and the most valuable features of these systems.

For example, Montalti *et al*[101] functionalized silica nanoparticles with dansyl groups and evaluated the sensing ability of the new hybrid system in the presence of Cd^{2+}, Zn^{2+}, Cu^{2+}, Ni^{2+} and Co^{2+} (Figure 18). The authors chose silica as inorganic solid support because this is photophysically inert, *i. e*., cannot be involved in quenching or photodecomposition processes and doesn´t present intrinsic toxicity. Moreover silica nanoparticles can be easily synthesized by Stöber´s method. In this process, which was discovered in 1968 by Werner Stöber et al,[102] occurs the hydrolysis of a silyl ether such as tetraethyl silicate into silanols using ammonia in a mixture of water and alcohol followed by the condensation into 50-200 nm silica particles. The characterization of silica nanoparticles can be done through Dynamic light scattering (DLS) and their visualization by transmission electron microscopy (TEM).

During the sensorial assays it was verified that the addition of Cd^{2+} and Zn^{2+} did not affect the dansyl fluorescence while even small amounts of Cu^{2+}, Ni^{2+} and Co^{2+} caused a strong intensity decrease. The authors estimated that a single Cu^{2+} ion caused a fluorescence decrease which corresponds to the total quenching of 13 dansyl moieties. They justified this signal amplification with the existence of communications between the dyes and with their pre-organization on the surface of nanoparticles.

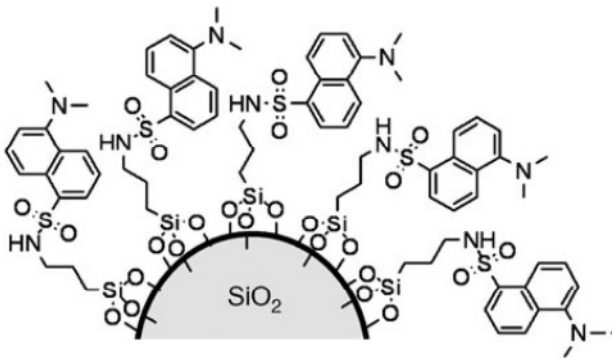

Figure 18- Silica nanoparticles functionalized with dansyl groups.[101]

Hybrid systems based on gold nanoparticles (AuNPs) have also been studied.[103] These systems are very appealing, because the gold nanoparticles can be easily synthesized and are stable. This stability is due to the strong interactions gold-thiol. Moreover, the plasmon surface ressonance of gold allow their detection by UV-Vis studies.[104] Recently Lodeiro and co-workers determined the sensorial ability for cations of hybrid systems resulting from the coating gold nanoparticles with coumarins that presented in their structure a cysteine amino acid unit.[105] The sensorial studies were performed in dicloromethane and involved the following metal ions: Hg^{2+}, Cd^{2+}, Zn^{2+}, and Ag^{+}. Only in the case of mercury(II) was observed alterations. The addition of Hg^{2+} caused a color change from pink to dark red/brown in both systems (Scheme 23), as well as an increase of 100-fold in the nanoparticle size, raising the AuNPs aggregation. The change of colour observed upon aggregation can be explained by the coupling of the dipoles which occur when the interparticle distances decrease.

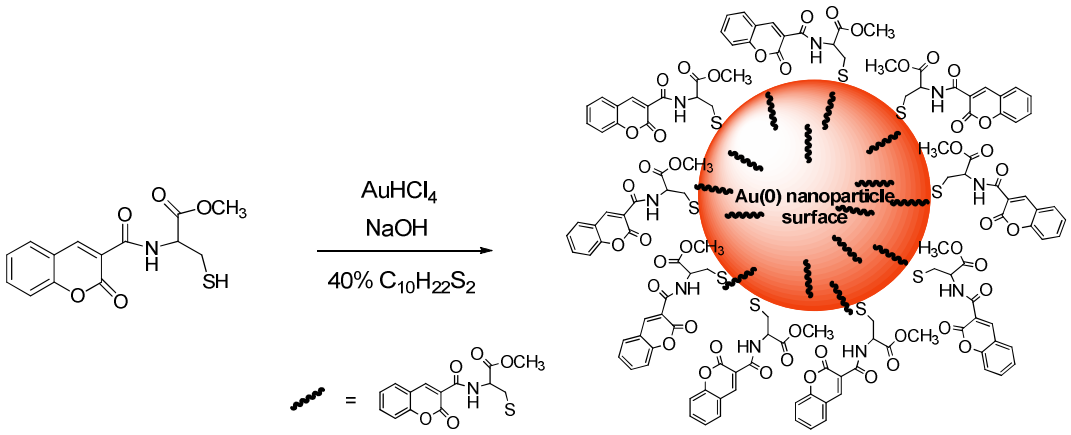

Scheme 23

2.5 Sensing Targets

After having described the type of chemosensors related to the scope of this thesis, some attention will now be given to some of the analytes that were the subject of the sensing studies.

Metal ions

In the present section are introduced most of the metals studied in this thesis, in order to better understand their coordinating properties, and consequently, their effects upon recognition.

Metal ions are extremely important in fields such as biology, chemistry, medicine and environment.[106] The role of metal cations in biological processes ranges from maintaining potentials across cell membranes to triggering muscle contraction, among other functions. They are also involved in catalytic functions at the active sites of many enzymes. Therefore they must exist in adequate quantities. In fact, they can promote metabolic disorders, when they are absorbed and accumulated from the environment causing toxicity and diseases.[91]

Among the metal ions present in nature, the ones studied in this thesis were alkali, alkaline earth and transition type.

Alkaline Na^+, K^+ and alkaline earth, Mg^{2+}, Ca^{2+} are present in large quantities in the human body and under Pearson theory[107] are considered hard metal ions. Contrary the transition metal ions Cu^{2+}, Ni^{2+} and post-transition metals Zn^{2+}, Cd^{2+} and Hg^{2+}, (d-block elements) are present in small quantities.[91]

Copper is one of the most well-known metals, and finds application in many areas of everyday life. It is also the less reactive of the first row transition metals. It can be found in a great number of metalloproteins. This metal is the only first row d block metal that exhibits a stable +1 oxidation state, even though the most stable one is +2 (copper(I) is easily oxidized and copper(III) is very difficult to obtain). Copper (II) is highly toxic for some bacteria and viruses, and it is suspect to cause infant liver damage. Their alteration in cellular environmental can causes neurodegenerative diseases such as Alzheimer's disease.[108] In terms of molecular recognition, Cu(II) usually quenches the emission of fluorophores, because it is a d^9 ion, and can undergo electron transfer or energy transfer processes.[109-110]

Zinc(II) is the second abundant metal ion in human body, is an important structural or catalytic cofactor of many proteins (for example carbonic anhydrase and zinc finger proteins) and can chelate on brain and pancreas.[111] The Zn(II) ion has a $3d^{10}$ electronic configuration, and it cannot be strictly considered as a transition metal ion. Due to this electronic configuration, its compounds are colorless and diamagnetic and there is no ligand-field stabilization energy associated with this ion, for what no particular geometry is preferred in the formation of complexes. Regarding its sensing, Zn(II) is not a redox active center, and for this reason cannot participate in electron-transfer processes. Plus, it is a hard metal center[101] and has affinity for nitrogen and oxygen donors. After complexation it usually enhances the fluorescence of the system, by blocking PET from the donor atoms to the fluorophore.

Nickel is rarely found in its pure form on the Earth's surface, although it is believed that a significant amount is present at the core. Its most stable oxidation state is +2, while +1 and 0 are only found in organometallic chemistry. It has a very rich coordination chemistry, and can form complexes with different geometries (octahedral, trigonal bipyramidal, tetrahedral, square-based pyramidal and square planar).[112-113]

Mercury has unique properties, since it is the only metallic element that exists in liquid form at room temperature. Another unusual property for this metal is its poor heat conductivity (even though it is a good conductor of electricity). It has many practical uses (e.g. barometers, electrodes, etc.), but it is extremely toxic to humans.[114] Both (I) and (II) oxidation states are stable, but in terms of sensing it was chosen in this thesis to detect Hg(II). The d^{10} configuration of Hg(II) should, in principle, predict a similar behavior to Zn(II) in terms of CHEF effect, with the difference that mercury(II) is a soft metal

center.[115] The metals cadmium (II) and lead (II) are extremely toxic and polluting, such as Hg(II). They can cause serious environmental contamination.[116]

Anions

The recognition and detection of anions is another field which has attracted increasing interest in recent years due to the fundamental importance of these species in many chemical and biological processes.[117] Throughout this thesis some studies with the spherical halide ion F^-, the linear anion CN^- and the bulky anions CH_3COO^- and $H_2PO_4^-$ were performed. Fluoride is an essential anion in humans and it is used to prevent dental caries and osteoporosis. However, its ingestion in high or in low levels may result in fluorosis, nephrotoxic changes and urolithiasis in humans.[118-119] Another interesting anion in terms of detection is CN^-, which is lethal in very small amounts due to its ability to bind strongly to the active site of cytochrome c oxidase, leading to the inhibition of the mitochondrial electron transport chain, and to a decrease in the oxidative metabolism. This anion has many applications in metallurgy, fishing, mining, and in the fabrication of polymers.[111] The development of simple acetate and phosphate chemosensors is also of great interest, since these anions are widely used in food additives and in agricultural fertilizers.[120]

3 Scope of the Present Thesis

In the previous sections, some important notions related to this work were introduced. By putting together some of these concepts it is possible to define the main objective of this thesis - to develop new efficient and sensitive chemosensors based on corrole derivatives for the recognition of anions and metal ions. It can be theoretically divided in two parts: one part deals with corrole functionalization studies and other with the recognition of different analytes.

Several functionalization studies were developed on the 5,10,15-tris(pentafluorophenyl)corrole **6**, which is one of the most studied macrocycles of the corrole family.

In chapter II is described the synthesis of the new β-vinylcorrole (3-vinyl-5,10,15-tris(pentafluorophenyl)corrolatogallium(III)). The possibility of using β-vinylcorroles as dienes in Diels-Alder reaction was also investigated. The reactivity of the 3-vinyl-5,10,15-tris(pentafluorophenyl)corrolatogallium(III) as the 4π component was studied in the presence of 1,4-benzoquinone and 1,4-naphthoquinone in refluxing toluene. The main products were isolated in yields of 76% and 64%, and were fully characterized by elemental analysis, ^{1}H-NMR, ^{13}C-NMR, ^{19}F-NMR, MALDI-TOF-MS, UV-Vis absorption and emission spectroscopy. The sensing ability of the new corrole derivatives and of their precursors was studied in solution towards the spherical halide ions F^-, Cl^-, Br^-, I^-, the linear anion CN^- and the bulky anions CH_3COO^- and $H_2PO_4^-$.

Taking into account the importance of colorimetric chemosensors, in chapter III two new colorimetric corrole probes are presented. The selected synthetic methodology involved, again, the synthesis of the 3-vinyl-5,10,15-tris(pentafluorophenyl)corrolatogallium(III) (pyridine) by the Wittig reaction of 3-formyl-5,10,15-tris(pentafluorophenyl)corrolatogallium(III) (pyridine) with phosphorus ylide and the subsequent reaction with dimethyl acetylenedicarboxylate. The derivatives obtained were fully characterized, and their application in the sensing of F^-, CN^-, CH_3COO^- and $H_2PO_4^-$ was tested by absorption and emission spectroscopies.

For *in vivo* applications, fluorescent chemosensors must to be water soluble. The change in the solubility of the corrole macrocycle resulting from the insertion of coumarin-type units in its structure is the subject of chapter IV. Two new corrole-coumarin derivatives were synthetized and their sensing ability compared with porphyrin-coumarin analogues. The insertion of a coumarin moiety conferred an unusual solubility of these

conjugates in ethanol. One of the porphyrin free-base conjugate was fully studied in a mixture EtOH:H_2O (50:50) and showed an unprecedented selectivity for Hg^{2+}. A colorimetric effect was also observed. A strong colour change from purple to yellow was detected. The sensorial ability of this conjugate was yet evaluated in the solid state. Two non-expensive solid supports of agarose and natural cellulose were developed. In the cellulose support material the colorimetric effect for Hg^{2+} reveals a similar behaviour as in solution.

Knowing that the incorporation of organic dyes in silica nanoparticles could improve the affinity, versatility and sensitivity of the chromophores to the guests, in chapter V silica nanoparticles are coated with an alkoxisilane corrole with an imine linkage. The sensorial ability of these nanoparticles was evaluated towards Hg^{2+}, Ag^{+} and Cu^{2+}. Interestingly, upon addition of Ag^{+}, groups of satellite AgNPs were formed around the SiNPs and were checked by transmission electron microscopy (TEM). At same time, a change of color from green to yellow was observed.

In this chapter was also studied the sensorial response of 5,10,15-tris(pentafluorophenyl)corrole and its monoanionic species towards Ag^{+}, Na^{+}, $Ca^{2+,}$ Zn^{2+}, Cd^{2+}, Cu^{2+}, Pb^{2+}, Hg^{2+}, Zn^{2+}, Ni^{2+}, Cr^{3+}, Ga^{3+}, Fe^{3+}, and Al^{3+} metal ions in toluene and acetonitrile. The 5,10,15-tris(pentafluorophenyl)corrole showed to be colorimetric for Hg^{2+}.

4 References

[1] http://www.nobel.se/chemistry/laureates/1964/press.html 19/11/2013.

[2] Rickes, E. L.; Brink, N. G.; Koniuszy, F. R.; Wood, T. R.; Folkers, K. *Science*, **1948**,107, 396-397.

[3] Pierce, J. V.; Page A. C.; Stokstad, E. L. R; Jukes, T. H. *J. Am. Chem. Soc.* **1949**, 71, 2952-2952.

[4] Emerson, G. A.; Folkers, K. *Ann. Rev. Biochem.* **1951**, 20, 559-598.

[5] Hodgkin, D. C.; Kamper, J.; Maureen, M; Pickworth, J.;Trueblood, K. N.; White, J. G. *Nature*, **1956**, 178, 64-66.

[6] Jonhson, A. W.; Price, R. J. *Chem. Soc*. **1960**, 1649-1653.

[7] Jonhson, A. W.; Kay, I. T. J. *Chem. Soc*. **1965**, 1620-1629.

[8] Harrison, D. C.; Hodder, O. J. R.; Hodgkin, D. C. *J. Chem. Soc*. (B). **1971**, 640-645.

[9] Gross, Z.; Galili, N.; Simkhovich, L.; Saltsman, I.; Botoshansky, M.; Blser, D.; Boese, R.; Goldberg, I. *Org. Lett*. **1999**, 1, 599-602.

[10] Gross, Z.; Galili, N.; Saltsman, I. *Angew. Chem. Int. Ed.* **1999**, 38, 1427-1429

[11] Dyke, J. M.; Hush, N. S.; Williams, M. L.; Woolsey, I. S. *Mol. Phys.* **1971,** *20* 1149-1161.

[12] Ghosh, A.; Jynge, K., *Chem. Eur. J.* **1997**, *3*, 823-833.

[13] Ding, T.; Alemán, E. A.; Modarelli, D. A.; Ziegler, C. J. *J. Phys. Chem. A* **2005**, 109, 7411-7417.

[14] Tasior, M.; Gryko, D.T.; Shen, J.; Kadish, K.M.; Ventura, B.; Flamigni, L. *J. Phys. Chem.C.* **2008***,*112*,*1699-19709.

[15] Aviv-Harel, I.; Gross, Z. *Chem. Eur. J.* **2009** , 15, 8382-8394.

[16] Tasior, M.; Gryko, D.T.; Shen, J.; Kadish, K.M.; Ventura, B.; Flamigni, L. *J. Phys. Chem.C.* **2008***,*112*,*1699-19709.

[17] Paolesse, R.; Sagone, F.; Macagnano, A.; Boschi, T.; Prodi, L.; Montalti, M.; Zaccheroni, N.; Bolleta, F.; Smith, K. M. *J. Porphyrins Phthalocyanines* **1999**, *3*,364–370.

[18] Bendix, J.; Dmochowski, I. J.; Gray, H. B.; Mahammed, A.; Simkhovich, L.; Gross, Z. *Angew. Chem. Int. Ed.* **2000**, 39, 4048–4051.

[19] (a) Tardieux, C.; Gros, C. P.; Guilard. R.; *J. Het. Chem*. **1998**, 35, 965-970. (b) Nardis, S.; Mandoj, F.; Paolesse, R.; Fronczek, F. R.; Smith, K. M.; Prodi, L.; Montalti, M.; Battistini, G. *Eur. J. Inorg. Chem*. **2007**, 2345-2352. (c) Swider, P.; Voloshchuk, R.; Lewtak, J.; Gryko D.T., *J. Mass. Spectrom.* **2010**, *45*, 1443–1451.

[20] Nardis, S.; Pomarico, G.; Fronczek, F. M.; Vicente, M. G. H; Paolesse. R.; *Tetrahedron Lett.***2007**, 48, 8643-8646.

[21] Barata J. F. B.; Neves M. G. P. M. S.; Tome A. C.; Faustino M. A. F.; Silva A. M. S.; Cavaleiro J. A. S. *Tetrahedron Lett.* **2010**, 51, 1537-1540.

[22] Hirabayashi, S.; Omote, M.; Aratani, N.; Osuka, A. *Chem. Soc. Jpn.* **2012**, 85, 558-564.

[23] Balazs, Y. S.; Saltsman, I.; Mahammed, A.; Kachenko, E.; Golibkov, G.; Levine, J.; Gross, Z. *Magn. Reson. Chem.* **2004**; 42: 624–635.

[24] Paolesse, R.; Jaquinod, L.; Nurco, D. J.; Mini, S.; Sagone, F.; Boschi, T.; Smith, K. M. *Chem. Commun.* **1999**, 1307–1308.

[25] Adler, A. D.; Longo, F. R.; Finarelli, J. D.; Goldmacher, J.;. Assour, J.;Korsakoff, L. *J. Org. Chem.* **1967**, 32, 476-476.

[26] Paolesse, R.; Nardis, S.; Sagone, F.; Khoury R. G. *J. Org. Chem.* **2001**, 66, 550-556

[27] Gryko, D. T.; Jadach, K., *J. Org. Chem* **2001,** *66* , 4267-4275.

[28] Collman, J. P.; Decreau, R. A., *Tetrahedron Lett.* **2003**, *44* , 1207-1210.

[29] Gryko, D. T.; Koszarna, B., *Org. Biomol. Chem* **2003**, *1* , 350-357.

[30] Koszarna, B.; Gryko, D. T., *J. Org. Chem.* **2006**, *71* , 3707-3717.

[31] Kumari, P.; Chauhan, S. M. S., *J. Heterocyclic. Chem.* **2008**, *45* , 779-783.

[32] Zhan H-Y.; Yang, H-Y.; Liu, H-Y.; Chen, H-J; Jian, H-F. *Tetrahedron Lett* . **2009**, *50*, 2196–2199

[33] Dogutan,D.K.; Schwalbe, M.; Teets, T. S.; Nocera, D. G. *J. Am. Chem. Soc***. 2011**, *133*, 131–140

[34] Paolesse, R.; Kadish, K.M.; Smith, K.M.; Guilard, R. *in The Porphyrins Handbook*; Eds; Academic Press: New York, **2000**, Vol.II.

[35] (a) Saltsman, I.; Simkhovich, L.; Balazs, Y. S.; Goldberg, I.; Gross, Z.; *Inorg. Chim. Acta* **2004**, *357*, 3038-3046. (b) Licoccia, S.; Paolesse, R.; Tassoni, E.; Polizio, F.; Boschi, T. *J. Chem. Soc., Dalton Trans.* 1995, 3617-3621.

[36] Saltsman, I.; Goldberg,I.; Gross, Z. *Tetrahedron Lett*. **2003**, *44*, 5669-5704.

[37] Buckley, H. L.; Chomitz, W. A.; Koszarna, B.; Tasior, M.; Gryko, D. T.; Brothers, P.; Arnold, J. *Chem. Commun*. **2013**, 49, 3104-3106.

[38] Barata, J. F. B.; Santos, C. I. M.; Neves, M. G. P. M. S.; Faustino, M. A. F.; Cavaleiro, J. A. S.; *Topics in Heterocyclic Chemistry*, Springer- Verlag: Berlin, 2013, in press.

[39] Costa, J. I. T.; Tomé, A. C.; Neves, M. G.P.M.S.; Cavaleiro, J. A.S. *J. Porphyrins Phthalocyanines,* **2011***,* 15, 1116-1133.

[40] Hori, T.; Osuka, A. *Eur J. Org. Chem*. **2010**, 2379-2386.

[41] Cardote, T. A. F.; Barata J. F. B.; Faustino, M. A. F.; Preuß, A; Neves, M. G. P. M. S.; Cavaleiro, J. A. S.; Ramos, C. I. V.; Santana-Marques, M. G. O; Röder, B. *Tetrahedron Lett*. **2012**, *53*, 6388-6392.

[42] Barata, J. F. B.; da Silva, D. A. L.; Neves, M.G. P. M. S.; Cavaleiro, J. A. S.; Trindade, T. *RCS Advances.* **2013**, 3, 274-279.

[43] Mahammed, A.; Botoshansky, M.; Gross, Z. Chlorinated corroles. *Dalton. Trans.* **2012**, *41*, 10938-10940.

[44] Vestfrid, J.; Botoshansky, M.; Palmer, J. H.; Durrell, A. C.; Gray, H. B.; Gross, Z. *J. Am. Chem. Soc.* **2011**, *133*, 12899-12901.

[45] Du, R-B.; Liu, C.; Shen, D-M.; Chen, Q-Y. *Synlett* **2009**, 16, 2701-2705.

[46] Nardis, S.; Mandoj, F.; Paolesse, R.; Fronczek, F. R.; Smith, K. M.; Prodi, L.; Montalti, M.; Battistini, G. *Eur. J. Inorg. Chem.* **2007**, 2345-2352.

[47] Palmer, J. H.; Day, M. W.; Wilson, A. D.; Henling, L. M.; Gross, Z.; Gray, H. B. *J. Am. Chem. Soc.* **2008**, *130*, 7786-7787.

[48] Golubkov, G.; Bendix, J.; Gray, H. B. Mahammed, A.; Goldberg, I.; DiBilio, A. J.; Gross, Z. *Angew. Chem. Int. Ed.* **2001**, *40*, 2132-2134.

[49] Nardis, S.; Pomarico, G.; Mandoj, F.; Fronczek, F. R.; Smith, K. M.; Paolesse, R. *J. Porphyrins Phthalocyanines* **2010**, 14, 752-757.

[50] Agadjanian, H.; Weaver, J. J.; Mahammed, A.; Rentsendorj, A.; Bass, S.; Kim, J.; Dmochowski, I. J.; Margalit, R.; Gray, H. B.; Gross, Z.; Medina-Kauwe, L. K. *Pharm. Res.* **2006**, *23*, 367-377.

[51] Lim, P; Mahammed, A.; Okun, Z.; Saltsman, I.; Gross, Z.; Gray, H. B.; Termini, J. *Chem. Res. Toxicol.* **2012**, *25*, 400-409.

[52] Hwang, J. Y.; Lubow, D. J.; Sims, J. D.; Gray, H. B.; Mahammed, A.; Gross, Z.; Medina-Kauwe, L. K.; Farkas, D. L. *J. Biomedical. Optics.* **2012**, *17*, 015003-1.

[53] Agadjanian, H.; Ma, J.; Rentsendorj, A.; Valluripalli, V.; Hwang, J. Y.; Mahammed, A.; Farkas, D. L.; Gray, H. B.; Gross, Z.; Medina-Kauwe, L. K*P Natl Acad Sci USA* **2009**, *106*, 6105-6110.

[54] Haber, A.; Aviram, M.; Gross, Z. *Inorg. Chem.* **2012**, *51*, 28-30.

[55] Catrinescu, M-M.; Chan, W.; Mahammed, A.; Gross, Z.; Levin, L. A. *Exp. Eye. Res.* **2012**, *97*, 31-35.

[56] Hwang, J. Y.; Lubow, J.; Chu, D.; Ma, J.; Agadjanian, H.; Sims, J.; Gray, H. B.; Gross, Z.; Farkas, D. L.; Medina-Kauwe, L. K. A *Mol. Pharmaceut.* **2011**, *8*, 2233-2243.

[57] Hwang, J. Y.; Lubow, J.; Chu, D.; Sims, J.; Alonso-Valenteen, F.; Gray, H. B.; Gross, Z.; Farkas, D. L.; Medina-Kauwe, L. K. *J. Controll. Release* **2012**, *163*, 368-373.

[58] Stefanelli, M.; Mastroianni, M.; Nardis, S.; Licoccia, S.; Fronczek, F. R.; Smith, K. M.; Zhu, W.; Ou, Z.; Kadish, K. M.; Paolesse, R. *Inorg. Chem.* **2007**, *46*, 10791-10799.

[59] Saltsman, I.; Mahammed, A.; Goldberg, I.; Tkachenko, E.; Botoshansky, M.; Gross, Z. Selective substitution of corroles: *J. Am. Chem. Soc.* **2002**, *124*, 7411-7420.

[60] Nardis, S.; Stefanelli, M.; Mohite, P.; Pomarico, G.; Tortora, L.; Manowong, M.; Chen, P.; Kadish, K. M.; Fronczek, F. R.; McCandless, G. T.; Smith, K. M.; Paolesse, R. *Inorg. Chem.* **2012**, *51*, 3910-3920.

[61] Mastroianni, M.; Zhu, W.; Stefanelli, M.; Nardis, S.; Fronczek, F. R.; Smith, K. M.; Ou, Z.; Kadish, K. M.; Paolesse, R*Inorg. Chem.* **2008**, *47*, 11680-11687.

[62] Stefanelli, M.; Mandoj, F.; Mastroianni, M.; Nardis, S.; Mohite, P.; Fronczek, F. R.; Smith, K. M.; Kadish, K. M.; Xiao, X.; Ou, Z.; Chen, P.; Paolesse, R. *Inorg. Chem.* **2011**, *50*, 8281-8292.

[63] Barbe, J-M.; Canard, G.; Brandès, S.; Guilard, R*Eur. J. Org. Chem.* **2005**, 4601-4611.

[64] Collman, J. P.; Decréau, R. A. *Org. Lett.* **2005**, *7*, 975-978.

[65] Saltsman, I.; Mahammed, A.; Goldberg, I.; Tkachenko, E.; Botoshansky, M.; Gross, Z. *J. Am. Chem. Soc.*, **2002**, *124*, 7411-7420.

[66] Vale, L. S.H. P.; Barata, J. F. B.; Santos, C. I. M.; Neves, M. G. P. M. S.; Faustino, M. A. F.; Tomé, A.C.; Silva, A. M. S.; Paz, F. A. A.; Cavaleiro, J. A. S. *J. Porphyrins Phthalocyanines* **2009**, *13*, 358-368.

[67] Paolesse, R.; Nardis, S.; Venanzi, M.; Mastroianni, M.; Russo, M.; Fronczek, F. R.; Vicente, M. G. H. *Chem. Eur. J.* **2003***,* 9, 1192-1197

[68] Saltsman, I.; Goldberg, I.; Gross, Z. *Tetrahedron Lett*. **2003**, *44*, 5669-5704.

[69] Sudhakar, K.; Velkannan, V.; Giribabu, L.; *Tetrahedron Lett.* **2012**, 53,991-994.

[70] Barata, J. F. B.; Silva, A. M. G.; Faustino, M. A. F.; Neves, M. G. P. M. S.; Tomé, A. C.; Silva, A. M. S.; Cavaleiro, J. A. S. *Synlett.* **2004**, Synlett, 7, 1291-1293.

[71] Barata, J. F. B. Thesis. *Synthesis and reactivity studies of new corrole derivatives Department of Chemistry.* University of Aveiro, Aveiro, **2009** p 248

[72] Vale, L. S. H. P.; Barata, J. F. B.; Neves, M. G. P. M. S.; Faustino, M. A. F.; Tomé, A. C.; Silva, A. M. S.; Paz, F. A. A.; Cavaleiro, J. A. S.; *Tetrahedron Lett.* **2007,** 48, 8904-8908.

[73] (a) Gross, Z.; Simkhovich, L.; Galili, N. *Chem. Commun*. **1999**, *7*, 599-600. (b) Aviv, I.; Gross, Z.; *Synlett*, **2006**, *6*, 951-959. (c) Aviv, I.; Gross, Z. *Chem. Eur. J.* **2008**, *14*, 3995-4001. (d) Mahammed, A.; Gray, M.B.; Weaver, M.; Sorasaenee, G.; Gross, Z. *Bioconjugate Chem.* **2004**, *15*, 738-742. (e) Mahammed, A.; Gross, Z.; *Angew. Chem., Int. Ed.* **2006**, *45*, 6544-6612.

[74] Walker, D.; Chappel, S.; Mahammed, A.; Weaver, J. J.; Brunschwig, B.F.; Winkler, F.J.; Gray, H.B.; Zaban, A.; Gross, Z. *J. Porphyrins Phthalocyanines,* **2006**, *10*, 1259-1305.

[75] Agadjanian, H.; Rentsendorj, A.; Valluripalli, V.; Hwang, J.Y.; Mahammed, D. L.; Gross, Z. ; Medina-Kauwe, L. M. *Proc. Natl. Acad. Sci. USA* **2009**, *106*, 6105-6116.

[76] (a) Li, Y.; Zhang, X.; Han, Y.; Akermark, B.; Sun, L.; Shen, G.; Yu, Q. *Analyst*, **2006**, *133*, 388-407. (b) Li, Y.; Zhang, X.; Han, Z.H.; Fang, G. L.; Shen, G.; Yu, Q. *Anal. Chim. Acta*, **2006**, *562*, 210-215.

[77] Pariyar, A.; Bose, S.; Chhetri, S. S.; Biswasb, A. N.; Bandyopadhyay, P. *Dalton Trans.* **2012**, 41, 3826–3831.

[78] Mahammed, A.; Weaver, J. J.; Gray, H. B. ; Abdelas, M.; Gross, Z.*Tetrahedron Lett*. **2003**, 44, 2077–2079.

[79] Pariyar, A.; Bose, S.; Chhetri, S. S.; Biswasb, A. N.; Bandyopadhyay, P. *Dalton Trans.* **2012**, 41, 3826–3831.

[80] Li, Y.; Zhang, X.; Han, Y.; Akermark, B.; Sun, L.; Shen, G.; Yu, Q. *Analyst*, **2006**, *133*, 388-407.

[81] Li, Y.; Zhang, X.; Han, Z.H.; Fang, G. L.; Shen, G.; Yu, Q. *Anal. Chim. Acta*, **2006**, *562*, 210-215.

[82] Leininger, S.; Olenyuk, B.; Stang, P. J. *Chem Rev*. **2000**, 100, 853-907.

[83] Pedersen, C. J. *J. Am. Chem. Soc*., **1967**, 89, 7017-7036.

[84] Hulanicki, A.; Glab, S.; Ingman, F.; *Pure and Applied Chemistry*, **1991**, *63*, 1247-1250.

[85] Czarnik, A.W.; *Fluorescent Chemosensors for Ion and Molecule Recognition*, American Chemical Society, Washington DC, **1993**, vol. 538.

[86] (a) Silva, de A. P.; Gunaratne, H. Q. N.; Gunnlaugsson, T.; Huxley, A. J. M.; Mccoy, C. P.; Rademacher, J. T.;. Rice, T. E *Chem. Rev*. **1997**, *97*, 1515–1566. (b) Lodeiro, C.; Pina,F.; Parola AJ. Bencini A.; Bianchi A.; Bazzicalupi C.; Ciattini S.; Giorgi C.; Masotti A.; Valtancoli B.; Melo, J. S. *Inorg Chem*. **2001**, 40, 6813-6819.

[87] Prodi, L.; Bollta, F.; Montalti, M.; Zaccheroni, N. *Coord. Chem. Rev.* **2000**, 205, 59-83.

[88] Bell, T. W.; Hext, N. M. *Chem. Soc. Rev.* **2004**, 33, 589-598

[89] (a) Martínez-Máñez, R.; Sancenón, F. *Coord. Chem. Rev*. **2006**, 250, 3081.

[90] Valeur, Bernard; *Molecular Fluorescence: Principles and Applications*, Wiley-VCH Verlag GmbH, **2001.**

[91] Lodeiro, C.; Capelo, J.L.; Mejuto J.C.; Oliveira, E.; Santos, H.M. ; Pedras, B.; Nuñez, C. *Chem. Soc. Rev.* **2010**, *39*, 1-29.

[92] Lodeiro, C.; Pina, F. *Coord. Chem. Rev.* **2009**, 253, 1353-1383.

[93] Basabe-Desmonts, L.; Reinhoudt, D.N.; Grego-Calama, M. *Chem. Soc. Rev.* **2007**, *36*, 993-1017.

[94] (a) Akkaya, E. U.; Huston, M. E.; Czarnik, A. W. *J. Am. Chem. Soc.* **1990**, *112*, 3590–3593. (b) Lakowicz, J. R. *Mechanisms and dynamics of fluorescence quenching*, Chapter 9. In: *Principles of fluorescence spectroscopy*, 3rd ed. Springer, New York**, 2006**, 64.

[95] Sapsford, K. E.; Berti, L.; Medintz, I. L. *Angew. Chem., Int. Ed*. **2006**, 45, 4562-4588.

[96] Rurack, K. *Spectrochim. Acta. A*. **2001**, 57, 2161-2195.

[97] Rettig, W.; Lapouyade, R. Fluorescence probes based on twisted intramolecular charge transfer (TICT) states and other adiabatic photoreactions, in *Topics in Fluorescence Spectroscopy, Probe Design and Chemical Sensing*, ed. Lakowicz, J. R. Plenum Press, New York, **1994,** vol. 4, p. 109

[98] Kurishita, Y.; Kohira,T.; Ojida, A.; Hamachi, I.; *J. Am. Chem. Soc*. **2010**, 132,13290-13299.

[99] (a) Huang, Y-J.; Jiang, Y.-B. ; Bull, S. D.; Fossey, J. S. James, T. D. *Chem. Commun*. **2010**, 46, 8180. (b) Wu, J. S.; Zhou, J. H.; Wang, P. F.; Zhang, X. H.; Wu, S. K. *Org. Lett.* **2005**, 7, 2133

[100] (a) Montalti, M.; Rampazzo, E.; Zaccheroni, N.; Prodi, L. *New. J. Chem*, **2013**, 37, 28-34. (b) Baú, L.; Tecilla, P.; Mancin, F. *Nanoscale.* **2011**, 3, 121-133. (c) Jung, J.; Lee, J. H.; Shinkai, S. *Chem. Soc. Rev.* **2011***,* 40, 4464-4474.

[101] Montalti, M.; Prodi, L.; Zaccheroni, N. *J. Mater. Chem*. **2005**, 15,2810 – 2814.

[102] Bohn, E.; Fink, A.; Stöber,W. Journal Colloid and Interface Science, 1968, 26, 62-69.

[103] (a) Seo, S.; Lee, H. Y.; Park, M.; Lim, J. M.; Kang, D.; Yoon, J.; Jung, J. H. *Eur. J. Inorg. Chem.* **2010**, 843–847. (b) P. D. Beer, D. P. Cormode, J. J. Davis, *Chem. Commun.* **2004**, 414 – 415.

[104] Saha, K.; Agasti, S. S.; Kim, C.; Li, X.; Rottello, V. M. *Chem. Rev.* **2012**, 112, 2739-2779.

[105] Oliveira, E.; Nunez, C.; Gonzalez, B. R.; Capelo, J. L.; Lodeiro, C. *Inorg. Chem.* **2011**, 50, 8797–8807

[106] Mameli, M.; Aragoni, M.C.; Arca, M.; Caltagirone, C.; Demartin, F.; Farruggia, G.;Filippo, G. D.; Devillanova, F. A.; Garau, A., Isaia, F.; Lippolis, V.; Murgia, S.; Prodi, L.; Pintus, A., Zaccheroni, N. *Chemistry-A European Journal,* **2010**, *16*, 919-930.

[107] Pearson, R. G. *J. Am. Chem. Soc.* **1963**, 85, 3533-3539.

[108] Zhao, Y.; Zhang, X.-B.; Han, Z.-X.; Qiao, L.; Li, C.-Y.; Jian, L.-X.; Shen, G.-L.; Yu, R.-Q. *Anal. Chem.* **2009**, 81, 7022-7030.

[109] Oliveira E., Vicente M., Valencia L., Macías A., Bértolo E., Bastida R., Lodeiro C.*Inorg. Chim. Acta.* **2007**, *360*, 2734-2743.

[110] Costa, S.P.G.; Oliveira, E.; Lodeiro, C.; Raposo, M.M.M. *Tetrahedron Lett.*, **2008**, *32*,49, 5258-5261.

[111] Hanaoka, K.; Muramatsu, Y.; Urano, Y.; Terai, T.; Nagano, T. *Chemisty –A European Journal*, **2010**, *16*, 568-572

[112] McNeil, Ian. "*The Emergence of Nickel". An Encyclopaedia of the History of Technology*.Taylor & Francis. **1990**. pp. 96–100.

[113] Kasprzak; S. J, F. W.; Salnikow, K. *Mutat Res*. **2003**, *533* 1-2: 67–97 .

[114] Cotton, F. A.; Wilkinson, G.; Murillo, C. A.; *Advanced Inorganic Chemistry* (6th ed.).New York: Wiley, **1999**.

[115] Li, W.; Guo, Y.; McGill, K.; Zhang, P.; *New. J. Chem.*, **2010**, *34*, 1148-1156.

[116] (a) Jensen, W. B. *J. Chem. Edu.* **2003**, *80*, 8, 952. (b) Hussain, S. M.; Hess, K. L.; Gearhart, J. M.; Geiss, K. T.; Schlager, J. *J. Toxicol. In Vitro.* **2005**, *19*, 975-983.

[117] Landsdown, A. B. G. *Crit. Rev. Toxicol.* **2007**, *37*, 237-250.

[118] Gale, P. A. *Chem. Commun.,* **2011**, 47, 82–86.

[119] Beer, P. D.; Gale, P. A. *Angew. Chem., Int. Ed.*, **2001**, 40, 486–516.

[120] 3º Guidelines for Drinking-Water Quality,*World Health Organization,* Geneva, **1996**.

Chapter II

Exploiting the fluorescence behavior of a new corrole family as anions chemosensors: From solution to solids-supported devices

Published in *J. Mat. Chem*. **2012**, 22, 13811-13819

INDEX

2- Exploiting the fluorescence behavior of a new corrole family as anions chemosensors: From solution to solids-supported devices

Resumo

Neste trabalho sintetizou-se pela primeira vez o complexo de gálio(III) do 3-vinil-5,10,15-trispentafluorofenilcorrol **4** e avaliou-se a sua reatividade como dieno em reacções de Diels-Alder, na presença dos dienófilos 1,4-benzoquinona e 1,4-naftoquinona. Das reacções de Diels-Alder resultaram os aductos desidrogenados **5** e **6**. Os novos derivados corrólicos **4**-**6** foram completamente caracterizados por ^{1}H-RMN, ^{13}C-RMN, ^{19}F-RMN, análise elementar, espectrometria de massa (MALDI-TOF) e por espectroscopia de absorção e de emissão.

A habilidade sensorial dos compostos **4**-**6** e dos seus percursores **1**-**3** foi determinada em solução na presença dos aniões esféricos F^-, Cl^-, Br^-, I^-, do anião linear CN^- e dos aniões volumosos CH_3COO^- e $H_2PO_4^-$, tendo sido determinadas as correspondentes constantes de associação em tolueno. Este estudo sensorial foi ainda realizado em fase gasosa com os aniões F^- e CN^-. A adição de fluoreto aos compostos **1**, **3** e **5** originou no espectro de absorção um deslocamento das bandas para a região do vermelho e um aumento da intensidade da emissão de fluorescência tendo-se verificado que o composto **1** na presença de F^- foi o que originou a constante de associação mais elevada, sendo capaz de quantificar 0,69 ppm de F^-. O composto **2** juntamente com o derivado **1** apresenta uma elevada sensibilidade para o anião CN^-, tendo ocorrido no estado fundamental um deslocamento das bandas Q para a região do vermelho e no estado excitado para além do deslocamento para o vermelho, um aumento da intensidade da emissão de fluorescência, sendo possível quantificar CN^- a partir de 1,43 ppm. Para além disso os compostos **1** e **5** foram utilizados na preparação de dois polímeros de baixo custo baseados em poliacrilamida e polimetilmetacrilato, sendo o primeiro promissor, uma vez que os aniões F^- e CN^- conseguem atravessar o gel em soluções aquosas, permitindo a deteção de CN^- em água a partir de concentrações na ordem dos 70.0 ppb. Os compostos **2a** e **5** foram também testados na presença das aminas, 4,4´-bipiridina, cafeína e nicotina. O composto **2a** provou ser muito sensível para a 4,4´-bipiridina, enquanto que o composto **5** foi realmente efetivo na deteção da cafeína e da nicotina.

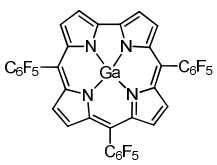
C6F5
N
Ga
N
N
C6F5
C6F5
C6F5

2a

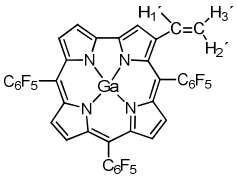
H1´
C=C
H3´
H2´
C6F5
N
Ga
N
N
C6F5
C6F5
C6F5

4

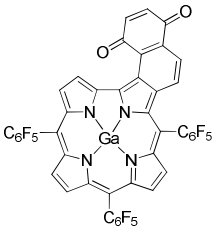
O
O
C6F5
N
Ga
N
N
C6F5
C6F5
C6F5

5

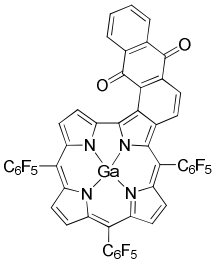
O
O
C6F5
N
Ga
N
N
C6F5
C6F5
C6F5

6

Abstract

In this chapter is described, for the first time, the synthesis of the gallium(III) complex of 3-vinyl-5,10,15-tris(pentafluorophenyl)corrole **4** through a Wittig reaction. It is also evaluated their reactivity in Diels-Alder reactions using 1,4-benzoquinone and 1, 4-naftoquinone as dienophiles. In these reactions, only the dehydrogenated adducts **5** and **6** were isolated. All the new corrole derivatives **4**-**6** were fully characterized by elemental analysis, ^{1}H-, ^{13}C- and ^{19}F-NMR, MALDI-TOF-MS, UV-Vis absorption and emission spectroscopy. The sensing ability of compounds **4**-**6** and of their precursors **1**-**3** was studied in solution towards the spherical halide ions F^-, Cl^-, Br^-, I^-, the linear anion CN^- and the bulky anions CH_3COO^-, $H_2PO_4^-$. This study was also realized in gas-phase with the anions F^- and CN^-. From the photophysical results, it was observed that compounds **1**, **3** and **5**, are strongly reactive to F^-, with these compounds a red-shift in the absorption spectra and an enhancement in the emission intensity were observed. The highest association constant was obtained for **1** with F^-, being able to quantified 0.69 ppm of anion. Compounds **1** and **2** also present a high sensitivity towards CN^- anions, producing a red-shift in the absorption and emission spectra and an increasing in the emission intensity, being able to quantify a minimal amount of 1.43 ppm. Moreover, compounds **1** and **5** were used to prepare two low-cost solid films, based on polymethylmethacrylate (PMMA) and polyacrylamide. The film obtained from PMMA is the most promising since it is able to detect *ca*. 70.0 ppb of CN^- in water. Compounds **2a** and **5** were also tested in the presence of 4,4´-bipyridine, caffeine and nicotine. Compound **2a** proved to be very sensitive to 4,4´-bipyridine while compound **5** was really effective for detecting caffeine and nicotine.

2.1 Introduction

In recent years, several studies have been carried out in order to explore different fluorescent materials for the development of chemical sensors. According to the literature, three basic units could constitute a classical chemosensor: i) a receptor (responsible for molecular recognition), ii) a fluorophore (responsible for signalling the recognition) and iii) a spacer (a chemical bridge that links the receptor and the fluorophore controlling their separation and geometric arrangement).[1] Through the controlling of these three moieties it is possible to design a specific fluorescent chemosensor for analytical sensing. However, a good fluorescent chemosensor must have a strong affinity and selectivity for the analyte, environmental interferences should not interfere in the fluorescence signal, and must be photostable.[2] The approach of the chemosensor to the analyte in solution can occurs in five different ways, such as, fluorescent ligands, as intrinsic fluorescence probes, as extrinsic probes (*Fluorophore–spacer–receptor* systems (FRS) and as *exciplex* or *excimer* forming probes (EPs)) and as chemodosimeters.[3-5]

The high number of substrates that can be recognized by tetrapyrrolic macrocycles like porphyrins and analogues make them particularly attractive to be considered as receptors.[6] From the porphyrinoid family, corroles are meriting in recent years a special attention since the discovery of facile methodologies to obtain synthetic triarylcorroles and the corresponding metal complexes. These contracted macrocycles bearing one direct pyrrole-pyrrole linkage exhibit unique spectral properties[7] with potentiality in several scientific areas namely for optical and sensing applications.[8] In general, corroles show strong fluorescence emission, high radiative rate constants, large Stoke´s shift and absorption (> 400 nm) and emission (> 600 nm) bands in the visible region of the electromagnetic spectrum and good photostability in most solvents.[9] All these aspects are quite positive, when the applications of these compounds are considered *in vivo* and in environmental targets, since these chromophores are visible excitable. Corroles also display unusually high N–H acidity, which makes them very interesting and useful for utilization as anion sensors.[10]

Anion recognition plays an important role in the supramolecular chemistry being their quantification really important in the chemistry industry, environmental science and biochemistry.[11] For instance, fluoride is an essential anion in human and it is used to prevent dental caries and osteoporosis.[12] However, its ingestion in high or in low levels may result in fluorosis, nephrotoxic changes and urolithiasis in humans.[13] Cyanide is also

considered one of the most acting and poison anion. Its toxicity is derived from their ability to bind to the iron in cytochrome c oxidase, interfering with electron transport chain, which results in hypoxia.[12] Herein we report the synthesis of three new corrole derivatives **4**-**6**. We show that the *β*-vinyl-corrole **4** can be efficiently prepared by the Wittig reaction of the *β*-formyl-corrole **3** with a phosphorus ylide. It is also demonstrated that the subsequent treatment of the *β*-vinyl- corrole with dienophiles afford the corresponding Diels–Alder adducts.

The sensing ability of the corrole macrocycles towards the sphericals halide ions F, Cl^-, Br^- and I^-, the linear anion CN^- and the bulky anions CH_3COO^- and $H_2PO_4^-$ was also studied. These studies were yet extended to corrole precursors **1**-**3**. Additionally, interaction studies with different amines such as caffeine, nicotine and 4,4´-bypiridine with compounds **2a** and **5** were also performed. In order to consider the application of these compounds as solid support sensors corroles **1** and **5** were incorporated on PMMA (polymethylmethacrylate) and in 10% of polyacrylamide. The sensing ability of these solid supports towards F^- and CN^- was also studied.

2.2 Results and Discussion

2.2.1 Synthesis and Structural Characterization of Corrolic Ligands

2.2.1.1 Synthesis of gallium(III)complex of 3-vinyl-5,10,15-tris(pentafluorophenyl)corrole

In chapter I it was shown that the chemistry of corroles remained in its infancy for many decades due to severe synthetic obstacles. However, with the discovery of facile methodologies for the synthesis of *meso*-triarylcorroles, from commercially available reagents, these aromatic macrocycles become more accessible. In recent years the synthesis and functionalization of corroles have received much attention within the scientific community.[14] This fact has been undoubtedly due to the promising applications of such compounds in several areas. Their use in medicine, in catalysis and in the production of sensors and electrodes are certainly of great significance. There is therefore a need for corrolic systems with new and well-defined substitution patterns.

In recent years Cavaleiro and co-workers[15] have demonstrated that the functionalization of the corrole and porphyrin cores via cycloaddtion reactions is an important approach to gain access to a wide variety of novel tetrapyrrolic macrocycles. The great success of such cycloaddition methodologies led us to study the possibility to

introduce a vinyl group in the corrole macrocycle and to evaluate the reactivity of the new 4π system as diene in the presence of different dienophiles. The method chosen for the introduction of the unsaturated substituent in the corrole core was the Wittig reaction.

General considerations about the Wittig reaction

The Wittig reaction is a reaction between a carbonyl compound (an aldehyde or a ketone) and a species known as phosphonium ylide, to give an olefin and phosphine oxide. An ylide (or ylid) is a species with positive and negative charges on adjacent atoms, and a phosphonium ylide carries its positive charge on phosphorus. Phosphonium ylides result from the deprotonation of phosphonium salts by a strong base. They can alternatively be represented as doubly bonded species, called phosphoranes (Scheme 1).[16]

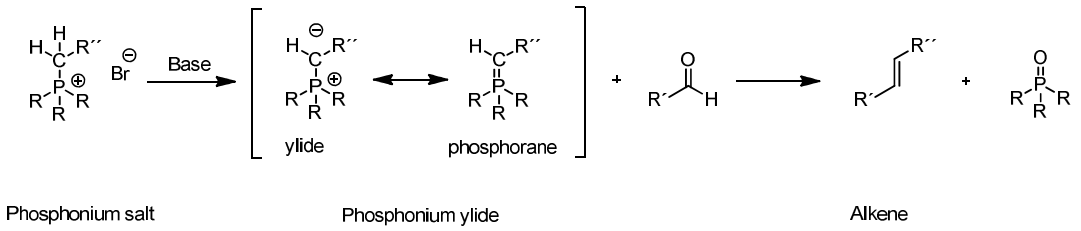

Scheme 1

The mechanism of the Wittig reaction is somewhat controversial and hasn´t been fully defined. However it´s known that after the treatment of the phosphonium salt with a strong base, there is an attack on the carbonyl group by the carbon of the phosphonium ylide affording a four-membered ring intermediate known as oxaphosphetane. This unstable intermediate after elimination of phosphine oxide gives the desired alkene (Scheme 2).[17]

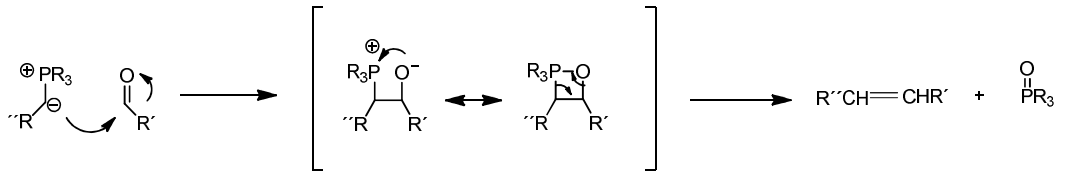

Scheme 2

The reactivity/stability of phosphonium ylides depends essentially on the substituents present in carbon, being the effect less relevant when the substituents are in phosphorus atom. Depending on the ylide structure, these can be classified as:

unstabilized ylides: these ylides are very reactive and they present on the carbon atom neutral substituents or electron-donating groups (*eg*: alkyl, alkoxy or dialkylamino);

stabilized ylides: these ylides are less reactive and the negative charge is stabilized not only by the phosphorus atom but by the adjacent functional group. These ylides hardly react with aldehydes and ketones, requiring higher reaction temperatures.

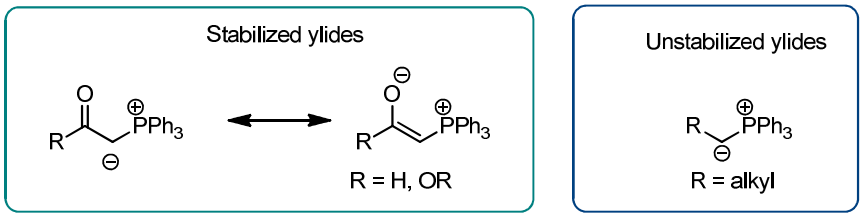

Figure 1-Structures of the stabilized and unstabilized ylides.

The Wittig reaction is stereoselective and this feature is dependent on the nature of the substituent on the carbon atom of the ylide. Usually stabilized ylides give *E*-alkenes on reaction with aldehydes and the unstabilized ylides give *Z*-alkenes. The alkene configuration depends on the decomposition step of the oxaphosphetane. In the case of unstabilized ylides the formation of oxasphosphetane is irreversible, yielding after decomposition, the (Z)-alkene (kinetic control). In the case of the stabilized ylides, the formation of oxaphosphetane is reversible and yielding an *anti* diastereoisomer and a *syn* diastereoisomer. However the *syn* diastereoisomer is instable and only the *E*-alkene is produced (Scheme 3).[17]

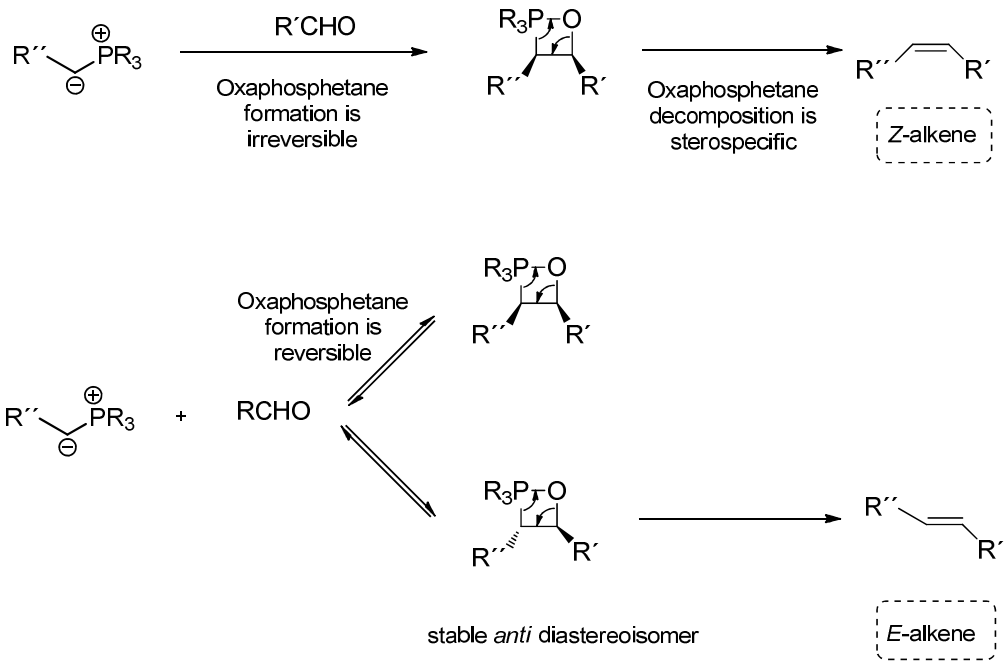

Scheme 3

Synthesis and characterization of gallium(III) complex of 3-vinyl-5,10,15-tris(pentafluorophenyl)corrole

The synthesis of the gallium(III) complex of 3-vinyl-5,10,15-tris(pentafluorophenyl)corrole involved the synthetic work compiled in schemes 4 and 5. The starting materials, 5,10,15-tris(pentafluorophenyl)corrole **1** and 5,10,15-tris(pentafluorophenyl)corrolatogallium(III)(pyridine) **2** were synthesized according to procedures described in literature: the free base by condensation of pyrrole with pentafluorobenzaldehyde using Gryko and Koszarna´s method[18] and the gallium(III) complex by refluxing corrole **1** in pyridine with $GaCl_3$ (Scheme 4).[19] Complex **2a** without pyridine as axial ligand was obtained quantitatively by treating a solution of complex **2** dissolved in CH_2Cl_2 with an aqueous solution of HCl (36%). After neutralization and the usual work-up the desired complex was isolated quantitatively.

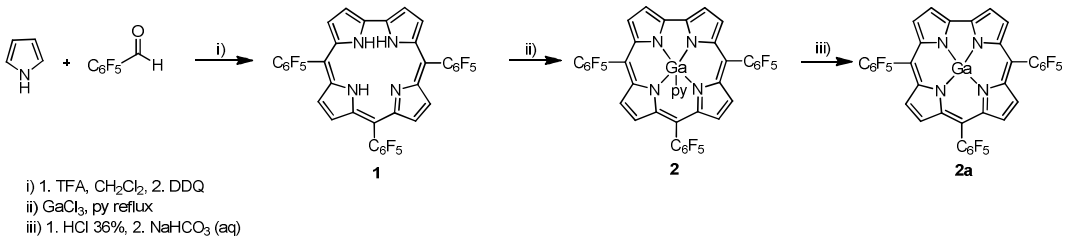

Scheme 4

Subsequently it was performed the Vilsmeier-Haack formylation of corrole **2a**. This reaction was carried out by adding to a solution of corrole **2** in dry dichloromethane and under nitrogen, the Vilsmeier-Haack reagent $POCl_3$/DMF (1:110 molar ratio); the final reaction mixture was maintained under stirring at room temperature, until the TLC control and the motorization by UV-Vis spectroscopy confirmed that all the starting corrole was consumed. Then, a $NaHCO_3$ saturated aqueous solution was added to hydrolyze the intermediate iminium salt. After the work up, the crude product was purified by preparative TLC, affording after recrystallization the desired 3-formyl corrole **3** in 70% yield.[20] This compound was used to prepare the vinyl-corrole **4** by a Wittig reaction (Scheme 5).

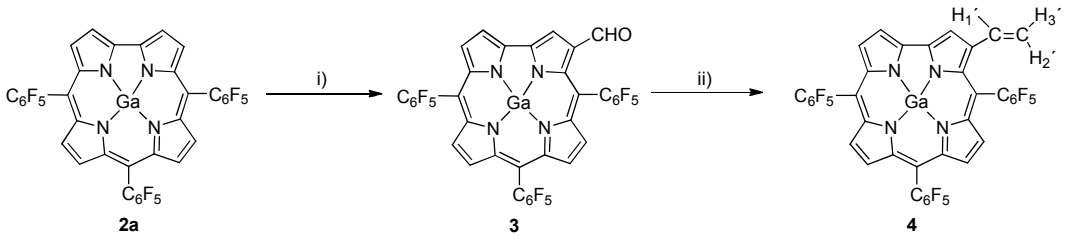

Scheme 5

The new corrole **4** was obtained in 74% yield, from the reaction of the gallium(III) complex **3** with the phosphonium ylide generated *in situ* from triphenylmethylphosphonium bromide and sodium hydride in tetrahydrofuran (THF). The coupling was performed at room temperature and under nitrogen and the reaction was stopped when the TLC control confirmed the total consumption of the starting corrole (approximately 4 h). The structure of the novel corrole **4** was unambiguously determined by spectroscopic data, namely by NMR techniques (^{1}H, ^{19}F,^{13}C, COSY, HSQC), UV-Vis and elemental analysis. In particular, from the analysis of ^{1}H NMR spectrum (Figure 2)

and 2D COSY experiment, it was possible to assign unequivocally all of the resonances of the protons. In the aromatic region it was identified a doublet at δ 9.29 ppm due to the resonance of the β-pyrrolic proton H-18 two multiplets at δ 8.84-8.82 and 8.81-8.78 ppm and a doublet at δ 8.62 ppm corresponding to the resonances of the remaining six β-pyrrolic protons. It was also possible to assign three doublet doublets at δ 6.65 (H_2´), δ 5.91 (H_3´) and δ 8.43 (H_1´) ppm due to the resonances of the vinylic protons (Figure 2).

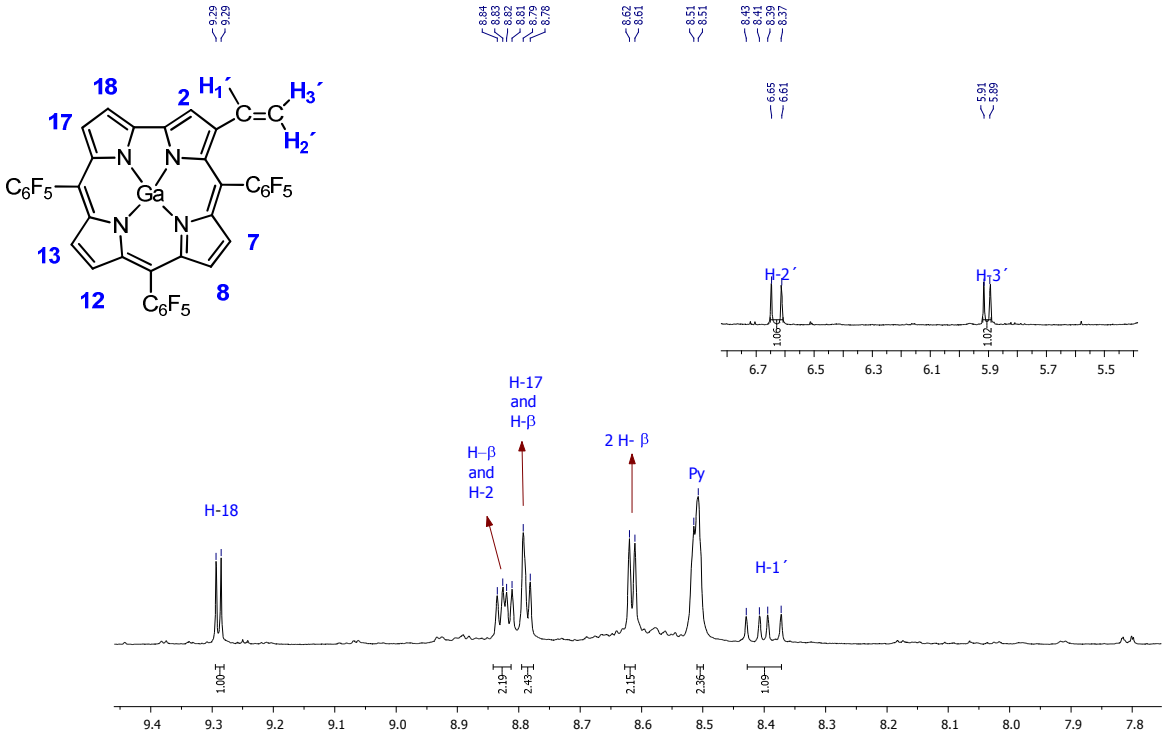

Figure 2- Partial ^{1}H NMR spectrum of vinyl-corrole **4** in $CDCl_3$ with a few drops of pyridine-d_5.

*Note: The pyridine signals observed in the spectrum are from pyridine d_5.

The ^{13}C NMR spectrum showed two distinctive signals at δ 130.5 and 116.9 ppm corresponding to the resonances of the vinyl group carbons (Figure 3). The interpretation and the assignments of this spectrum were facilitated by the aid of the HSQC spectrum.

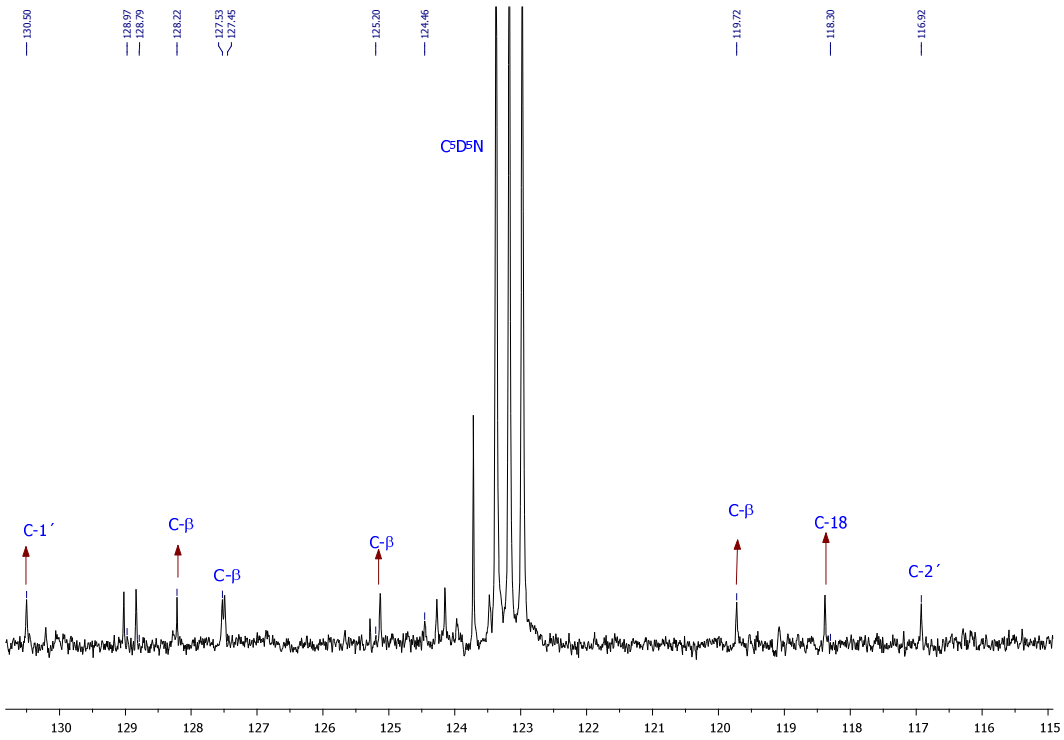

Figure 3- Partial ^{13}C NMR spectrum of vinyl-corrole 4 in $CDCl_3$ with a few drops of pyridine-d_5.

The MALDI mass spectra also showed the expected molecular ion at *m/z* 890 $[M+H]^+$. All the spectroscopic data found are compatible with the structure of corrole **4**, whose reactivity was evaluated in Diels-Alder reactions.

2.2.1.2. Reactivity of gallium(III)complex of 3- vinyl-5,10,15-tris(pentafluorophenyl)corrole 4 as diene in Diels-Alder reactions

General considerations about Diels-Alder reactions

The Diels-Alder reaction, also known as a [4+2] cycloaddition reaction is a transformation that involves a conjugated diene (the 4π system) and a dienophile (the 2π system; that can be a alkene or alkyne) affording a new six-membered ring (Scheme 6).[21]

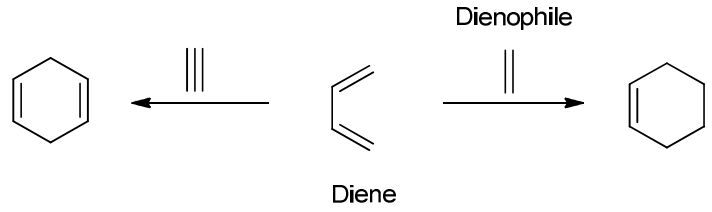

Scheme 6

This type of reaction is included in the group of pericyclic reactions and in general involves a transition state in which the six π electrons are delocalized by the six carbon atoms (Scheme 7). When one or more heteroatoms are present in the diene or in the dienophile the cycloaddition can be called hetero-Diels-Alder reaction.[22]

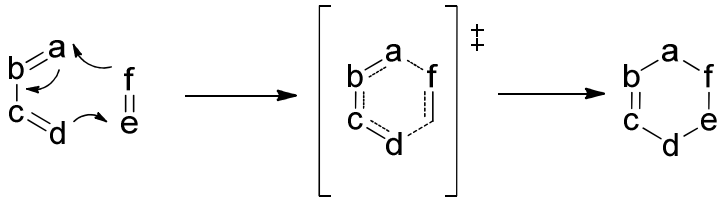

Scheme 7

The diene component in the Diels-Alder reaction can be an open-chain or a cyclic system but it is fundamental that this component is able to adopt a *s-cis* conformation. In fact, cyclic dienes that have a permanent *s-trans*-conformation do not react in Diels-Alder reactions (Figure 4).[22]

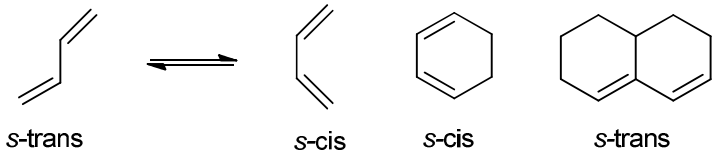

Figure 4-- *s-cis* and *s-trans* conformations of dienes

The dienophile can be also an open-chain or cyclic derivatives bearing different substituents. Actually, the electronic effect of the substituents either in the diene or in the dienophile can strongly influence the kinetic of the reaction. In the so called normal electron demand Diels-Alder, the reaction is accelerated when the reaction occurs between dienes with electron donating groups and dienophiles with electron withdrawing groups. In the reverse electron demand Diels-Alder reaction the opposite situation is required: dienes with electron withdrawing groups react faster with dienophiles with electron-donating

groups. Another important aspect of this type of reactions is the stereochemistry of the reactants that it is maintained in the final product (Scheme 8).[23]

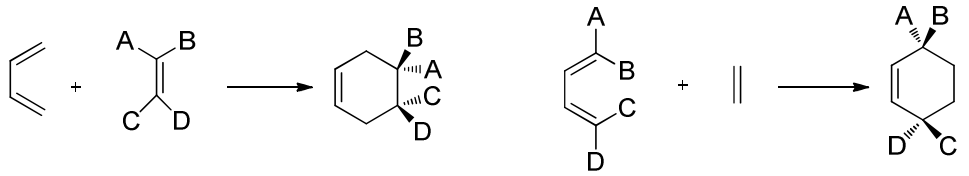

Scheme 8

Synthesis and characterization of new adducts obtained from Diels–Alder reactions of corrole 4 with quinones

The reactivity of the *β*-vinylcorrole **4** as a diene in Diels-Alder reactions was studied in the presence of 1,4-benzoquinone and 1,4-naphthoquinone as dienophiles. The reactions were carried out by heating corrole **4** with an excess of the dienophile (2 equiv.) in refluxing toluene, and were finished when the control by TLC showed the total consumption of corrole **4**. In both cases, the main products were identified after the usual work up and purification, as the dehydrogenated adducts **5** (76%) and **6** (64%) (Scheme 9).

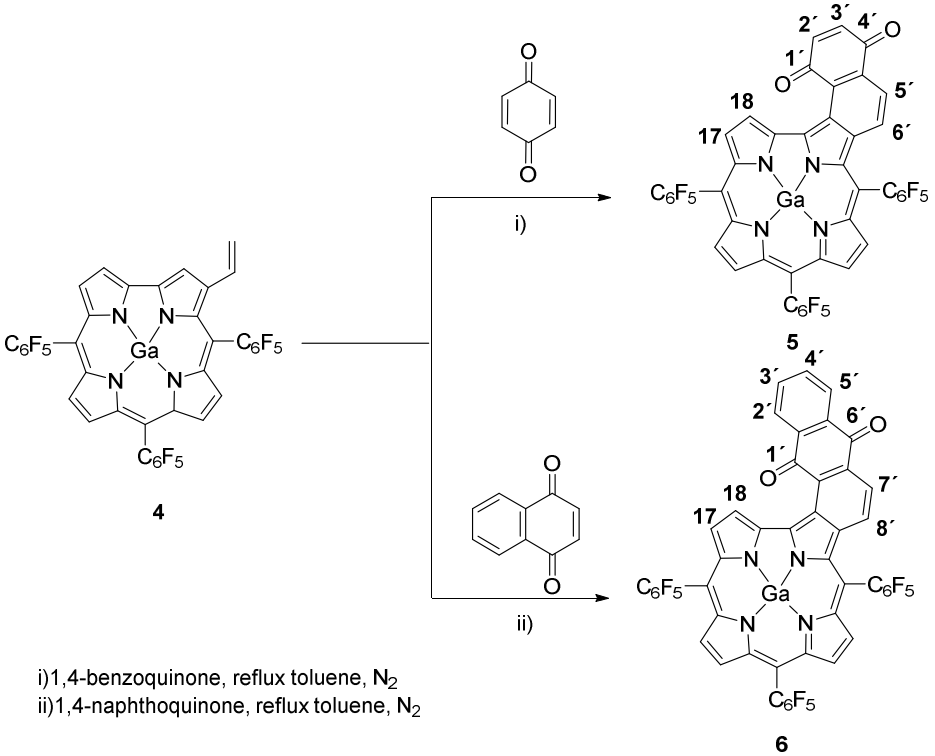

Scheme 9

The structures of the new compounds were established by spectroscopic data, namely NMR, UV-Vis, MS and elemental analysis. The MALDI spectra showed the expected molecular ions at *m/z* 992 $[M]^{+\cdot}$ for **5** and at 1042 $[M]^{+\cdot}$ for **6**. The presence of the naphthoquinone and anthraquinone fused residues on the corrole macrocycle were also confirmed by the ^{13}C NMR spectra, which showed the carbonyl resonances at δ 185.8 and 185.4 for compound **5** and at δ 183.7 and 183.1 for compound **6**. From the ^{1}H NMR spectrum of compound **5** it was possible to assign the doublet at δ 9.84 as the resonance of proton H-5', and the doublet at δ 9.53 as the resonance of the β-pyrrolic proton H-18. It was also possible to identify three doublets at δ 8.90, 8.65 and 8.62 ppm and a multiplet at δ 8.81-8.77 which are due to the resonance of the remaining five β-pyrrolic protons. From the 2D HSQC spectrum it was possible to conclude that the resonance of H-6´ is overlapped with the resonances of two β pyrrolic protons in the multiplet at δ 8.81-8.77 ppm. The doublets at δ 7.09 and 6.86 ppm were due to the resonances of H-2´ and H-3´ of the quinone residue (Figure 5).

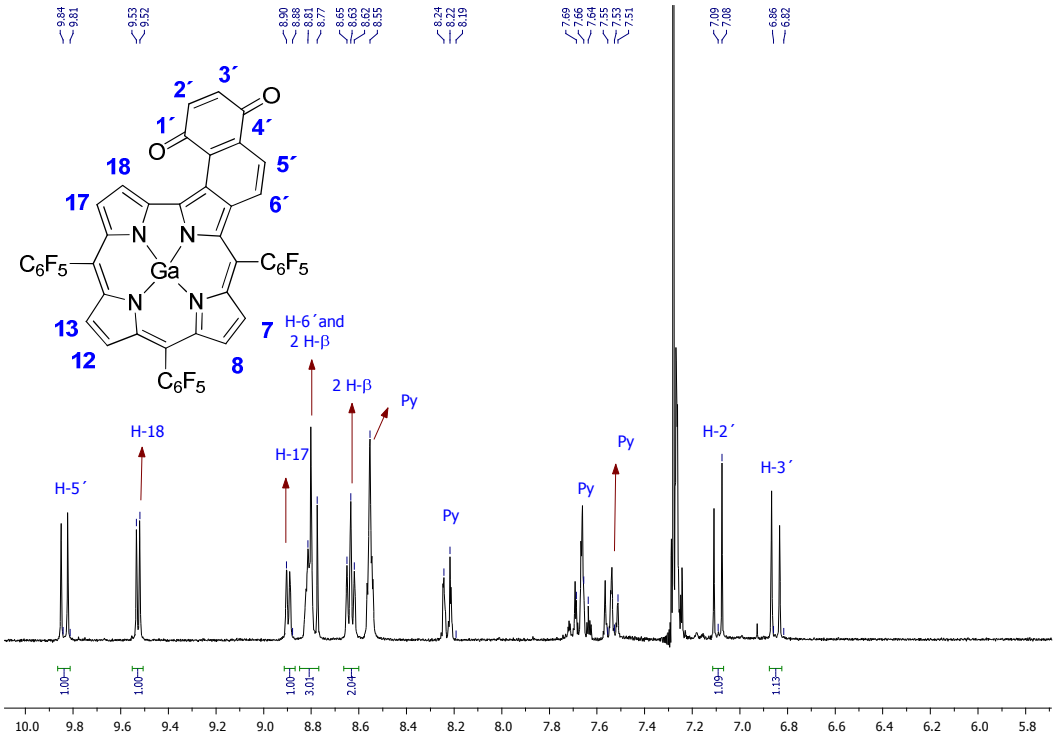

Figure 5- Partial ^{1}H NMR spectrum of compound **5** in $CDCl_3$ with a few drops of pyridine-d_5.

The proton resonances due to the extra anthraquinone residue in compound **6** were identified, through 2D studies, as two doublets at δ 8.72 (H-5´) and 8.66 (H-2´) ppm and as two multiplets at 7.89-7.87 (H-3´) and at 7.86-7.84 (H-4´) ppm The multiplet at δ 8.84-8.80 ppm is related to resonance of protons H-7´and H-8´. The high chemical shift of H-18 (9.66 ppm) is due to the deshielding anisotropic effect of the anthraquinone residue.

2.2.2. The sensing ability of corroles 1-6 in solution

2.2.2.1. Photophysical characterization

The photophysical characterization of compounds **1** to **6** was performed at 298 K in toluene and for compounds **1** and **2** also in dichloromethane. In Table 1 are gathered the main photophysical data obtained and the results show that only small differences were detected for compounds **1** and **2** in the two solvents.

Table 1: Selected photophysical data of compounds **1** to **6** in toluene. Solvents: a – toluene b – dichloromethane.

Compounds.	λ_{max}(nm) : log ε	λ_{em} (nm)	Stoke's shift (nm)	ϕ
1	565: 4.37[a]	645	80	0.05
	561: 4.36[b]	642	81	0.03
2	570: 3.82[a]	601	31	0.06
	569: 3.97[b]	600	31	0.03
2a	570:4.32[a]	600	30	0.03
3	599: 4.29[a]	626	28	0.02
4	599: 3.29[a]	612	13	0.02
5	590: 4.22[a]	629	39	0.02
6	597: 3.98[a]	624	27	-

The absorption spectra of corroles show a Soret-type band between 400 and 420 nm and Q-type bands around 500–650 nm. Figure 6 shows the absorption spectrum of 5,10,15-trispentafluorophenylcorrole (Figure 6) .

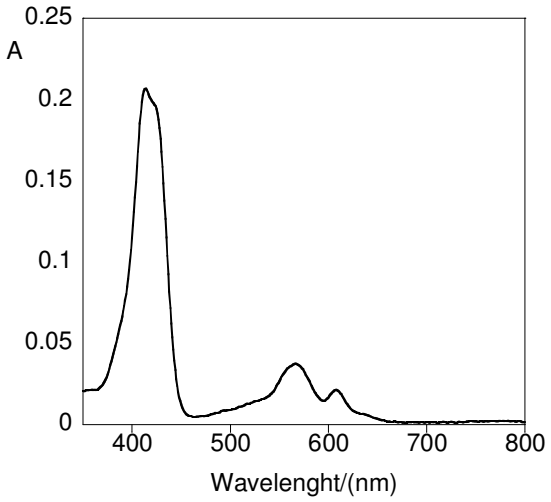

Figure 6- Absorption spectrum of 5,10,15-trispentafluorophenylcorrole **1** in toluene ([1]= $1*10^{-6}$ M.) .

From Table 1 it can be observed that for compounds **1** to **6** the Q absorption and emission bands of highest energy are centered at maximum wavelenghts between 565 and 599 nm, and 600-645 nm respectively. The emission spectra were collected on the Q-bands, in order to avoid the re-absorption phenomena.

As an example, figure 7 shows the absorption (only Q band region), emission and excitation spectra in toluene of compound **1**.

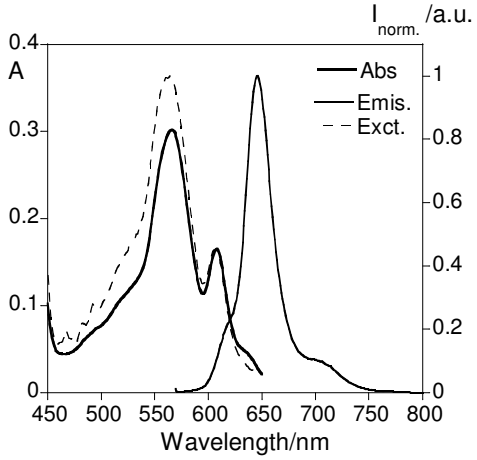

Figure 7- Room temperature absorption (bold line), normalized emission (full line, λ_{exc} = 565 nm) and excitation spectra (dotted line, λ_{em} = 645 nm) of compound **1** in toluene.

The perfect match between the absorption and excitation spectra, rules out in all cases the presence of any emissive impurity. The fluorescence quantum yields of **1-5** are in general in the same order, varying between ϕ = 0.02 – 0.07, with an exception of

compound **6** which was not emissive. As it was already mentioned, compounds **1** and **2** were also characterized in dichloromethane, and no significant changes were observed in the maximum of absorption and emission bands. However, in dichloromethane, both compounds showed lower fluorescent quantum yields than in toluene (Table 1). It is also possible to verify that in the same solvent, the presence of the metal ion Ga^{3+} coordinated with pyridine does not produce variations in the fluorescent quantum yield (**1** – ϕ = 0.05; **2** – 0.06). Otherwise, the insertion of a substituted on the position 3 of the corrole unit leads to a decrease of the luminescent quantum yield from 0.06 in compound **2** to 0.02 in compounds **3**-**5**, being compound **6** not emissive. It is known that quinone moiety is a well established fluorescent quencher.[24] In this way quinone moiety fused to corrole macrocycle can be responsible by the decrease of fluorescence quantum yield.

After the photophysical characterization of corrole macrocycles **1**-**6** their sensorial ability in the presence of different anions was evaluated and will be discussed in the following sections.

2.2.2.2. Spectrophotometric and spectrofluorimetric titrations and anion sensing effects

The sensorial ability of compounds **1**-**5** towards the spherical (F^-, Cl, Br^-, I^-), linear (CN^-) and bulky anions (CH_3COO^-, $H_2PO_4^-$) was carried out by ligand titrations with the addition of small amounts of the adequate anion tetrabutylammonium salt. The titrations were followed by UV-vis and fluorescence measurements in toluene. The most significant data are gathered in Table 2.

Table 2: Association constants of compounds **1**-**3** and **5** in toluene

Compounds	Anions (A)	Association constants A:L
1	F^-	9.43 ± 0.03 (2:1)
	CN^-	10.57 ± 0.01 (2:1)
	CH_3COO^-	9.87 ± 0.02 (2:1)
	$H_2PO_4^-$	9.88 ± 0.01 (2:1)
2	F^-	-
	CN^-	10.52 ± 0.02 (1:2)
	CH_3COO^-	8.52 ± 0.02 (1:2)
	$H_2PO_4^-$	9.40 ± 0.02 (1:2)
2a	4,4- bipyridine	26.27± 0.03 (3:2)
	caffeine	-
3	F^-	5.28 ± 0.01 (1:1)
	CN^-	6.39 ± 0.01 (1:1)
	CH_3COO^-	6.11 ± 0.01 (1:1)
	$H_2PO_4^-$	6.02 ± 0.01 (1:1)
5	F^-	6.81 ± 0.01 (1:2)
	CN^-	6.89 ± 0.01 (1:2)
	CH_3COO^-	-
	$H_2PO_4^-$	-
	caffeine	7.93 ± 0.01 (2:1)
	nicotine	10.01 ± 0.02 (2:1)

2.2.2.2.1. Spherical halide ions F^-, Cl^-, Br^-, I^-.

The most significant changes in the ground and excited states for compounds **1**, **3** and **5** were observed in the presence of fluoride (F^-) anion. No changes were detected with compound **2** and **4** in the presence of this anion and also when all compounds (**1**-**5**) were titrated with Cl^-, Br^- and I^-.

As already mentioned, free-base corroles display unusually high N-H acidity and due to this fact, they can be highly sensitive to basic anions. The ionic size and electronegativity of F^- when compared with other halides can explain the strongest interaction, via hydrogen bonds with the inner N-H of the corrole core, observed between this anion and compound **1**.[10] Considering the best performance of complexes **3** and **5** when compared with **2** and **4**, these results can be justified by the presence of electron withdrawing groups that can increase the Lewis acidic character of gallium and consequently make these compounds highly sensitive to fluoride anions. Figure 8 shows the spectral changes in the ground and excited state obtained for compound **1**. The addition of F^- to **1** promotes in the absorption spectrum (fig.8A), a decrease in the band at 570 nm and an increase in the one at 606 nm, accompanied by a red shift from 606 nm to 619 nm ($\Delta\lambda$ = 13 nm). An isosbestic point at 586 nm is also observed.

Considering the emission spectrum of **1** (fig. 8B), the titration with F^- is responsible for an enhancement of intensity of *ca*. 91% at 628 nm.

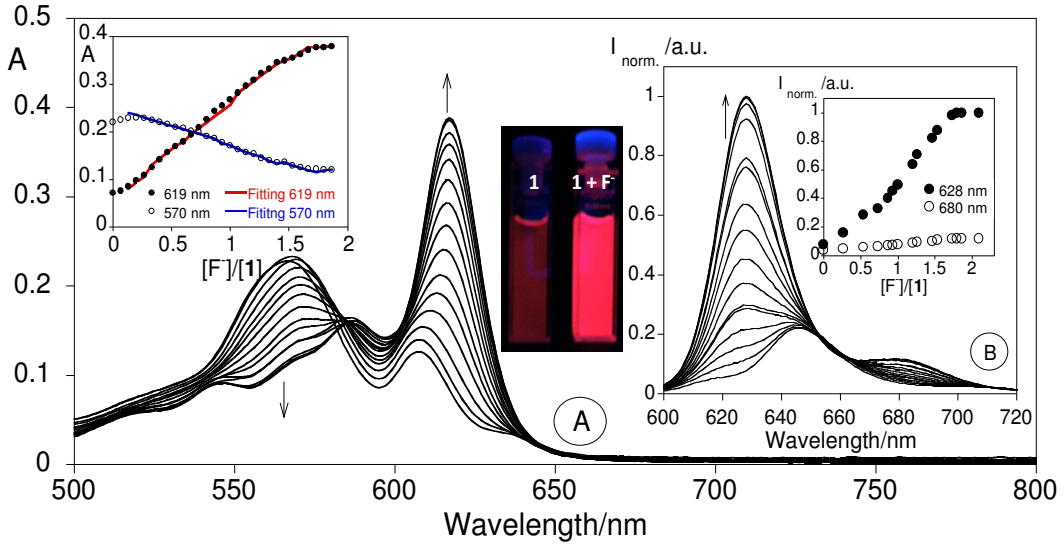

Figure 8- Spectrophotometric (A) and spectrofluorimetric (B) titration of compound **1** with the addition of F^- in toluene. The inset represents the absorption (A) and the emission intensity (B) as a function of $[F^-]/[1]$ at 570 nm, 619 nm for (A) and 628 nm, 680 nm for (B). ($[1] = 1 \times 10^{-5}$M, λ_{exc}= 565 nm, T=298 K).

Taking into account compound **3**, the addition of F^- produces a decrease in the absorption bands at 599 nm and 618 nm and an increase in the band centred at 638 nm. In the emission a quenching of *ca.* 50% at 626 nm and an enhancement of *ca.* 20% at 642 nm were detected (Figure 9). A similar spectral behaviour was obtained for compound **5** (Figure 10).

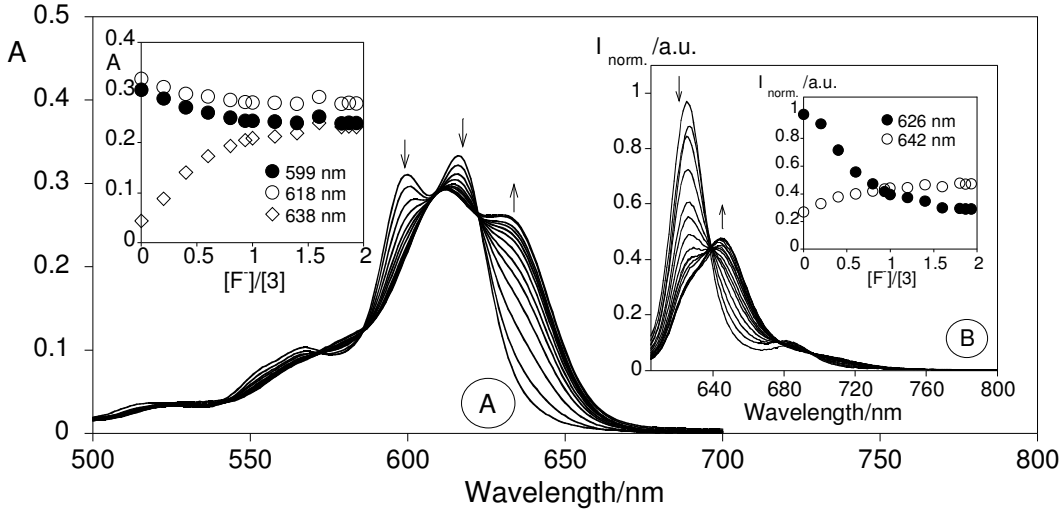

Figure 9- Spectrophotometric (A) and spectrofluorimetric (B) titration of compound 3 with the addition of F^- in toluene. The inset represents the absorption (A) and the emission intensity (B) as a function of $[F^-]/[3]$ at 599 nm, 618 nm, and 638 nm for (A) and 626 nm and 642 nm for (B). ([3] = 1 $\times 10^{-5}$M, λ_{exc}= 599 nm, T=298

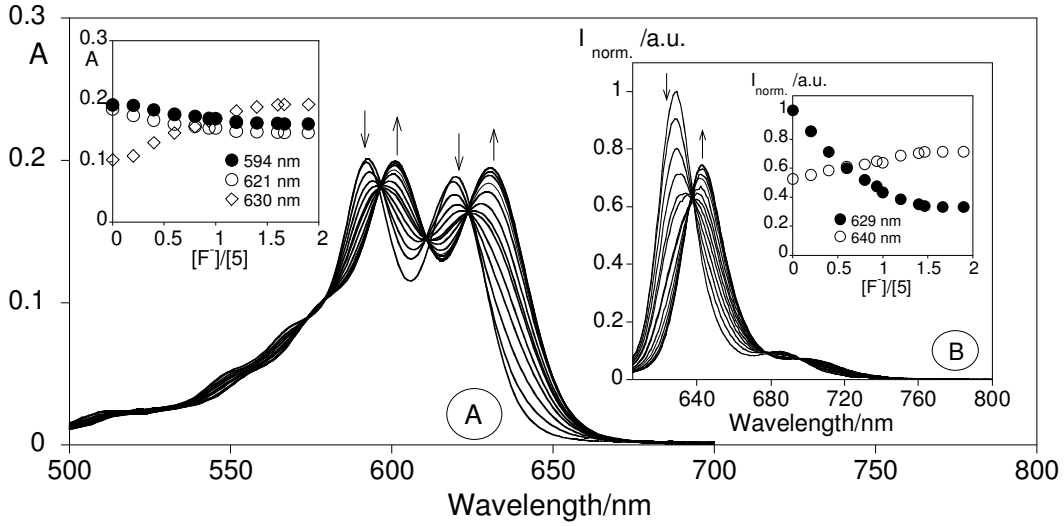

Figure 10- Spectrophotometric (A) and spectrofluorimetric (B) titration of compound **5** with the addition of F^- in toluene. The inset represents the absorption (A) and the emission intensity (B) as a function of $[F^-]/[\mathbf{5}]$ at 594 nm, 621, and 630 nm for (A) and 629 nm, 640 nm for (B). ([**5**] = 1 $\times 10^{-5}$M, λ_{exc}= 590nm, T=298 K).

The association constants for F^- interaction were determined using the HypSpec program[25] (Table 2) and compound **1** shows the highest constant (log K_{ass} = 9.43 ± 0.03) with a stoichiometry of two anions per ligand. In this case, the anion interaction probably occurs inside the corrole skeleton through the NH groups (Scheme 10). For compound **3** a value of log K_{ass} = 5.28 ± 0.01 was obtained, corresponding to one anion per ligand, while a different stoichiometry was obtained for compound **5**. In this case a value of log K_{ass} = 6.81 ± 0.01 for an adduct formation of one anion per two ligands was obtained (scheme 10). For complexes **3** and **5** the interaction with the anion will probably take place through coordination with the metal.

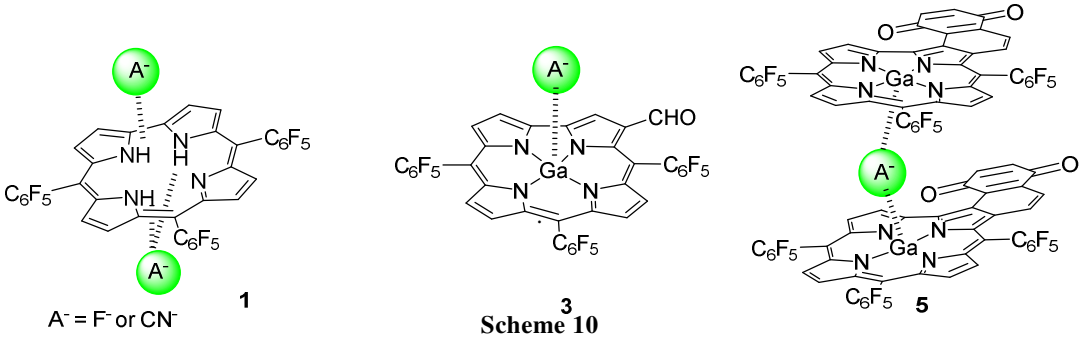

Scheme 10

According to the results described above, compound **1** was shown to be the best sensor for F^- with a highest association constant. On the other hand, the coordination of corrole with gallium(III) leads to a decrease in the affinity of the ligand for fluoride anions and consequently lower association constants were observed.

The detection (LOD) and quantification (LOQ) limits for the analyte (F^-) were also determined in the presence of compound **1**. In the absorption band centred at 619 nm the LOD was 0.078 ± 0.006 and the LOQ was 0.092 ± 0.02. Thus, the minimal amount of fluoride detectable by compound **1** was 0.35 ppm and the minimal amount quantified was 0.69 ppm.

2.2.2.2.2 Linear anion CN^-

It is well known that cyanide is one of the most powerful poisonous and toxic anions. It is a lethal anion for humans, as well as for aquatic life. Its quantification is really important and due to its high toxicity, the highest allowable level of cyanide according to the World Health Organization in drinking water is around 1.9 µM.[26, 27]

All compounds were shown to be sensitive towards cyanide anion, with exception of

the compound **6**. Notice that, the antraquinone moiety in compound **6** is responsible for a different fate of the electronic excited molecule. In this case, it is probably that the dominant de-excitation phatway is via intersystem crossing (see. fig.15, pg.30, chapter I).[28]

In the presence of CN^-, compound **1** presents a similar behaviour to that obatined with F^-. The addition of CN^- to **1** promotes in the absorption spectrum a decrease in the band at 570 nm and an increase in the one at 609 nm followed by a red-shift ($\Delta\lambda$=10 nm). An enhancement in the emission of 93% at 628 nm is also detected (Figure 11).

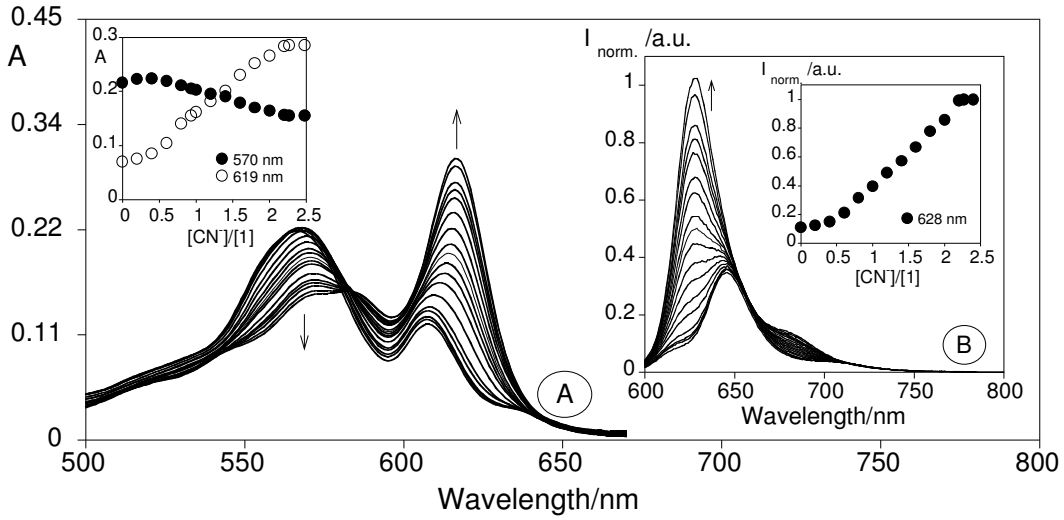

Figure 11- Spectrophotometric (A) and spectrofluorimetric (B) titration of compound **1** with the addition of CN^- in toluene. The inset represents the absorption (A) and the emission intensity (B) as a function of [CN^-]/[**1**] at 570 nm and 619 nm for (A) and 628 nm for (B). ([**1**] = 1×10^{-5}M, λ_{exc}= 565nm, T=298 K).

However, the determination of the association constant shows a higher value in the presence of CN^- (log K_{ass}= 10.57 ± 0.01) than that obtained with F^- (log K_{ass} = 9.43 ± 0.03) for the same stoichiometry of two anions per ligand (scheme 10). In this case the minimal amount of cyanide anion detectable by compound **1** at 619 nm was 0.54 ppm and the minimal amount quantified was 1.43 ppm.

Figure 12 presents the spectrophotometric and spectrofluorimetric titration of compound **2** in toluene in the presence of CN^-.

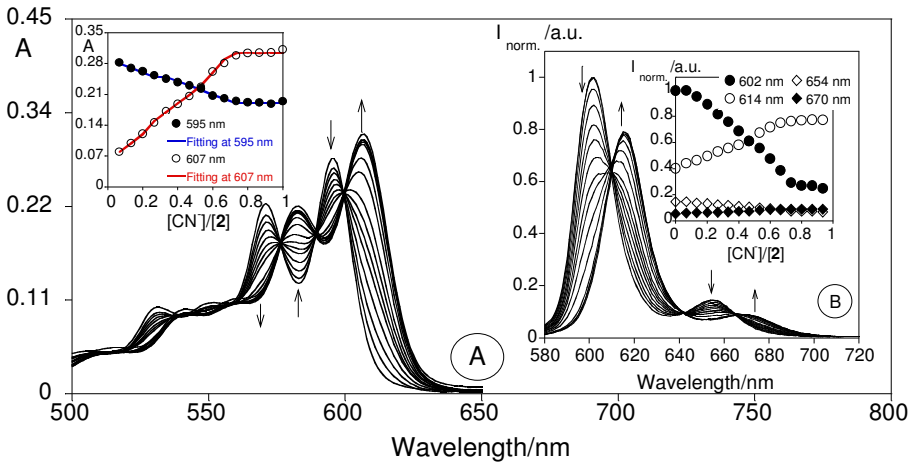

Figure 12- Spectrophotometric (A) and spectrofluorimetric (B) titration of compound **2** with the addition of CN^- in toluene. The inset represents the absorption (A) and the emission intensity (B) as a function of [CN^-]/[**2**] at 570 nm, 619 nm for (A) and 628 nm, 680 nm for (B). ([**2**] = 1 $\times 10^{-5}$M, λ_{exc}= 570 nm, T=298 K).

The titration of compound **2** with CN^-, induces strong changes in the ground state (fig. 12 A). A decrease in the intensity of the initial bands centred at 570 nm and 595 nm is observed with a concomitant appearance of new bands centred at 582 nm and 607 nm. Two isosbestic points are detected at 577 nm and 600 nm. Taking into account the emission spectra (excited state), a quenching at 602 nm (ca. 40%) and at 654 nm (12%) is observed, accompanied by a red shift ($\Delta\lambda$ = 15-20 nm) and an enhancement of the emission intensity at 614 nm and 670 nm (fig. 12 B). A similar behaviour was detected for compounds **3** and **5** and the main results are presented in figure 13 and figure 15.

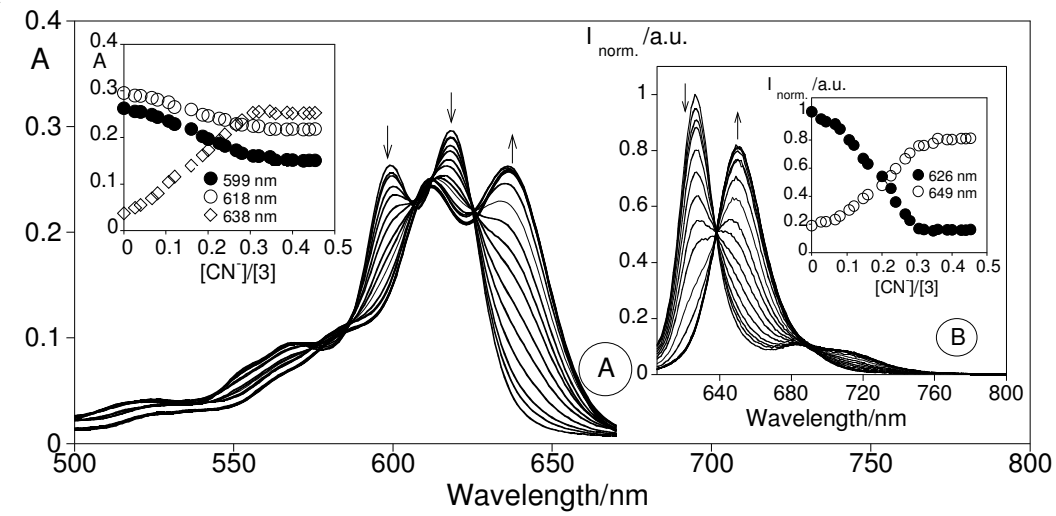

Figure 13- Spectrophotometric (A) and spectrofluorimetric (B) titration of compound **3** with the addition of CN^- in toluene. The inset represents the absorption (A) and the emission intensity (B) as a function of [CN^-]/[**3**] at 599 nm, 618 nm and 638 nm for (A) and 626 nm, 649 nm for (B). ([**3**] = 1 ×10^{-5}M, λ_{exc}= 599nm, T=298 K).

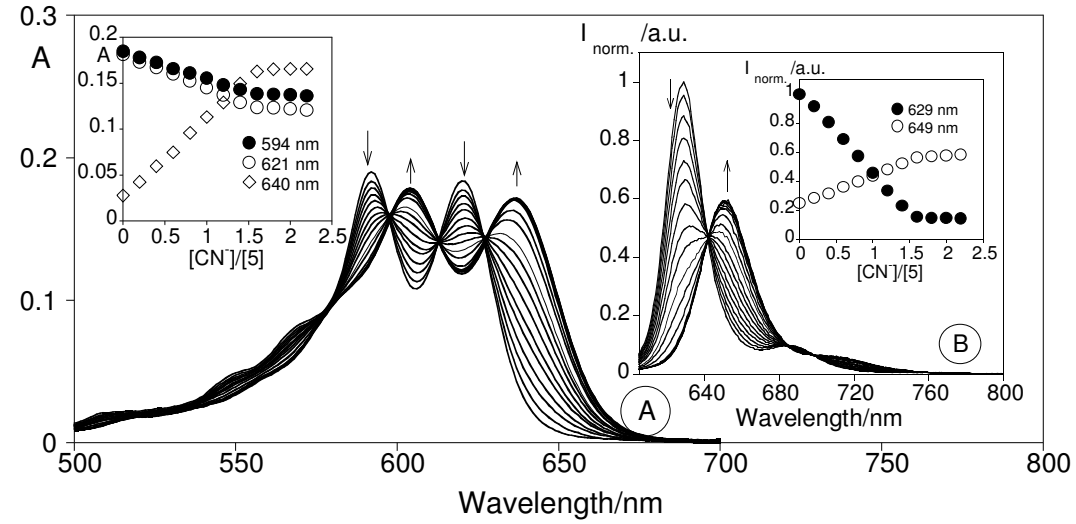

Figure 14- Spectrophotometric (A) and spectrofluorimetric (B) titration of compound **5** with the addition of CN^- in toluene. The inset represents the absorption (A) and the emission intensity (B) as a function of [CN^-]/[**5**] at 594 nm, 621 nm and 640 nm for (A) and 629 nm, 649 nm for (B). ([**5**] = 1 ×10^{-5}M, λ_{exc}= 590 nm, T=298 K).

The association constant for compound **2** (log K_{ass} = 10.52 ± 0.02) is similar to that obtained for compound **1** but with a different stoichiometry one anion per two

ligands. A decrease of the association constant value for CN^- occurs, in the presence of substituted corroles at position 3. The value log K_{ass} = 6.39 ± 0.01 was found for compound **3**, for the interaction of one ligand per anion and of log K_{ass} = 6.89 ± 0.01 for **5** for one anion per two ligands (scheme 10).

Taking into account compounds **2** and **5**, which present the same stoichiometry towards the same anion, the presence of the quinone unit in **5** is probably responsible for its lower ability to recognize cyanide, due to some electronic repulsion from oxygen atoms.

2.2.2.2.3. Bulky anions CH_3COO^- and $H_2PO_4^-$.

The anions acetate and phosphate, which are widely used in food additives and in agricultural fertilizers [29] interact with compounds **1**, **2**, and **3**. No changes in the ground and excited state were observed for compounds **4**, **5** and **6**. The addition of CH_3COO^- to **1** results a decrease in the band at 570 nm in the absorption spectra and an increase in the band at 609 nm, followed by a red-shift from 609 to 620 nm (Δλ= 15 nm). In the emission an enchament of *ca.* 89% at 628 nm was observed, with the formation of a new band at 684nm (Figure 15).

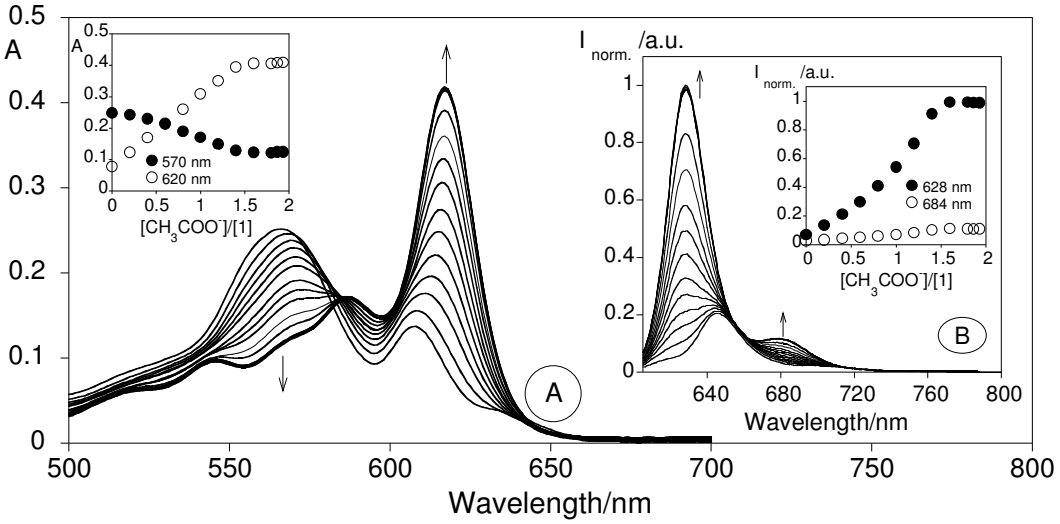

Figure 15- Spectrophotometric (A) and spectrofluorimetric (B) titration of compound **1** with the addition of CH_3COO^- in toluene. The inset represents the absorption (A) and the emission intensity (B) as a function of $[CH_3COO^-]/[\mathbf{1}]$ at 570 nm, and 620 nm for (A) and 628 nm, 684 nm for (B). ([**1**] = 1 $\times 10^{-5}$M, λ_{exc}= 565nm, T=298 K).

A similar spectral behaviour was detected during the titration of compound **1** with the phosphate anion (Figure16).

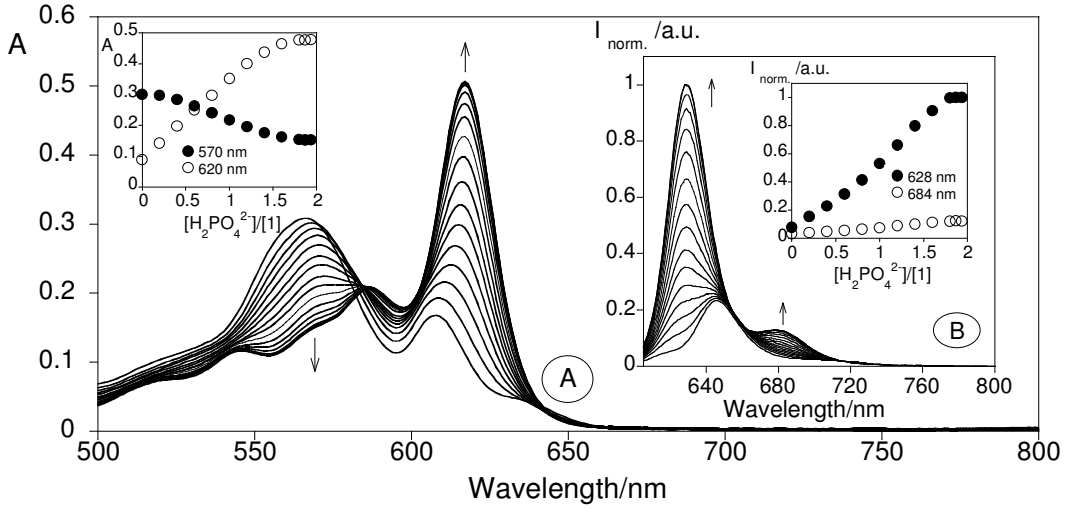

Figure 16- Spectrophotometric (A) and spectrofluorimetric (B) titration of compound 1 with the addition of $H_2PO_4^-$ in toluene. The inset represents the absorption (A) and the emission intensity (B) as a function of $[H_2PO_4^-]/[1]$ at 570 nm and 620 nm for (A) and 628 nm and 684 nm for (B). ($[1] = 1 \times 10^{-5}$ M, $\lambda_{exc} = 565$nm, T = 298 K).

The interaction of coumpound **2** with phosphate produces a decrease in the intensity of bands centred at 570 and 595 nm. Two new bands appear at 582 and 607 nm. In the excited state a quenching at 601nm of *ca.* 32% and at 650nm (8%) occurred (Figure 17). During the tritations of coumpounds **2** and **3** with the acetate anion a similar behaviour was observed (See figure 18 and figure 19).

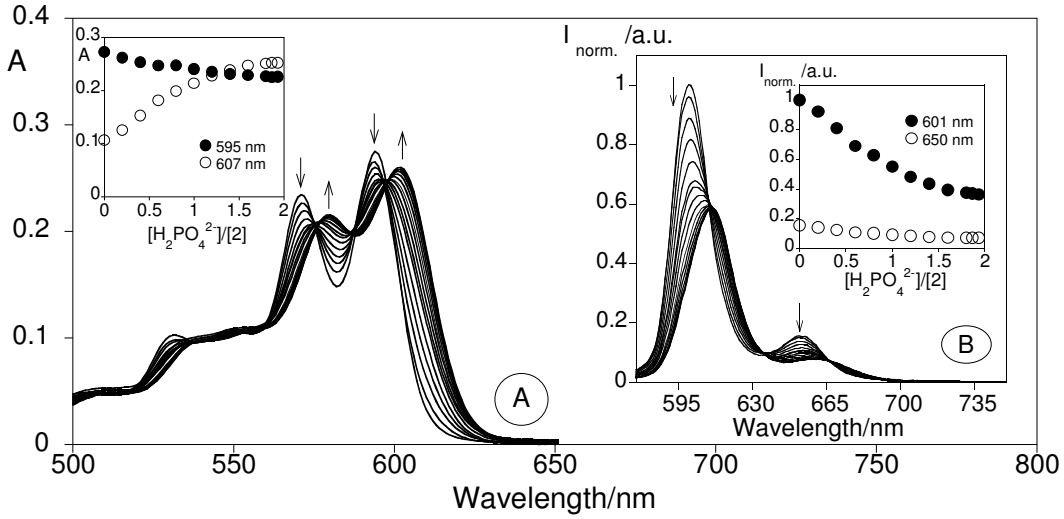

Figure 17- Spectrophotometric (A) and spectrofluorimetric (B) titration of compound **2** with the addition of $H_2PO_4^-$ in toluene. The inset represents the absorption (A) and the emission intensity (B) as a

function of $[H_2PO_4^-]$/[**2**] at 595 nm and 607 nm for (A) and 601 nm and 650 nm for (B). ([**2**] = 1 $\times 10^{-5}$ M, λ_{exc} = 570 nm, T = 298 K).

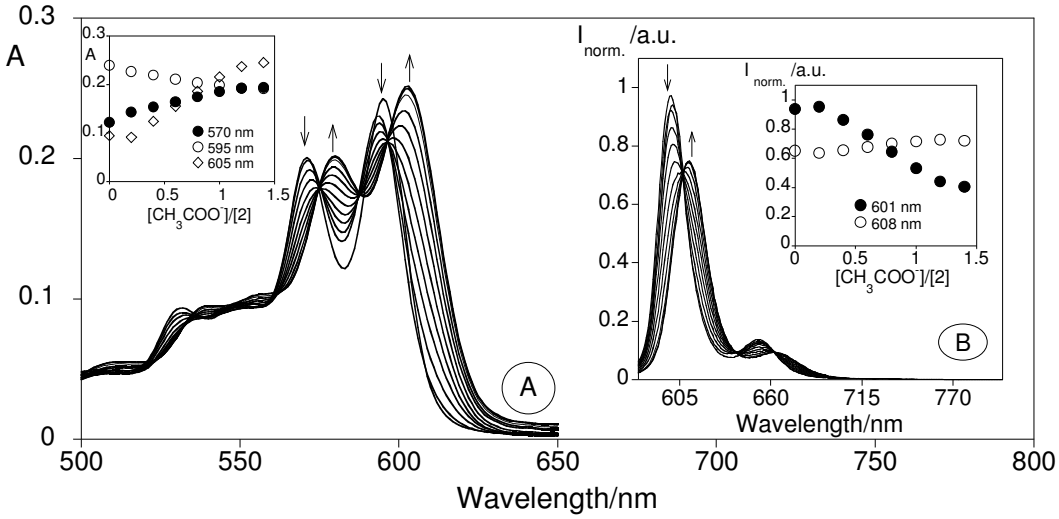

Figure 18- Spectrophotometric (A) and spectrofluorimetric (B) titration of compound 2 with the addition of CH_3COO^- in toluene. The inset represents the absorption (A) and the emission intensity (B) as a function of $[CH_3COO^-]$/[2] at 570 nm, 595 nm and 605 nm for (A) and 601 nm and 608 nm for (B). ([2] = 1 $\times 10^{-5}$ M, λ_{exc} = 570nm, T = 298 K).

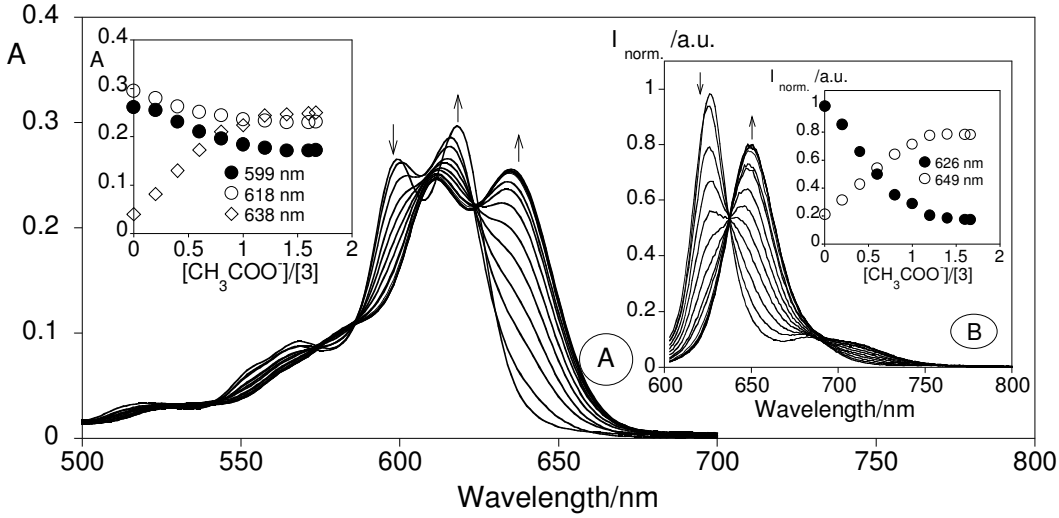

Figure 19- Spectrophotometric (A) and spectrofluorimetric (B) titration of compound **3** with the addition of CH_3COO^- in toluene. The inset represents the absorption (A) and the emission intensity (B) as a function of $[CH_3COO^-]$/[**3**] at 599 nm, 618 and 638 nm for (A) and 626 nm and 649 nm for (B). ([**3**] = 1 $\times$ 10^{-5} M, λ_{exc} = 599 nm, T = 298 K).

The association constants obtained with the anions CH_3COO^- and $H_2PO_4^-$ are lower than those obtained for the CN^- analyte and higher than those obtained for fluoride (see Table 2) .

2.2.2.2.4. Interaction of corroles 2a and 5 with 4,4-bipyridine, caffeine and nicotine.

In order to study the interaction of different amines with the corrole-gallium center, the pyridine unit was removed from compound **2** by acid treatment, affording the corresponding derivative **2a** as it was already referred. The sensorial ability of this free pyridine derivative, and of compound **5** was studied in the presence of 4,4'-bipyridine, caffeine and nicotine, but no spectral alterations were detected in their absorption spectra, suggesting that their ground state is not affected by the amine coordination. A different situation was observed for the excited state. For compound **2a,** the titration with 4,4'-bipyridine lead to an important emission quenching of *ca.* 60% at 600 nm (see figure 20A), while a less significant decrease (*ca.* 10%) was induced by the addition of caffeine and nicotine.

For compound **5** the most significant effects were observed after the addition of caffeine or nicotine that lead to an enhancement in the emission intensity at 635 nm of *ca.* 25% (see figure 20B). With this derivative no spectroscopic changes were observed in the presence of 4,4'-bipyridine.

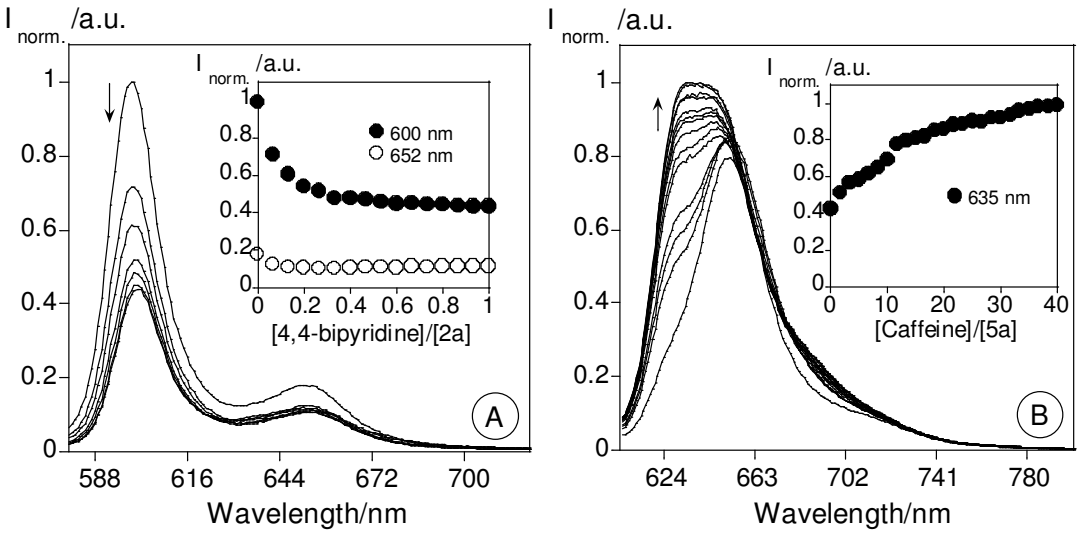

Figure 20- Spectrofluorimetric titration of compound **2a** (A) and **5** (B) with the increasing addition of 4,4-bipyridine and Caffeine in toluene at room temperature. [**2a**] = [**5**] = 1.00×10^{-5} M, $\lambda_{exc\mathbf{2a}}$ = 570 nm.

Based on the association constants calculated by HypSpec program [25], an adduct of three ligand **2a** per two molecules of 4, 4'-bypiridine (scheme 11) with a value of log K_{ass} = 23.12± 0.02 was postulated (see Table 2). Otherwise, in compound **5** an interaction of two units of caffeine or nicotine per ligand was determined (scheme 11), with values of log K_{ass} = 7.93 ± 0.01 and log K_{ass} = 10.01 ± 0.02, respectively (see Table 2).

The minimum amount of analytes that compounds **2a** and **5** are able to detect and to quantify was also determined by emission. For compound **2a** the minimum amount of 4,4-bypiridine detectable was 30.0 ppb and the minimum amount quantified was 50.0 ppb. Relative to compound **5** the minimum amount of caffeine and nicotine detectable was respectively 1.61 ppm and 2.70 ppm, and the minimum amount quantified was 3.24 ppm and 5.6 ppm. According to these results, it can be conclude that compound **2a** is a strong probe for sensing 4,4'-bypiridine allowing the detection and quantification of very small amounts of this analyte.

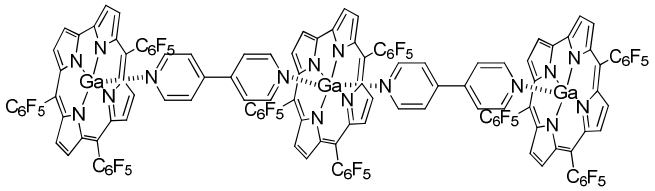

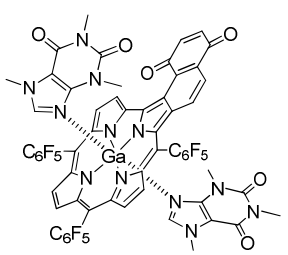

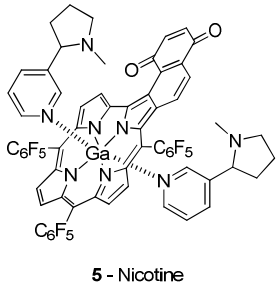

Scheme 11

2.2.3. Solid Support Sensors based on corrole ligands 1 and 5

The potentiality of these compounds as solid support sensors was evaluated by preparing two low-cost polymers in the presence of compounds **1** and **5**. One of them was based on polymethylmethacrylate (PMMA) and the other in 10% polyacrylamide. The emission of the four polymers was measured in solid state using a fiber optic system connected to the Horiba Jobin-Yvon Fluoromax 4. The PMMA polymers doped with compounds **1** and **5** show a purple colour, and a strong red emission under UV lamp irradiation (λ=365 nm) or when excited in the spectrofluorimeter at 565 nm. However, the system did not show significant changes to the naked eye in the presence of the analytes. On the other hand, the acrylamide gel based on the same derivative **1** that in the absence of the analyte was not emissive was able to switch on the emission after being submersed in a fluoride solution. The reason of this enhancement in the emission intensity is probably due to the large pores in the acrylamide gel that allow the entry of fluoride anions into the gel. The enhancement in the emission intensity with the time of submersion in a fluoride solution was performed with this polymer and the main results are gathered in Figure 21. With cyanide a similar behavior was observed (Figure 22).

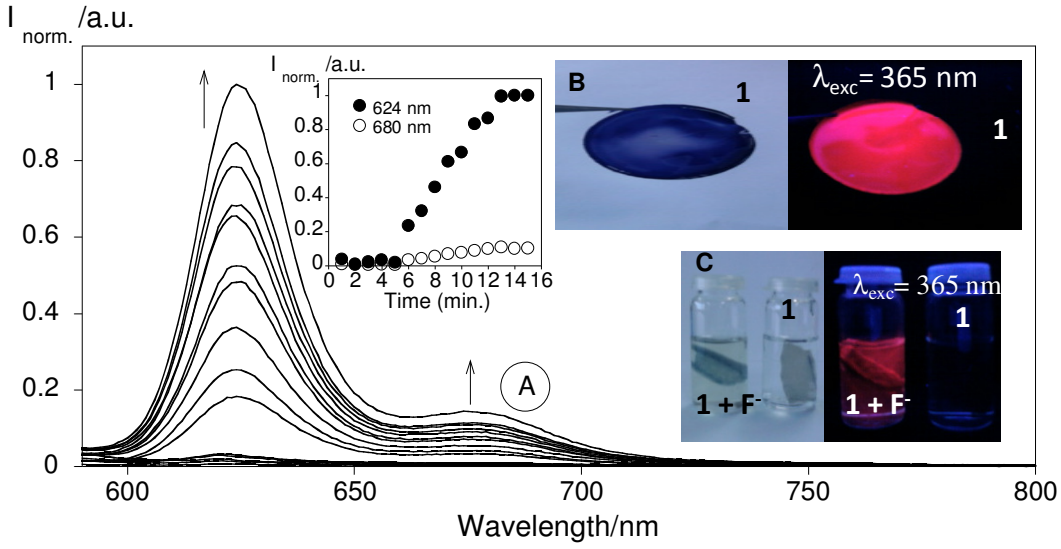

Figure 21- (A) Emission spectra of acrylamide gel dopped with compound **1** in the presence of fluoride as function time (T= 298 K, λ_{exc}= 570 nm. (B) Polymethylmethacrylate film with 1 and (C) polyacrilamide gel of **1** in the presence of fluoride (F^-).

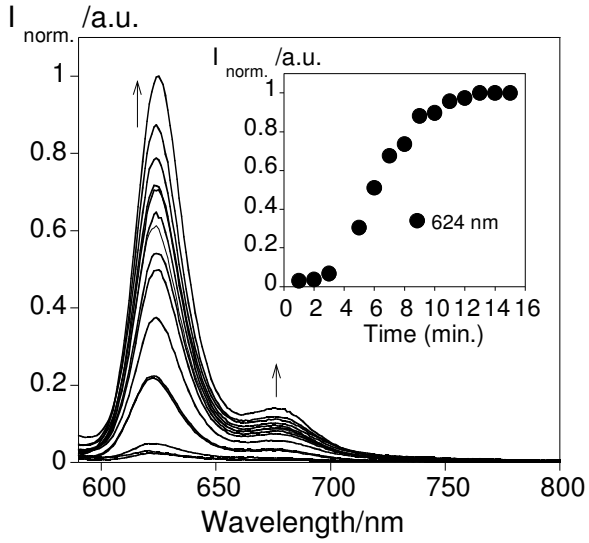

Figure 22- Emission spectra of acrylamide gel dopped with compound 1 in the presence of cyanide anion with time. (T=298 K, λ_{exc} = 565 nm).

The two polymers based on derivative **5** present a blue coloured film, detectable to the naked eye, and a strong emission under the UV lamp at 365 nm. Furthermore, when the acrylamide gel doped with compound **5** was submersed in a solution containing nicotine or caffeine an important enhancement in the emission intensity was observed. In figure 23 is presented the emission spectra of the gel doped with compound 5 in the presence of a solution containing caffeine, as a function of time. A similar behaviour was obtained for nicotine**.**

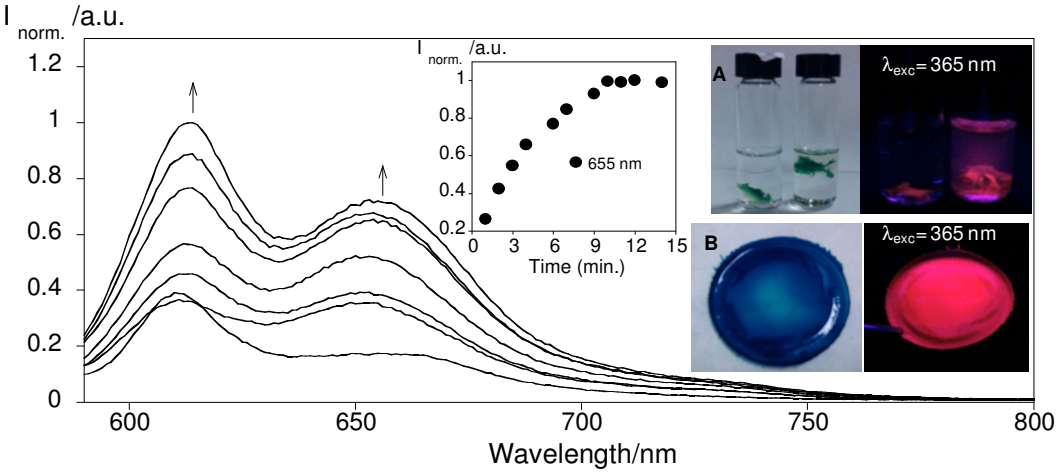

Figure 23- Emission spectra of acrylamide gel dopped with compound 1 in the presence of cyanide anion with time. (T=298 K, λ_{exc} = 565 nm).

These studies were also extended to water samples; a polyacrylamide gel dopped with compound **1** was introduced in water previously doped with different concentrations of cyanide such as, 0, 0.5, 1, 2 and 4 ppm. Figure 24 shows the variations of the emission intensity upon the addition of CN^-. As it can be seen the linear regression is maintained until 1 ppm of CN^-, and over this value a saturation point is detected. Overall, compound **1** in a solid support is able to detect a maximum of 1 ppm of cyanide in water and a minimal amount of 70.0 ppb in water.

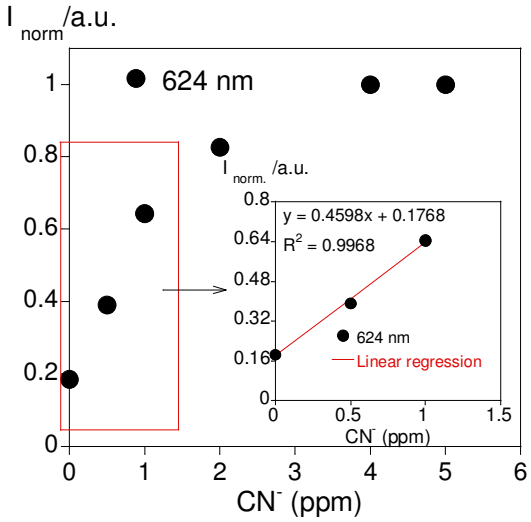

Figure 24- Normalized emission intensity of a polyacrylamide gel doped with compound **1** in water upon de addition of 0, 0.5, 1, 2 and 4 ppm of CN^-. (T=298 K, λ_{exc} = 565 nm).

2.2.4. MALDI-TOF-MS titrations with fluoride and cyanide anions

Compounds **1**-**6** were characterized in gas phase by MALDI-TOF-MS spectrometry and all the measurements were realized in negative mode. In general, the peaks corresponding to the deprotonated compounds were perfectly observed.

Table 3: MALDI-TOF-MS peaks of free compounds **1, 2**, **3** and **5** (negative mode).

Compounds	Species	MALDI-TOF-MS Calc./Found (%)
1	[**1**]$^-$	795.48 / 795.04 (100%)
2	[**2**-Pyr]$^-$	861.97 / 861.99 (100%)
	[**2**]$^-$. MeOH	974.32 / 974.97 (50%)
	[**2**-Pyr]$^-$. $2H_2O$	898.21 / 898.956 (70%)
3	[**3**]$^-$. $2H_2O$	924.99 / 924.96 (100%)
5	[**5**]$^-$. $2H_2O$	1028.01 / 1028.96 (70%)

In order to explore these compounds as molecular probes in gas phase, several MALDI-TOF-MS titrations of compounds **1**-**6** with fluoride and cyanide anions were performed in a dichloromethane solution. To realize the anion titration a dried droplet solution and a layer-by-layer deposition sample preparation were carried out. In gas phase, it was observed that only compounds **2** and **5** show interaction with cyanide anions in which were detected the species [2.CN$^-$] at calc./ found (%): 887.98/887.97 (100%) m/z, [2.CN]$^{2-}$ at calc./ found (%): 443.49/443.50 (90%) m/z for **2** and the specie [5.CN]$^-$ at calc./ found (%): 1017.99/ 1017.84 (100%) m/z for **5**. Figure 26 shows the mass spectra of compound **2a** alone and after the titration with 1 and 2 equivalents of cyanide anions.

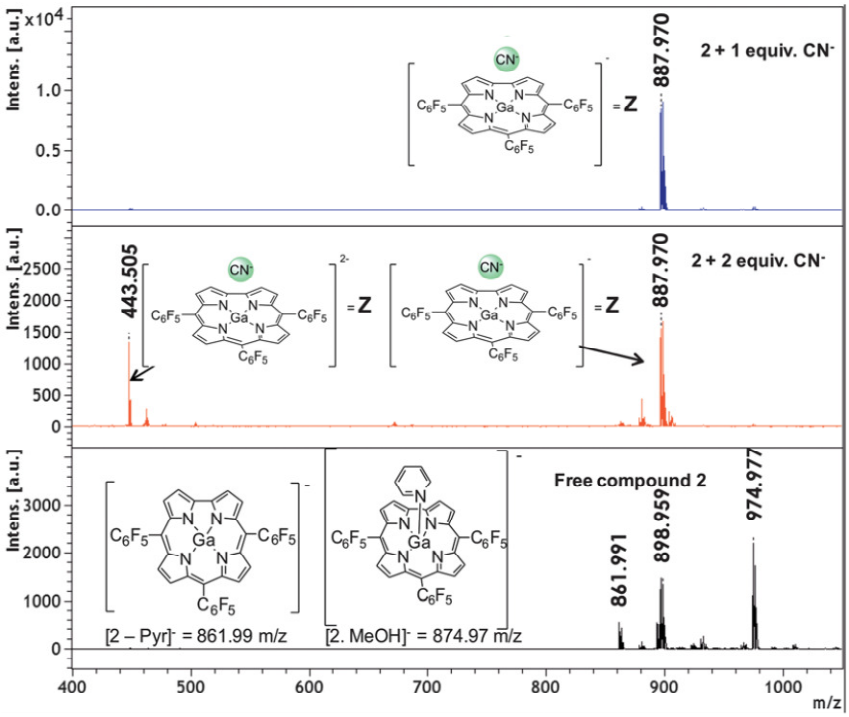

Figure 25- MALDI-TOF-MS mass spectra of free compound **2** and after the addition of **1** and **2** equivalents of cyanide anions.

2.3 Conclusions

Three new corrole derivatives **4–6** were successfully prepared and fully characterized by elemental analysis, ^{1}H-NMR, ^{13}C-NMR,^{19}F-NMR, MALDI-TOF-MS, UV-Vis absorption and emission spectroscopy. The gallium(III) complex of 3-vinyl-5,10,15-tris(pentafluorophenyl)corrole **4** was obtained efficiently through a Wittig reaction. The results show that the vinyl group and the peripheral double bond can act as a diene in Diels–Alder reactions. In the presence of 1,4- benzoquinone and 1,4-naftoquinone as dienophiles the dehydrogenated derivatives **5–6** were obtained in very good yields.

The sensing ability of the new corrole derivatives and of theirs precursors towards the spherical halide ions F^-, Cl^-, Br^-, I^-, the linear anion CN- and the bulky anions CH_3COO^-, $H_2PO_4^-$ was carried out in toluene. This study was also realized in gas-phase with the anions $F^-$and CN^-.

Compounds **1** and **2** show the highest fluorescence quantum yield of *ca*. 0.05–0.06; however the insertion of a substituent on position **3** of the corrole unit leads to a decrease of the quantum yield from 0.06 to 0.02, with compound **6** not being emissive.This behaviour can be probably attributed to the quencher character of quinones.

From all compounds, the most sensitive to fluoride anions is **1**, where a strong association constant of log K_{ass}= 9.43±0.03 was determined. This compound is able to detect and quantify 0.35 and 0.69 ppm of this anion, respectively.

The coordination of the corrole core with gallium(III) decreases the affinity for fluoride anions and consequently, lower association constants were obtained. In general, all compounds show interaction with cyanide anions; a red-shift in the absorption and emission spectra and an increase in the emission intensity are observed. Compounds **1** and **2** show the highest association constants: log K_{ass}= 10.57± 0.01 (anion : ligand = 2 : 1) for **1** and log K_{ass}=10.52 ± 0.02 (anion : ligand = 1 : 2) for **2**. The minimal amount of cyanide quantified by compound **1** was 1.43ppm. The interaction of CN^- with compound **2** and **5** was also observed in the gas-phase. Lower association constants were obtained in the presence of the bulky anions CH_3COO^- and $H_2PO_4^-$ than with CN^-, probably due to their higher size. The interaction of sensors **2a** and **5**, with amines, such as 4,4´-bipyridine, caffeine and nicotine shows that compound **2a** is very sensitive to 4,4´-bipyridine with a log K_{ass} = 26.27± 0.03 (amine : ligand =3: 2) and is able to detect a very small amount of this amine (30.0 ppb); compound **5** is really effective for detecting nicotine and caffeine with log K_{ass} = 7.93±0.01 and log K_{ass}= 10.01± 0.02 (amine : ligand = 2 : 1), respectively.

With compound **5** the minimum amount of caffeine and nicotine detectable was respectively, 1.61 ppm and 2.70 ppm, and the minimum amount quantified was 3.24 ppm and 5.6 ppm.

The most promising results come from the application of these chemosensors as solid support polymers, by preparing two low cost polymers based on PMMA and polyacrylamide. The PMMA films prepared with compounds **1** and **5** show a purple and a blue colour to the naked eye, respectively, and under an UV lamp a very strong red emission.

The non-emissive doped-polyacrylamide gel film when exposed to water solution containing amounts of fluoride, cyanide for compound **1** and nicotine, caffeine for compound **5** shows a very strong emission. Overall, the film doped with **1** was able to detect a maximum of **1** ppm of cyanide and a minimal amount of 70.0 ppb in water. These results are really positive for the determination of contaminants and toxic anions, like cyanide, in water.

2.4 Experimental Section

2.4.1 Chemicals and starting reagents

$(CH_3CH_2CH_2CH_2)_4NF$, $(CH_3CH_2CH_2CH_2)_4N(OCOCH_3)$, $(CH_3CH_2CH_2CH_2)_4N(CN)$, $(CH_3CH_2CH_2CH_2)_4N(H_2PO_4)$, $(CH_3CH_2CH_2CH_2)_4NBr$, $(CH_3CH_2CH_2CH_2)_4NCl$, $(CH_3CH_2CH_2CH_2)_4NI$ salts, pyrrole, pentafluorobenzaldehyde, 2,3-dichloro-5,6-dicyanobenzoquinone (DDQ), 4,4´-bipyridine caffeine and nicotine were purchased from Sigma–Aldrich and 1,4-naphthoquinone, 1,4-benzoquinone, $CH_3P(C_6H_5)_3Br$ were obtained from Alfa Aesar. All these chemicals were used without further purification. The solvents were obtained from Panreac and Riedel-de Häen and used as received or distilled and dried using standard procedures.

2.4.2 Physical measurements

Elemental analyses were carried out with Fisons Instruments EA1108 microanalyser at the University of Vigo (CACTI), Spain. ^{1}H and ^{13}C NMR spectra were recorded on Bruker Avance 500 (at 500 and 125 MHz, respectively) and 300 (at 300 and 75 MHz, respectively) spectrometers. ^{19}F NMR spectra were also obtained on Bruker Avance 300 at 282 MHz. $CDCl_3$ and pyridine-d_5 were used as solvents and tetramethylsilane (TMS) as internal reference; the chemical shifts are expressed in δ (ppm) and the coupling constants (*J*) in Hertz (Hz). Unequivocal ^{1}H assignments were made using 2D COSY and NOESY experiments (mixing time of 800 ms), while ^{13}C assignments were made on the basis of 2D HSQC and HMBC experiments (delay for long-range *J* C/H couplings were optimized for 7 Hz). Preparative thin-layer chromatography was carried out on 20×20 cm glass plates coated with silica gel (0.5 mm thick). Analytical TLC was carried out on precoated sheets with silica gel (Merck 60, 0.2 mm thick).

The MALDI-MS analyses have been performed with a MALDI-TOF-TOF-MS model Ultraflex II Bruker, Germany, equipped with nitrogen, from the BIOSCOPE group, University of Vigo, FCOU- Ourense Campus. Each spectrum represents accumulations of 5×50 laser shots. The reflection mode was used. The ion source and flight tube pressure were less than 1.80×10^{-7} and 5.60×10^{-8} Torr, respectively. The MALDI mass spectra of the soluble samples (1 μg/μL) were recorded using the conventional sample preparation method for MALDI-MS. 1μL with 1 or 2 equivalents of anions F^- or CN^- were put on the sample holder on which the compounds **1** to **6** had been previously spotted. The sample holder was inserted in the ion source. Chemical reaction between

the ligand and the anions occurred in the holder and complexed species were produced. The samples were prepared in dichloromethane, and dithranol was used as matrix.

2.4.3 Photophysical measurements

Absorption spectra were recorded on a Perkin Elmer lambda 45 and JASCO 650 spectrophotometers and fluorescence emission on a Perkin Elmer LS55. The linearity of the fluorescence emission vs. concentration was checked in the concentration range used (10^{-4} – 10^{-6} M). A correction for the absorbed light was performed when necessary. The spectroscopic characterizations and titrations were performed using stock solutions of the studied compounds (*ca.* 10^{-3} M), prepared by dissolving the appropriate amount of the corrole in toluene or dichloromethane in a 10 mL volumetric flask. The studied solutions were prepared by appropriate dilution of the stock solutions up to 10^{-5} to 10^{-6} M. Titrations of the ligands **1** to **6** were carried out by the addition of microliter amounts of standard solutions of anions or amines in DMSO or toluene, respectively. All the measurements were performed at 298 K.

Luminescence quantum yields were measured using a solution of cresyl violet perchlorate in absolute ethanol as a standard ($[\phi] = 0.54$)[29] and were corrected for different refraction indexes of solvents.

Fluorescence spectra of the solid samples were recorded using a fiber optic system connected to a Horiba Jobin-Yvon Fluoromax 4 spectrofluorimetric, exciting at appropriate λ (nm) for the solid compounds. The limit of detection (LOD) and the limit of quantification (LOQ) for the anions were performed, having in mind their use for real anion detection and for analytical applications. For these measurements, ten different analyses for the selected receptor were performed in order to obtain the LOQ.

The LOD was obtained by applying the formula:

$$Ydl = yblank + 3std$$

where ydl = signal detection limit and std = standard deviation.

2.4.4 Synthesis of organic ligands

2.4.4.1. Synthesis of the corrole precursors:

The 5,10,15-tris(pentafluorophenyl)corrole **1,** the corresponding gallium(III)(pyridine) complex **2** and the gallium(III) complex of 5,10,15-tris(pentafluorophenyl)corrole-3-carbaldehyde **3** were synthesized according to procedures described in literature.[18-20]

2.4.4.1.1 Synthesis of 5,10,15-tris(pentafluorophenyl)corrole 1

In a round bottom flask, 0.22 ml of pentafluorbenzaldeyde (2.00 mmol) was mixed with 20 µL (24 µmol) of a pre-prepared solution of TFA (10 mL) in CH_2Cl_2 (100 mL) and with 0.21 mL (3 mmol) of pyrrole. After stirring this reaction mixture for 10 min at room temperature, it was added 20 mL of CH_2Cl_2 and a solution of DDQ (545 mg, 2.40 mmol) in toluene:THF (4:4 mL); the resulting solution was then stirred for further 5 min. A pre-purification of the final reaction mixture by flash chromatography (silica, CH_2Cl_2 : hexane 2 : 3) afforded impure corrole **1** contaminated with porphyrin and unidentified compounds. Subsequent chromatography (column chromatography, silica, hexane, then CH_2Cl_2 : hexane, 1 : 4) afforded after recrystallization from hexane the pure corrole **1** (64 mg, 12%) as dark purple crystals.

Compound 1:

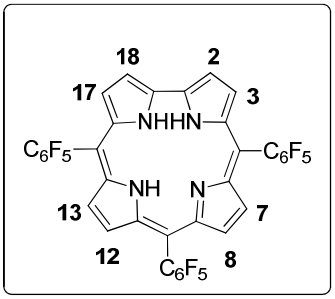

^{1}H NMR (300.13, $CDCl_3$): δ9.12 (d, 2 H, *J* 4.4 Hz, H-2 and H-18), 8.77 and 8.59 (2d, 4 H, *J* 4.8 Hz, H-7, H-13 or H-8, H-12) 8.58 (2d, 2 H, *J* 4.4 Hz, H-3 and H-17).

UV-Vis λ_{max} (log ε, $CHCl_3$): 408 (4.74), 408 (4.74), 560 (2.87), 602(2.23).

Yield: 12%, Colour: dark purple.

2.4.4.1.2 Synthesis of 5,10,15-tris (pentafluorophenyl)corrolatogallium(III)(pyridine)/ (gallium(III)(pyridine) complex)

A large excess of flame-dried $GaCl_3$ (5 g) was added to a solution of corrole **1** (500 mg) in dry pyridine and the resulting mixture was refluxed for 1h under argon. After this period the solvent was evaporated under reduced pressure and the resulting residue was purified by flash chromatography (silica, hexane:CH_2Cl_2:pyridine 150:50:1). Compound **2**

was obtained as purple crystals (45 mg; 76%) after recrystallization in CH_2Cl_2/hexane in the presence of few drops of pyridine.

Compound 2:

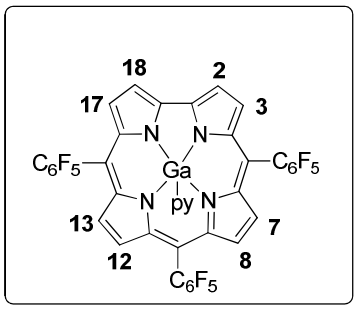

^{1}H NMR (500.13, $CDCl_3$, few drops of pyridine-d_5): δ 9.24 (d, 2 H, *J* 3.9 Hz, H-12 and H-18), 8.86 (d, 2 H, *J* 4.4 Hz, H-7 and H-13), 8.80 (d, 2 H, *J* 3.9 Hz, H-7, H-3 and H-17), 8.65 (d, 2 H, *J* 4.4 Hz, H-2, H-8 and H-12), 6.64 (t, 1 H, *J* 7.5 Hz, H_{para}-Py), 5.84 (dd not resolved, 2H, H_{meta}-Py), 4.71 (d, 2H, *J* 5.3 Hz, H_{orto}-Py).

UV-Vis λ_{max} (log ε, $CHCl_3$): 398 (4.81) 420 (5.42) 568 (4.20) 594 (4.41).

Yield: 76% Colour: purple.

2.4.4.1.2.1 Elimination of pyridine from compound 2

A solution of corrole **2** in dichloromethane was treated with 5 mL of HCl (36%) and maintained under magnetic stirring for 30 min. Then, the reaction mixture was carefully neutralized with sodium hydrogen carbonate solution and extracted with dichloromethane. The organic layer was separated, washed with water and dried with Na_2SO_4. The solvent was evaporated and the residue after crystallization from dichloromethane/hexane afforded quantitatively the pyridine free compound **2a**.

2.4.4.1.3 Synthesis of gallium(III) complex of 3-carbaldehyde-5,10,15-tris(pentafluorophenyl)corrole 3

Dry DMF (0.16 mL) was cooled to 5-10 °C, then it was added $POCl_3$ (0.12 mL, 1.16 mmol) under N_2 and the mixture was maintained under stirring for 15 min. After this period, the ice bath was removed and the reaction mixture was maintained under stirring for further 15 min. Dry dichloromethane (4 mL) was then added, and the reagent was cooled to 0-5 °C. A limited amount of this reagent (0.428 mL) was added dropwise to a solution of **4** (100 mg, 0.106 mmol) in 8 mL of CH_2Cl_2. During the addition, the solution turned from red to deep green, and after 3-5 min, the TLC control (silica, CH_2Cl_2:hexane, 2:1, and some drops of pyridine) confirmed that no starting corrole was present. Then, it was added a saturated solution of Na_2CO_3 (50 mL), and the mixture was stirred overnight, after which the organic phase was separated. The water phase was extracted more three times with CH_2Cl_2, and the combined organic extracts were washed with brine, dried with Na_2SO_4 and the solvent was removed under vacuum. The reaction mixture after being

purified by preparative TLC [hexane/ethyl acetate/pyridine (15:5:0.1)] afforded, after recrystallization from CH_2Cl_2/hexane and some drops of pyridine, the 3-formyl-5,10,15-tris(pentafluorophenyl)corrolato gallium(III)(pyridine) as green-blue crystals (75 mg, 70%). The elimination of pyridine was carried out according with the procedure described in the previous point affording compound 3.

Compound 3:

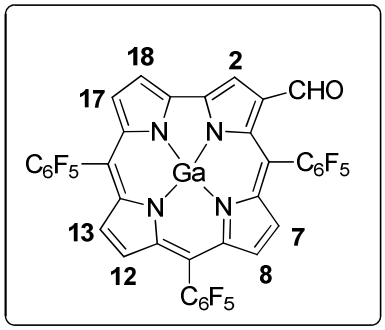

^{1}H NMR (500.13, $CDCl_3$, few drops of pyridine-d_5): δ 10.53 (s, 1 H, CHO), 9.14 (d, 1 H, *J* 4.1 Hz, H-18), 8.77 (d, 1 H, *J* 4.7 Hz, H-β), 8.75 (d, 1 H, *J* 4.1 Hz, H-17), 8.69 (d,1 H, *J* 4.7 Hz, H-β), 8.54 (d, 1 H, *J* 4.7 Hz, H-β), 8.50 (d, 1 H, *J* 4.7 Hz, H-β).

UV-Vis λmax (log ε, $CHCl_3$): 410 (4.62), 432 (5.23), 602 (4.39), 620 (4.46).Yield: 70% Colour: green.

2.4.4.1.4 Synthesis of gallium(III) complex of 3-vinyl-5,10,15-tris(pentafluorophenyl)corrole 4: Sodium hydride (95 %, 14.5 mg, 0.57 mmol) was added to a suspension of triphenylmethylphosphonium bromide (129.0 mg, 0.36 mmol) in dry THF (6 mL) under a nitrogen atmosphere. The resulting mixture was stirred until an intense yellow color was observed (ca. 30 min), which indicated the formation of the ylide. Then, the gallium(III) complex of 3-carbaldehyde-5,10,15-tris(pentafluorophenyl)corrole **3** (20 mg, 0.021 mmol) was added and the reaction mixture was maintained under stirring for 4 h at room temperature. After this period, the reaction mixture was washed with water and the corrolic material was extracted with dichloromethane. The organic layer was separated, washed with water and dried with Na_2SO_4. The solvent was evaporated and the residue after crystallization from dichloromethane/hexane afforded the 3-vinyl corrole **4** (15.2 mg, 76% yield).

Compound 4:

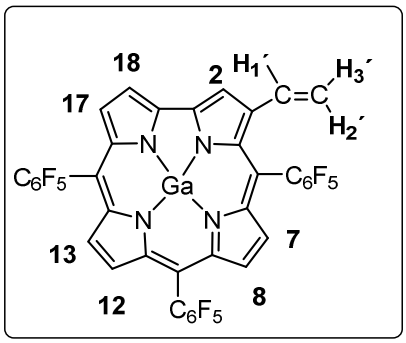

^{1}H NMR (500.13, $CDCl_3$, few drops of pyridine-d_5): δ 9.29 (d, 1H, *J* 4.1 Hz, H-18), 8.84-8.82 (m, 2H, H-2 and H-β), 8.81-8.78 (m, 2H, H-β and H-17), 8.62 (d, 2H, H-β), 8.43 (dd, 1H, *J* 17.6 and 10.9 Hz, H-1´), 6.65 (dd, 1H, *J* 17.6 and 1.0 Hz, H-2´), 5.91(dd, 1H, *J* 10.9 and 1.0 Hz, H-3´).

^{19}F NMR (282.37, $CDCl_3$, a few drops of pyridine-d_5): δ- 161.15 to -161.40 (m, 6F, F_{ortho}), -176.89 to -177.08 (m, 2F, F_{para}), -178.88 (t, J 21.2 Hz, 1F, F_{para}), -185.06 to -185.22 (m, 2F, F_{meta}), -185.61 to -185.92 (m, 4F, F_{meta}).

^{13}C NMR (125.77, $CDCl_3$, few drops of pyridine-d_5): δ 149.6-149.0 (m, C_5D_5N), 143.6, 141.2, 136.9, 136.6, 135.9-135.1 (m, C_5D_5N), 132.5, 130.9, 130.5 (C-1´), 128.9, 128.2, 127.53 (C-β), 127.45 (C-β) 125.2 (C-17), 124.4 (C-β), 123.4-122.9 (m, C_5D_5N), 119.7 (C-17), 119.1 (C-2), 118.3 (C-18), 116.9 (C-2´ and C-3´) Anal. Calc. for $C_{39}H_{12}F_{15}GaN_4$ (Fw: 887.99) C, 52.68; H, 1.13; N, 6.30. Found: C, 52.60; H, 1.38; N, 6.33.

UV-Vis λ_{max} (log ε, toluene): 421(4.41), 429 (4.68), 599 (3.29).

Yield: 74% Colour: Green.

2.4.4.2 General procedure for the Diels-Alder reactions with quinones:

A solution of corrole **4** (0.025 mmol) and the dienophile (1,4-benzoquinone or 1,4-naphthoquinone) (0.050 mmol) in toluene (0.5 mL) was gently refluxed for 48 h under a nitrogen atmosphere. After cooling to room temperature, the solvent was evaporated. Then, the adducts **5** or **6** were further purified by preparative TLC [silica, hexane/ethyl acetate/pyridine (15:5:0.1)]. The isolated adducts were then crystallized from dichloromethane/methanol.

Compound 5:

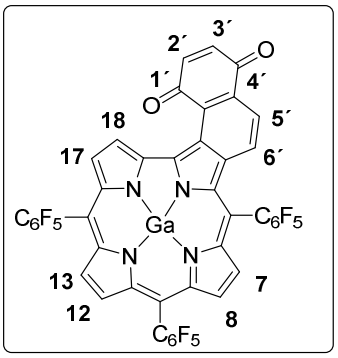

^{1}H NMR (300.13, $CDCl_3$, few drops of pyridine-d_5): δ 9.84 (d, 1H, *J* 8.2 Hz, H-5'), 9.53 (d, 1H, *J* 4.1 Hz, H-18), 8.90 (d, 1H, *J* 4.1 Hz, H-17), 8.81-8.77 (m, 3H, H-6', 2 H-β), 8.65-8.62 (m, 2H, H-β), 7.09 (d, 1H, *J* 10.1 Hz, H-2'), 6.86 (d, 1H, *J* 10.1 Hz, H-3'). ^{19}F NMR (282.37, $CDCl_3$, few drops of pyridine-d_5): δ-161.15 to -161.40 (m, 6F, F_{ortho}), -176.89 to –177.08(m, 2F, F_{para}), -178.88 (t, *J* 21.2 Hz, 1F, F_{para}), -185.06 to -185.22 (m, 2F, F_{meta}), - 185.61 to -185.92 (m, 4F, F_{meta}).

^{13}C NMR (125.77, $CDCl_3$, few drops of pyridine-d_5): δ 185.8 (C-1', C=O), 185.4 (C-4', C=O), 149.6 (t, C_5D_5N, *J* 27.1 Hz), 142.9, 142.6, 142.0, 140.9, 138.0 (C-3'), 137.9, 137.4 (C-2'), 135.9 (t, C_5D_5N, *J* 24.8 Hz), 132.9, 132.3, 131.6, 131.0, 130.5, 127.6, 127.5, 127.3 (C-5', 2 C- β), 125.2 (C-17), 124.9 (C-β), 123.69 (C-6´), 123.67 (C- β), 123.3 (t, C_5D_5N, *J* 25.0 Hz), 118. 3 (C-18).

Anal. Calc. for $C_{45}H_{11}F_{15}GaN_4O_2$ (Fw: 993.29) C, 54.41; H, 1.01; N, 5.64. Found: C, 54.40; H, 1.18; N, 5.67.

Uv-Vis λ_{max} (log ε, toluene): 409 (4.57), 429 (4.79), 590 (4.22), 607 (4.40).

Yield: 76% Colour: Dark blue.

Compound 6:

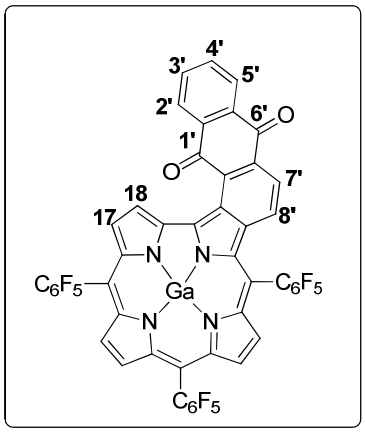

^{1}H NMR (300,13, $CDCl_3$, few drops of pyridine): δ 9.66 (d, 1H, *J* 4.3 Hz, H-18), 8.84-8.80 (m, 2H, H-7´and H-8´), 8.79-8.77 (m, 2H, H-β, H-17); 8.72 (d, 1H, *J* 4.6 H-5'), 8.66 (d, 1H, *J* 4.6 Hz, H-2´), 8.59 (d, 1H, *J* 4.3 Hz, H-β), 8.42-8.38 (m, 3H, H-β), 7.89-7.87 (m, 1H, H-3'), 7.86-7.84 (m, 1 H, H-4´).^{13}C NMR (75.47, $CDCl_3$, few drops of pyridine-d_5): δ 183.7 (C-1', C=O), 183.1 (C-6', C=O), 149.7 (t, C_5D_5N, *J* 27.2Hz) 141.5, 140.5, 139.7, 138.9, 138.3, 137.7, 135.9-135.4 (m, C_5D_5N), 134.3 (C-4´), 134.1 (C-3´), 133.8, 133.6, 132.6, 132.5, 131.4, 129.7 (C-7´), 129.3 (C-8´), 127.3-126.9 (m, 3 C-β), 126.0 (C-5´), 124.6 (C-2´), 124.3 (C-β), 123.7 C-β), 123.4-123.1 (m, C_5D_5N), 122.9 (C-17), 119.8 (C-18), Anal. Calc. for $C_{49}H_{12}F_{15}GaN_4O_2$ (Fw: 1043.34). C, 56.41; H, 1.16; N, 5.37 Found: C, 56.44; H, 1.19; N, 5.39.

UV-Vis λ_{max} (log ε, toluene): 407 (4.66), 477 (4.80), 597 (4.17).

Yield: 64%. Colour: Brownish Green.

2.4.5 Preparation of the solid supports dopped with compounds 1 and 5

The solid supports based on polymethylacrylate (PMMA) were prepared by dissolving 0.1g of polymethylmethacrylate powder in dichloromethane, followed by the addition of the compounds **1** or **5** (0.001g) also dissolved in the same solvent. The polymer film was obtained after the solvent evaporation at 40ºC (~48 hours).

The solid supports based on the polyacrylamide gel were prepared by addition of compounds **1** or **5** (0.001g) to acrylamide (10%) using the conventional 1D-Gel Electrophoresis procedure described for proteins separation.[30]

2.5 References:

[1] (a) Desvergne, J. P.; Czarnik. A. W. *Chemosensors of Ion and Molecule Recognition* (NATO Science Series, Serie C:Mathematical and Physical Sciences), Kluwer Academic, London, **1997**. (b) Lodeiro, C.; Pina, F.; Parola, AJ.; Bencini,A.; Bianchi, A.; Bazzicalupi, C.; Ciattini, S.; Giorgi, C.; Masotti, A.; Valtancoli, B.; Melo, J. S. *Inorg. Chem.* **2001**, 40, 6813-6819.

[2] Xu, Z.; Yoon, J.; Spring, D.R. *Chem. Soc. Rev*. **2010**, 39, 1996-2006.

[3] Silva, A.P. ; Gunaratne, H.Q.N.; Gunnlaugsson, T.; Huxley, A. J. M.; Mccoy, C. P.; Rademacher, J. T.; Rice, T. E. *Chem. Rev*. **1997**, 97, 1515-1566.

[4] Akkaya, E. U.; Huston, M. E.; Czarnik, A. W. *J. Am. Chem. Soc.* **1990**, 112, 3590-3593.

[5] Rurack, K. *Spectrochimica Acta Part A*, **2001**, 57, 2161-2195.

[6] Aviv-Harel, I.; Gross, Z. *Coord. Chem. Revs*, **2011**, 255, 717-736.

[7] Ventura, B.; Degli Esposti, A.; Koszarna, B.; Gryko, D. T. ; Flamigni, L. *New J. Chem.*, **2005**, 29, 1559–1566. (b) Ding, T.; Alemán, E. A.; Mordarelli, D. A. ; Ziegler, C. J. *J. Phys. Chem. A*, **2005**, 109, 7411–7417. (c) Paolesse, R. *The Porphyrin Handbook*, ed. Kadish, K. M. ; Smith, K. M.; Guilard, R. Academic Press, New York, **2000**, vol. 2, ch. 11, pp. 202–203.

[8] Flamigni, L.; Gryko, D. T. *Chem. Soc. Rev.*, **2009**, 38, 1635-1646.

[9] (a) He, C-L.; Ren, F-L.; Zhang, X-B.; Han, Z-X. *Talanta*, **2006**, 70, 364-369. (b) Aviv-Harel, I.; Gross, Z. *Chem. Eur. J.* **2009**, 15, 8382-8394.

[10] Mahammed, A.; Weaver, J. J.; Gray, H. B.; Abdelas, M.; Gross, Z. *Tetrahedron Letters*, **2003**, 44, 2077-2079.

[11] (a) Gale, P. A. *Chem. Commun.* **2011**, 47, 82-86. (b) Beer, P. D.; P. A. Gale, P. D. *Angew. Chem. Int. Ed*. **2001**, 40**,** 486-516.

[12] Kleerekoper, M. *Endocrinol. Metab. Clin. North Am.* **1998**, 27, 441-452.

[13] Wiseman, A. *Handbook of Experimental Pharmacology XX/2*, Part 2, Springer-Verlag: Berlin, **1970**, 48-97.

[14] Barata, J. F. B.; Santos, C. I. M.; Neves, M. G.. P. M. S.; Faustino, M. A. F.; Cavaleiro, J. A. S.; *Topics* in *Heterocyclic Chemistry*, Springer- Verlag: Berlin, **2013**, 79-143.

[15] (a) Vale, L. S. H. P.; Barata, J. F. B.; Neves, M. G. P. M .S; Faustino, M. A. F.; Tomé, A. C.; Silva, A. M. S.; Paz, F. A. A.; Cavaleiro, J. A. S. *Tetrahedron Lett*. **2007**, 48, 8904-8908. (b) Barata, J. F. B.; Santos, C. I. M.; Faustino, M. A. F.; Neves, M. G. P. M. S.;

Cavaleiro, J. A. S. *Topics Heterocyclic Chemistry,* **2013**, DOI: 10.1007/7081. (c) Cavaleiro, J. A. S.; Tomé, A. C.; Neves, M. G. P. M. S. in *Handbook of Porphyrin Science*, (Ed. K. M. Kadish, K. M. Smith, R. Guilard) **2010**, Vol 2. Ch. 9, pp. 194–294.

[16] Kolodiazhnyi, O. I. *Phosphorous Ylides - Chemistry and Application in Organic Synthesis*, Wiley-VCH, Weinheim, Germany, **1999**, 359-538.

[17] (a) McNulty, J.; Das, P. *Eur. J. Org. Chem.* **2009**, 4031-4035. (b) McNulty, J.; Das, P. *Tetrahedron Lett.* **2009**, *50*, 5737-5740. (c) McNulty, J. ; Das, P.; McLeod, D.; *Chem. Eur. J.* **2010**, *16*, 6756-6760. (d) Gosney, I.; Rowley, A. P. *Organophosphorous Reagents in Organic Synthesis*, Ed. J. I. G. Cadogan, Academic Press, London, **1979**, 17-153.

[18] Gryko, D. T.; Koszarna, B. *Org. Biomol. Chem.* **2003**, 2, 350-357.

[19] Bendix, J.; Dmochowski, I. J.; Gray, H. B.; Mahammed, A.; Simkhovich, L.; Gross, Z. *Angew. Chem. Int. Ed*., **2000**, 39, 4048-4051.

[20] (a) Saltsman, I. ; Mahammed, A. ; Goldberg, I.; Tkachenko, E.; Botoshansky, M.; Gross, Z. *J. Am. Chem. Soc.* **2002**, 124, 7411–7420, (b) Vale, L. S. H. P.; Barata, J. F. B., Santos, C. I. M.; Neves, M. G. P. M. S.; Faustino, M. A. F.; Tomé, A. C.; Silva, A. M. S.; Paz, F. A. A.; Cavaleiro, J. A. S. *J. Porphyrins Phthalocyanines* **2009**, 13, 358–368.

[21] Carey, F. A. ; Sundberg, R. J. *Advanced Organic Chemistry - Part A: Structure and Mechanisms*, 5ª Ed., Springer Science-Business Media, LLC, **2007**, 833-872.

[22] Smith, M. B.; March, J.; *March's Advanced Organic Chemistry*, 6ª Ed., John Wiley & Sons, Inc., **2007**, 1194-1218.

[23] Fringuelli, F.; Taticchi, A.; *The Diels-Alder Reaction: Selected Practical Methods*, John Wiley & Sons, Ltd, **2002**, 1-138.

[24] Illos, R. A.; Harlev, E.; Bittner, S. *Tetrahedron Lett*. **2005**, 46, 8427–8430.

[25] Gans, P.; Sabatini, A.; Vacca, A. *Talanta*, **1996**, 43, 1739-1753.

[26] Guidelines for Drinking-Water Quality, World Health Organization, Geneva, **1996**.

[27] Gee, H-C.; Lee, C-H.; Jeong, Y-H. ; Jang, W.-D. *Chem. Commun.*, **2011**, 47, 11963-11965.

[28] Valeur, B. *Molecular Fluorescence: Principles and Applications*, Wiley-VCH Verlag GmbH, **2001**.

[29] Esipenko, N. A.; Koutnik, P.; Minami, T.; Mosca, L.; Lynch, V. M.;Anzenbacher, P. *Chem. Sci*. **2013**, 4, 3617-3623

[30] Galesio, M.; Vieira, D. V.; Rial-Otero, R. ; Lodeiro, C. ; Moura, I. ; Capelo, J. L. *J. Proteome. Res.* **2008**, 7, 2097-2106.

Chapter III

New Gallium(III) Corrole Complexes as Colorimetric Probes for Toxic Cyanide Anion

Published in *Inorg. Chim. Acta, **2013**, in Press*
doi.org/*10.1016/j.ica.2013.09.049*

INDEX

3-New Gallium(III) Corrole Complexes as Colorimetric Probes for Toxic Cyanide Anion

Resumo

Nos últimos anos a procura de quimiossensores colorimétricos para a detecção de aniões tóxicos tem aumentado de forma significativa, uma vez que, estes dipositivos moleculares permitem a deteção do analito a olho nu e sem recurso a técnicas ou equipamentos sofisticados. Neste capítulo é descrita a preparação de dois novos derivados corrólicos **2** e **3** bem como a sua caracterização estrutural por análise elementar, espectroscopia de ressonância magnética nuclear de protão (^{1}H-RMN), espectrometria de massa (MALDI-TOF) e por espectroscopia de absorção e de emissão de fluorescência. Estes derivados foram obtidos durante a reação de cicloadição de Diels-Alder do complexo de gálio do 3-vinil-5,10,15-tris(pentafluorofenil)corrol, também denominado de 3-vinil-5,10,15-tris(pentafluorofenil)corrolatogálio(III)(piridina), **1** com acetilenodicarboxilato de dimetilo. A habilidade sensorial dos novos derivados corrólicos para os aniões fluoreto, cianeto, acetato, e fosfato foi avaliada por espectroscopia de absorção e emissão. O composto **2** mostrou comportar-se como um quimiossensor colorimétrico para o anião cianeto, uma vez que na presença deste, observou-se-se a uma mudança de cor da solução de verde para incolor. Para além disso, as constantes de associação mais elevadas para os compostos **2** e **3** foram obtidas na presença do anião cianeto. Ambos os derivados mostraram ser capazes de detetar quantidades muito pequenas de cianeto (*ca*. 1.00 μM).

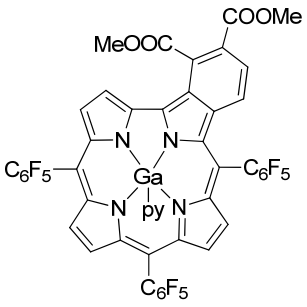

2

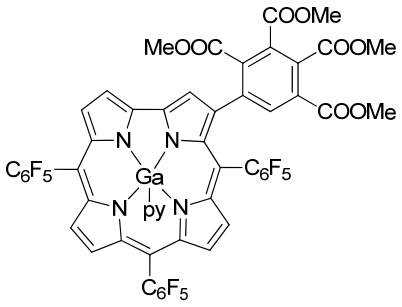

3

Abstract

Demand for new colorimetric sensors for toxic anions has widely increased in the last ten years, because, as was referred in the introduction (chapter I), this is an inexpensive technique, in which the analyte is naked-eye detectable. In this chapter is described the synthesis of two new corrole derivatives **2** and **3** and their structural and photophysical characterization by elemental analysis, ^{1}H-NMR, MALDI-TOF-MS, UV-Vis absorption and emission spectra. These derivatives were obtained from the Diels-Alder cycloaddition reaction of gallium (III)(pyridine) complex of 3-vinyl-5,10,15-tris(pentafluorophenyl)corrole **1** with dimethyl acetylenedicarboxylate. The sensorial ability of the new corrole derivatives towards several anions, namely, fluoride, cyanide, acetate and phosphate anions was carried out by absorption and emission spectroscopy. Compound **2** shows to be colorimetric to cyanide, since a change of colour from *green* to *colourless* was visualized. In addition the highest association constants were obtained for compounds **2** and **3** in the presence of cyanide that are able to quantify a minor amount of cyanide (*ca.* 1.00 μM).

3.1 Introduction

Nowadays, a huge number of colorimetric and fluorescent chemosensors have been developed targeting the detection of anions. They have a widely application on chemical and biological processes.[1] Among all anions, fluoride and cyanide are the most attractive targets, because of their significant importance in health and environmental matters.[2] Fluoride is an essential anion being widely used in toothpaste for dental caries prevention and in osteoporosis treatment, as well. Like for the other anions, an excess of fluoride anion could induce several diseases, such as fluorosis, which might cause nephorotoxic alterations in humans leading to urolithiasis.[3] The detection and quantification of fluoride anion is often controlled in urine samples, and the standard amount of this anion in water given by the United States Environmental Protection Agency (EPA)[4] must be around 2 and 4 $mg.L^{-1}$.

Cyanide is one of the most poison and toxic anion for the environmental and human health.[5] Despite its toxicity cyanide is up to now applied in industrial fields, such as in gold and silver mining, in nitriles and nylon polymers and in acrylic plastic production.[6,7] Its quantification is really important and due to its high toxicity the highest allowable level of cyanide according to the World Health Organization in drinking water is around 1.9 μM.[8,9] There are many techniques to detect cyanide such as spectrophotometric analysis, electrochemical and optical sensors.[10] The most inexpensive methods are the use of colorimetric sensors, which allows the naked-eye detection of cyanide by a change of colour. As an example, Kang *et al*.[11] reported a specific naked eye sensor for cyanide over other competitive anions in protic solvents, whereas a colour change from colourless to yellow in the presence of cyanide was observed.

Consequently, the search for methods that can rapidly detect such few amount of anions is a challenge, where the use of high sensitive techniques as absorption and emission fluorescence spectroscopy enable their detection.

The design and synthesis of chemosensors with fluorophores visible excitable have increased due to their potential application *in* environmental control, biology or medicine[12]

Corroles, porphyrins and metalloporphyrins are excellent multifunctional candidates for a great variety of sensing material applications. In particular, corroles have many advantages such as high radiative rate constants, large Stoke's shift, absorption and emission bands in the visible and high luminescent quantum yield.[13] Also, corrole derivatives are sensitive to anions, because of their high N-H acidity.[14] In fact, most part of

the supramolecular interactions between the fluorophore and the anion are mainly hydrogen bond, acid-base and anion – π interactions.[15]

Following our interest, on the functionalization of corroles via cycloaddition rections,[16] and in the study of fluorescent chemosensors,[17] herein we present the synthesis and the sensorial ability of new corrole derivatives **2** and **3** towards fluoride, cyanide, acetate and phosphate anions by absorption and emission spectroscopy.

3.2 Results and Discussion

3.2.1 Synthesis and structural characterization of corrolic ligands

The synthetic route used to prepare the corrolic derivatives **2** and **3** is outlined in Scheme 1. The corrole precursors 5,10,15-tris(pentafluorophenyl)corrole and 5,10,15-tris-(pentafluorophenyl)corrolatogallium(III)(pyridine) were synthesized, according to procedures described in literature, and as it was referred in chapter II of this dissertation.[18,19]

The synthesis of the gallium(III)(pyridine) complex of 3-vinyl-5,10,15-tris(pentafluorophenyl)corrole **1** involved the Vilsmeier–Haack formylation of 5,10,15-tris-(pentafluorophenyl)corrolatogallium(III)(pyridine) using $POCl_3$/DMF, followed by a Wittig reaction using CH_3PPh_3Br/NaH/THF.[17] This synthetic step was described in detail in chapter II of this dissertation.

After having assessed the reactivity of the gallium(III)(pyridine) complex of 3-vinyl-5,10,15-tris(pentafluorophenyl)corrole **1** in the presence of dienophiles of quinone type (see chapter II), it has been decided to extend the study to dimethyl acetylenedicarboxylate. This linear dienophile is well known by its high reactivity in Diels-Alder reactions.[20] The reaction was carried out by heating corrole **1** with an excess of the dienophile (2 equiv.) in refluxing toluene, and was finished when the control by TLC showed the total consumption of the starting reagent. After the usual work up and purification, two novel compounds were isolated and identified, as the benzocorrole **2** ($[M+H]^+$ *m/z* 1029) obtained in 81% yield and compound **3** ($[M+H]^+$ *m/z* 1171) obtained in 16% yield (Scheme 1). The synthesis of compound **2** results from a Diels-Alder reaction followed by oxidation. However the formation of compound **3** *via* a cyclotrimerization process[21] is quite surprising, since a similar reaction with a *β*-vinylporphyrin and the same dienophile only afforded the expected adduct.[20] This result shows a clear difference in the reactivity of porphyrins and corroles, and further studies will be performed in order to clarify this unexpected transformation.

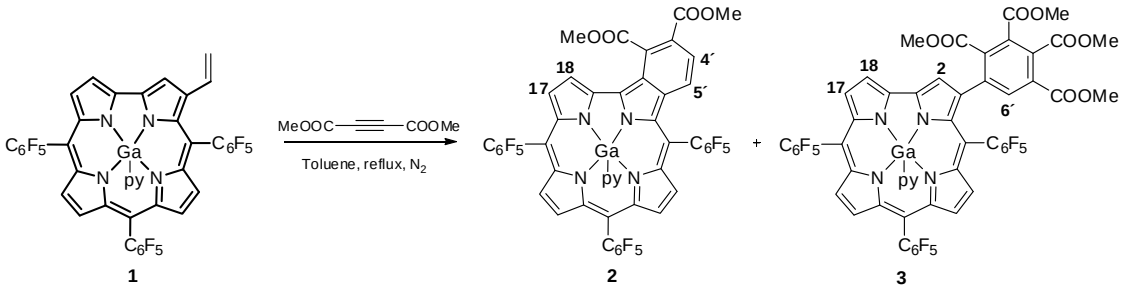

Scheme 1

The structures of the new compounds were established by spectroscopic data, namely NMR (^{1}H,^{19}F and COSY), UV-Vis, MS and elemental analysis.

The ^{1}H NMR spectrum of the adduct **2** showed in the aromatic region two doublets at δ 9.47 and 8.91 due to the resonance of protons H-18 and H-17, respectively. The multiplet existing at *δ* 8.72-8.67 was attributed to the resonances of other four *β*-pyrrolic protons. The signals at δ 8.53 and 8.17 were assigned to the resonances of the aromatic protons H-5´ and H-4'. In the aliphatic region were identified two singlets at *δ* 4.58 and 4.09, which are due to the resonance of the methyl ester groups (Figure 1).

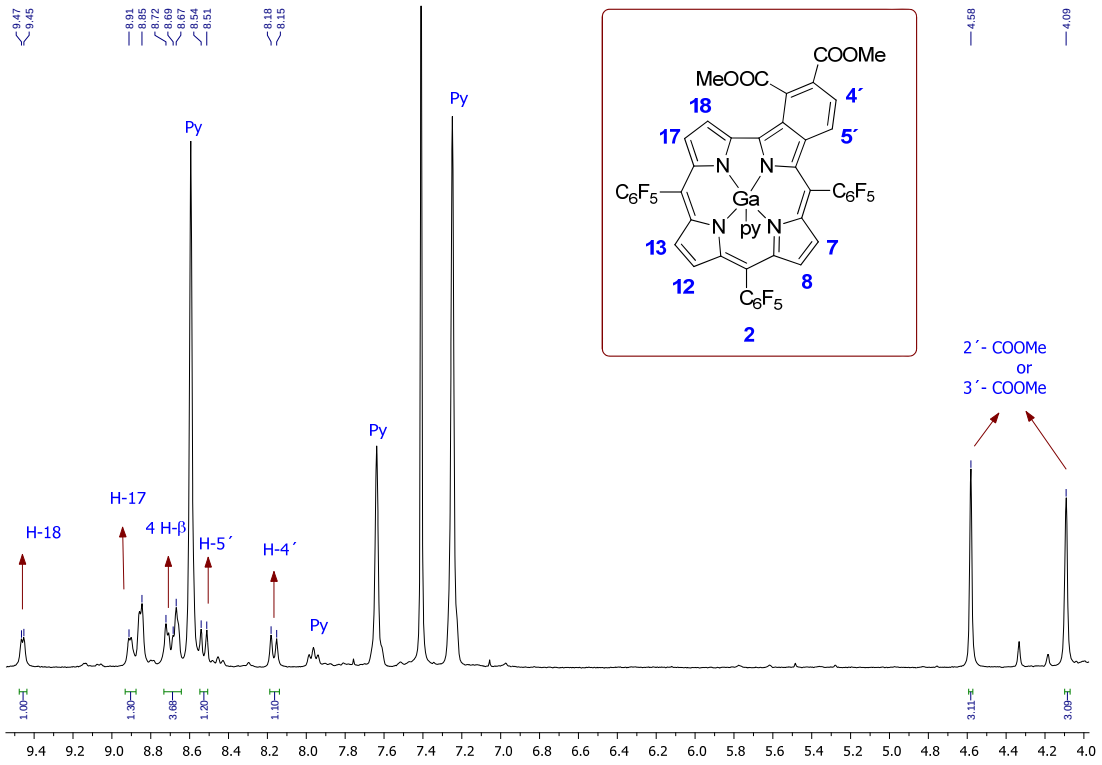

Figure 1- Partial ^{1}H NMR spectrum of corrole **2** in $CDCl_3$ with a few drops of pyridine-d_5.

From the ^{1}H NMR spectrum of compound **3** it was possible to assign in the aromatic region, two singlets at δ 10.53 and 9.66 corresponding to the resonances of protons H-6' and H-2 and a doublet at δ 9.12 due to the resonance of proton H-18. In the same region, it was also possible to identify four signals, three doublets at δ 8.68, 8.53 and 8.49 ppm and a multiplet at 8.77-8.72 ppm corresponding to the resonances of the remaining five *β*-pyrrolic protons. In the aliphatic region were identified four singlets at δ 4.23, 3.95, 3.86 and 3.80, corresponding to the resonances of the methyl ester groups (Figure 2).

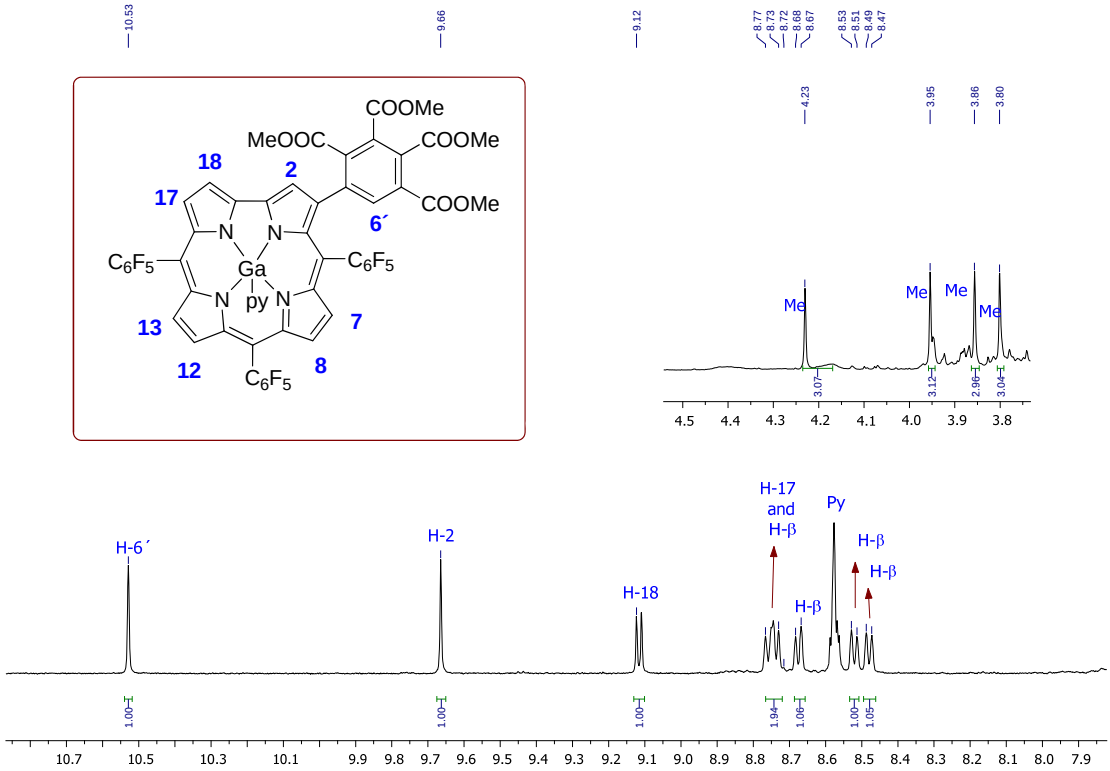

Figure 2- Partial ^{1}H NMR spectrum of the aromatic and aliphatic regions of corrole **3** in $CDCl_3$ with a few drops of pyridine-d_5.

3.2.2 The sensing ability of corroles 2 and 3 in solution

3.2.2.1 Photophysical characterization

The photophysical characterization of compounds **2** and **3** was performed in toluene solution at 298 K. The benzocorrole **2** shows the highly intense Soret band at 440 nm and two weak Q bands at 590 and 614 nm. The *β*-substituted corrole **3** exhibits the Soret band at 443 nm and the two weak Q bands at 596 nm and 616 nm. The emission bands of highest energy of the compounds **2** and **3** are centered at 616 and 618 nm, respectively. Some selected photophysical data are reported in Table 1.

Compounds	λ_{max} (log ε)/nm	λ_{em} (nm)	Δλ (nm)	Φ
2	440 (5.21); 590 (3.82); 614 (3.08)	616	26	0.24
3	443 (5.21); 596 (3.78); 616 (3.17)	618	22	0.08

Table 1- Selected photophysical data of compounds 2 and 3 in toluene

As an example, figure 3 shows the absorption (only Q bands region), emission and excitation spectra in toluene of compound **2**. Notice that, a careful inspection of figure 3 rules out the presence of any emissive impurity due to the total overlap between the absorption and excitation spectra. The fluorescence quantum yield of β-substituted corrole **3** (ϕ =0.08) is relatively lower than that obtained with the benzocorrole **2** (ϕ =0.24). The high value observed by derivative **2** is probably related with conformation issues, with the increase of the rigidity of the molecular structure.[22] It is known that in a rigid structure the radiationless deactivation due to rotation or vibration of fluorophore side groups is minimized, and that, in these conditions, the compounds can show higher values of fluorecence quantum yield. Compound 2 is the most rigid one having then a major value of fluorescence quantum yield.

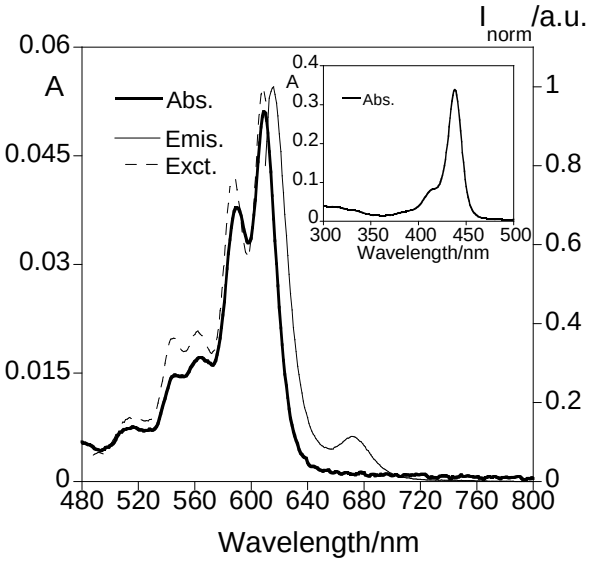

Figure 3 - Room temperature absorption (Q region) (bold line), normalized emission (full line, λ_{exc}=590 nm) and excitation spectra (dotted line, λ_{em}= 620nm) of compound **2** in toluene. Inset:Absorption spectrum of compound **2** (Soret band region).

3.2.2.2 Spectrophotometric and spectrofluorimetric titrations and fluoride, cyanide, acetate and phosphate sensing effects.

The sensorial ability of compounds **2** and **3** for spherical (F^-), linear (CN^-) and bulky anions (CH_3COO^- and $H_2PO_4^-$) was carried out by the increasing addition of the corresponding tetrabutylammonium salts to a solution of each corrole derivatives. The titrations were followed by absorption and emission fluorescence spectroscopy in toluene. The addition of F^- anion produces spectral changes in the ground and excited states of compounds **2** and **3**, as can be observed in Figure 4. In all compounds in the ground state a red shift from *ca* 440 to 450 nm followed by a small decrease in the absorbance is noticed in the Soret type band (see figure 4 Aa). In the Q-bands region upon addition of F^- to derivative **2** a red shift from 590 to 600 nm and from 616 to 620 nm is detected, as well as, an increase in the absorbance at 600 and 620 nm (see figure 4A). In the emission spectra a red shift from 616 to 630 nm, accompanied by a quenching of 40% is visualized (see figure 4B). A similar behaviour was observed for compound **3**. Considering the absorption spectrum of **3** (see figure 4C) the titration with F^- is responsible for a decrease in the band at 596 nm and an increase in the one at 606 nm, accompanied by a red-shift from 596 to 606 nm and from 618 to 624 nm. In the excited state a quenching at 618 nm of *ca.* 40% occurred, followed by a red-shift from 618 to 635 nm (see figure 4D).

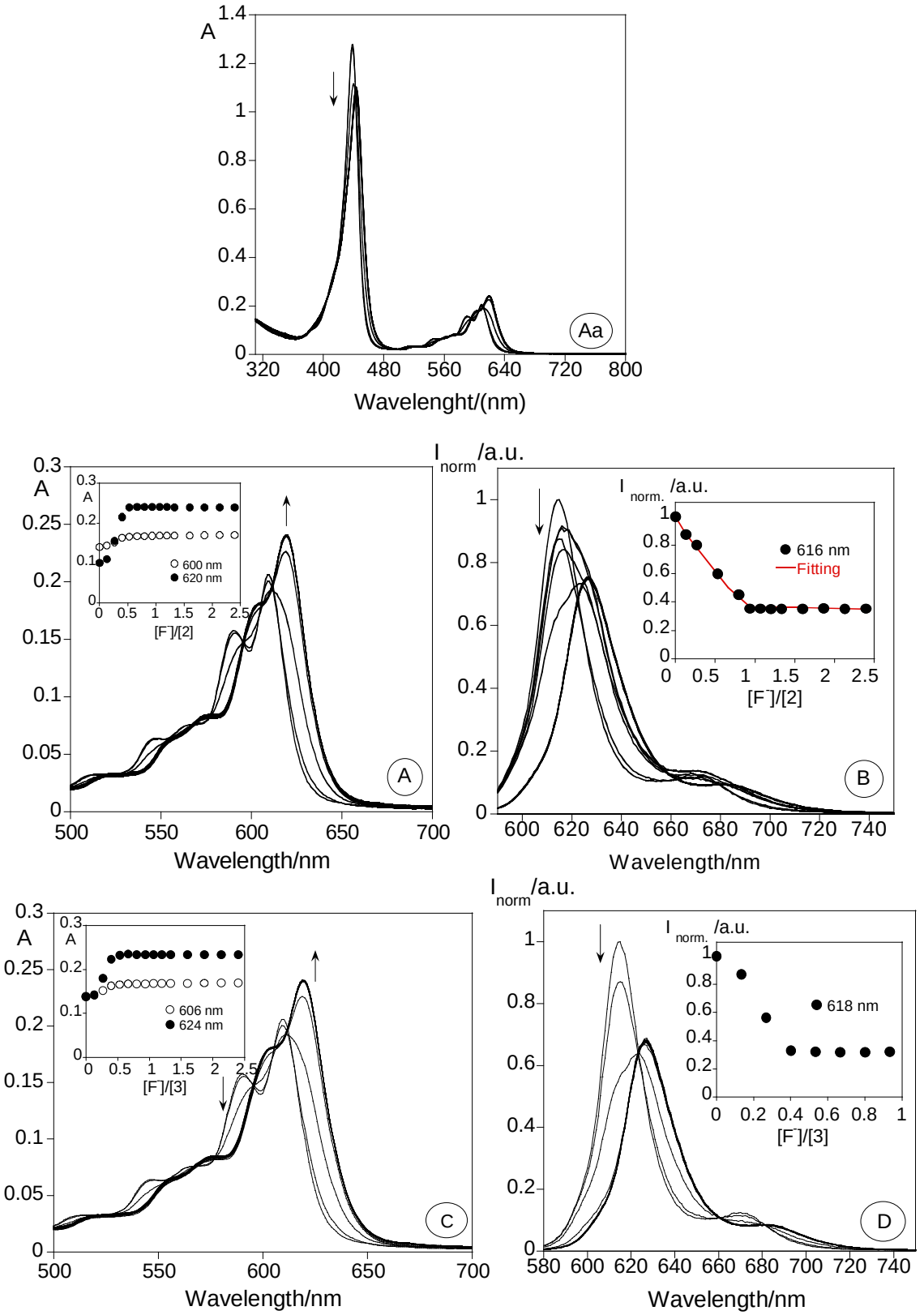

Figure 4- Spectrophotometric (Aa, A, C) and spectrofluorimetric (B, D) titration of compounds **2** (**Aa,** A, B) and **3** (C, D) with the addition of F^- in toluene. The inset represents the absorption at 600, 620 nm (A), 606, 624 nm (C) and the emission intensity at 616 nm (B), 618 nm (D) as a function of $[F^-]/[\mathbf{2}]$, $[F^-]/[\mathbf{3}]$ ($[\mathbf{2}] = [\mathbf{3}] = 1 \times 10^{-5}$M, λ_{exc2}= 590 nm, λ_{exc3}= 596 nm,T=298 K).

Figure 5 shows the absorption (ground state; Q band region,) and emission (excited state) spectra of compounds **2** and **3** with the increasing amount of cyanide. For compound **2** in the Q band region, a red shift from 590 to 605 nm and from 616 to 630 nm, with an absorbance increase at 630 nm are detected. These alterations are accompanied by a colour change from *green* to *colourless* (see figure 5A). Compound **2** shows to be colorimetric, being its interaction with the anions cyanide naked-eye detectable. A red shift in the emission spectra of **2** from 616 to 637 nm is detected, as well as an emission quenching at 616 nm (see figure 5B). For compound **3** in the ground state it is also detected a red shift from 596 to 607 nm (see figure 5C). Subsequently, in the excited state a red shift from 618 to 636 nm, is perceived, as well as, a turn-off in the emission intensity at 618 nm (see figure 5D).

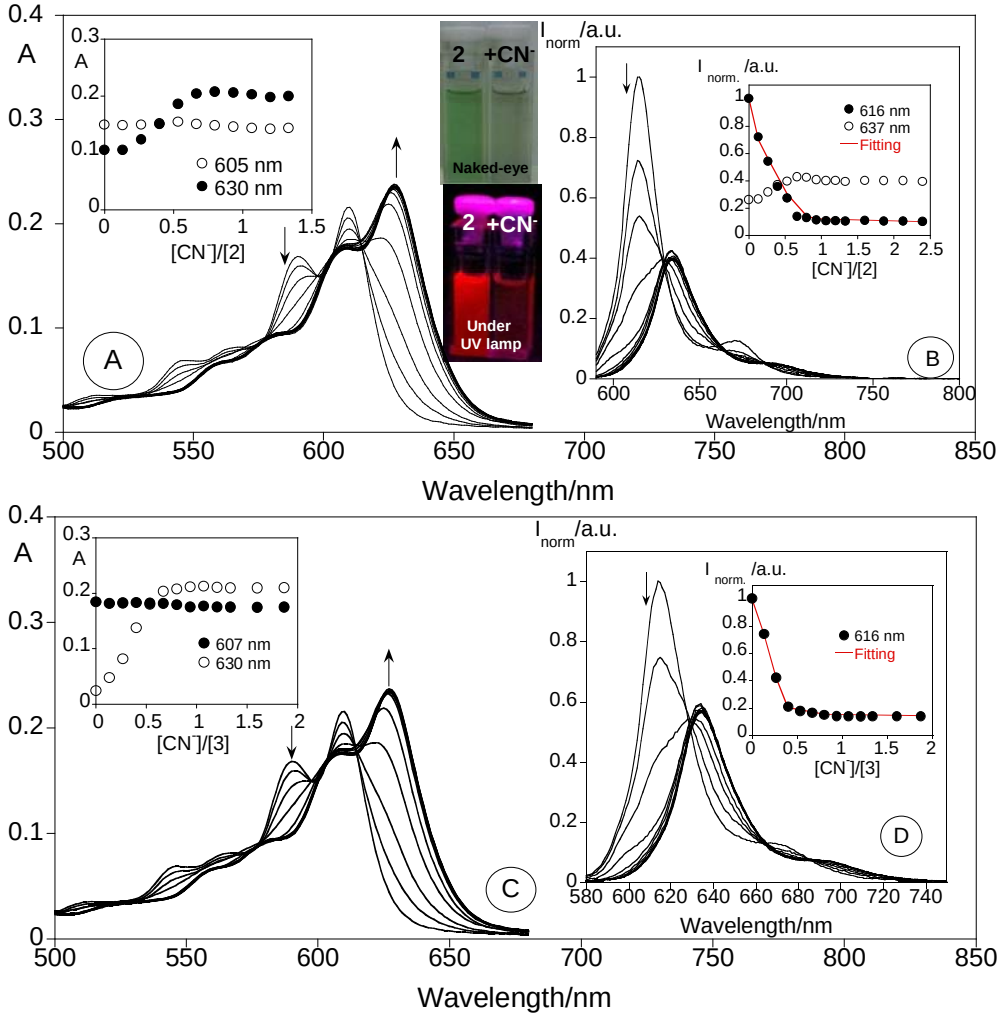

Figure 5 - Spectrophotometric (A, C) and spectrofluorimetric (B, D) titration of compounds **2** (A, B) and **3** (C, D) with the addition of CN^- in toluene. The inset represents the absorption at 605, 630 nm (A), 607, 630 nm (C) and the emission intensity at 616, 637 nm (B), 616 nm (D) as a function of $[CN^-]/[\mathbf{2}]$, $[CN^-]/[\mathbf{3}]$ ($[\mathbf{2}] = [\mathbf{3}] = 1 \times 10^{-5}$M, λ_{exc2}= 590 nm, λ_{exc3}= 596 nm, T=298 K).

The bulky anions as acetate and phosphate can be found in food additives and in agricultural fertilizers.[8] Their interactions with corrole **2** did not produce changes in the ground state (see figure 6A and 6C). However, in the excited state a quenching of *ca* 40% at 616 nm was observed for macrocycle **2** in the presence of CH_3COO^- and $H_2PO_4^-$ anions (see figure 6B and 6D). A different situation occurs with corrole **3** where no changes in the ground and excited state were observed, during the titrations performed with the anions above referred.

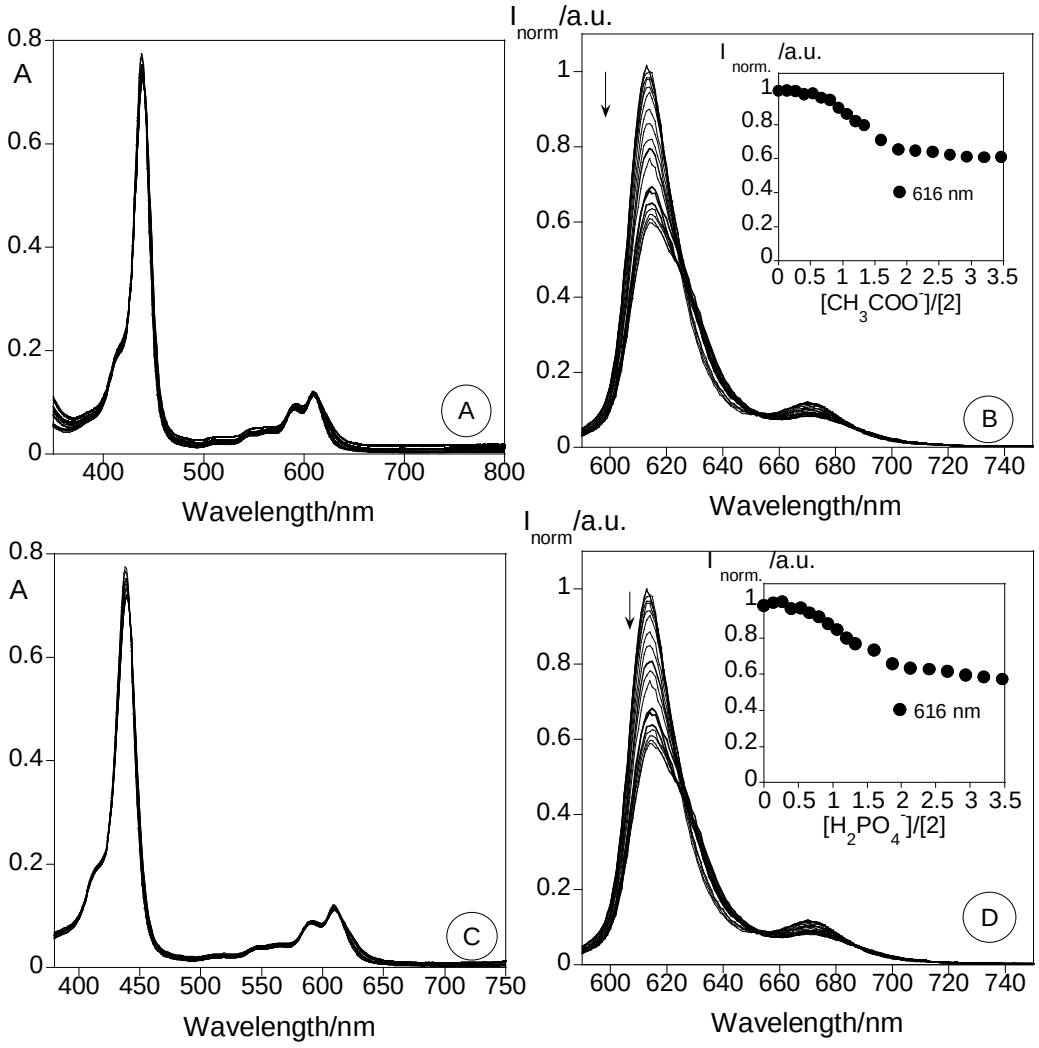

Figure 6 -- Spectrophotometric (A, C) and spectrofluorimetric (B, D) titration of compound 2 with the addition of CH_3COO^- and $H_2PO_4^-$ in toluene. The inset represents the emission intensity at 616 nm for (B) and (D) as a function of $[CH_3COO^-]/[2]$ and $[H_2PO_4^-]/[2]$ ($[2] = 1 \times 10^{-5}$M, λ_{exc2}= 590 nm, T=298 K).

The association constants for anions interaction were determined using the HypSpec program[23] and the main results are gathered in Table 2. For both compounds, the highest association constants were obtained for cyanide anion (corrole **3** Log $K_{ass.}$ = 6.82 ± 0.02) and (corrole **2** Log $K_{ass.}$ = 6.73 ± 0.02). A stoichiometry of two ligands per anion was postulated for both derivatives. Concerning the sensorial ability of compounds **2** and **3** studied towards cyanide anion and future application of these probes, the detection (LOD) and quantification (LOQ) limits for the analyte (CN^-) were also determined (see table 2). It was found that compounds **2** and **3** are able to detect and quantify a fewer amount of cyanide with values of 0.33-0.34 µM and of 1.00-1.01 µM, respectively.

Table 2- Association constants, detection (LOD) and quantification (LOQ) limits of compounds 2 and 3. [LOD and LOQ were measured at 616 and 618 nm for 2 and 3].

Compound	Anion	Log K_{ass}	A:L	LOD (µM)	LOQ (µM)
2	F^-	5.48±0.02	(2:1)	-	-
	CN^-	6.73±0.02	(2:1)	0.33	1.00
	CH_3COO^-	4.28±0.02	(2:1)	-	-
	$H_2PO_4^-$	3.78±0.02	(2:1)	-	-
3	F^-	5.86±0.01	(2:1)	-	-
	CN^-	6.82±0.02	(2:1)	0.34	1.01

3.3 Conclusions

Two new corrole derivatives **2** and **3** were synthetized and fully characterized. Corrole **2** shows a colorimetric behaviour in the presence of cyanide, whereas a change of colour from *green* to *colourless* was visualized. Corroles **2** and **3** show good affinity for cyanide presenting the highest association constant for the tested anions. At the same time, the low detection and quantification limits obtained for corrole derivatives **2** and **3** opens new avenues for their future application in real environmental samples.

3.4 Experimental

3.4.1. Materials

$(CH_3CH_2CH_2CH_2)_4NF$, $(CH_3CH_2CH_2CH_2)_4N(CN)$, $(CH_3CH_2CH_2CH_2)_4N(CH_3CO_2)$, $(CH_3CH_2CH_2CH_2)_4NCl$, $(CH_3CH_2CH_2CH_2)_4N(H_2PO_4)$ salts were purchased from Sigma-Aldrich and dimethyl acetylenedicarboxylate were obtained from Alfa Aesar. All these chemicals were used without further purification. The solvents were obtained from Panreac and Riedel-de Haen and used as received or distilled and dried using standard procedures.

3.4.2. Physical measurements

Elemental analyses were carried out with a Fisons Instruments EA1108 microanalyser at the University of Vigo (CACTI), Spain. ^1H and ^{19}F NMR spectra were recorded on Bruker Avance 300 (at 300 and 282 MHz, respectively) spectrometer. $CDCl_3$ and pyridine-d_5 were used as solvents with tetramethylsilane (TMS) as the internal reference; the chemical shifts are expressed in δ (ppm) with the coupling constants (*J*) in Hertz (Hz). Unequivocal ^1H assignments were made using 2D COSY experiments (mixing time of 800 ms). Preparative thin-layer chromatography (TLC) was carried out on 20 × 20 cm glass plates coated with silica gel (0.5 mm thick). Analytical TLC was carried out on precoated sheets with silica gel (Merck 60, 0.2 mm thick).

3.4.3. Spectrophotometric and spectrofluorimetric measurements

Absorption spectra were recorded on a JASCO V-650 Spectrophotometer and the fluorescence emission on a Spectrofluorimeter HORIBA-JY Scientific Fluromax-4. The linearity of the fluorescence emission versus the concentration was checked out in the concentration used (10^{-4} – 10^{-6} M). A correction for the absorbed light was performed when necessary. The spectrometric characterizations and titrations were performed as follows: the stock solutions of compounds **2** and **3** (*ca*. 10^{-3} M) were prepared by dissolving an appropriated amount of each compound in a 10 mL volumetric flask and diluting it to the mark with toluene. The solutions were prepared by appropriate dilution of the stock solutions up to 10^{-5} – 10^{-6} M. Titrations of compounds **2** and **3** were carried out by adding microliter amounts of standard solutions of the anions in DMSO.

Fluorescent quantum yields of compounds **2** and **3** were measured using a solution of cresyl violet perchlorate in absolute ethanol as a standard ([ϕ]=0.54)[24] and was corrected

for different refraction indexes of solvents. The limit of detection (LOD) and the limit of quantification (LOQ) for the anions were performed, having in mind their use for real anion detection and for analytical applications. For these measurements, ten different analyses for the selected receptor were performed in order to obtain the LOQ. The LOD was obtained by applying the formula:

$$Y_{dl} = y_{blank} + 3std$$

where y_{dl} = signal detection limit and std =standard deviation

3.4.4. Synthesis of corrole ligands.

The precursor gallium(III) complex of 3-vinyl-5,10,15-tris(pentafluorophenyl)corrole **1** was synthesized according to the procedures described in chapter II.[17]

3.4.4.1. General procedure for preparing compounds 2 and 3.

A solution of **1** (0.025 mmol) and the dienophile (dimethyl acetylenedicarboxylate) (0.050 mmol) in toluene (0.5 mL) was gently refluxed for 48 h under a nitrogen atmosphere. After cooling to room temperature, the solvent was evaporated and the compounds **2**, and **3** were separated and further purified by preparative TLC (silica: hexane–ethyl acetate–pyridine (15:5:0.1)). Compound **2** and **3** were obtained after crystallization in dichloromethane/methanol in 81% and 16% yield respectively.

Compound 2:

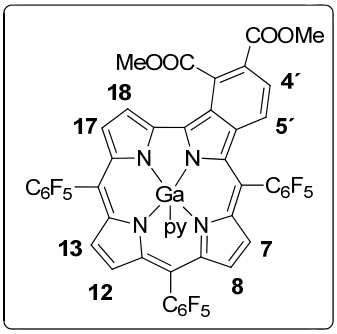

^{1}H NMR (300.13, $CDCl_3$, few drops of pyridine-d_5): δ 9.47 (d, 1 H, *J* 3.6 Hz, H-18), 8.91 (d, 1H, *J* 3.6 Hz, H-17), 8.72-8.67 (m, 4 H, H-β), 8.53 (d, 1 H, *J* 8.7 Hz, H- 5'), 8.17 (d, 1 H, *J* 8.7 Hz, H- 4'), 4.58 (s, 3H, 3'-CO_2Me), 4.09 (s, 3H; 2'-CO_2Me).^{19}F NMR (282.37, $CDCl_3$, a few drops of pyridine-d_5): δ -161.49 to -161.69 (m, 6F, F_{orto}), -175.38 (t, 1F, *J* = 21.1 Hz, F_{para}), -177.38 (t, 1F, *J* 21.3 Hz, F_{para}), -177.57 (t, 1F, *J* 21.1 Hz, F_{para}), -184.85 to -185.14 (m, 2F, F_{meta}), -185.89 to -186.15 (m, 2F, F_{meta}), -186.15 to -186.42 (m, 2F, F_{meta}).

MALDI-MS *m/z*: 1029 $[M+H]^+$. Anal. calc. for $C_{45}H_{14}F_{15}GaN_4O_4$: C, 52.51; H, 1.37; N, 5.44; found: C, 52.48; H, 1.46; N, 5.47%.

Uv-Vis λ_{max} (log ε) Toluene: 418 (sh), 440 (5.21), 590 (3.82), 614 (3.08) nm.

Yield: 81%. Colour: Green.

Compound 3:

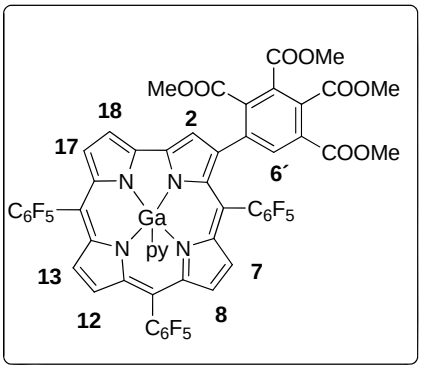

^{1}H NMR (300.13, $CDCl_3$, few drops of pyridine-d_5): δ 10.53 (s, 1 H, H-6´), 9.66 (s, 1 H, H-2), 9.12 (d, 1 H; *J* 4.1 Hz, H-18), 8.77-8.73 (m, 2 H, H-β and H-17), 8.68 (d, 1 H, *J* 4.7 Hz, H-β), 8.53 (d, 1 H, *J* 4.7 Hz, H-β), 8.49 (d, 1 H, *J* 4.5 Hz, H-β), 4.23 (s, 3H, CO_2Me), 3. 95 (s, 3H, CO_2Me), 3.86 (s, 3H, CO_2Me), 3.80 (s, 3H, CO_2Me). ^{19}F NMR (282.37, $CDCl_3$, a few drops of pyridine-d_5): δ -161.41 (dt, 4F, *J* 23.5, 11.8 Hz, F_{orto}); -162.19 (dd, 2F, *J* 24.5, 8,4 Hz, F_{orto}),), -176.19 to -176.40 (m, 1F, F_{para}), -176.67 (t, 1F, *J* 21.0 Hz, F_{para}); -185.17 to -185.42 (m, 2F, F_{meta}), -185.49 to -185.69 (m, 2F, F_{meta}), -185.76 to -185.95 (m, 2F, F_{meta}).

MALDI-MS *m/z* 1171 $[M+H]^+$. Anal. calc. for $C_{51}H_{20}F_{15}GaN_4O_{8.1/3}$Py: C, 52.81 ; H, 1.82; N, 5.07; found: C, 52.62 ; H, 1.50; N, 5.39.

UV-Vis λ_{max} (log ε) Toluene: 417 (sh), 443 (5.21), 596 (3.78), 616 (3.17) nm.

Yield: 16%. Colour: Brownish Green.

3.5 References:

[1] (a) Duke, R. M.; Veale, E. B.; Pfeffer, F. M.; Kruger, P. E.;Gunnlaugsson, T. *Chem. Soc. Rev.* **2010**, 39, 3936-3953. (b) Galbraith, E.; James, T. D. *Chem. Soc. Rev.* **2010**, 39, 3831-3842. (c) Amendola, V.; Esteban-Gómez, D.;Fabbrizzi, L.;Licchelli, M. *Acc. Chem. Res.* **2006**, 39, 343-353. (d) Gale, P. A. *Coord. Chem. Rev*. **2001**, 213, 79-128. (e) Sessler, J. L.; Davis, J. M. *Acc. Chem. Res.* **2001**, 34, *989*-997. (f) Martínez, R.; Sancenon, F. *Chem. Rev*. **2003**, 103, 4419-4476. (g) Gunnlaugsson, T.; Glynn, M.; . Tocci, G. M.; Kruger, P. E.; Pfeffer, F. M. *Coord. Chem. Rev*. **2006**, 250, 3094-3117. (h) Hudson, Z. M.; Wang, S. *Acc. Chem. Res*. **2009**, 42, 1584-*1596*. (i) Swinburne, A. N.; Paterson, M. J.; Beeby, A.; Steed, J. W. *Chem. Eur. J.* **2010**, 16, 2714-2718. (j) Zeng, Z. H.; Torriero, A.A.J.; Bond, A. M.; Spiccia, L. *Chem. Eur. J.* **2010**, 16, 9154-9163.

[2] (a) Wade, C. R.; Broomsgrove, A. J.; Aldridge, S.; Gabbai, F. P. *Chem. Rev*. **2010**, 110, 3958- 3984. (b) Xu, Z.; . Kim, S. K.; Han, S. J; Lee, C.; Kociok-Kohn, G.; James, T. D.; Yoon, J. *Eur. J. Org. Chem.* **2009**, 3058-3065. (c) Lam, S. T.; Zhu, N.; Yam, V. W. W. *Inorg. Chem*. **2009**, 48, 9664-9670. (d) Broomsgrove, A. E. J.; Addy, D. A.; Bresner, C.; Fallis, I. A.; Thompson, A. L.; Aldridge, S. *Chem. Eur. J.* **2008**, 14, 7525-7529. (e) Perry-Feigenbaum, R.; Sella, E.; Shabat, D. *Chem. Eur. J.* **2011**, 17, 12123-12128.

[3] (a) Horowitz, H. S. *J. Public Health Dent*. **2003**, 63, 3. (b) Farley, J. R.; Wergedal, J. E.; Baylink, D. J. *Science* **1983**, 222, 330-332. (c) Kleerekoper, M. *Endocrinol. Metab. Clin. North Am.* **1998**, 27, 441- 452.

[4] Water: Basic Information about Regulated Drinking Water Contaminants, United States Environmental Protection Agency (EPA) (http://water.epa.gov/drink/contaminants/basicinformation/fluoride. cfm/).

[5] (a) Gale, P. A. *Chem. Commun.* **2011**, 47, 4902-4904. (b) Beer, P. D.; Gale, P. A. *Angew. Chem. Int. Ed*, **2001**, 40, 486-516.

[6] (a) Liu, Z. Q.; Shi, M.; Li, F. Y.; Fang, Q.; Chen, Z. H.; Yi, T.; Huang, C. H. *Org. Lett.* **2005**, 7, 5481-5484. (b) Xu, W. J.; Liu, S. J.; Zhao, X.Y.; Sun, S.; Cheng, S.; Ma, T.C.; Sun, H. B.; Zhao, Q.; Huang, W. *Chem. Eur. J.* **2010**, 16, 7125-7133. (c) Liu, X. J.; Bai, D. R.; Wang, S. N. *Angew. Chem.* **2006**, 118, 5601-5605. (d) Zhao, C. H.; Sakuda, E.; Wakamiya, A.; Yamaguchi, S. *Chem. Eur. J.* **2009**,15, 10603-10612. (e) Kubo, Y.; . Ishida, T.; Kobayashi, A.; James, T. D, *J. Mater. Chem.* **2005**, 15, 2889-2895.

[7] Hachiya, H.; Ito, S.; Fushinuki, Y.; Masadome, T.; Asano, Y.; . Imato, T. *Talanta* **1999**, 48, 997- 1004.

[8] Guidelines for Drinking-Water Quality, World Health Organization, Geneva, **1996**.

[9] Gee, H. C.; Lee, C. H.; Jeong, Y. H.; Jang, W. D. *Chem. Commun.* **2011**, 47, 11963-11965.

[10] (a) Deep, B.; Balasubramanian, N.; Nagaraja, K. S. *Anal. Lett.* **2003**,2865-2874. (b) Geetha, K.; Balasubramanian, N. *Anal. Lett.* **2001**, 34, 2507-2519. (c) Wang, M.; Luo, D. L. *Chin. J. Anal. Chem.* **2000**, 28, 519- 527. (d) Haj-Hussein, A. T. *Talanta* **1997**, 44, 545-551. (e) Ishii, H.; Kohata, *K. Talanta* **1991**, 38, 511-14.

[11] Kang, J.; Song, E. J.; Kim, Y. H.; Kim, S. J.; Kim, C. *Tetrahedron Lett*. **2013**, 54, 1015-1019.

[12] Sessler J L, Karnas E, Sedenberg E, **2012,** Porphyrins and expanded porphyrins as receptors. In:Philip A, Jonathan W (eds) Supramolecular chemistry: from molecules to nanomaterials, Wiley, Chichester.

[13] (a) He, C. L.; Ren, F. L.; Zhang, F. L.; Han, Z. X. *Talanta* **2006**, 70, 369-364. (b) Aviv-Harel, I.; Gross, Z. *Chem. Eur. J.* **2009**, 15, 8382-8394.

[14] Mahammed; A.; Weaver, J. J.; Gray, H. B.; Abdelas; M.; Gross, Z. *Tetrahedron Lett.* **2003**, 44, 2077-2079.

[15] (a) Kubo, Y.; Kobayashi, A.; Ishida, T.; Misawa, Y.; James, T. D. *Chem. Commun.* **2005**, 2846- 2848. (b) Koskela, S. J. M.; Fyles, T. M.; James, T. D. *Chem. Commun*. **2005**, 945-947. (c) Kubo, Y.; Yamamoto, M., Ikeda, M.; Takeuchi, M.; Shinkai, S.; Yamaguchi, S.; Tamao, K. *Angew. Chem.* **2003**, 115, 2082-2086. (d) Boiocchi, M.; Boca, L. D.; Gomez, D. E.; Fabbrizzi, L.; Licchelli, M.; Monzani, M., *J. Am. Chem. Soc*. **2004**, 126, 16507-16514.

[16] (a) Barata, J. F. B.; Santos, C. I. M.; Faustino, M. A. F.; Neves, M. G. P. M. S.; Cavaleiro, J. A. S. *Topics Heterocyclic Chemistry.* **2013**, 11, 79-142. (b) Barata, J. F. B.; Silva, A. M. G.; Faustino, M. A. F; Neves, M. G. P. M. S.; Tomé, A. C.; Silva, A. M. S; Cavaleiro, J. A. S. *Synlett* **2004**, 7, 1291- 1293.(c) Vale, L. S. H. P.; Barata, J. F. B.; Faustino, M. A. F.; Neves, M. G. P. M. S.; Tomé, A. C.; Silva, A. M. S.; Cavaleiro, J. A. S. *Tetrahedron Lett.* **2007**, 48, 8904- 8908. (d) Barata, J. F. B.; Neves, M. G. P. M. S.; Tomé, A.C.; Cavaleiro, J.A.S- *J. Porphyrins Phthalocyanines* **2009**, 13, 415- 418.

(e) Vale, L. S. H. P.; Barata, J. F. B.; Santos, C. I. M; Neves, M. G. P. M. S.; Faustino, M. A. F.; Tomé, A. C.; Silva, A. M. S.; Paz, F. A. A.; Cavaleiro, J. A. S. *J. Porphyrins Phthalocyanines* **2009**, 13, 418-424.

[17] (a) Santos, C. I. M.; Oliveira, E.; Barata, J. F. B.; Faustino, M. A. F.; Cavaleiro, J. A. S; Neves, M. G. P. M. S.; Lodeiro, C. J. Mater. Chem. 2012, 22, 13811-13819. (b) Lodeiro, C.; Capelo, J. L; Mejuto, J. C.; Oliveira, E.; Santos, H. M; Pedras, B.; Nunez, C. *Chem. Soc. Rev.* **2010**, 39, 2948- 2976. (c) Santos, C. I. M.; Oliveira, E.; Menezes, J. C. J. M. D. S.; Barata, J. F. B.; Faustino, M. A F: Ferreira, V. F.; Cavaleiro, J. A. S; Neves, M. G. P. M. S.; Lodeiro, C. *Tetrahedron*, *in press*, (d) Santos, C. I. M; Oliveira, E.; Fernández-Lodeiro, J.; Barata, J. F. B.; Santos, S. M.; Faustino, M. A. F.; Cavaleiro, J. A. S; Neves, M. G. P. M. S.; Lodeiro, C. *Inorg. Chem*. DOI: 10.1021/ic4006295.

[18] Gryko, D. T.; Koszarna, B. *Org. Biomol. Chem.* **2003**, 1, 350- 357.

[19] Bendix J.; Dmochowski, I. J.; Gray, H. B.; Mahammed, A.; Simkhovich, L.; Gross, Z. *Angew. Chem. Int. Ed*. **2000**, 39, 4048-4051.

[20] (a) Faustino, M. A. F.; Neves, M. G. P. M. S.; Tomé, A. C.; Silva, A. M. S; Cavaleiro, J. A. S. *Arkivoc* **2005**, 10, 332- 343. (b) Faustino, M. A. F; Neves, M. G. P. M. S.; Vicente, M. G. H.; Silva, A. M. S.; Cavaleiro, J.A.S. *Tetrahedron Lett.* **1996**, 37, 3569-3570.

[21] (a) Domínguez, G.; Pérez-Castells, J.; Chem. Soc. Rev., 2011, **40**, 3430–3444. (b) Mantovani, L.; Ceccon, A.; Gambaro, A.; Santi, S.; Ganis, P.; Venzo, A.; *Organometallics* **1997,** *16,* 2682-2690.

[22] (a) Rurack, K. *spectrochim.Acta, Part A*. **2001**, 57, 2161-2195. (b) Lakowicz, J. R. *Principles of Fluorescence Spectroscopy*, 3rd ed.; Springer: New York, **2006**;

[23] Gans, P.; Sabatini, A; Vacca, A. *Talanta* **1996**, 43, 1739-1753.

[24] (a) Berlman, I. B. *Handbook of Fluorescence Spectra of Aromatic Molecules, Academic Press*, New York, 2nd edn, **1971**. (b) Montalti, M.; Credi, A.; Prodi., L.; Gandolfi, M.T. *Handbook of Photochemistry,* Taylor & Francis, Boca Raton, 3rd edn, **2006**.

Chapter IV

New coumarin-corrole and -porphyrin conjugate as multifunctional probes for anionic or cationic interactions: Synthesis, spectroscopy and solid supported studies

Published in *Tetrahedron, **2013**, in Press.*
doi.org/10.1016/j.tet2013.07.022

INDEX

4- New coumarin-corrole and –porphyrin conjugate as multifunctional probes for anionic or cationic interactions: Synthesis, spectroscopy and solid supported studies

Resumo

Os corróis e as porfirinas possuem características que fazem destes macrociclos potenciais sondas para a deteção de aniões e catiões. Neste trabalho é apresentada, não só, a síntese e caracterização de conjugados do tipo corrol-cumarina (**7** - **8**), mas também**,** a sua habilidade sensorial para a deteção de aniões. Os novos derivados corrólico resultaram de reações de Hetero-Diels-Alder entre o complexo de gálio do 3-vinil-5,10,15-tris(pentafluorofenil)corrole **2** e *orto*-quinodimetanos gerados *in situ* a partir de reacções de Knoevenagel entre cumarinas e paraformaldeído.

A habilidade sensorial dos conjugados **7** e **8** foi avaliada, em tolueno, na presença de aniões esféricos (F^-, Cl^-), lineares (CN^-) e volumosos (CH_3COO^-). Estes estudos sensoriais foram também realizados com conjugados porfirina-cumarina análogos **3** e **4**. Foi ainda avaliada a habilidade sensorial dos conjugados do tipo porfirina-cumarina de base-livre **5** e **6**, na presença dos catiões Na^+, Ca^{2+}, Zn^{2+}, Cd^{2+}, Pb^{2+}, Fe^{2+}, Ba^{2+}, Cu^{2+}, Ag^+ e Hg^{2+}, tendo-se assistido a um efeito colorimétrico (mudança de cor de roxo para amarelo) e a uma inédita seletividade para o Hg^{2+}.

A inserção de uma unidade cumarina conferiu solubilidade aos macrociclos, estes tornaram-se solúveis em etanol. O conjugado porfirina-cumarina de base-livre **5** foi completamente estudado numa mistura de etanol:água (50:50) e apresentou um comportamento análogo ao obtido em tolueno, mas com uma constante de associação para Hg^{2+} superior. Neste sistema de solventes o derivado **5** conseguiu detectar e quantificar o catião Hg^{2+} em valores de 0.6 e 1.2 ppm.

Tendo em mente as possíveis aplicações biológicas e ambientais destes conjugados, desenvolveram-se ainda dois suportes sólidos de baixo custo: um polímero de agarose e um de celulose. O suporte sólido à base de celulose revelou um efeito colorimétrico para o catião Hg^{2+} semelhante ao observado em solução.

Por fim, realizaram-se ainda estudos de pH com o conjugado **5**. A baixos valores de pH visualizou-se uma coloração verde e a valores de pH mais elevados uma coloração amarela. Este comportamento foi observado tanto em solução como nos suportes sólidos.

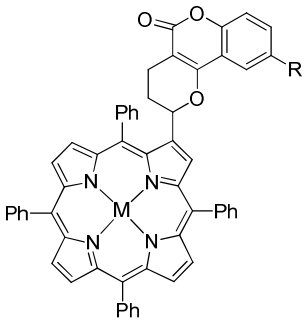

3 M= Zn, R= H
4 M= Zn, R= CH_3
5 R= H
6 R= CH_3

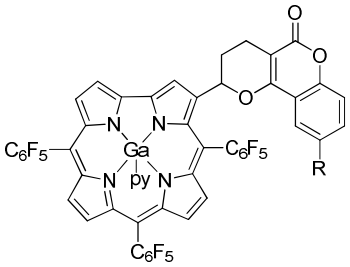

7 R=H
8 R=CH_3

Abstract

Corroles and porphyrins have very promising properties to be used as molecular probes for anion and metal ion detection. Here, we present the synthesis and characterization of two new corrole-coumarin derivatives **7** and **8**. The new corrole-coumarin conjugates resulted from hetero Diels-Alder reaction between the gallium(III) complex of 3-vinyl-5,10,15-tris(pentafluorophenyl)corrole **2** and *o*-quinone methides (*o*-QM) generated *in situ* from Knoevenagel reactions of 4-hydroxycoumarin or 4-hydroxy-6-methylcoumarin with paraformaldehyde.

The sensing ability of the conjugates **7** and **8** was studied in toluene, in the presence of spherical (F^-, Cl^-), linear (CN^-) and bulky anions (CH_3COO^-). These sensorial studies were extended to porphyrin-coumarin analogues **3** and **4**. Porphyrin free-base conjugates **5** and **6** were also studied with Na^+, Ca^{2+}, Zn^{2+}, Cd^{2+}, Pb^{2+}, Fe^{2+}, Ba^{2+}, Cu^{2+}, Ag^+ and Hg^{2+}, showing a colorimetric effect (colour change from purple to yellow) and an unprecedented selectivity for Hg^{2+}.

The insertion of the coumarin moiety confers an unusual solubility of these conjugates in ethanol. The porphyrin free-base conjugate **5** was fully studied in a mixture EtOH:H_2O (50:50) and showed a similar behaviour with Hg^{2+}. Under these conditions, the conjugate **5** presented a higher association constant than in toluene and was able to detect and quantify a minimal amount of 0.6 ppm and 1.2 ppm of Hg^{2+}, respectively. Having in mind the biological and environmental application of these conjugates, non-expensive solid supports, like agarose and natural cellulose polymers were developed. In the cellulose support material (filter paper) the colorimetric effect for Hg^{2+} reveals a similar behaviour as in solution.

In addition pH studies carried out with the same conjugate showed a green colour at low pH and a yellow colour at high pH values in solution and in solid supports.

4.1 Introduction

Corroles and porphyrins are excellent candidates for a great variety of sensing material applications. Chemosensors based on these tetrapyrrolic macrocycles are being pursued as active materials owing to their large absorption coefficient and well tunable fluorescence emission.[1-6.]

Porphyrin combined with other classes of molecules have been used as fluorophores in the detection of heavy metals like Cd(II), Pb(II) and Hg(II).[7] Also, metalloporphyrins, depending on the metal ion incorporated into the inner core of the complex, offers an excellent method to develop ion-selective electrode and optical sensor devices.[8] In particular, optical sensors based on porphyrinic complexes of Zn(II), Cd(II) and Hg(II) with amide functionality have shown higher anion binding abilities in more competitive solvent medium than those with metals like Fe(III), Co(III), Ni(II) and Cu(II).[9] For instance, a cage receptor based on tetra-triazole Zn(II) metalloporphyrin shows a naked-eye colorimetric response when strongly bound to anions.[10] Also, a Zn(II)-porphyrin bearing naphthalimide or aza-crown ether-capped moieties created a fluoride ion-triggered dual fluorescence molecular switch,[11] or colour change in the presence of sodium cyanide.[12]

In the case of corroles, these macrocycles coordinate with a large number of metals,[13] and are very promising materials for optical and sensing applications.[14] Although a few number of free-base corroles or their derivatives are being explored as selective sensors for Hg(II) ion,[5,15] the Ga(III) complex is presently a selective sensor for F^- and CN^- ions,[6] which empowers newer corrole derivatives to be explored as sensors for anion selectivity.

A good fluorescent chemosensor must have a strong affinity and selectivity for the analyte, no environmental interferences with the fluorescence signal, and it must be photostable. It should also be easily accessible by organic reactions and be robust in nature. A good strategy to develop new probes or chemosensors is the coupling of two different molecules with well-established sensory activities.

Coumarin derivatives have been utilized as sensors for Hg(II),[16-18] fluoride[19-23] and cyanide[24,25] ions either in organic solvents or aqueous mixtures at biological pH. The inclusion of the coumarin nucleus in the porphyrin or corrole frameworks can enhance the

fluorescence emission and furnish better solubility in aqueous medium. It is reported that coumarins transfer energy to the porphyrin molecule and increase the fluorescence lifetimes.[26,27] Similarly corroles coumarin dyads also have shown efficient energy transfer from the coumarin moiety to corrole.[28,29]

Recently the Aveiro group reported the hetero Diels-Alder reaction of 2-vinyl-5,10,15,20-tetraphenylporphyrinatozinc(II) **1a** with *o*-quinone methides (*o*-QM) generated *in situ* from Knoevenagel reaction of 4-hydroxycoumarin or 4-hydroxy-6-methylcoumarin with paraformaldehyde that afforded respectively, derivatives **3** and **4** (Scheme 1).[30] Using this methodology the authors were able to functionalize the 5,10,15,20-tetraphenylporphyrinatozinc(II) **1b** at the *β*-pyrrolic position with coumarin units.

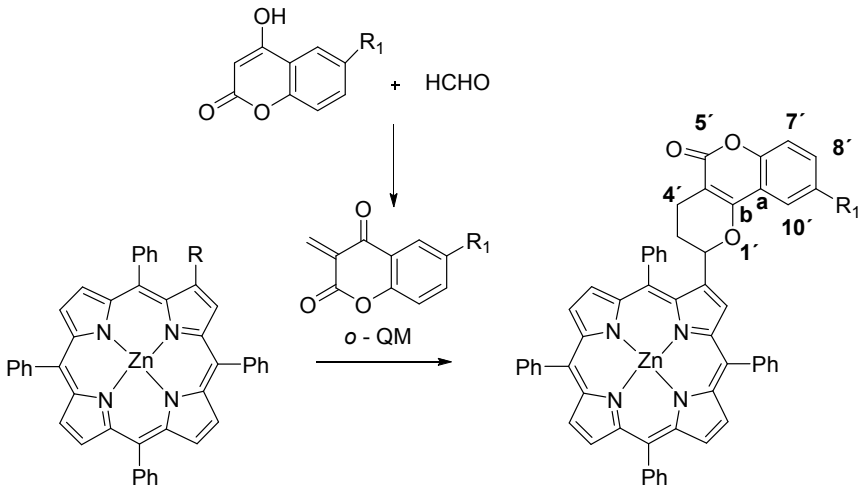

Scheme 1[30]

Following the importance in the development of sensing materials,[31] we envisaged the design of corroles with coumarin moieties **7** and **8** from the recently developed gallium(III)(pyridine) complex of 3-vinyl-5,10,15-tris(pentafluorophenyl)corrole **2** (Scheme 2).[6] The photophysical characterizations of compounds **3**-**6** and **7**-**8** were also carried out. The sensing ability of the metalloconjugates towards the spherical halide ions F^-, Cl^-, the linear anion CN^- and the bulky anion CH_3COO^- was evaluated. Additionally, the interaction of the coumarin-porphyrin conjugates **5** and **6** towards the metal ions Na^+,

Ca^{2+}, Ba^{2+}, Fe^{2+}, Cd^{2+}, Cu^{2+}, Pb^{2+}, Hg^{2+}, Zn^{2+}, Ag^{+} was evaluated. pH studies were also performed with these two free-base conjugates (**5** and **6**).

Considering the environmental monitoring of heavy metals[7] and pH[32] the potential of conjugate **5** was tested using non-expensive natural solid supports, with simple fabrication and handling towards Hg(II) and pH studies. The polymeric materials selected were agarose[33] used in gel electrophoresis, and cellulose. The use of these compounds for on-site Hg(II) detection, was carried out by immersing a filter paper with compound **5** in a solution and drying in air.

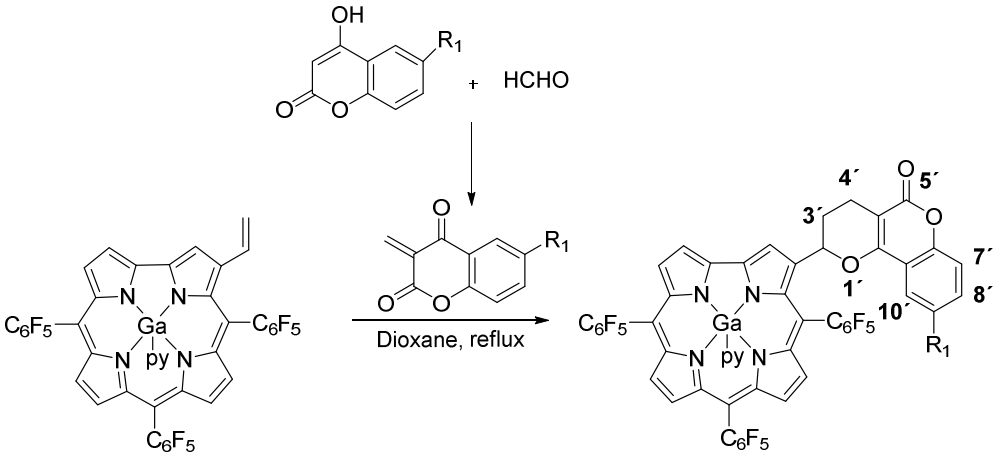

2

7 (92%) R_1=H
8 (87%) R_1= CH_3

Scheme 2

4.2 Results and Discussion

4.2.1 Synthesis and characterization of gallium(III)(pyridine) complex of 3-coumarin-corrole conjugates

Before presenting the synthetic strategy used to obtain the new corrole derivatives some considerations about *o*-quinone methides and their role in cycloaddition reactions will be discussed.

O-quinone methides are very reactive dienes that have been proposed to be intermediates in a large number of chemical and biological transformations and they have been widely used in the synthesis of polycyclic compounds.[34] The precursors used to

generate *o*-quinone methides have a common structural motif: a phenol with a substituent in the *ortho* position that can be readily converted to an alkylidene by elimination of a leaving group. In the most common protocols, these intermediates are generated *in situ* from an *o*-hydroxybenzyl alcohol or a phenol Mannich base by elimination of water or a secondary amine respectively; these eliminations can occur under thermal or photoinduced conditions or in the presence of a Lewis acid. The oxidation of substituted *o*-alkyl phenols and the thermal or photochemically induced cheletropic extrusion of carbon monoxide, or sulfur dioxide are some of the other methods to obtain *o*-quinone methides (Scheme 3).[35]

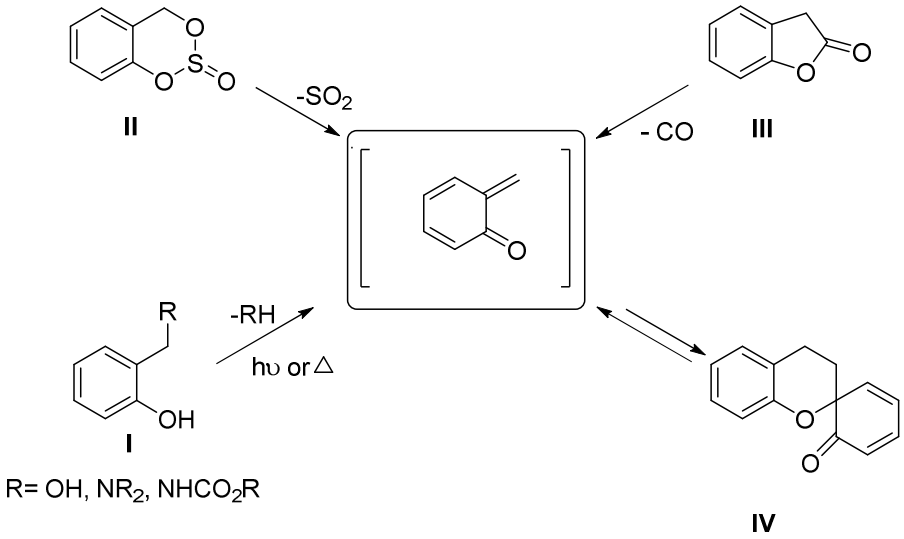

Scheme 3

In general, the *o*-quinone methides can only be isolated when they are part of a π-extended system. Otherwise they are generated in *situ* for direct use in the next step of an intended reaction sequence. These intermediates can be utilized in different type of reactions, namely as acceptors of nucleophiles like carbanions, nitriles, amines, alcohols, thiols, halides and phosphites (Scheme 4).[36]

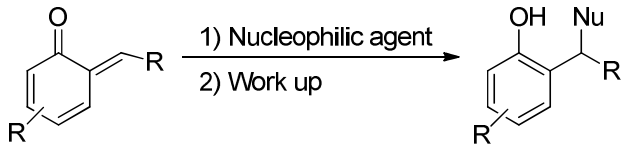

Scheme 4

However the most important and well studied reactions of *o*-quinone methides are [4+2] cycloadditions reactions. In fact, the inter and intramolecular cycloaddition reaction of *o*-quinone methides have been exploited in the elegant syntheses of several natural products.[37] One of the simplest examples of such reactions is given in scheme 5, where a *o*-

quinone methide formed by condensation of a α,β-unsaturated aldehyde with a 1,3-diketone afforded a 2H-pyran-*cis*-dienone system.[38]

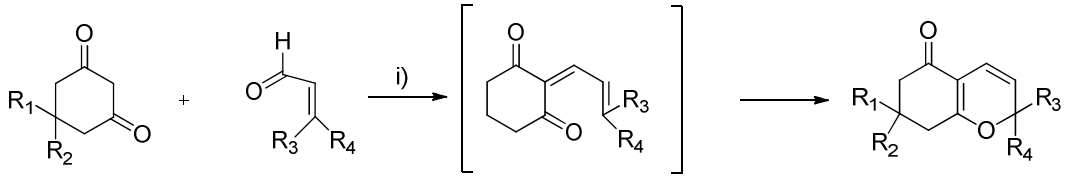

Scheme 5

Considering the tetrapyrrolic macrocycles, Cavaleiro *et al*.[39] also demonstrated that the peripheral double bonds of the porphyrins, in the presence of a reactive *o*-quinone methide can participate in [4+2] cycloadditions as the two-π -electron component.

In this chapter, it was evaluated the reactivity of the gallium(III) (pyridine) complex of 3-vinyl-5,10,15-tris(pentafluorophenyl)corrole **2** as dienophile in the presence of *o*-quinone methides resulting from Knoevenagel reactions. The synthetic strategy used is shown in scheme 2. The gallium(III)(pyridine) complex of 3-vinyl-5,10,15-tris(pentafluorophenyl)corrole **2** reacted with the *o*-quinone methides, generated *in situ* from *ca* 1.4 equivalent of 4-hydroxycoumarins and 11 equivalents of paraformaldehyde, under reflux in 1,4-dioxane. The TLC control of these reactions showed after 1 h the complete consumption of the vinyl-corrole **2**. The adducts **7** and **8** were isolated, after workup and preparative purification in excellent yields, 92% and 87% respectively.

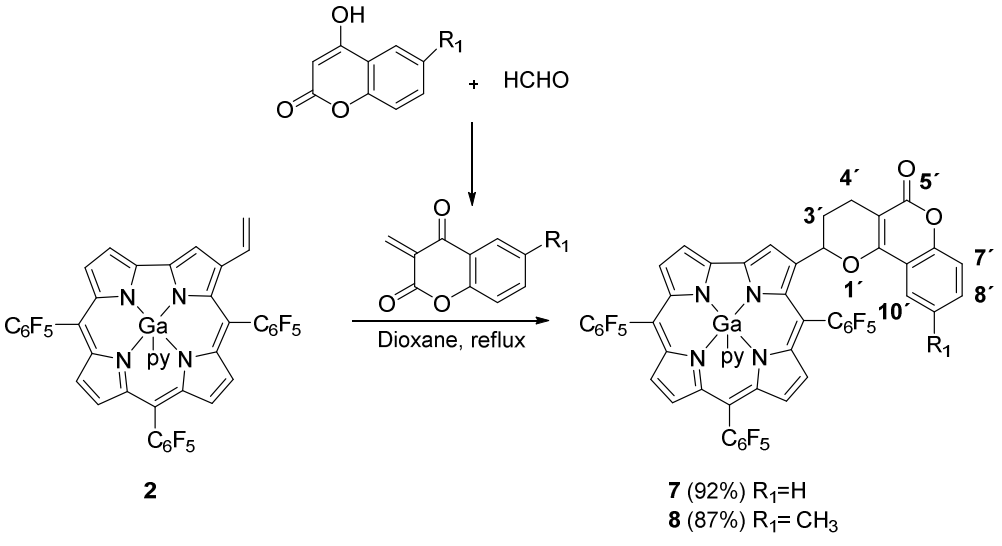

Scheme 6

The structures of these corrole-coumarin conjugates were confirmed by NMR (1D and 2D), UV-vis and high resolution mass spectrometry. In particular, from the analysis of ^{1}H NMR spectra of **7** (for numbering see Scheme 2) it was possible to assign, the four multiplet between δ 2.65-3.04 to the H-3′ and H-4′ protons of the dihydropyran ring and the double doublet at δ 5.83 to the H-2′ proton (this feature is due to the non-equivalence of H-3′ protons). In the aromatic region, the multiplet at δ 7.19-7.24 was assigned to the H-9′ of coumarin nucleus, the ones at δ 7.38-7.42 and δ 7.66-7.68 to H-7′ and H-8′, respectively, and finally the doublet at δ 7.84 to H-10′. The beta substitution pattern of the corrole nucleus was confirmed by the presence of the singlet at δ 9.40 due to H-2 proton resonance (Figure 1).

The *β*-pyrrolic protons of the corrole core were also identified. The signals corresponding to protons H-2 and H-18 appeared as a singlet and as a doublet at *δ* 9.40 and 9.25, respectively. The signals corresponding to the resonance of the remaining *β*-pyrrolic protons emerged between *δ* 8.87 and 8.63.

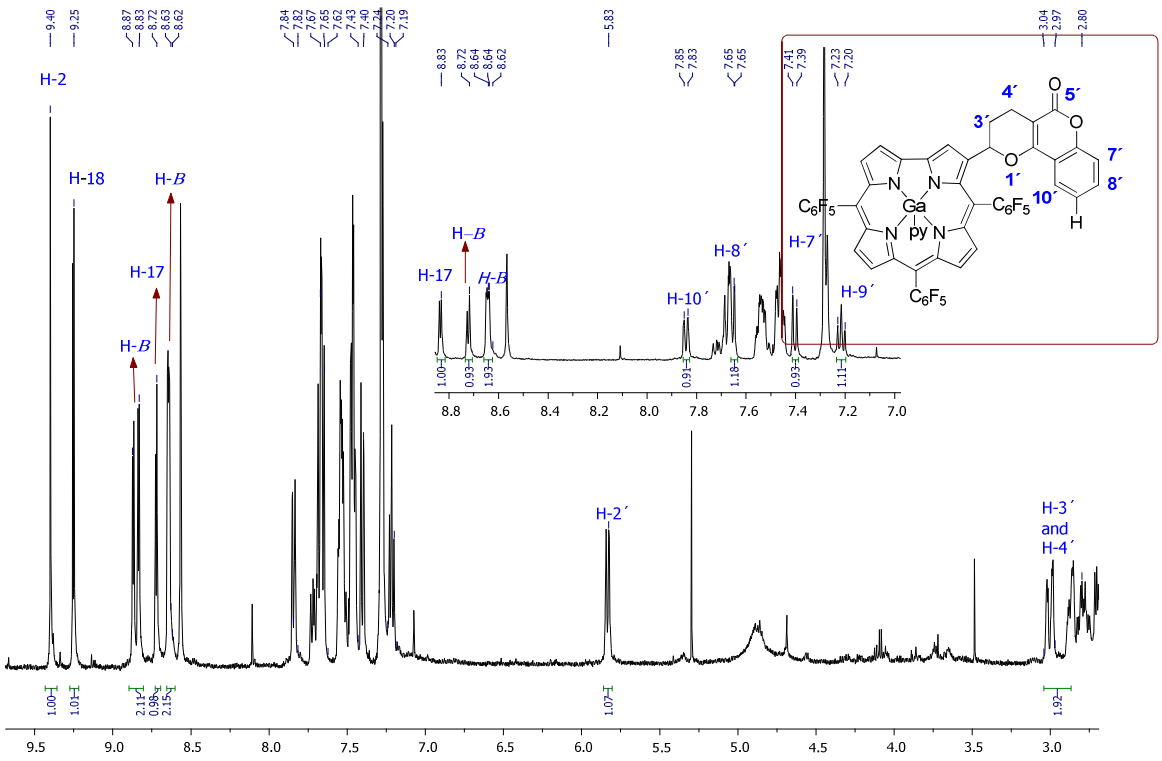

Figure 1- Partial ^{1}H NMR spectrum of conjugate **7** in $CDCl_3$ with a few drops of pyridine-d_5.

The analysis of the ^{13}C NMR spectrum of **7** showed the signal at δ 163.2 and δ 75.0 assigned to the coumarin carbonyl C5′ and C2′ respectively, which is in accordance with the proposed structure; this shows that the addition occurred selectively at the 3,4-position of the coumarin nucleus (Figure 2).[30]

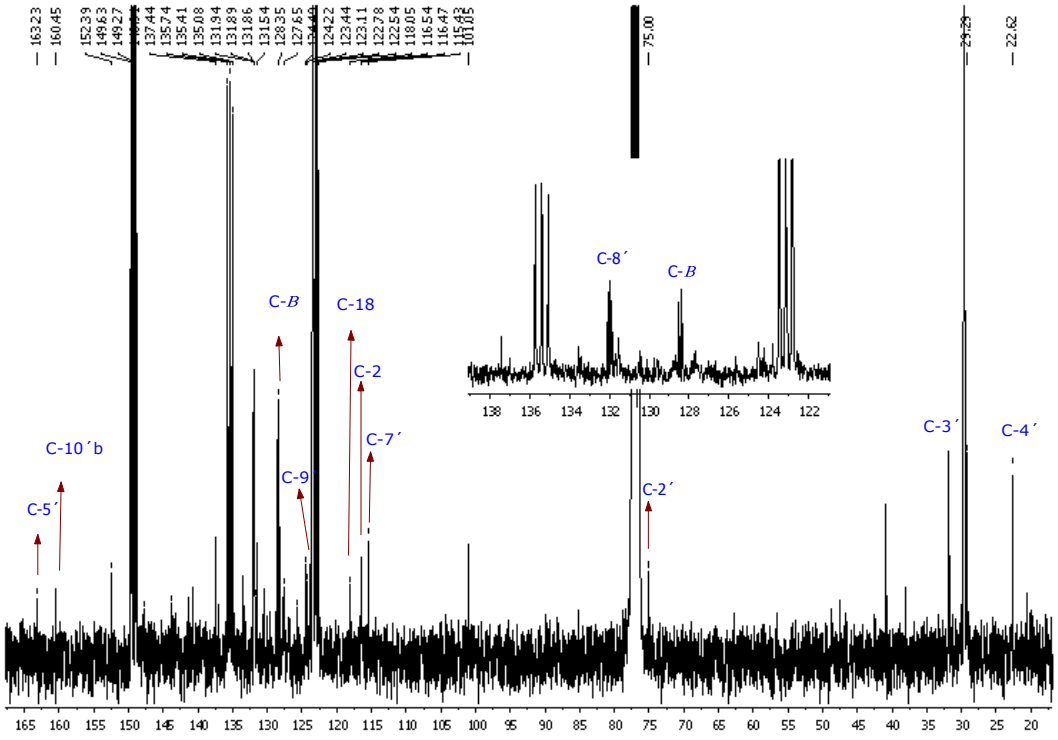

Figure 2- ^{13}C NMR spectrum of conjugate 7 in $CDCl_3$ with a few drops of pyridine-d_5.

In the ^{1}H NMR spectrum of compound **8**, the presence of the methyl group on the coumarin moiety was confirmed by the appearance of a singlet at δ 2.27.

Similarly, the reaction of 2-vinyl-5,10,15,20-tetraphenylporphyrinatozinc(II) (**1a**) with the *o*-quinone methide, generated *in situ* from 4-hydroxycoumarins and paraformaldehyde afforded the porphyrin-coumarin conjugates **3** (88% yield) and **4** (95% yield).[30] The decomplexation of these porphyrin-coumarin conjugates **3** and **4** with 5% TFA/$CHCl_3$ gave the corresponding free-bases **5** (97% yield) and **6** (92% yield).[30] These compounds were synthesized by the group of organic chemistry at the University of Aveiro in the framework of another project. However as they never has been exploited as fluorescent chemosensors, we decided to exploit their potentialities along with compounds **7** and **8**.

4.2.2.The sensing ability of coumarin-corrole and –porphyrin conjugates

4.2.2.1 Photophysical Studies

The photophysical characterization of compounds **3** to **8** were performed in dichloromethane, DMSO, toluene and ethanol solutions at 298 K. Compound **5** was characterized in the solvents referred above and also in a mixture of ethanol:water (50:50). In Table 1, the main photophysical data for all compounds in toluene are reported and the results obtained in the other solvents are presented in experimental section (Table SN1).

Table 1 -Photophysical data of conjugates **3**-**8** in dichloromethane, DMSO, toluene and ethanol at 298 K.

Conjugates	Solvent	λ_{max}(log ε) / nm	λ_{em} (nm)	Stoke's shift (nm)	Φ
3	Toluene	426(5.23);565(3.95);599 (3.21)	599, 646	47	0.02
4	Toluene	426(5.28); 560(4.15);599(3.31)	599, 646	47	0.01
5	Toluene	421(5.32);523(4.15);557(3.85) 603(3.78); 652(3.56)	652, 719	67	0.02
6	Toluene	420(5.38); 519(4.15);560(3.86) 607(3.72); 652(3.40)	652, 713	61	0.02
7	Toluene	427(5.51);580(4.30);601(3.81)	602, 650	48	0.06
8	Toluene	426(5.53);582(4.27);601(3.76)	602, 651	49	0.09

In toluene and in the other solvents, the absorption spectra of the metalloporphyrin conjugates **3** and **4** showed the Soret band between 423 and 426 nm (due to the allowed transition from $S_0 \rightarrow S_2$) and two weak Q bands (due to the transition from $S_0 \rightarrow S_1$) at *ca* 560-565 and 599 nm. The free-base derivatives **5** and **6** exhibit the Soret band between 417 and 424 nm and four Q bands centered between 519 and 654 nm. The absorption spectra of corroles **7** and **8** present the Soret-type band between 426 and 430 nm and two Q bands at *ca* 580 and 603 nm except for compound **8** in DMSO. In this case a bathochromic shift was

visualized with the increase of solvent polarity, being the absorbance band centered at *ca* 582 nm (toluene) < 585 nm (CH_2Cl_2) < 587 nm (EtOH) < 605 nm (DMSO). This positive solvatochromic effect can be detected by naked eye for compound **8**, which shows different colours in different solvents (colourless, yellow and purple - Figure 3).

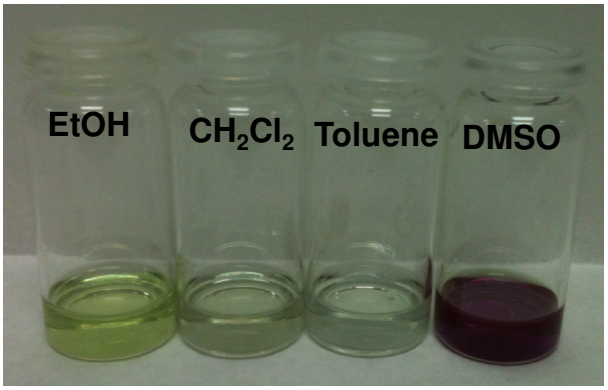

Figure 3- Solvatocromic effect on compound 8.

In order to characterize quantitatively this solute-solvent interaction the multiparametric fitting of Kamlet-Taft equation[40] was realized by using of solvent parameters gathered in table 2. Through this fitting a liner plot of ν_{exp} *versus* ν_{calc} was determined for compound **8**, being the fitted parameters ν_0 = 17887 cm^{-1}, a = -2274 cm^{-1}, b = 2156 cm^{-1} and p = -2283 cm^{-1} with a correlation factor of 1. The negative value of p shows that the contribution of dipolarity/polarizability decreases the stabilization of the excited state in compound **8**. The ground (μ_g) and excited (μ_e) states dipole moments were estimated based on Kawski theory,[41,42] whereas, a linear curve fitting of ν_a-ν_f and ν_a+ν_f as a function of $f(\varepsilon,n)$ and $f(\varepsilon,n)$ + $2g(n)$. Values of μ_g = 0.42 D and μ_e = 0.15 D were determined, which indicate that in compound **8**, the ground state is slightly more polar than the excited state.

Table 2- Spectroscopic polarity parameters, physical properties and polarity functions of solvents used for photophysical characterization of compound **8**.

Solvent	ε_r	N	E_T (30)	α	β	π*	*f*(ε,n)	*g*(n)
Toluene	2.38	1.4969	-	0.00	0.11	0.54	0.029	0.335
Dichloromethane	8.93	1.4242	40.7	0.13	0.10	0.73	0.590	0.288
Ethanol	24.30	1.3610	51.9	0.86	0.75	0.54	0.812	0.246
DMSO	47.24	1.4790	45.1	0.00	0.76	1.00	0.841	0.324

Figure 4 shows the absorption (only Q band region), excitation and emission spectra, of compound **3** (Fig. 4A) as an example of metalloporphyrin series and of compound **7** (Fig. 4B) as an example of the corrole series.

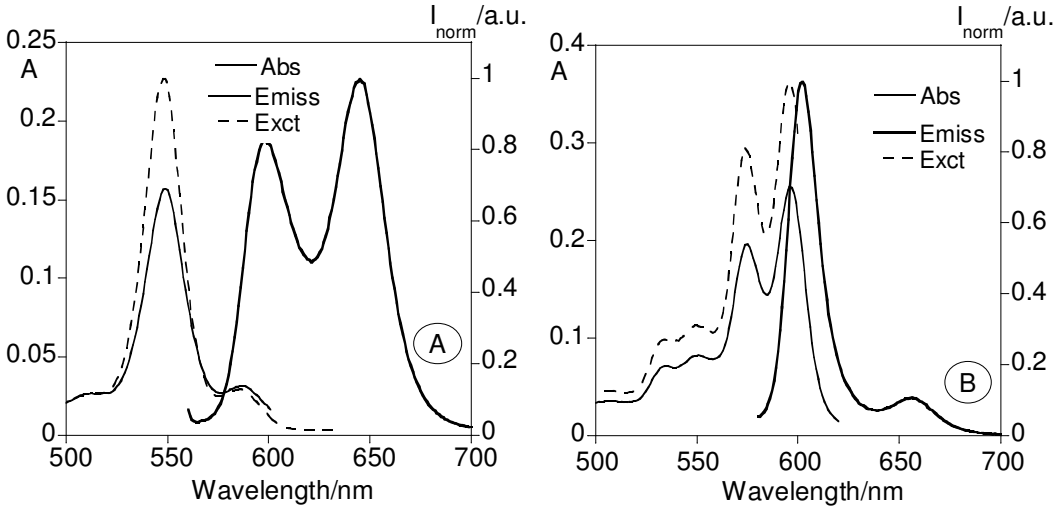

Figure 4- Absorption, normalized emission and excitation spectra of porphyrin 3 (A) and corrole 7 (B) in toluene, ([3] = [7] = 5.0×10^{-6} M, $\lambda_{exc(full\ line)3}$ = 565 nm, $\lambda_{exc\ (full\ line)7}$ = 580 nm and $\lambda_{emiss(dotted\ line)3}$ = 646 nm $\lambda_{emiss(dotted\ line)7}$ = 650 nm).

The perfect match between the absorption and excitation spectra in figure 4, indicates the absence of any emissive impurity in all cases. The fluorescence emission spectra of zinc(II) porphyrins **3** and **4** obtained after excitation at *ca* 560-565 nm, present two bands centered at 599 and 646 nm, that are characteristic of metalloporphyrins derivatives (see table 1). Otherwise, the excitation of **5** and **6** at *ca.* 605 nm afforded two

emission bands, one centered at *ca.* 652 nm and the other between 713 and 719 nm. In the case of corrole derivatives **7** and **8** the emission bands are centered between 601 and 652 nm.

As can been seen in table 1, the excited state of conjugates **3**-**7** are not affected by the dipole moment of the solvent. The fluorescence quantum yields of porphyrin and corrole derivatives were determined by the internal reference method with respect to a solution of crystal violet in methanol as a standard ([ϕ] = 0.54) and the values are present in Table 1. The fluorescence quantum yields of porphyrinic conjugates **3**-**6** ($0.01 < \phi < 0.03$) are relatively lower than those obtained with the corrole derivatives ($0.04 < \phi < 0.13$), being the highest value determined for compound **8** in an ethanolic solution. This behavior can be due to the inherent differences of the tetrapyrrolic macrocycle.[43] On the other hand, a better solubility conferred by the coumarin unit to corrole may favor the decay of excited molecules by fluorescence in ethanol.

4.2.2.2 Spectrophotometric and spectrofluorimetric sensing studies

Corroles, porphyrins and metalloporphyrins as it was already referred are excellent multifunctional candidates for a great variety of sensing material applications. These molecules are rather stable compounds and their properties can be finely tuned by simple modifications of their basic molecular structure. These macrocycles offers a large variety of interaction mechanisms that can be exploited for chemical sensing. Hydrogen bonds, polarization, and polarity interactions are expected to take place between analyte molecules and these tetrapyrrolic macrocycles.

For these reasons it was decided to study the potentialities of these macrocycles in conjunction with coumarins in the signaling of different anions and metals. The measurement of sensory activity is generally undertaken in purely organic solvents or less efficiently in aqueous mixtures. The combination of the corrole or porphyrin macrocycles with coumarin moiety, conferred solubility to all synthesized compounds in ethanol and in ethanol:water mixtures. This fact also prompted us to perform pH sensing studies.

4.2.2.2.1 Anion sensing effects

The sensorial ability of metallocompounds **3**, **4**, **7** and **8** towards the spherical (F^-, Cl^-), linear (CN^-) and bulky anions (CH_3COO^-) was carried out by ligand titrations with the addition of small amounts of the adequate anion as tetrabutylammonium salt. The titrations were followed by UV-Vis and fluorescence measurements in toluene and the most significant data are gathered in Table 3.

Table 3-. Association constants of conjugates 3, 4, 7 and 8 in toluene**.**

Compound	Analyte (A)	Log K_{Ass} (A:L)
3	Cl^-	5.43 ± 0.03 (1:1)
	CN^-	6.57 ± 0.01(1:1)
	CH_3COO^-	4.87± 0.02 (1:1)
4	Cl^-	5.40 ± 0.03 (1:1)
	CN^-	6.53 ± 0.01(1:1)
	CH_3COO^-	4.85± 0.02 (1:1)
7	F^-	5.28± 0.01(1:1)
	CN^-	6.11± 0.01(1:1)
	CH_3COO^-	4.32± 0.01(1:1)
8	F^-	5.04± 0.01(1:1)
	CN^-	6.08± 0.01(1:1)
	CH_3COO^-	4.11± 0.01(1:1)

As is was already referred in the previous chapters, fluoride ion is added in drinking water and dental hygiene products for the purpose of reducing the frequency of dental caries. However, its ingestion in high or in low levels may result in fluorosis, nephrotoxic changes and urolithiasis in human.[44] The fluoride anion is known to be used in many industrial applications, and in human diet, but, recently it has been accused for several human pathologies (osteoporosis and poor dental health).[45] The EPA-recommended F^- level in drinking water is 1 ppm, and over 2 ppm is considered a health-risk.[46] The chloride ion has significant role in biological, medical and environmental fields.[47]

The addition of Cl^- to the porphyrin derivatives **3** and **4,** it was responsible for mild alterations in their emission spectra. No spectral alterations were detected in their absorption spectra, suggesting that their ground state is not affected by the interaction with this spherical halide ion. Figure 5A shows the spectral changes, in the excited state, obtained for compound **3** during the titration with Cl^-. This addition leads to an emission quenching of *ca* 40% at 599 and of *ca* 60% at 646 nm, followed by a red-shift from 599 to

605 nm and from 646 to 656 nm. A similar spectral behavior was obtained for compound **4**. Considering the addition of F^- to these two chromophores **3** and **4** no significant spectral changes were detected.

In the case of corrole conjugates **7** and **8** no spectral modifications were observed, in the ground state, during the titrations with those two anions and in the excited state with Cl^-. However, the titrations of these compounds with F^- were responsible for a quenching of *ca* 40% at 602 nm. Figure 5B, shows the spectrofluorimetric titration of compound **7,** in toluene, in the presence of F^-. Similar spectral changes were detected for compound **8** with the addition of fluoride.

The association constants for the interaction of F^- and Cl^- with the different ligands were determined using the HypSpec[48] program and are summarized in Table 3. Looking at table 3, for the anions chloride and fluoride a stoichiometry of one ligand per anion was postulated, and was confirmed by Job's plot method.[49] Thus, a value of Log $K_{Ass.Cl^-}$ = 5.43 ± 0.03 (1:1); and of Log $K_{Ass.F^-}$ = 5.28 ± 0.01 (1:1), were determined for compound **3** and **7**, respectively. Similar interactions were found for compounds **4** and **8**.

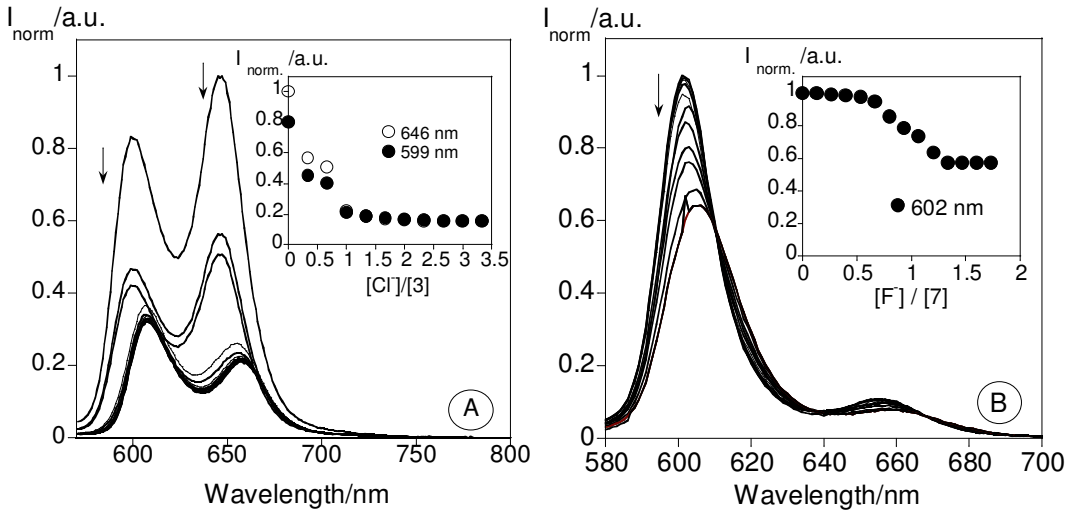

Figure 5- Spectrofluorimetric titrations of compound 3 (A) and 7 (B) with the addition of Cl^- and F^- in toluene at room temperature. ([3] = [7] = 1.0×10^{-5} M, $\lambda_{exc.\ 3}$ = 565 nm, $\lambda_{exc.\ 7}$ = 580 nm).

On the other hand, cyanide is one of the most poisonous and toxic anions. It is a lethal anion for humans, as well as for aquatic life.[50] Most environmental cyanides are released by industries involved in gold mining, electroplating, and metallurgy.[51] Due to its high toxicity, the highest allowable level of cyanide in drinking water by the World Health Organization (WHO) is 1.9 μM.[52] The cyanide anion interacts with all metallocorroles and

metalloporphyrins conjugates. The addition of CN^- to **3** promotes in the absorption spectrum (Fig. 6A) a small red-shift from 426 to 429 nm ($\Delta\lambda$ = 3 nm), accompanied by an increase of *ca* 40% in the band at 429 nm. An isosbestic point at 427 nm was also observed. A similar behavior was observed in the case of Q-bands. Initially there was a decrease in the intensity of the band centered at 550 nm, and an increase at 573 nm, with an isosbestic point at 560 nm. A new band appears at 600 nm (Fig. 6B). Considering the emission spectrum of **3** (Fig. 7A), the titration with CN^- was responsible for a decrease of intensity of *ca* 60% at 599 nm and also at 646 nm (*ca* 80%), followed by a red-shift from 599 to 605 nm and from 646 to 656 nm. Similar spectral modifications were observed in compound **4**.

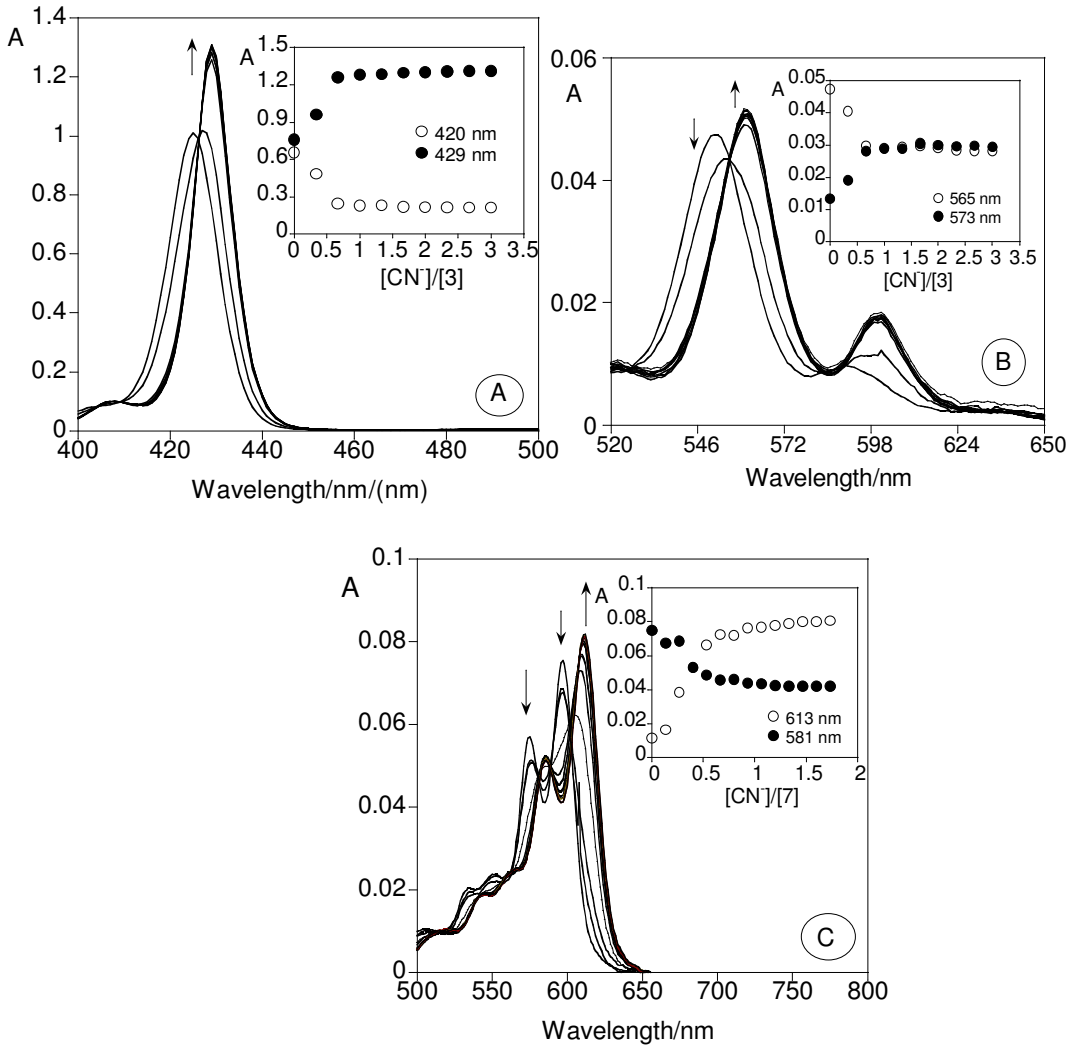

Figure 6- Spectrophotometric titration of compound **3** (A, B) and **7** (C) in toluene with the addition of CN^- in DMSO at 298 K. The insets show the absorption at 426 and 429 nm (A), 565 and 573 nm (B), and at 581 and 613 nm (C) ([3] = [7] = 1.0 x10^{-5} M).

In the presence of CN^-, compound **7** and **8**, undergo strong changes in the ground state. The addition of the anion produces a decrease in the intensity of the initial bands centered at *ca* 580 and 601 nm, with the concomitant appearance of two new bands centered at 588 and 613 nm. Two isosbestic points were detected at 586 and 607 nm (Fig. 6C). Taking into account the emission spectra (excited state), a quenching of *ca* 40% at 601 nm was observed (Fig. 7B) followed by a red shift of 12 nm.

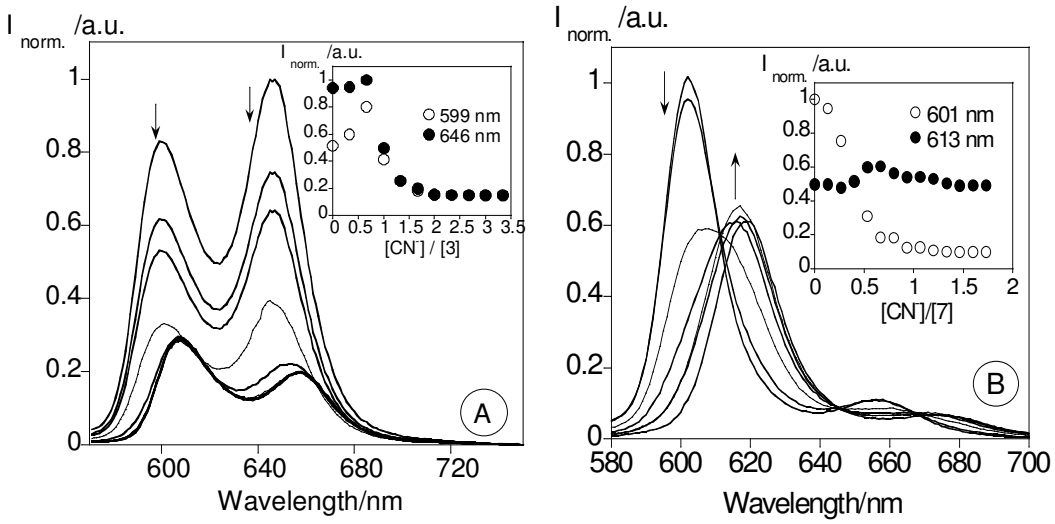

Figure 7-Spectrofluorimetric (A, B) titrations of compounds 3 and 7, in toluene, with the addition of CN^- in DMSO. The insets show the normalized emission intensity at 599 and 646nm (A) and at 601 and 613 nm (B) ([3] = [7] = 1.0 x10^{-5} M, $\lambda_{exc\ 3}$ = 565 nm, $\lambda_{exc\ 7}$ = 580 nm, T = 278 K) .

With respect to the association constants a value of Log $K_{ass.}$ = 6.57 ± 0.03 (1:1) and of Log $K_{ass.}$ = 6.11 ± 0.01 (1:1) were determined for compound **3** and **7**, respectively (Table 3).

Compounds **3**, **4** and **7**, **8** were titrated with the acetate anion (CH_3COO^-), and spectral changes in the ground and excited state were observed, in both macrocycle types. In compound **3**, like in **4**, a red shift in the absorption spectra from 426 to 430 nm, as well as, an emission quenching of *ca* 80% at 599 and 646 nm, were observed, with the addition of 1 equivalent of the anion (Figure 8).

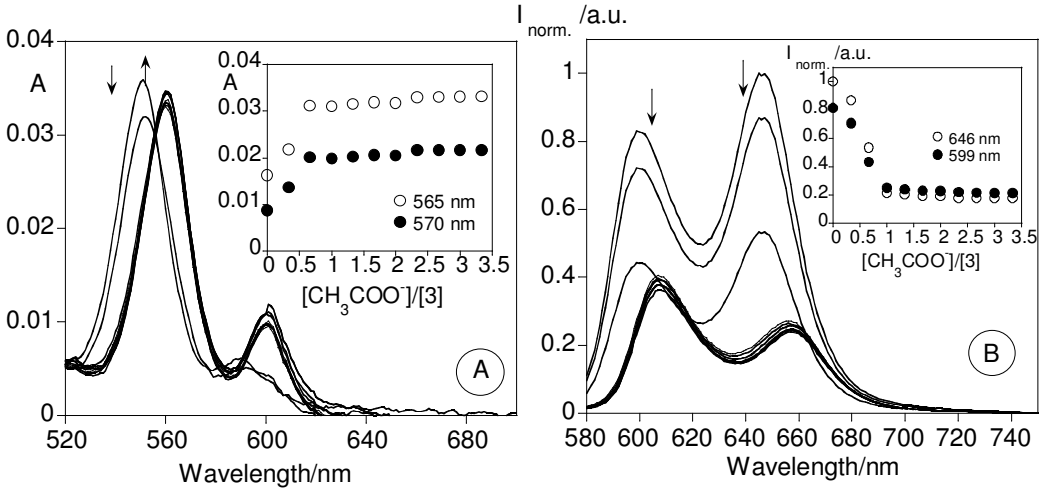

Figure 8- (A) Spectrophotometric and (B) spectrofluorimetric titrations of compound 3 with the addition of CH_3COO^- in toluene at 298 K. ([3] = 5.0×10^{-6} M, $\lambda_{exc.\ 3}$ = 565 nm).

With respect to the interaction of compound **7** and **8** with acetate a similar behaviour to the one observed for cyanide was found (Figure 9). An association constant of Log $K_{ass.}$ = 4.87 ± 0.02 and of Log $K_{ass.}$ = 4.32 ± 0.01, with a stoichiometry of one ligand per anion was determined for compounds **3** and **7**, respectively. Similar interactions were found for compounds **4** and **8** (Table 3).

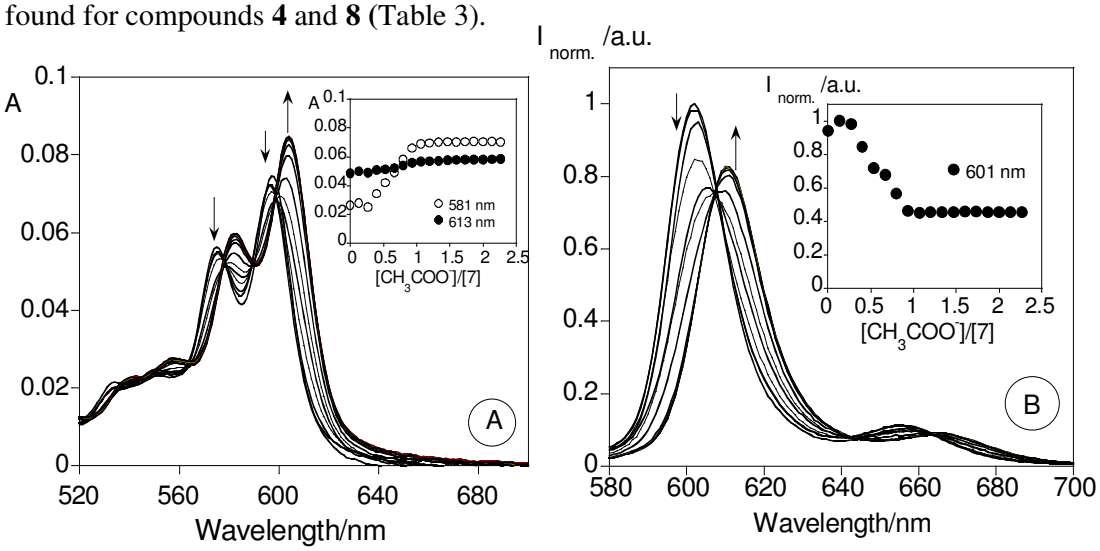

Figure 9- .(A) Spectrophotometric and (B) Spectrofluorimetric titrations of compound 7 with the addition of CH_3COO^- in toluene at 298 K. ([7] = 5.0×10^{-6} M, $\lambda_{exc.\ 7}$ = 565 nm).

It is to be noted that the sensing ability of porphyrin precursor **1b** (scheme 1) was also evaluated for all the anions and under the experimental conditions used, no changes in the ground and excited states were observed (Figure 10). These results are in accordance with literature.[9]

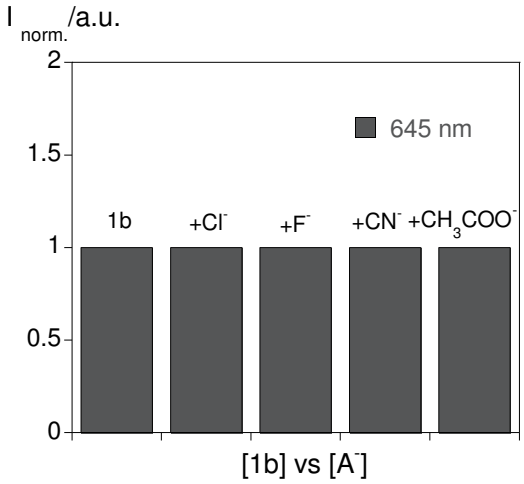

Figure 10- Normalized emission at 645 nm of compound 1b, and 1b with the addition of 2 equivalents of Cl^-, F^-, CN^- or CH_3COO^- in toluene at 298 K. ([1b] = 1.0×10^{-5}M, $\lambda_{exc.}$ = 563 nm).

Additionally, the detection (LOD) and quantification (LOQ) limits for the anions studied were determined and the values gathered in Table 3 show that the lowest values for LOD (0.09 and 0.10 ppm) and LOQ (0.18 and 0.19) were obtained for conjugates **3** and **4**, respectively, with the addition of chloride anion.

Table 4- Detection (LOD) and quantification (LOQ) limits of conjugates **3**, **4**, **7** and **8** in toluene**.**

Compound	Analyte (A)	LOD (ppm)	LOQ (ppm)
3	Cl^-	0.09	0.18
	CN^-	0.13	0.27
	CH_3COO	0.20	0.40
4	Cl^-	0.10	0.19
	CN^-	0.13	0.27
	CH_3COO^-	0.21	0.42
7	F^-	0.52	0.87
	CN^-	0.18	0.27
	CH_3COO^-	0.40	0.60
8	F^-	0.50	0.85
	CN^-	0.19	0.28
	CH_3COO^-	0.41	0.62

4.2.2.2.2 Metal sensing effects

The sensorial ability of porphyrinic free-bases **5** and **6** towards the metal ions Na^+, Ca^{2+}, Zn^{2+}, Cd^{2+}, Pb^{2+}, Fe^{2+}, Ba^{2+}, Cu^{2+}, Ag^+ and Hg^{2+} was investigated by the titration of the ligands, dissolved in toluene, with small amounts of the adequate metal salt dissolved in acetonitrile. These experiments were followed by UV-Vis and fluorescence emission spectroscopy. It is worth to refer that, mercury ions are environmentally toxic ions and are responsible for pollution and adverse effects to human health.[53]

In these conditions, only the Hg(II) cation caused significant changes in the ground and excited states of porphyrins **5** and **6**. No changes were detected upon addition of the other metal ions to the derivatives **5** and **6**. Figure 11A-B and 11C show the alterations observed in the absorption and emission spectra of compound **5** with the increasing addition of Hg^{2+}, in toluene. In the absorption spectra, the addition of Hg^{2+} to **5** results in a decrease in the band at 421 nm and an increase at 434 nm. A colorimetric effect was observed (a change of colour from purple to yellow) which allows a naked-eye detection of Hg^{2+} (figure 11A). In the emission spectra a quenching in the emission intensity at 654 nm

was visualized (figure 11C). The association constant was determined by HypSpec program and the value of Log $K_{Ass.Hg(II)}$ = 5.51 ± 0.01, was obtained with a stoichiometry of one ligand per metal ion.

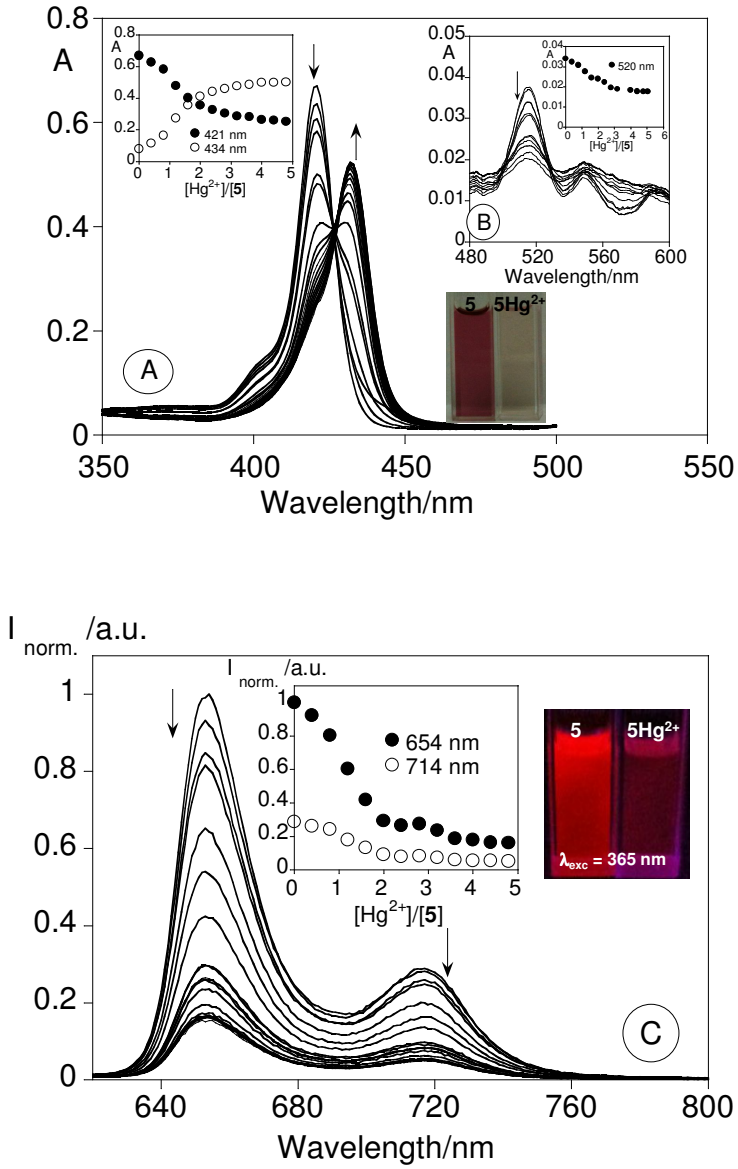

Figure 11. Spectrophotometric (A and B) and spectrofluorimetric (C) titration of porphyrinic free-base 5 with the addition of Hg^{2+} in toluene. The inset represents the absorption (A, B) at 421 nm, 434 nm for (A) and 520 nm for (B); and represents the emission intensity (C) at 654 and 714 nm, as function of $[Hg^{2+}]/[5]$. ($[5] = 1 \times 10^{-5}$ M, λ_{exc}= 592 nm, T = 298 K).

Compound **5** was also titrated with Hg^{2+} in a mixture of EtOH:H_2O (50:50), and in the emission spectra (figure 12B) a similar behavior, to the one found in toluene was detected. In the ground state a slight decrease in the absorbance at 421 nm was observed (figure 12A). An higher association constant for Hg^{2+} was obtained for EtOH:H_2O with respect to toluene, yielding a value of Log $K_{Ass.}$ = 7.13 ± 0.01. At 654 nm the detection (LOD) and quantification (LOQ) limits were of 1.05 ± 0.11 and 1.31 ± 0.40, respectively. Thus, the minimal amount of Hg^{2+} detectable in an aqueous solution (EtOH:H_2O/50:50) by compound **5** was 0.6 ppm and the minimal amount quantified was 1.2 ppm.

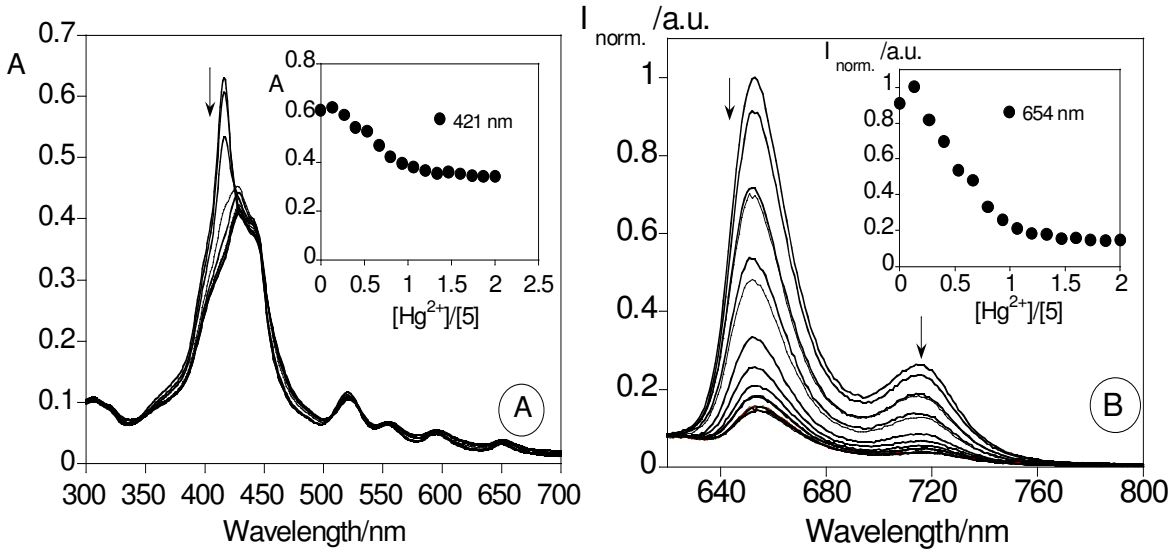

Figure 12- Spectrophotometric (A) and spectrofluorimetric (B) titration of compound 5 with the addition of Hg^{2+} in EtOH:H_2O (50:50) at 298 K. The inset represents the absorption (A) at 421 nm; and the emission intensity (B) at 654 nm, as function of $[Hg^{2+}]/[5]$. ([5] = 1.0×10^{-5} M, λ_{exc}= 592 nm).

In competitive studies with compound **5** in toluene a higher affinity and an unprecedented selectivity for Hg^{2+} metal was found (figure 13). In this figure, the normalized emission intensity presented as black bars was measured towards the addition of 2 equivalents of Na^{+}, Ca^{2+}, Zn^{2+}, Cd^{2+}, Pb^{2+}, Fe^{2+}, Ag^{+} and Hg^{2+} metal ions; the red bars confirmed that even upon the addition of 100 equivalents of the other metals the affinity towards Hg^{2+} is not altered.

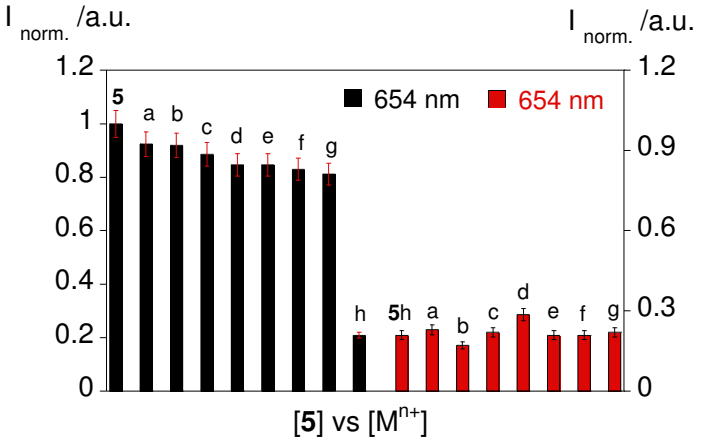

Figure 13- *Black bar*: normalized relative emission intensity of compound 5 upon the addition of 2 equivalents of a (Na^+), b (Ca^{2+}), c (Zn^{2+}), d (Cd^{2+}), e (Pb^{2+}), f (Fe^{2+}), g (Ag^+) and h (Hg^{2+}). *Red bar*: normalized emission intensity of 5 with Hg^{2+} upon addition of 100 equivalents of the metal ions a to g. ([5] = 1×10^{-5} M, λ_{exc} = 603 nm.).

4.2.2.2.3 Solid supports and pH studies

Several pH studies with compound **5** were carried out in mixtures of ethanol: water (50:50). Figure 14 shows the absorption spectra of compound **5** at different pH's. Compound **5** behaves as a colorimetric sensor with the change in pH. Increasing the pH, compound **5** change its colour from green (low pH) to yellow (high pH) (figure 15A).

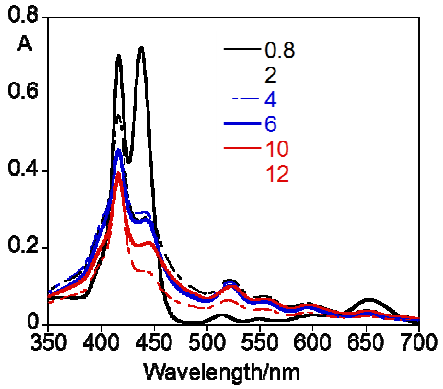

Figure 14- Absorption spectra of compound 5 at different pH (from 0.8 to 12) in an mixture EtOH:H_2O (50:50) at 298 K,([5] = 1.0×10^{-5} M).

This behavior is typical of *meso*-tetraarylporphyrins like 5,10,15,20-tetraphenylporphyrin (the free-base of **1b**),[54] but the great advantage of conjugate **5** is its high solubility in polar solvent such as ethanol and water, which allows its use in non-expensive solid supports. The green colour at very low pH, according with literature,[55] is due to the formation of dicationic species, confirmed by the appearance of a band at 650 nm, in the absorption spectra (figure 14).

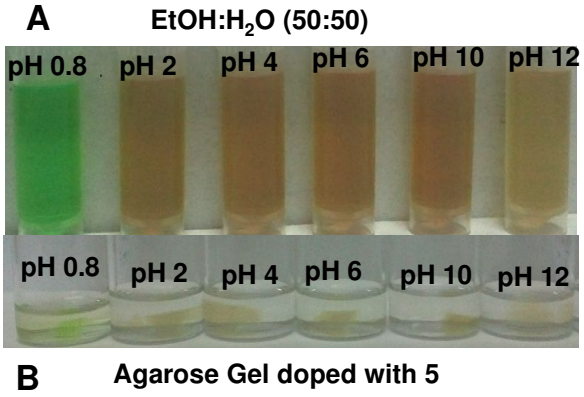

Figure 15- (A) Colour change (from green to yellow) at different pH, of compound 5 in EtOH:H_2O (50:50). (B) Agarose gel doped with compound 5 exposed at different pH (from pH 0.8 -12).

During the pH experiments with conjugate **5**, two low-cost polymers, agarose and cellulose, were tested (see figure 15B and 16). Thus, an agarose and a natural cellulose polymer (carboxymethylcellulose sodium salt) doped with compound **5** were exposed to different pH's (from 0.8 to 12). The same colour changes (green at low pH to yellow at higher pH) were observed in solution EtOH:H_2O (50:50) when the compound **5** was doped in the agarose and cellulose polymers. The emission of both polymers at different pH's was also recorded in solid state, using a fiber optic system connected to the Horiba Jobin-Yvon Fluoromax 4.

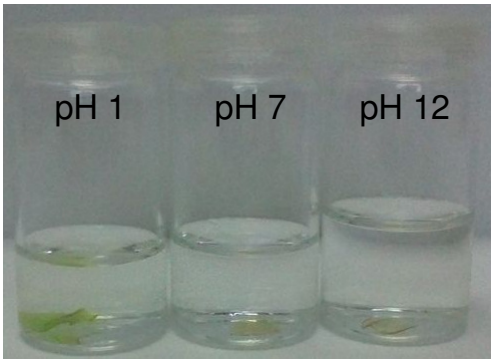

Figure 16- Image of natural cellulose polymer (carboxymethylcellulose sodium salt) doped with compound 5 at pH's 1, 7 and 12.

As can be seen in figure 17 with the pH, the emission intensity of the polymers doped with **5** was practically not affected. From these results compound **5** can be considered as a colorimetric pH probe, which can be applied in low cost materials, such as, agarose and cellulose. It is worthwhile to mention that under the same conditions (EtOH:H_2O) the free-base of **1b** showed limited solubility.

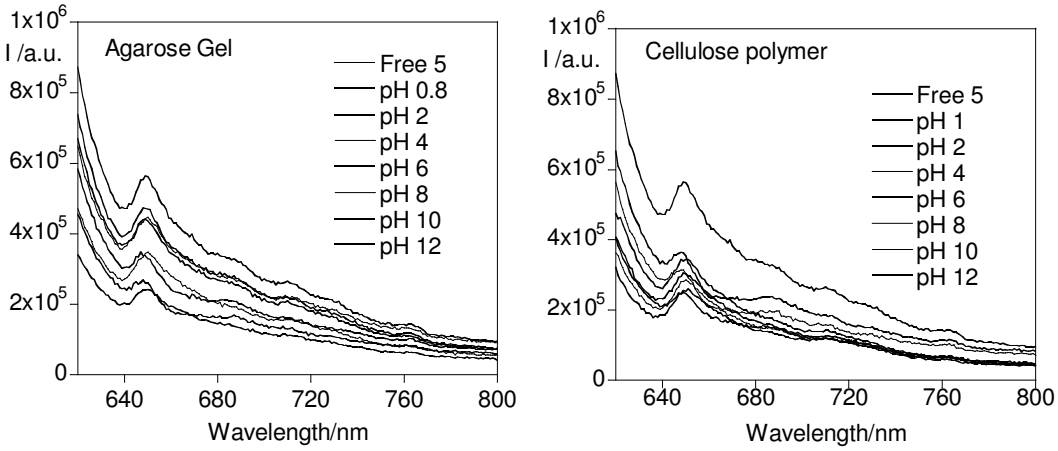

Figure 17- (A) Emission spectra of compound 5 in an Agarose Gel and in a Cellulose Polymer (carboxymethylcellulose sodium salt) at different pH ($\lambda_{exc.}$ = 592 nm, T = 298 K).

In order to explore the colorimetric properties of compound **5** and its application in solid support materials, cellulose paper, in this case filter paper, containing compound **5** was exposed to different amounts of mercury(II) metal ion. As can be seen in figure 18, the

cellulose paper with **5** was purple and showed a strong red emission under a UV lamp λ_{exc} = 365 nm. After the addition of Hg^{2+} metal ion, the colour of the cellulose paper changes from purple to yellow, and under the UV lamp the strong red emission disappears. This emission quenching in solid state was monitored using a fiber optic system and the results are presented in figure 18A.

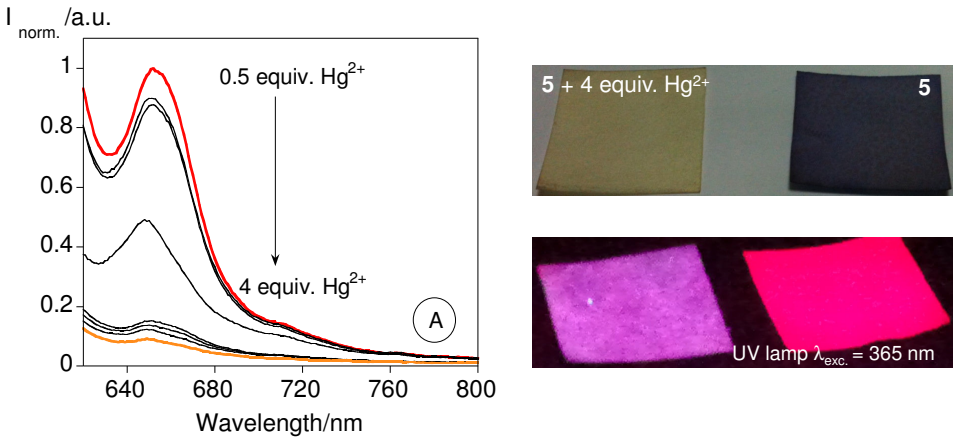

Figure 18- Spectrofluorimetric titration of compound 5 in a cellulose paper with the addition of 0 to 4 equivalents of the metal ions Hg^{2+} in water, $\lambda_{exc.}$ = 592 nm.

4.3 Conclusions

New corrole-coumarin derivatives **7** and **8** were successfully obtained and fully characterized. The coumarin-corrole and the analogues coumarin--porphyrin conjugates were photophysically characterized in different solvents (dichloromethane, DMSO, toluene and ethanol). Compound **8** is slightly more polar in the ground state (μ_g = 0.42 D) than in the excited state (μ_e = 0.15 D), showing a positive solvatochromic effect, while the other conjugates were practically not affected by the solvent. A strong colour change from purple to yellow (colorimetric effect) and an unprecedented selectivity for Hg^{2+} was detected for compound **5** in EtOH:H_2O (50:50); the association constant in EtOH:H_2O (50:50) was higher than in toluene (Log $K_{Ass.\ EtOH:Water}$ = 7.13 ± 0.01; Log $K_{Ass\ Toluene}$ = 5.51 ± 0.01). In addition, compound **5** was able to detect and quantify the minimal amount of 0.6 ppm and 1.2 ppm of Hg^{2+} in aqueous solution (EtOH:H_2O, 50:50).

The naked eye sensorial ability of the colorimetric effect of **5** for Hg^{2+} was successfully applied in a solid support material, a cellulose paper (filter paper). The sensorial ability of conjugate **5** for Hg^{2+} was maintained when applied in cellulose paper allowing naked eye detection. Moreover, pH studies carried out with conjugate **5** showed a green colour at low pH and a yellow colour at high pH values in solution and solid supports.

4.4. Experimental Section

4.4.1 Chemicals and starting materials

$NaCH_3SO_3$, $Ca(CH_3SO_3)_2$, $Ba(CH_3SO_3)_2$, $Cd(CH_3SO_3)_2$, $Cu(BF_4)_2.6H_2O$, $Pb(BF_4)_2.6H_2O$, $Hg(CH_3SO_3)_2$, $Zn(CH_3SO_3)_2$, $Fe(CH_3SO_3)_2$, $AgCH_3SO_3$, $(CH_3CH_2CH_2CH_2)_4NF$, $(CH_3CH_2CH_2CH_2)_4NCl$, $(CH_3CH_2CH_2CH_2)_4N(CN)$, $(CH_3CH_2CH_2CH_2)_4N(CH_3CO_2)$ salts, paraformaldehyde, methanesulfonic acid (CH_3SO_3H), carboxymethylcellulose sodium salt, agarose, 4-hydroxycoumarin and 4-hydroxy-6-methylcoumarin were purchased from Sigma-Aldrich. All these chemicals were used without further purification. The solvents were obtained from Panreac and Riedel-de Haen and used as received or distilled and dried using standard procedures.

4.4.2 Physical measurements

HRMS were carried out at the University of Vigo (CACTI), Spain. ^{1}H and ^{13}C NMR spectra were recorded on Bruker Avance 500 (at 500 and 125 MHz, respectively) and 300 (at 300 and 75 MHz, respectively) spectrometers. ^{19}F NMR spectra were also obtained on a Bruker Avance 300 at 282 MHz. $CDCl_3$ and pyridine-d_5 were used as solvents with tetramethylsilane (TMS) as the internal reference; the chemical shifts are expressed in δ (ppm) with the coupling constants (*J*) in Hertz (Hz). Unequivocal ^{1}H assignments were made using 2D COSY experiments (mixing time of 800 ms), while ^{13}C assignments were made on the basis of 2D HSQC and HMBC experiments (delay for long-range *J* C–H couplings was optimized for 7 Hz). Preparative thin-layer chromatography (TLC) was carried out on 20 × 20 cm glass plates coated with silica gel (0.5 mm thick). Analytical TLC was carried out on precoated sheets with silica gel (Merck 60, 0.2 mm thick).

4.4.3 Photophysical measurements

Absorption spectra were recorded on JASCO V-650 spectrophotometer and fluorescence emissions were performed on a Spectrofluorimeter HORIBA-JOBIN-YVON Fluoromax 4. The linearity of the fluorescence emission vs. concentration was checked in the concentration range used (10^{-4} to 10^{-6} M). A correction for the absorbed light was performed when necessary. The spectroscopic characterizations and titrations were performed using stock solutions of the studied compounds (*ca.* 10^{-3} M), prepared by

dissolving the appropriate amount of porphyrin/corrole derivatives in toluene, dichloromethane, ethanol or DMSO in a 10 mL volumetric flask. The studied solutions were prepared by appropriate dilution of the stock solutions up to 10^{-5} to 10^{-6} M. Titrations of the ligands **3-8** were carried out by the addition of microliter amounts of standard solutions of cations in acetonitrile and anions in DMSO or toluene, respectively. All the measurements were performed at 298 K. Fluorescence quantum yields were measured using a solution of cresyl violet perchlorate in absolute ethanol as a standard ([ϕ] 0.54)[18], and were corrected for different refraction indexes of solvents. Fluorescence spectra of the doped solid supports were recorded using a fiber optic system connected to a Horiba Jobin-Yvon Fluoromax 4 spectrofluorimeter, exciting at appropriate λ (nm) for the solid supports. The limit of detection (LOD) and the limit of quantification (LOQ) for the analytes were performed, having in mind their use for real ions detection and analytical applications. For these measurements, ten different analyses for the selected receptor were performed in order to obtain the LOQ. The LOD was obtained by applying the formula:

$$y_{dl} = y_{blank} + 3std$$

where y_{dl} = signal detection limit and std = standard deviation.

4.4.4 Synthesis of organic ligands

The porphyrin-coumarin derivatives **3-6** were prepared in the ambit of other project according with literature.[30]

The precursor gallium(III)(pyridine) complex of 3-vinyl-5,10,15-tris(pentafluorophenyl)corrole **2** was synthesized according to the procedure described in chapter 2.

4.4.4.1 General procedure for preparing 7 and 8

In a round-bottom flask, equipped with a magnetic stirring bar, a solution of 4-hydroxycoumarin (5.7 mg, 35.5 μmol) / 4-hydroxy-6-methylcoumarin (6.2 mg; 35.5 μmol), 1,4-dioxane (5 mL), paraformaldehyde (8.5 mg, 284 μmol) and corrole **2** (25 mg, 25.8 μmol) was heated at reflux until consumption of the starting corrole **2** (1 h). 1,4-Dioxane was then removed under reduced pressure, chloroform (50 mL) was added to the residue and the mixture was washed with saturated aqueous sodium bicarbonate (2 × 20

mL). The organic phase was concentrated under vacuum and the corrole compounds were purified by preparative TLC using hexane:ethyl acetate:pyridine (150:50:1) system.

Compound 7 {3-(5-oxo-2,3,4,5-tetrahydro-2*H*-pyrano[3,2-*c*]chromen-2-yl)-5,10,15-tris(pentafluorophenyl)corrolato}gallium(III):

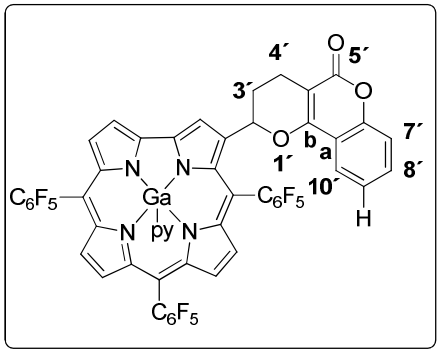

^{1}H NMR ($CDCl_3$, a few drops of pyridine-d_5, 500 MHz): δ 9.40 (s, 1 H, H-2), 9.26 (d, 1H, *J* = 4.0 Hz, H-18), 8.87 (d, 1H, *J* = 4.5 Hz, H-*β*), 8.83 (d, 1H, *J* = 4.0 Hz, H-17), 8.72 (d, 1H, *J* = 4.5 Hz, H-*β*), 8.64-8.63 (m, 2H, H-*β*), 7.84 (dd, *J* = 7.9, 1.0 Hz, H-10′), 7.68-7.66 (m, 1H, H-8′), 7.40 (dd, 1H, *J*= 8.4, 0.6 Hz, H-7′), 7.22 (dt, 1H, *J*= 7.8 Hz, H-9′), 5.83 (dd, 1H, *J* = 9.7, 1.8 Hz, H-2′), 3.04-2.97 (m, 2H, H-3′ and H-4′), 2.98-302, 2.89-2.85, 2.81-2.75, 2.72-2.65.^{13}C NMR ($CDCl_3$, a few drops of pyridine-d_5, 125 MHz): δ 163.2 (C-5′), 160.4 (C-10′b), 152.3, 147.6, 143.7, 141.4, 140.8, 137.4, 137.0, 135.7, 133.4 (C-8′), 132.0, 131.9, 131.8, 131.7, 131.5, 128.3 (C-β), 125.6 (C-17), 124.5 (C-β), 124.4 (C-β), 124.2 (C-9′), 118.0 (C-10′), 116.5 (C-2), 116.4 (C-7′), 115.4, 101.1, 75.0 (C-2′), 29.3 (C-3′), 22.6 (C-4′). ^{19}F NMR ($CDCl_3$, a few drops of pyridine-d_5, 282 MHz,): -161.3 to -161.4 (m, 6F, F*ortho*), -177.2 to -177.5 (m, 3F, F*para*), -185.7 to -186.2 (m, 6F, F*meta*). HRMS-ESI-TOF *m/z* calcd for $C_{49}H_{16}F_{15}N_4O_3Ga$ $[M+H]^{+\cdot}$ 1063.3830, found 1063.3816.

Yield: 92%. Colour: Dark Purple.

Compound 8 {3-(9-methyl-5-oxo-2,3,4,5-tetrahydro-2*H*-pyrano[3,2-*c*]chromen-2-yl)-5,10,15-tris(pentafluorophenyl)corrolato}gallium(III):

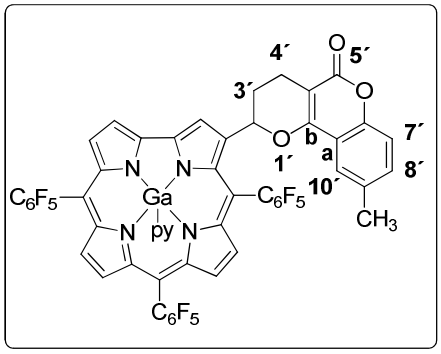

^{1}H NMR ($CDCl_3$, a few drops of pyridine-d_5, 300 MHz): δ 9.42-9.35 (m, 1H, H-*β*), 9.28-9.20 (m, 1H, H-*β*), 8.93-8.59 (m, 5H, H-*β*), 7.63 (d, 1H, *J* = 1.8 Hz, H-10′), 7.37-7.21 (m, 2H, H-7′ and H-8′),5.91-5.82 (m, 1H, H-2′), 3.06-2.63 (m, 4H, H-3′ and H-4′), 2.27 (s, 3H, CH_3).

^{13}C NMR (75 MHz, $CDCl_3$) δ 163.6, 160.5, 150.6, 143.2, 141.4, 140.9, 137.3, 136.0, 133.7, 133.6, 133.5, 132.6, 129.7, 128.6, 128.1, 127.8, 127.2, 125.6, 124.4, 123.7, 118.1,

116.3, 115.1, 101.0, 74.9 (C-2′), 29.4 (C-3′), 22.7 (C-4′), 20.8 (Ar-*C*H_3). ^{19}F NMR ($CDCl_3$, a few drops of pyridine-d_5, 282 MHz): δ - 159.1 to -159.2 (dd, 1F, *J* = 25.0, 7.2 Hz, F_{ortho}), -161.0 to -161.2 (dd, 1F, *J*= 25.4, 9.0 Hz, F_{ortho}), -161.4 to -161.5 (m, 4F, F_{ortho}), -174.9 (t, 1F, *J* = 21.2 Hz, F_{para}), -176.8 (t, 1F, *J* = 21.0 Hz, F_{para}), -177.0 (t, 1F, *J* = 21.0 Hz, F_{para}), -184.1 to -184.3 (m, 1F, F_{meta}), - 185.0 to -185.2 (m, 1F, F_{meta}), -185.5 to - 186.0 (m, 4F, F_{meta}); HRMS-ESI-TOF *m/z* calcd for $C_{50}H_{18}F_{15}N_4O_3Ga$ $(M)^{+\cdot}$ 1076.0412, found 1076.0362.

Yield: 87%. Colour: purple

4.4.4.2 Preparation of the solid supports doped with compounds 5 and 6.

The solid supports based on the agarose were prepared by the addition of compounds **5** or **6** (1 mg) to agarose (15%) using the conventional 1D-Gel Electrophoresis procedure described for protein separation.[56] The solid supports based on cellulose were prepared by dissolving 0.4 g of carboxymethylcellulose sodium salt in 8 mL of *ca.* 1×10^{-5} M solutions of **5** or **6**, and the final pH (pH=8) measured on a MeterLab 240 pH meter was slightly readjusted before gelification with the addition of small amounts of NaOH or HCl.

4.5 Supplementary data

Table SN1- All photophysical data of compounds **3**-**8** in solution[#]at 298K. ([#]solvents: a-toluene, b-dicloromethane, c-dimethylsulfoxide, d-ethanol, e-water:ethanol(50:50).

Conjugates	λ_{max}(logε) / nm	λ_{em} / nm	Stoke's shift /nm	Φ_{flu}
3	426[a] (5.23) 565(3.95) 599(3.21)	599, 646	47	0.02
	423[b] (5.28) 563(3.97) 599(3.25)	599, 646	47	0.02
4	426[a] (5.28) 560(4.15) 599(3.31)	599, 646	47	0.01
	426[b] (5.24) 561(3.87) 595(3.35)	595, 645	50	0.01
5	421[a] (5.32) 523(4.15) 557(3.85)	652, 719	67	0.02
	419[b] (5.34)526(4.11)560(3.86)	652, 713	61	0.02
	420[c] (5.33) 524(4.13) 562(3.88)	651, 712	61	0.02
	417[d](5.31) 519(4.13) 564(3.86)	652, 713	61	0.03
	424[e](5.33) 526(4.18) 562(3.90)	654, 714	60	0.01
6	420[a](5.38) 519(4.15) 560(3.86)	652, 713	61	0.02
	420[b](5.36) 523(4.12) 562(3.81)	653, 712	59	0.02
	420[d](5.38) 521(4.11) 562(3.84)	652, 713	60	0.03
7	427[a](5.51) 580(4.30) 602(3.81)	602, 650	48	0.06
	428[b](5.49) 585(4.28) 601(3.78)	601, 648	47	0.06
	427[c](5.49) 581(4.27) 603(3.79)	603, 651	48	0.04
	428[d](5.49) 585(4.26) 601(3.75)	601, 652	51	0.11
8	426[a](5.53) 582(4.27) 592(3.73)	602, 651	59	0.09
	430[b](5.51) 585(4.31) 595(3.71)	601, 648	53	0.05
	430[c] (5.51) 587(4.31) 605(3.75)	618, 668	63	0.04
	427[d](5.47) 597(4.26) 605(3.73)	609, 647	50	0.13

4. 6 References

[1] Sessler, J. L.; Karnas, E. ;Sedenberg, E. In: Gale, P. A.; Steed, J. W. (Eds), John Wiley & Sons, Chichester, **2012**, vol 3, pp 1045-1074.

[2] Choi, J. K.; Sargsyan,G.; Olive, A. M.; Balaz, M. *Chem. Eur. J.* **2013**, 19, 2515-2522.

[3] Liu, B.-W.; Chen, Y.; Song, B.-E.; Liu, Y. *Chem. Commun*. **2011**, 47, 4418-4420.

[4] Cho, Y.; Lee, S. S.; Jung, J. H. *Analyst* **2010**, 135, 1551-1555.

[5] Pariyar, A.; Bose, S.; Chhetri, S. S.; Biswas, A. N.; Bandyopadhyay, P. *Dalton Trans*. **2012**, 41, 3826-2831.

[6] Santos, C. I. M.; Oliveira, E.; Barata, J. F. B.; Faustino, M. A. F.; Cavaleiro, J. A. S.; Neves, M. G. P. M. S.; Lodeiro, C. *J. Mat. Chem.* **2012**, 22, 13811-13819.

[7] Kim, H. N.; Ren, W. X.; Kim, J. S.; Yoon, J. *Chem. Soc. Rev.* **2012**, 41, 3210-3244.

[8] Pietrzak, M.; Mroczkiewicz, M.; Malinowska, E. *Electroanalysis* **2012**, 24, 173-179.

[9] Cormode, D. P.; Drew, M. G. B.; Jagessar, R.; Beer, P. D. *Dalton Trans*. **2008**, 6732-6741.

[10] Gilday, L. C.; White, N. G.; Beer, P. D. *Dalton Trans.* **2012**, 41, 7092-7097.

[11] Li, Y.; Cao, L.; Tian, H. *J. Org. Chem.* **2006**, 71, 8279-8282.

[12] Liu, H.; Shao, X. B.; Jia, M.; Jiang, X. K.; Li, Z. T.; Chen, G. J. *Tetrahedron* **2005**, 61, 8095-8099.

[13] Aviv-Harel, I; Gross, Z. *Coord. Chem. Rev.* **2011**, 255, 717-736.

[14] Flamigni, L.; Gryko, D. T. *Chem. Soc. Rev.* **2009**, 38, 1635-1646.

[15] He, C. L.; Ren, F. L., Zhang, X. B; Han, Z. X. *Talanta* **2006**, 70, 364-369.

[16] García-Beltrán, O.; Mena, N.; Berríos, T. A.; Castro, E. A.; Cassels, B. K.; Núñez, M. T.; Aliaga, M. E. *Tetrahedron Lett.* 2012, 53, 6598-6601.

[17] Kim, H. J.; Park, J. E.; Choi, M. G.; Ahn, S.; Chang, S.-K. *Dyes Pigments* 2010, 84, 54-58.

[18] Voutsadaki, S.; Tsikalas, G. K.; Klontzas, E.; Froudakis, G. E.; Katerinopoulos, H. E. *Chem. Commun.* **2010**, 46, 3292-3294.

[19] Jiang, Y.; Hu, X.; Hu, J.; Liu, H.; Zhong, H.; Liu, S. *Macromolecules* **2011**, 44, 8780-8790.

[20] Sokkalingam, P.; Lee, C.-H., *J. Org. Chem.* **2011**, 76, 3820-3828.

[21] Zhuang, X.; Liu, W.; Wu, J.; Zhang, H.; Wang, P. *Spectrochim. Acta A*, **2011**, 79, 1352-1355.

[22] Cao, X.; Lin, W.; Yu, Q.; Wang, J. *Org. Lett.* **2011**, 13, 6098-6101.

[23] Upadhyay, K.K.; Mishra, R. K.; Kumar, V.; Roy Chowdhury, P. K. *Talanta*, **2010**, 82, 312-318.

[24] Yang, Z.; Liu, Z.; Chen, Y.; Wang, X.; He, W; Lud, Y. *Org. Biomol. Chem.* **2012**, 10, 5073.

[25] Kim, G.-J.; Kim, H.-J. *Tetrahedron Lett.* **2010**, 51, 185-187.

[26] Mao, M.; Song, Q.-H. *Dyes Pigments*, **2012**, 92, 975-981.

[27] Lin, W.; Long, L.; Feng, J.; Wang, B; Guo, C. *Eur. J. Org. Chem.* **2007**, 26, 4301-4304.

[28] Tasior, M.; Gryko, D. T.; Pielacińska, D. J.; Zanelli, A; Flamigni, L. *Chem. Asian J.* **2010**, 5, 130-140.

[29] Tasior, M.; Voloshchuk, R.; Poronik, Y. M.; Rowicki, T.; Gryko, D. T. *J. Porphyrins Phthalocyanines* **2011**, 15, 1011-1023.

[30] Menezes, J. C. J. M. D. S.; Gomes, A. T. P. C.; Silva, A. M. S.; Faustino, M. A. F.; Neves, M. G. P. M. S.; Tomé, A. C.; Silva, F. C.; Ferreira, V. F.; Cavaleiro, J. A. S. *Synlett* **2011**, 13, 1841-1844.

[31] Lodeiro, C.; Capelo, J. L.; Mejuto, J. C.; Oliveira, E.; Santos, H. M.; Pedras, B.; Nuñez, C. *Chem. Soc. Rev.* **2010**, 39, 2948–2976.

[32] Nordstrom, D. K.; Alpers, C. N.; Ptacek, C. J.; Blowes, D. W. *Environ. Sci. Technol.* **2000**, 34, 254-258.

[33] Gu, Z.; Zhao, M.; Sheng, Y.; Bentolila, L. A.; Tang, Y. *Anal. Chem.* **2011**, 83, 2324-2329.

[34] (a) Charlton, J. L.; Alauddin, M. M. *Tetrahedron,* **1987**, *43*, 2873-2889. (b) Segura, J. L.; Martín, N. *Chem. Rev.* **1999**, *99*, 3199-3246.

[35] (a) Nair, V.; Sheela, K. c., Radhakrislman, K. V.; Rath, N. P. *Tetrahedron Lett.***1998**, 39, 5627-5630. (b) Nair, Y.; Radhakrishnan, K. V.; Sheela, K. C.; Rath, N. P. *Tetrahedron,* **1999**, 55, 14199-14210. (c) Nair, V.; Shee1a, K. c., Rath, N. P. *Tetrahedron Lett.* **2000**, 41, 6217-6221.

[36] (a) Port. M.; Lett, R. *Tetrahedron Lett.* **2006**, *47*, 4671-4675; (b) Ibrahim-Ouali, M.*Tetrahedron Lett.* **2010**, *51*, 3610-3612. (c) Nemoto, H. *Chem. Pharm. Bull.* **2007**, *55*,

961.(d) Matsuya, Y. ; Masuda,S.; Itoh,T.; Murai, T.; Nemoto, H. *J. Org. Chem.* **2005**, *70*, 6898-6903.

[37] (a) Kitagaki, S.; Katoh, K.; Ohdachi, K.; Takahashi, y.; Shibata, D.; Mukai, C. *J. Org.Chem.* **2006**, *71*, 6908-6914. (b) Coll, G.; Costa, A.; Deya, P. M.; Flexas, F.; Rotger, C.; Saá, J. M. *J. Org. Chem.* **1992**, *57*, 6216-6222. (c) Nakamura, Y.; O-kawa, K.; Minami, S.; Ogawa, T.;Tobita, S.; Nishimura, J. *J. Org.Chem.* **2002**, *67*, 1247-1261.

[38] Groot, A; Janson B. M. *Tetrahedron Lett.* **1975**, 3407-3410.

[39] Tome´, A. C.; Lacerda, P. S.S,; Neves, M. G. P. M. S.; Cavaleiro, J. A. S. *Chem. Commun.* **1997**, 1199-1200.

[40] Kamlet, M.J.; Taft, R.W. *J. Am. Chem. Soc.* **1976**, 98, 377.

[41] Kawski, A. *Acta Physica Polonica* **1966**, 29, 507-518.

[42] Kawski, A. *Progress in Photochemistry and Photophysics* Boca Raton, Boston, **1992**.

[43] Ali, H.; Van Lier, J. E. In *Handbook of Porphyrin Science*: Kadish, K. M., Smith, K. M., Guilard, R. (Eds), World Scientific Publishing Company: Singapore **2010**; vol 4, pp 1.

[44] Kleerekoper, M. *Endocrinol. Metab. Clin. North Am.* **1998**, 27, 441-452.

[45] Cametti, M.; Rissanen, K., *Chem. Commun*. **2009**, 2809-2829.

[46] Ayoob, S.; Gupta, A. K. *Crit. Rev. Environ. Sci. Technol.* **2006**, 36, 433-487.

[47] Bai, Y.; Zhang, B.; Xu, J.;Duan, C-Y.;Dang, D-B.;Liu, D-E.; Meng, Q-E. *New J. Chem.* **2005**,29, 777-779.

[48] Gans, P.; Sabatini, A.; Vacca, A. *Talanta* **1996**, 43, 1739-1753.

[49] MacCarthy, P. *Anal. Chem.* **1978**, 50, 2165-2166.

[50] Boening, D. W.; Chew, C. M. *Water, Air and Soil Pollution* **1999**, 109, 67-79.

[51] Young, C.A.; Tidwell, L. G.; Anderson, C. G. Eds. *Cyanide*: *Social, Industrial, and Economic Aspects*; Minerals, Metals, and Materials Society: Warrendale, **2001**, 289-303.

[52] *Guidelines for Drinking-Water Quality*, World Health Organization, Geneva, **1996**.

[53] Boening, D. W. *Chemosphere* **2000**, 40, 1335-1351.

[54] Serra, V. V.; Andrade, S. M.; Neves, M. G. P. M. S.; Cavaleiro, J. A. S.; Costa, S. M. B. *New J. Chem.* **2010**, 34, 2757-2765.

[55] Finikova, O.; Galkin, A.; Rozhkov, V.; Cordero, M.; Hägerhäll, C.; Vinogradov, S. *J. Am. Chem. Soc.* **2003**, 125, 4882-4893.

[56] Galesio, M.; Vieira, D.V.; Rial-Otero, R.; Lodeiro, C.; Moura, I.; Capelo, J. L. *J. Proteome Res.* **2008**, 7, 2097-2106

Chapter V

Corrole and Corrole Functionalized Silica Nanoparticles as New Metal Ion Chemosensors: A Case of Silver Satellite Nanoparticles Formation

Published in *Inorg. Chem.* **2013**, 52, 8564−8572

INDEX

5- Corrole and Corrole Functionalized Silica Nanoparticles as New Metal Ion Chemosensors: A Case of Silver Satellite Nanoparticles Formation

Resumo

Os macrociclos corrólicos são fluoróforos muito interessantes para serem utilizados na formação de quimiosensores fluorescentes, uma vez que podem estabelecer interacções com os analitos quer através do seu núcleo de coordenação trianiónico quer através de grupos funcionais auxiliares que possam apresentar. Neste trabalho é determinada a habilidade sensorial do 5,10,15-tris(pentafluorofenil)corrol **1** e da respetiva espécie monoaniónica para os iões metálicos Na^{+}, Ca^{2+}, Cu^{2+}, Cd^{2+}, Pb^{2+}, Hg^{2+}, Ag^{+}, Al^{3+}, Zn^{2+}, Ni^{2+}, Cr^{3+}, Ga^{3+}, Fe^{3+} em tolueno e em acetonitrilo. As propriedades fotofísicas dos corróis na presença destes iões metálicos foram estudadas por espectroscopia de absorção de ultravioleta-visível e de emissão de fluorescência. Os resultados obtidos mostraram a formação de complexos de fórmula geral L_2M com Cd^{2+}, Pb^{2+}, Hg^{2+}, Ag^{+}, Cr^{3+} e Al^{3+} e LM com Cu^{2+}, Ga^{3+} e Fe^{3+} em tolueno. De entre todos os iões metálicos estudados, a forma monoaniónica do corrole 1 (**1**$^{-}$) mostrou ser colorimétrica para o Hg^{2+} permitindo a sua detecção a olho nu, através de uma mudança de cor de verde escuro para verde pálido em tolueno. O corrol **1** em acetonitrilo também mostrou ser selectivo e colorimétrico para o Hg^{2+}. Assistiu-se a uma mudança de cor da solução de roxo para verde-azulado.

Neste trabalho descreve-se ainda a síntese do derivado *β*-iminocorrol **4** que após funcionalização com 3- isocianatopropiltrimetoxisilano originou um derivado do tipo alcoxisilano **5**, que foi, posteriormente, ancorado a nanopartículas comerciais de sílica. Curiosamente, após a adição de Ag^{+}formaram-se grupos de nanopartículas satélites de prata em torno das nanopartículas de sílica. Ao mesmo tempo, foi observada uma mudança de cor na solução, esta passou de verde a amarela.

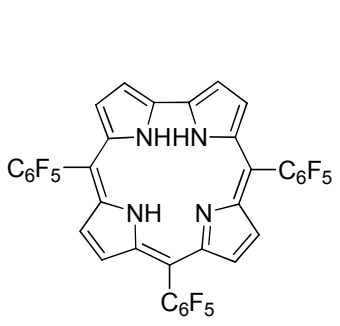

1

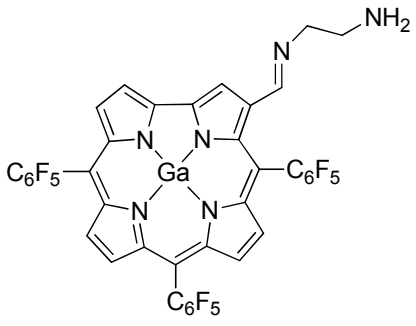

4

Abstract

Corrole macrocycles are very appealing fluorophores which not only offer coordination sites but can also induce dynamic interaction with the guest via auxiliary functional group. This work shows the sensorial ability of 5,10,15-tris(pentafluorophenyl)corrole **1** and its monoanionic species (**1**$^{-}$) towards Na^{+}, Ca^{2+}, Cu^{2+}, Cd^{2+}, Pb^{2+}, Hg^{2+}, Ag^{+}, Al^{3+}, Zn^{2+}, Ni^{2+}, Cr^{3+}, Ga^{3+} and Fe^{3+} metal ions in toluene and acetonitrile. The photophysical studies towards metal ions were carried out by absorption and emission spectroscopy. Metal complexes with formula L_2M, were obtained in the interaction of **1**$^{-}$ with Cd^{2+}, Pb^{2+}, Hg^{2+}, Ag^{+}, Cr^{3+} and Al^{3+}, while LM species were identified with Cu^{2+}, Ga^{3+} and Fe^{3+}, in toluene. Corrole **1** shows to be colorimetric for Hg^{2+} allowing a naked-eye detection of Hg^{2+} through a change of colour from purple to blue in acetonitrile. Also the species corrole 1^{-} reveals to be selective for Hg^{2+}, where a change of color from dark green to green was visualized. In addition a new *β*-imine corrole **4** was successful synthetized and further functionalized with 3-isocyanatopropyl-trimethoxysilane resulting in an alkoxysilane derivative **5**. The grafting of alkoxysilane derivative **5**, with optically transparent silica nanoparticles (SiNPs) was achieved succesfully. The new-coated silica nanoparticles with corrole **5** were studied in the presence of Cu^{2+}, Hg^{2+} and Ag^{+} as metal ion probes. Interestingly, upon addition of Ag^{+}, groups of satellite AgNPs were formed around the SiNPs and were checked by transmission electron microscopy (TEM). At same time, a change of color from green to yellow was observed.

5.1. Introduction

The design, synthesis and application of fluorescent molecular probes that selectively recognize the presence of biologically important analytes, such as metal ions, is an area in constant growth.[1] In the last few years the easy detection and quantification of pollutant metallic species by fluorescent molecular probes have attracted interest in fields such as waste management, environmental chemistry and clinical toxicology.[2]

Corroles are tetrapyrrolic macrocycles with one *meso* carbon less than porphyrin analogues, providing a trianionic coordination sphere that it is able to stabilize metal ions in high valent oxidation state.[3] Considering the synthetic approaches developed for corroles, their chemical functionalization can afford new compounds with potential applications as catalysts, dyes for solar energy conversion and in Medicine.[4,5]

These macrocyles have also useful properties to be used as fluorescent chemosensors for molecular recognition.[6] They absorb and emit light in the visible region, and show high excitation coefficients, fluorescent quantum yields and photostability. Corroles also display inner nitrogen donor atoms available for metal recognition.[7] However, in contrast to porphyrins, the sensorial ability of corroles has been under study. Up to date there are few reports about the use of corroles as sensing materials in analytical chemistry.[8,9]

The 5,10,15-tris(pentafluorophenyl)corrole **1** is one of the most studied macrocycle of the corrole family and one of our major interests is concerned with its functionalization and further applications.[10] Among the metal ions, there are particular interest in metals with biological and environmental impact.[1,11-17]In this way we decided to evaluate the sensorial ability of 5,10,15-tris(pentafluorophenyl)corrole **1** in the absence and in the presence of OH^- anion towards Na^+, Ag^+, Ca^{2+}, Cu^{2+}, Cd^{2+}, Pb^{2+}, Hg^{2+}, Ni^{2+}, Zn^{2+}, Al^{3+}, Cr^{3+}, Fe^{3+} and Ga^{3+} metal ions in the aprotic solvents, as toluene and acetonitrile (see figure 1).

Taking into account that the incorporation of a highly emissive corrole unit in silica nanoparticles[18] could improve the affinity, versatility and sensitivity of the chromophore to the guest, we decide to coat silica nanoparticles with corrole **5** bearing an imine linkage (see figure 1). The sensorial ability of these nanoparticles was also evaluated towards Hg^{2+}, Ag^+ and Cu^{2+}.

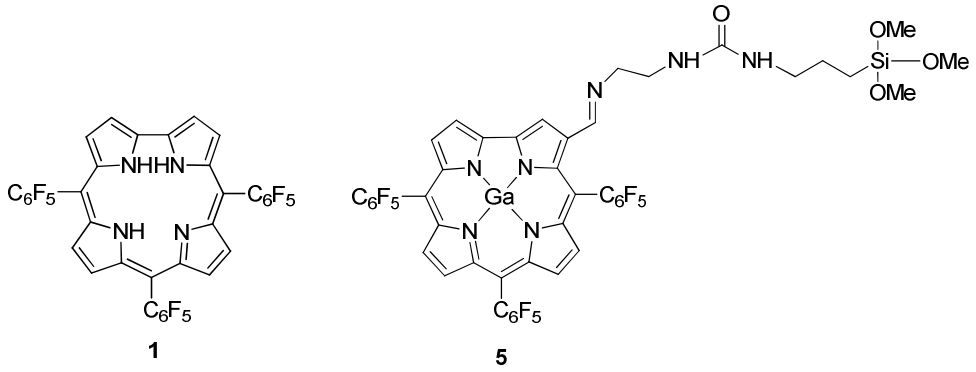

Figure 1: Structure of compounds **1** and **5**.

5.2. Results and Discussion

5.2.1 Photophysical studies with corrole 1

Spectrophotometric and spectrofluorimetric titrations and metal ion sensing effects in the presence of corrole 1

The 5,10,15-tris(pentafluorophenyl)corrole **1** is a macrocycle of the corrole family that displays unique properties to be used as a host (fluorophore) for metals since that it shows a trianionic coordination site available for establishing interactions. In this chapter we decided to study their host-guest interactions towards different cations.

The first studies concerning the sensorial ability of compound **1** towards the different metals, Ag^{+}, Na^{+}, Ca^{2+}, Cd^{2+}, Pb^{2+}, Zn^{2+}, Ni^{2+},Cu^{2+}, Hg^{2+}, Fe^{3+}, Cr^{3+}, Ga^{3+}, Al^{3+} were performed in toluene, where the decomposition of the corrole macrocycle is minimized.[19]

The absorption spectrum of compound **1** in toluene shows the Soret-type band at 415 nm and the Q-type band centered at 565 nm, while the emission spectrum shows a band at 645 nm with a fluorescence quantum yield of 0.05.[9] To avoid the reabsorption phenomena, the emission spectrum was collected on the Q-bands. However, no significant changes were detected in the ground and excited state of this corrole after titration in the presence of the metals selected.

Knowing that compound **1** presents a high N-H acidity being really sensitive to anions prompts us to evaluate if its metal sensing ability is modified after deprotonation with OH^{-}.[20] The addition of this anion to corrole **1** promotes in the absorption spectrum a decrease accompanied by a red shit in the Soret band from 415 to 440 nm ($\Delta\lambda$ = 25 nm) and in the

Q-band from 565 to 606 nm ($\Delta\lambda$ = 41 nm) (see figure 2). At same time, a naked-eye change of colour from purple to green is visualized upon addition of OH^-. In the fluorescence spectra a strong enhancement in the emission intensity at 644 nm was observed, as well as, a blue shift from 644 nm to 626 nm (see figure 2 and picture in figure 2). In addition in the emission spectra it was detected the appearance of a new band at 670 nm. These features are similar to the ones described for corroles in the presence of organic bases, [21] confirming that after titration we are in the presence of the monoanionic form of corrole $[(Cor)H_2]^-$. A similar spectroscopic profile was also reported by Gross and co-workers,[20] where a pH study was carried out, allowing to conclude that the pH range at which neutral corroles exist is extremely limited.

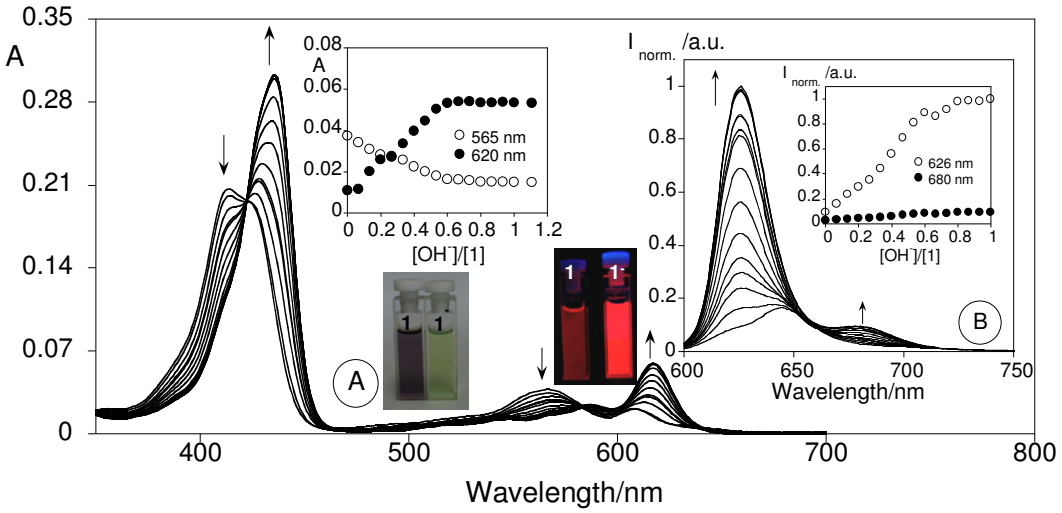

Figure 2: Spectrophotometric (A) and spectrofluorimetric (B) titration of corrole **1** with the addition of OH^- in toluene. The inset represents the absorption (A) and the emission intensity (B) as a function of [OH^-]/[**1**] at 415 nm, 440 nm, 565 nm and 620 nm for (A), 626 nm and 680 nm for (B). ([**1**] = 1 $\times 10^{-5}$ M, λ_{exc} = 565 nm, T = 298 K).

Corrole **1** does not present any spectral changes in the ground and excited states after addition of the metal ions mentioned above.

However, the addition of Cu^{2+}, Cd^{2+}, Pb^{2+}, Hg^{2+}, Ga^{3+}, Cr^{3+}, Fe^{3+}, Ag^+ or Al^{3+} to corrole **1** after its previous deprotonation with 0.5 equivalents of OH^-, is responsible for significant alterations in the absorption and emission spectra. Only the titrations with Na^+, Ca^{2+}, Ni^{2+}, Zn^{2+} did not affect the ground and the excited state of the monoanionic form of corrole **1** that will be referred here as **1**$^-$.

Figure 3 shows the modifications observed in the absorption and emission spectra of **1**$^{-}$ in the presence of Cd^{2+}, Cu^{2+} and in figure 4 in the presence of Hg^{2+}. The titrations with the other metal ions (Ga^{3+}, Fe^{3+}, Cr^{3+}, Pb^{2+}, Al^{3+} and Ag^{+}) presented a similar behavior and are shown in experimental section (Figures SN1 and SN2). The addition of Cd^{2+}, produces alterations in the absorption spectrum, such as, a decrease in the Q-type absorption band at 620 nm and in the Soret-type band at 440 nm that is accompanied with the concomitant appearance of blue-shift bands at 606 nm ($\Delta\lambda$ = 14 nm) and at 415 nm ($\Delta\lambda$ = 25 nm). An isosbestic point at 426 nm was observed.

Considering the fluorescence spectra, the addition of these metal ions promotes a quenching in the emission intensity at 626 nm, accompanied by a red shift from 626 nm to 645 nm ($\Delta\lambda$ = 19 nm).

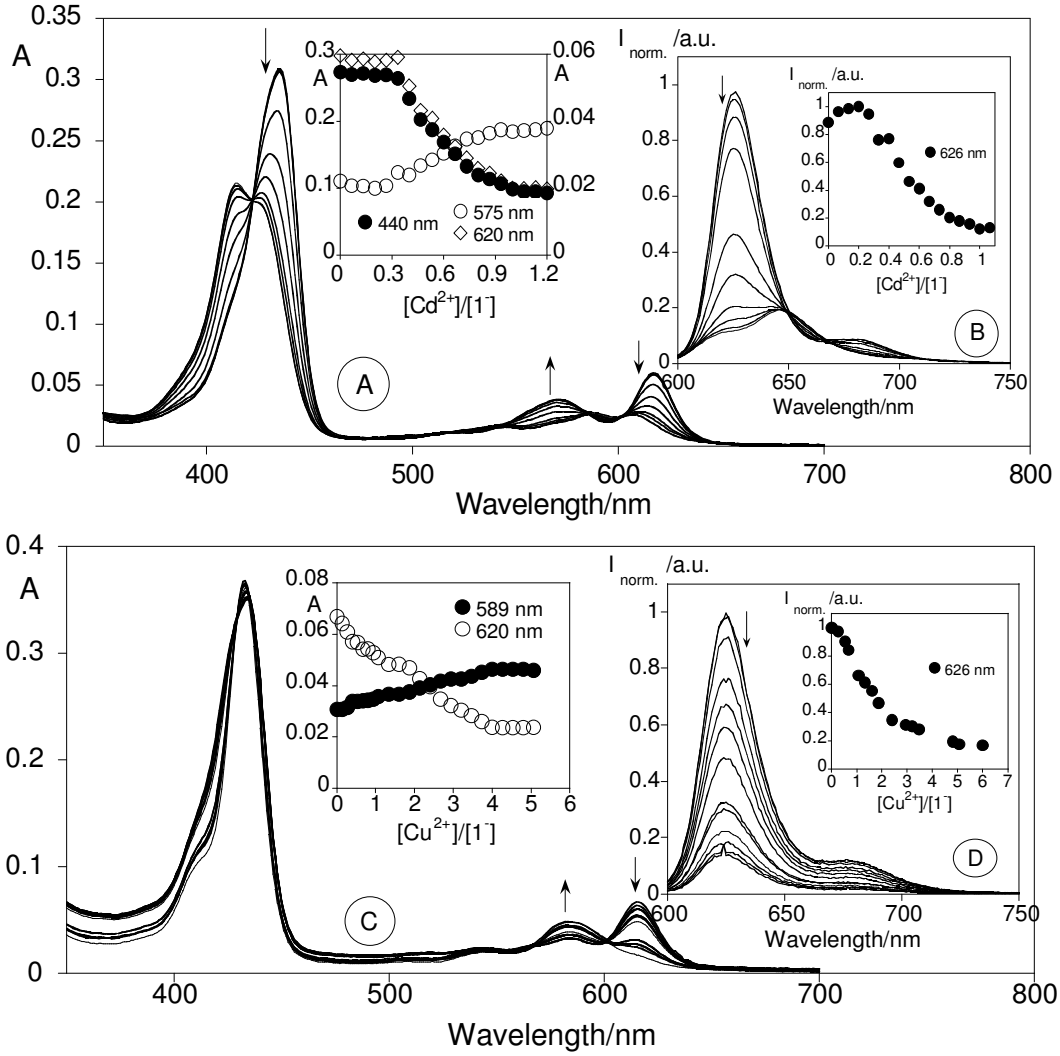

Figure 3: Spectrophotometric (A, C) and spectrofluorimetric (B, D) titration of $\mathbf{1}^-$ with the addition of Cd^{2+} (A, B) and Cu^{2+} (C, D) in toluene. The inset represents the absorption at 440 nm, 575 nm and 620 nm for A, at 589 nm and 620 nm for C; and the emission intensity at 626 nm (B, D) as a function of $[Cd^{2+}]/[\mathbf{1}^-]$, and $[Cu^{2+}]/[\mathbf{1}^-]$, respectively. ($[\mathbf{1}^-] = 1 \times 10^{-5}$ M for $[Cd^{2+}]$ and $[\mathbf{1}^-] = 1.2 \times 10^{-5}$ M for $[Cu^{2+}]$, $\lambda_{exc} = 565$ nm, T = 298 K).

The titration with Cu^{2+} produces only alterations in the Q-bands region in the absorption spectra where a decrease of the band at 620 nm with the concomitant appearance of a blue shift band at 589 nm is observed. In the emission spectra it was only observed a quenching in the emission intensity at 626 nm without any shift (figure 3D).

The most interesting results arise from the interaction of the monoanionic form of corrole **1** with Hg^{2+}, where a colorimetric effect was visualized, with a change of colour from dark *green* to *pale* green (see figure 4). The addition of Hg^{2+} to $\mathbf{1}^-$ results in a blue shift of the Soret band from 440 nm to 420 nm ($\Delta\lambda$ = 20 nm) and in the Q-type band from 620 nm to 575 nm ($\Delta\lambda$ = 45 nm) with a decrease in the absorbance. The appearance of a charge transfer bands (LMCT – Ligand to metal charge transfer) at 478 nm and at 720 nm was observed as well. The blue shift in the ICT (intramolecular charge transfer) transitions can be attributed to Hg^{2+} metal ion binding to free nitrogen atoms in the inner of the macrocycle. In the emission spectra, the addition of Hg^{2+} is responsible by the total quenching in the fluorescence intensity at 626 nm accompanied by a red shift from 626 nm to 650 nm. This behavior is not unexpected due to Hg^{2+} "heavy" metal ion nature, which increases the probability to occur non-radiative deactivation processes, such as intersystem crossing, responsible by chelation enhancement of quenching (CHEQ) in the emission intensity.[22]

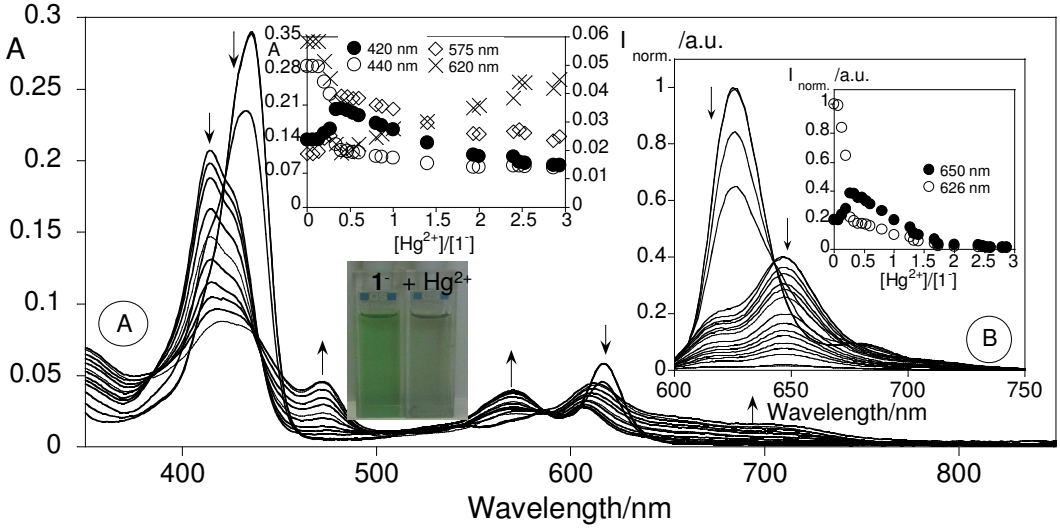

Figure 4 – Spectrophotometric (A) and spectrofluorimetric (B) titration of compound $\mathbf{1}^-$ with the addition of Hg^{2+} in toluene. The inset represents the absorption (A) and the emission intensity (B) as a function of $[Hg^{2+}]/[\mathbf{1}^-]$ at 420 nm, 440 nm, 575 nm and 620 nm for (A) 626 nm and 650 nm for (B). ($[\mathbf{1}^-] = 9.0 \times 10^{-6}$ M, $\lambda_{exc} = 565$ nm, T = 298 K).

The association constants for the interaction of compound $\mathbf{1}^-$ with the different metal ions were calculated using the HypSpec[23] program and are summarized in Table 1. The stoichiometry of two ligands per metal ion (L_2M) could be postulated for Cd^{2+}, Pb^{2+}, Hg^{2+}, Ag^+, Cr^{3+} or Al^{3+} and one ligand per metal in the presence of Cu^{2+}, Ga^{3+} and Fe^{3+}.

Table 1 - Association constants (emission data), detection (LOD) and quantification (LOQ) limits of $\mathbf{1}^-$ in toluene.

Metal	Log $K_{ass.}$ (L:M)	**LOD** (ppm)	**LOQ** (ppm)
$\mathbf{Al^{3+}}$	14.32±0.25 (2:1)	0.03	0.05
$\mathbf{Cd^{2+}}$	10.99±0.01 (2:1)	0.04	0.08
$\mathbf{Pb^{2+}}$	11.32±0.01 (2:1)	0.04	0.07
$\mathbf{Hg^{2+}}$	8.43±0.02 (2:1)	0.02	0.3
$\mathbf{Ag^{+}}$	12.33±0.07 (2:1)	0.02	0.03
$\mathbf{Cr^{3+}}$	12.61±0.02 (2:1)	0.09	0.12
$\mathbf{Fe^{3+}}$	7.66 ± 0.02 (1:1)	0.04	0.08
$\mathbf{Ga^{3+}}$	6.49 ± 0.02 (1:1)	0.02	0.04
$\mathbf{Cu^{2+}}$	4.23 ± 0.02 (1:1)	0.03	0.06

Looking at table 1 the most stable complexes were formed with Al^{3+}, Cr^{3+} and Ag^{+}, with log K_{ass} = 14.30 ± 0.25, log K_{ass} = 12.61 ± 0.02 and log K_{ass} = 12.33 ± 0.07, respectively. From the other association constant values: log $K_{ass\ Pb^{2+}}$ = 11.32 ± 0.01 (L_2M) > log $K_{ass\ Cd^{2+}}$ = 10.99 ± 0.01 (L_2M) > log $K_{ass\ Hg^{2+}}$ 8.43 ± 0.02 (L_2M) > log $K_{ass\ Fe^{3+}}$ 7.66 ± 0.02 (LM) > log $K_{ass\ Ga^{3+}}$ 6.49 ± 0.02 (LM) >log $K_{ass\ Cu^{2+}}$ = 4.23 ± 0.02 (LM) we can conclude that the monoanion of corrole **1** coordinated better with Pb^{2+} followed by Cd^{2+}, Hg^{2+} and finally Cu^{2+} metal ions.

Apart from the type of donor atoms present in the inner of the corrole, where the metal complexation occurs, other parameters in the macrocycle such as the cavity size, shape, conformation, topology and rigidity and the radius of the metal ion are important because they influence the thermodynamic and kinetics properties of the corresponding final metal complexes. Moreover, in macrocyclic ligands the chelate and macrocycle effects must be taken into account.[24,25]

Figure 5 shows the normalized fluorescence intensity of corrole **1** after being deprotonated with OH^- and after the addition to this monoanionic form of 0.5 equivalents of M^{n+} metal ions in toluene (M^{n+} = Na^+, Ca^{2+}, Ni^{2+}, Zn^{2+}, Cd^{2+}, Cu^{2+}, Pb^{2+}, Hg^{2+}, Ga^{3+}, Cr^{3+}, Fe^{3+}, Ag^+ and Al^{3+})

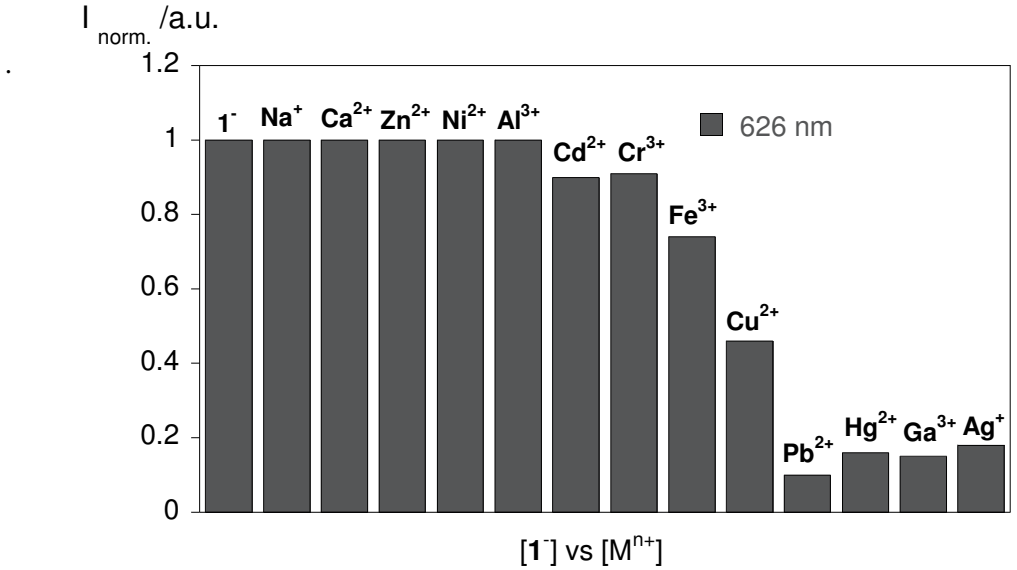

Figure 5: Normalized fluorescence at 626 nm of compound **1** with the first addition of OH^- (species $\mathbf{1}^-$), and after addition of 0.5 equivalents of [M^{n+} = Na^+, Ca^{2+}, Ni^{2+}, Zn^{2+}, Cd^{2+}, Cu^{2+}, Pb^{2+}, Hg^{2+}, Ga^{3+}, Cr^{3+}, Fe^{3+}, Ag^+ and Al^{3+}] = M^{n+} metal ions in toluene.

Taking into account the results of figure 5, we can see the evident CHEQ effect of the specie $\mathbf{1}^-$ in the presence of 0.5 equivalents of the heavy, pollutants and toxic, Pb^{2+}, Hg^{2+}, Cd^{2+} and Ag^+ metal ions, while a strong quenching between 50% and 80% was observed.

The detection (LOD) and quantification (LOQ) limits for the metal ions studied were also determined in the presence of the monoanionic form $\mathbf{1}^-$, using the emission band centred at 626 nm (Table 1). The values obtained show that the lowest values of LOD and LOQ were found for Ag^+; with this macrocycle the minimum amount of Ag^+ detectable was 0.02 and the minimum amount quantified was 0.03 ppm.

Since all the metal salts used, show good solubility in acetonitrile, it was decided to perform several titrations towards the same metal ions, in this solvent with and without the previous addition of OH^- anion. When the titrations were carried after desprotonation with OH^-, no spectral alterations were detected in the absorption and emission spectra. However, without the previous addition of OH^- anion, the increase of the dipole moment of the solvent from 0.36 D (toluene) to 3.92 D (acetonitrile), leaded to a better sensorial and selectivity capability of corrole **1** for Hg^{2+}. In figure 6 are presented the modifications observed in the absorption and emission spectra of compound **1** with the increasing

addition of Hg^{2+} metal ion. In these conditions, no changes were detected in the ground and excited state of corrole **1** upon addition of the other metal ions studied.

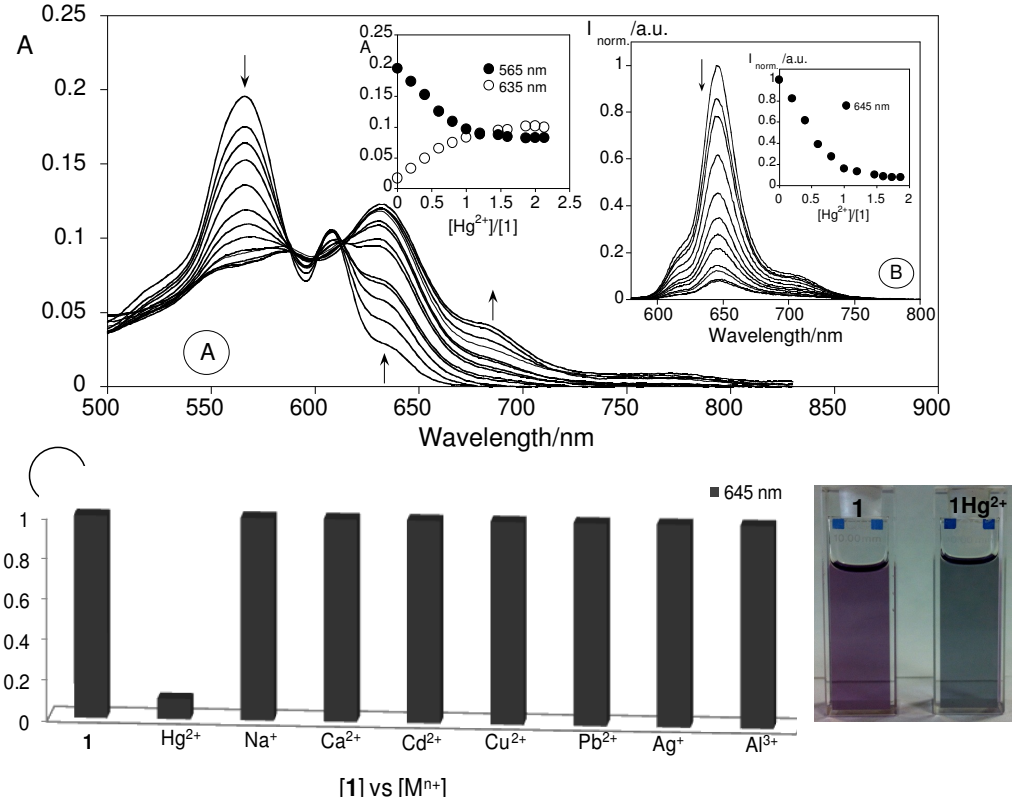

Figure 6- Spectrophotometric (A) and spectrofluorimetric (B) titration of **1** with the addition of Hg^{2+} in acetonitrile. The inset represents the absorption (A) and the emission intensity (B) as a function of $[Hg^{2+}]/[\mathbf{1}]$ at 565 nm and 635 nm for (A), 645 nm for (B). ($[\mathbf{1}] = 1 \times 10^{-5}$ M, $\lambda_{exc} = 565$ nm, T = 298 K). (C) - Normalized fluorescence at 645 nm of compound **1** with addition of 0.5 equivalents of metal ions in acetonitrile [(Na^+, Ca^{2+}, Cd^{2+}, Cu^{2+}, Pb^{2+}, Hg^{2+}, Ag^+ and Al^{3+})= M^{n+}]; and picture with a colour change from purple to green-blue with the addition Hg^{2+} in acetonitrile.

In this case, the Soret band of compound **1** upon addition of Hg^{2+} was practically not affected, whereas the Q-band region showed significant changes. Looking at figure 6A, it can be observed that the addition of the metal ion is responsible by a decrease in the absorbance band at 565 nm that is accompanied by the appearance of two bands at 635 nm and 680 nm. In these conditions it was also observed a colorimetric effect (a change of colour from purple to green-blue) which allows again a naked-eye detection of Hg^{2+} (see figure 6C). In the emission spectra a quenching in the emission intensity at 645 nm was visualized (figure 6B). The association constant was also determined by HypSpec program and the value obtained for **1** in the presence of Hg^{2+} (acetonitrile) was log $K_{ass\ Hg^{2+}}$ = 9.04 ±

0.01, with a stoichiometry of two ligands per one metal ion, which is slightly higher than the one obtained for **1**$^-$ in the presence of Hg^{2+} in toluene [log $K_{ass\ Hg^{2+}}$ = 8.43 ± 0.02, (L_2M)].

As a conclusion, corrole **1** in acetonitrile shows a higher affinity and an unprecedented selectivity for Hg^{2+} metal, as can be seen in figure 6C, where a normalized intensity of fluorescence towards the addition of 0.5 equivalents of metal ions studied is shown.

5.2.2 Theoretical Studies

To understand better the complex formation, the preferential stoichiometries and binding modes of corrole **1**$^-$ to Al^{3+}, Cu^{2+} and Ag^+ were assessed through a series of electronic calculations[26] performed at the density functional theory (DFT) level, using Gaussian09.[27] The energetics of the 1:1 and 2:1 (ligand:metal) binding stoichiometries was evaluated by calculating the energy gain/loss obtained upon formation of the complex from its individual components.

The complexation of Al^{3+} with **1**$^-$ occurs preferentially in a 2:1 stoichiometry, as shown in Figure 7. The coordination of the cation occurs with four nitrogens from one corrole unit and with one nitrogen from a second corrole, with $Al^{3+}\cdots N$ distances ranging from 1.91 to 2.12 Å, in what resembles a square pyramid coordination environment. Our DFT calculations revealed that this 2:1 binding arrangement is more stable than the 1:1 stoichiometry in ca. -0.127 Ha (-332.8 kJ mol^{-1}; see Figure 8 for the analogous 1:1 complex with Cu^{2+}).

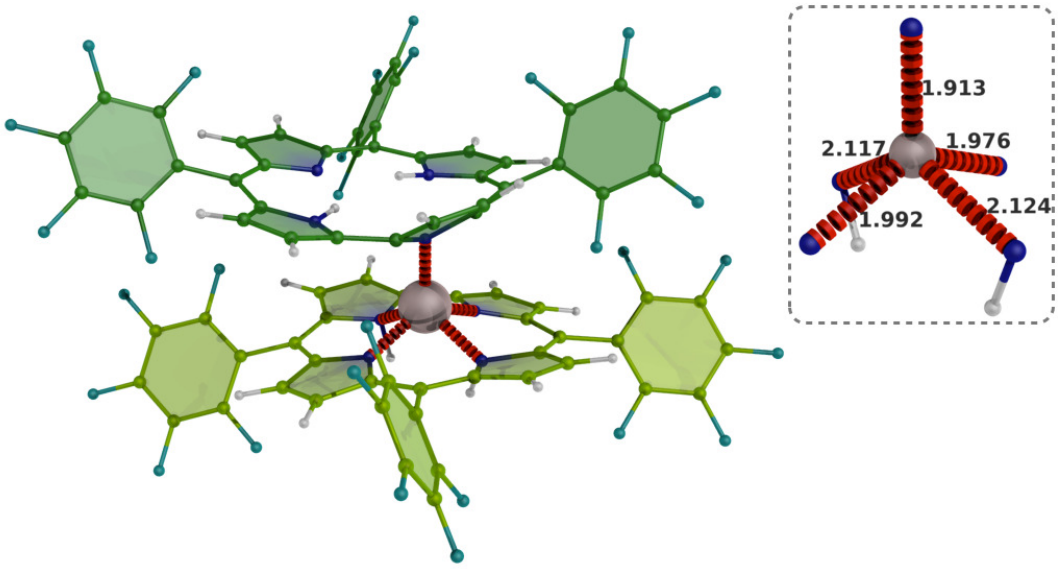

Figure 7. Lowest energy gas-phase complex of $\mathbf{1}^-$ with Al^{3+}, calculated at the B3LYP level. The inset provides details about the coordination environment of the cation, in the same orientation shown for the complex (only key particles were kept for sake of clarity). Coordinating interactions shown as red dashes; distances in Ångstrom. Color code: hydrogen–white; carbon–green (different shades for distinct macrocyles); aluminum–light pink; fluorine–teal, nitrogen–blue.

The lack of stability of the 1:1 complex with Al^{3+} seems to arise from the fact that the cation, in order to efficiently coordinate with all four nitrogens, needs to fully fit inside the corrole cavity, which then leads to electrostatic repulsion between the cation and the two positively charged interior protons. However, when considering the 1:1 binding arrangement of $\mathbf{1}^-$ with Cu^{2+}, as shown in Figure 7, the larger size of the Cu^{2+} cation requires that coordination occurs slightly above the corrole plane, thus minimizing the electrostatic hinderance between the cation and the interior protons. In this case, the coordination of the cation occurs with the four nitrogens of the corrole and one oxygen from a solvent molecule (in this case DMSO). The incorporation of two solvent molecules was required to provide the necessary stabilization of the overall complex. In fact, when solvent molecules were not incorporated at all, the 2:1 stoichiometry was slightly more stable than the "unsolvated" 1:1 model in ca. -0.11 Ha (-307.7 kJ mol^{-1}) which suggested that the completion of the coordination sphere of Cu^{2+} requires at least one solvent molecule, whereas the solvated model is more stable than the 2:1 one in ca. 0.07 Ha (-185.4 kJ mol^{-1}), thus supporting the 1:1 stoichiometry found experimentally.

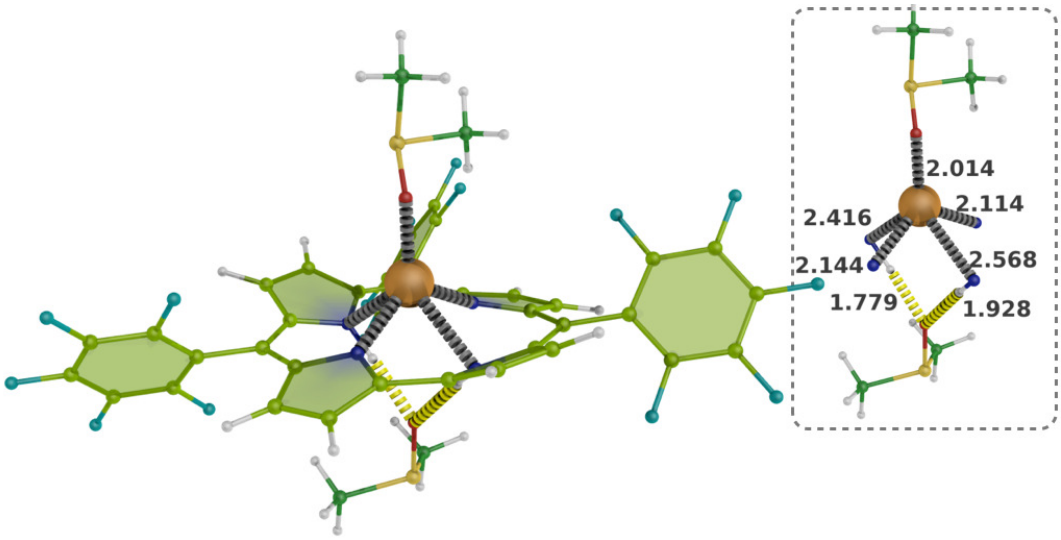

Figure 8. Lowest energy gas-phase complex of **1**$^-$ with Cu^{2+}. Details as in **Figure 8**; Cu^{2+} shown as orange sphere.

The coordination environment of the cation is a slightly distorted square pyramid involving the four corrole nitrogens and a nitrogen from a solvent molecule, having $Cu^{2+}\cdots X$ ($X=N_{corrole}$ or O_{DMSO}) distances ranging from 2.01 to 2.57 Å. As also shown in Figure 8, a second DMSO molecule is able to establish two simultaneous hydrogen bonds with the two interior corrole protons, with $O_{DMSO}\cdots H_{corrole}$ distances of 1.779 and 1.928 Å. Finally, the coordination of Ag^+ with **1**$^-$ (Figure 9) occurs, similarly to Al^{3+}, in a 2:1 stoichiometry, being this stoichiometry more stable than the 1:1 one in ca. -0.08 Ha (-251.15 kJ mol^{-1}). Coordination of the cation occurs mainly with three nitrogens from one corrole unit and three nitrogens from a second unit, in what resembles a distorted trigonal prismatic coordination environment. The $Ag^+\cdots N$ distances can be subdivided into set of two shorter distances involving the non-protonated nitrogens (2.217 and 2.238 Å) and four longer ones involving the protonated nitrogens (ranging from 3.30 to 3.43 Å). Due to the larger cationic radius of Ag^+ relatively to that of Al^{3+}, the efficient accommodation of Ag^+ into the binding pocket formed by the two corrole receptors does not impose large distortions on the planarity of the corrolic core, as happens with Al^{3+}.

It is possible that both complexes with Al^{3+} and Ag^+ gain further stabilization in solution from π-π interactions that can be established as result of the momentary alignment of aromatic fragments from adjacent units. However, evaluation of such hypothesis requires molecular dynamics simulations, which falls beyond the scope of the current analyses.

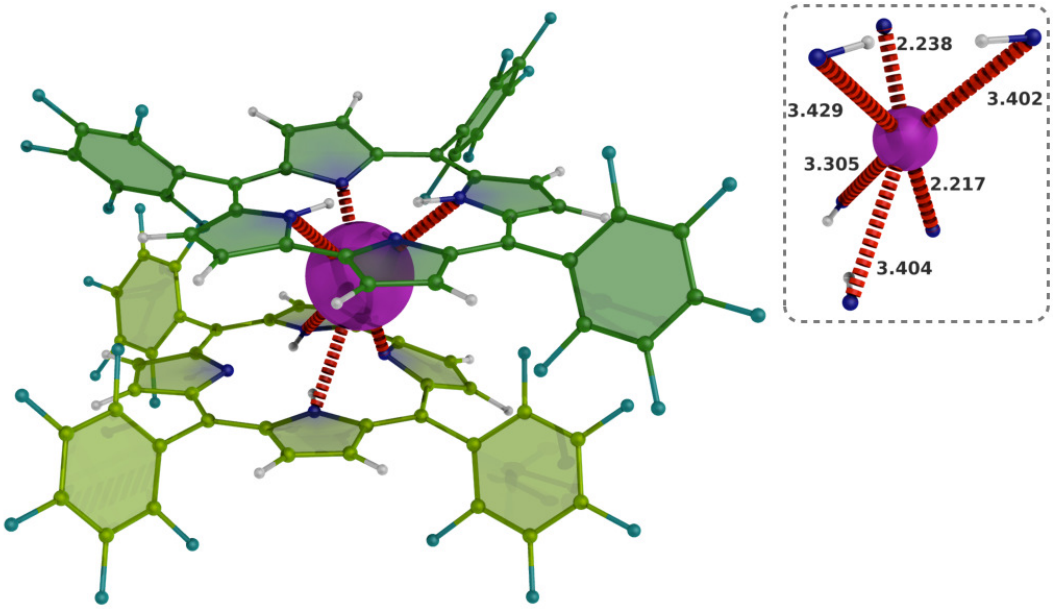

Figure 9. Lowest energy gas-phase complex of $\mathbf{1}^-$ with Ag^+. Details as in **Figure 8**; Ag^+ cation shown as purple sphere.

5.2.3 Synthesis

Before the description of the synthesis of derivative **5**, which was grafted with commercial silica nanoparticles, a brief introduction about nanoparticles, organic-inorganic hybrid materials and their utilization as alternative to classic fluorescent chemosensors will be presented.

Nanoparticles

Typically nanoparticles are defined as inorganic, metallic, magnetic or even polymeric particles with diameters of less than 100 nm and with potential use in several scientific areas as electronics, catalysis, drug carriers, sensors, pigments, magnetic and optical materials, etc. This multidisciplinarity is related to their properties. In fact, nanoparticles possess large specific surface area, high adsorption capacity and low temperature modification, which confer selectivity, sensitivity and efficacy to the new nanosystems.[28] Currently the nanoparticles most widely used in analytical sciences include silica nanoparticles, carbon nanoparticles (mainly fullerenes and carbon nanotubes) and metallic nanoparticles. All these types of nanoparticles can be chemically bonded to a

surface or functionalized with other organic or inorganic compounds or simply incorporated.

The combination of inorganic nanoparticles (*e.g.* gold, silver, silica nanoparticles or quantum dots) as solid supports with the intrinsic functionalities of organic dyes/fluorophores can led to the development of hybrid materials with improved functionalities.[29] Using this strategy some of the gaps associated to the classic chemosensors can be exceeded. In the literature, novel hybrid organic–inorganic sensing materials have been reported to display novel signaling properties that are hardly achievable by the individual components alone or when using analogous molecular-based systems.[30] In the presence of hybrid systems has been observed a signal amplification that arises from the preorganization of the units on the surface, and a reduction in the detection limit.[31]

For example, the research group of Beer[32] increased the sensitivity for anions detection by assembling metalloporphyrins on the surface of AuNPs (Figure 10). The preorganization of the binding sites resulted in a significant enhancement of guest coordination at the surface of the nanoparticle relative to the free receptor in solution. The preorganization of the receptors on the surface reduced their conformational flexibility (entropic contributions) and increased their effective sensitivity.

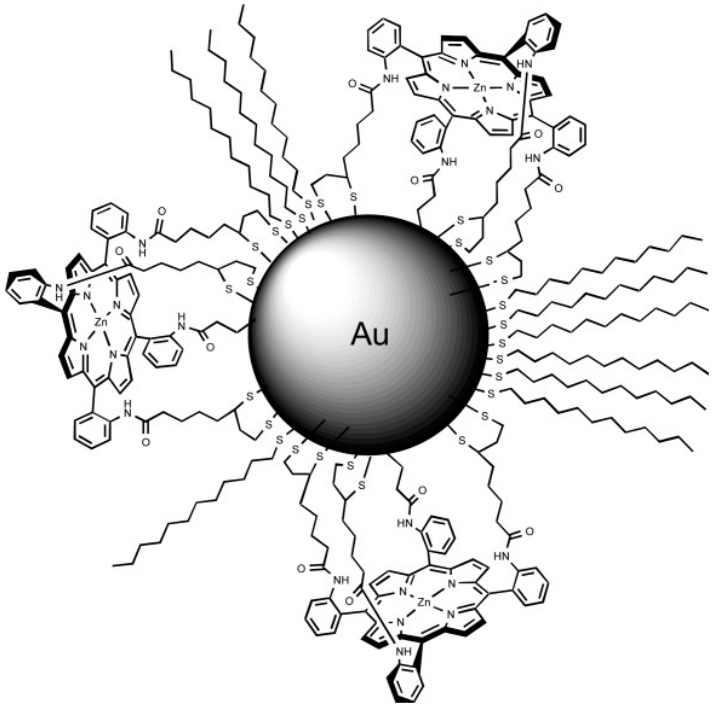

Figure 10- AuNPS functionalized with metalloporphyrin.[32]

It has also been described colorimetric effects involving organic-inorganic hybrid materials. Chen and co-workers[33] reported an efficient recognition of K^+ ions by gold nanoparticles functionalized with [15]crown-5 in aqueous solution through formation of 2:1 sandwich-type complexes; a color change from red to blue was observed (Figure 11). This alteration, which was detected upon aggregation, is due to a coupling of the dipoles which results in a significant red-shift of the plasmon band when the inter-nanoparticle distance in the aggregates decrease to less than the average particle radius.

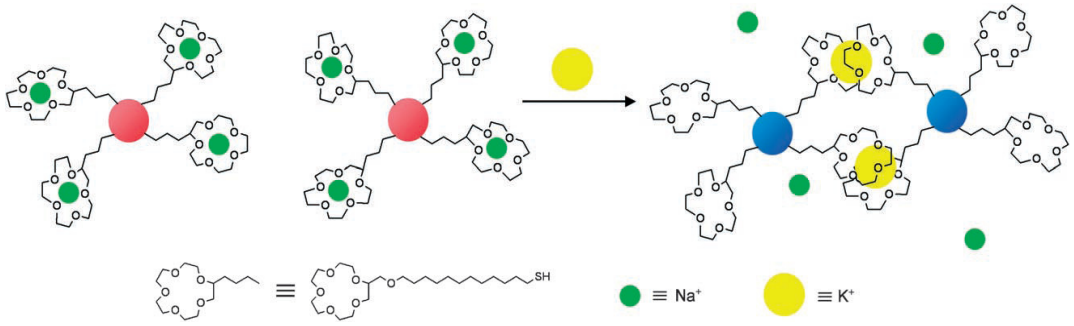

Figure 11- Potassium induced aggregation of AuNPS modified with crown ether/thiol groups through formation of sandwich complexes.

In spite of these interesting features, the organization of fluorescent groups and binding sites in the surface of inorganic materials for the development of fluorescent probes is still a relatively recent field. Among all the available inorganic supports we direct our attention to silica nanoparticles.

Silica nanoparticles are versatile supports, which can be easily synthesized (for example using Stöber´s method) and their surface can be straightforwardly modified by the use of the well-known alcoxysilane chemistry.[34] These features make silica nanoparticles a good choice as inorganic scaffoldings for the covalent grafting or coating of fluorophores and binding sites. Additionally silica is transparent to visible light and inert as far as energy and electron transfer processes are concerned.[35]

The use of silica nanoparticles as inorganic support in the development of fluorescent chemosensors for metal cations has also been reported.[36] For example, Tonellato *et al*.[37] developed a fluorescent sensor for Cu^{2+} ions based on silica nanoparticles functionalized on the surface with trialkoxysilane derivatives of picolinamide **I** as the

ligand and dansylamide **II** as the fluorescent dye (difunctionalization of the surface of nanoparticles). The picolinamide ligand complexes the Cu^{2+} ions strongly, and the bound ion still quenches the dansyl emission substantially in DMSO. The functionalization with two types of chemical groups allowed intercommunications between both subunits without the need for a direct covalent chemical link between them (Figure 12).

A

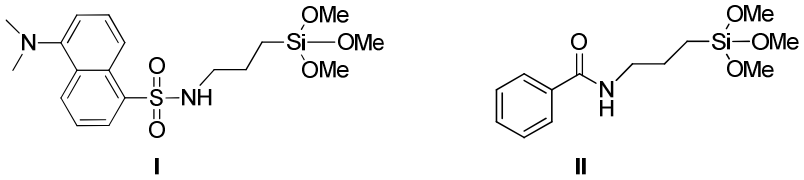

B

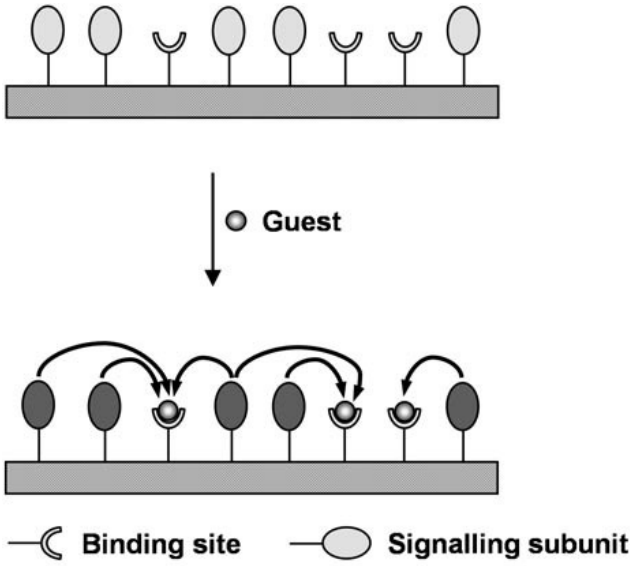

Figure 12- (A) units of picolinamide and danslyamide; (B) Difunctionalized surface, communication between the binding sites and signaling sites.

Also, in a recent published work, the same authors prepared silica nanoparticles coated with a 6-methoxy-8-(*p*-toluenosulfonamido)quinoline derivative which displayed a selective emission enhancement in the presence of Zn^{2+} cation in ethanol–water 1:1 mixtures.[38] Furthermore, silica nanoparticles functionalized with a fluorescein derivative

with suitable coordination sites have been prepared and used for Cu^{2+} imaging in living cells.[39]

As a continuation of our interest in the design of chemosensors we report in this chapter the synthesis of an alkoxysilane derivative **5** and its grafting inoptically transparent silica nanoparticles (SiNPs). The synthetic route used is outlined in Scheme 1. The 5,10,15-tris(pentafluorophenyl)corrole **1**,[40] the corresponding gallium(III) complex **2**[41] and the gallium(III) complex of 5,10,15-tris(pentafluorophenyl)corrole-3-carbaldehyde **3**[42] were synthesized according to the procedures described previously, and in the chapter II. The protection of the corrole **1** with gallium(III) was fundamental in order to obtain efficiently the 5,10,15-tris(pentafluorophenyl)corrole-3-carbaldehyde **3** under Vilsmeier-Haack conditions. The

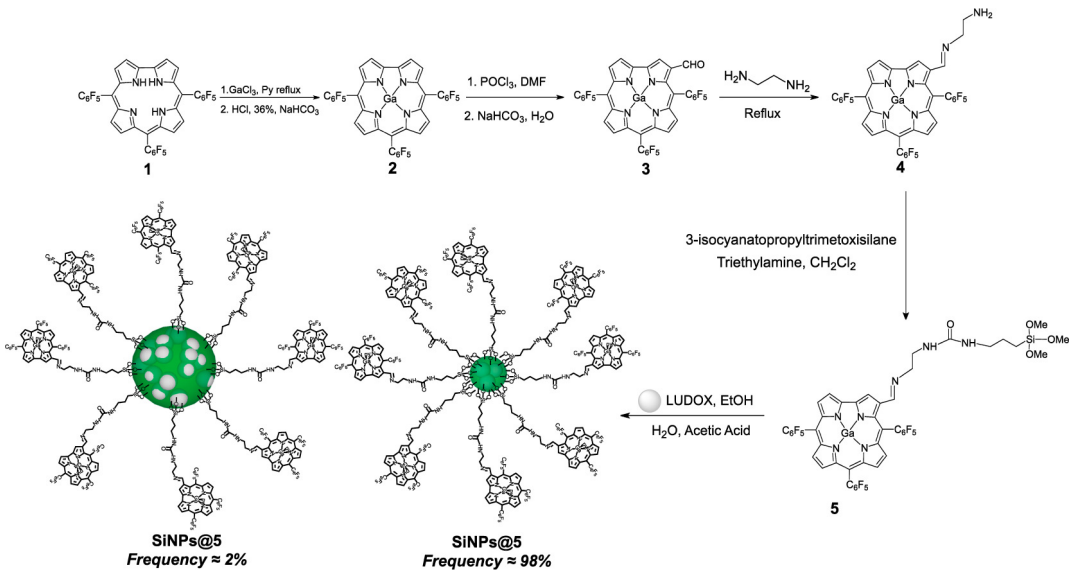

Scheme1

The synthesis of the new *β*-imine corrole **4** was carried out by adding ethylenediamine to an absolute ethanol solution of *β*-formyl corrole **3**. The reaction was performed at reflux, for 4 h. The TLC control revealed the absence of the starting corrole **3** and the presence of a new product. After work-up, this compound was identified by NMR and HRMS as the novel corrole derivative **4**, obtained in 69% yield. The ^{1}H NMR spectrum showed at lower field, a singlet at δ 9.27 corresponding to the resonance of *β*-pyrrolic H-2 and a doublet at δ 9.18 due to the resonance of proton H-18. Besides the resonances of the *β*-pyrrolic protons H-17 (δ 8.52, doublet) and H-7,8,12,13 (δ 8.74-8.80,

multiplet), the ^{1}H NMR spectrum showed a singlet at δ 8.66 identified as the resonance of proton H-1´, and a singulet at δ 4.13 due to the resonance of the NH_2 protons. In the aliphatic region, the spectrum presented two signals between δ 3.25 and δ 3.23 and δ 3.01 and δ 2.97 correspondents to the resonances of the protons of the aliphatic chain CH_2CH_2 (Figure 13).

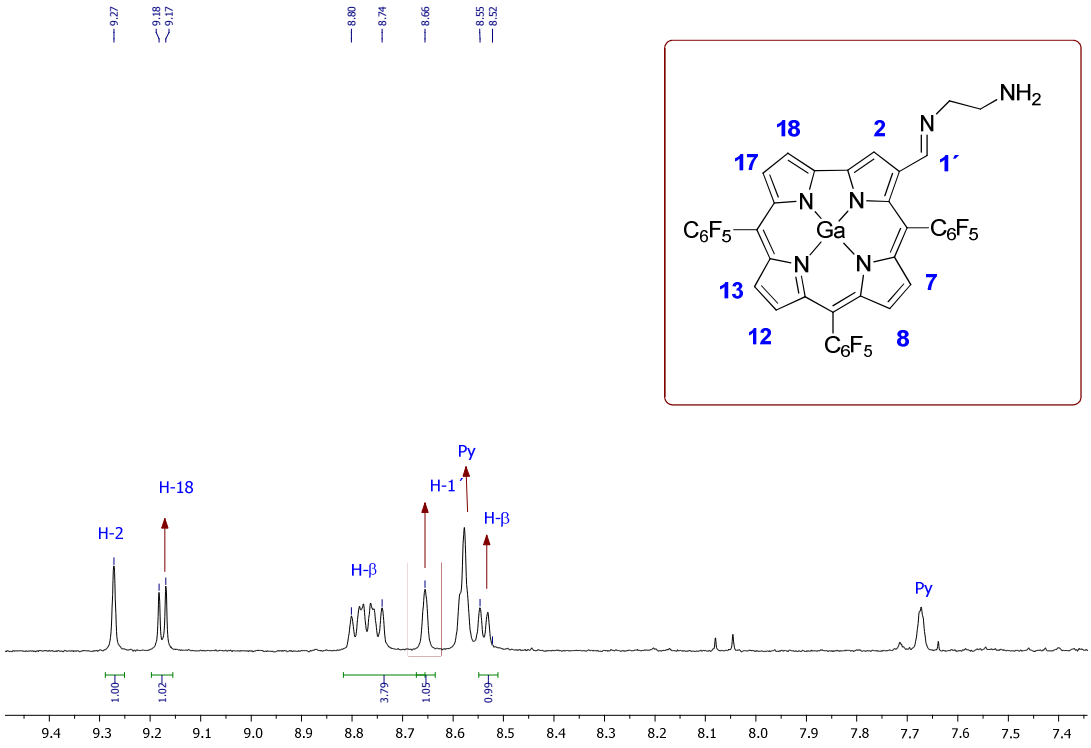

Figure 13 – Partial ^{1}H-NMR spectrum of corrole **4** in $CDCl_3$ with a few drops of pyridine- d_5.

The functionalization reaction of the *β*-imine corrole **4** with 3-isocyanatopropyl-trimethoxysilane was performed in dichloromethane in the presence of triethylamine. The success of the coupling was confirmed by HRMS; the mass spectrum of intermediate **5** showed the expected molecular ion $[M + H]^+$ at *m/z* 1138.1036. Although compound **5** seems to sufer some decompostion in solution it was possible to assign by analysis of ^{1}H-NMR spectrum a singulet at δ 9.63 due to the resonance of the *β*-pyrrolic proton H-2 and a doublet at δ 9.10 corresponding to the resonance of proton H-18 in the aromatic region. The remaining five β-pyrrolic protons appeared as three doublets at δ 8.67, 8.51 and 8.47 and as a multiplet between δ 8.76 and 8.72. The presence of two broad signals at δ 5.52 and 5.04 were assigned as due to the resonances of the NH protons.

The grafting of alkoxysilane derivative **5**, with LUDOX was achieved by magnetic stirring, at 80 ºC for two days. The resulting nanoparticles were further characterized by UV-Vis, fluorescence emission spectroscopy and transmission electron microscopy TEM.

5.2.4. Spectrophotometric and spectrofluorimetric titrations and metal ion sensing effects in the presence of nanoparticles functionalized with silane derivative 5.

To develop new corrole fluorescent materials to be used as new sophisticated metal ion chemosensors in environmental fields, the sensorial ability of the coated silica nanoparticles with compound **5** was studied and compared with the free precursor **4**.

The main photophysical data of compounds **4** and **5** are gathered in table 2. The Q-bands absorption of corrole **4** were centered at 599 and 601 nm in toluene and in CH_2Cl_2, the emission band at 624 and 623 nm, respectively. The alkoxysilane derivative **5** showed the highly intense Soret band at 430 nm and the two Q-bands at 603 and 626 nm. The emission band of highest energy was centered at 626 nm.

Table 2 - Photophysical data of corrole **4**, **5** and **SiNPs@5**.

Compound	Solvents	λ_{max} (nm)		λ_{em} (nm)	Stoke´s shift (nm)	ϕ (sd=0.01)
		Soret	Q-bands		Q-bands	
4	Dichloromethane	432	601	623	22	0.03
	Toluene	431	599	624	25	0.03
5	Dichloromethane	430	603	626	23	0.03
SiNPs@5	Dichloromethane	431	601	624	23	0.03

As an example figure 14 shows the absorption, emission and excitation spectra in dichloromethane of compound **5**.

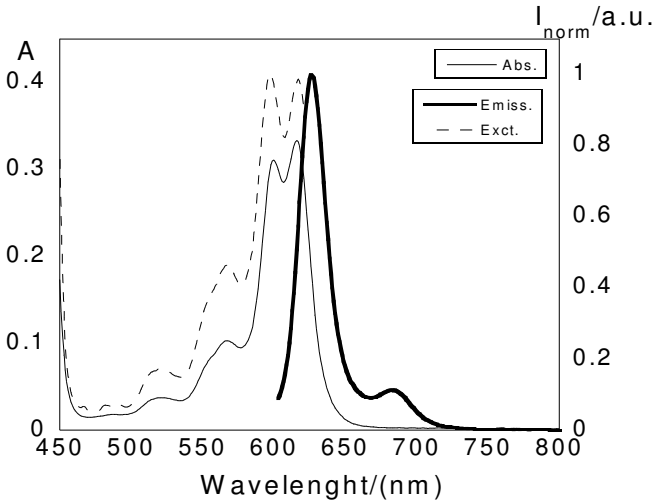

Figure 14- Room temperature absorption (bold line), normalized emission (full line, λ_{exc}=600 nm) and excitation spectra (dotted line, λem= 629nm) of compound **5** in dichloromethane.

The study of the sensorial ability of compound **4** toward metal ions Cu^{2+}, Hg^{2+} and Ag^{+} was carried out by ligand titrations with the addition of small amounts of the adequate metallic salts. The titrations were followed by UV-Vis and fluorescence measurements in toluene. The most significant alterations in the ground and excited states were observed in the presence of the ion Ag^{+}. No changes were detected in the presence of the ions Hg^{2+} and Cu^{2+}. The addition of Ag^{+} to compound **4** promoted a quenching of *ca*. 60% at 626 nm in the emission spectrum. In the ground state were not observed spectral alterations (Figure 15).

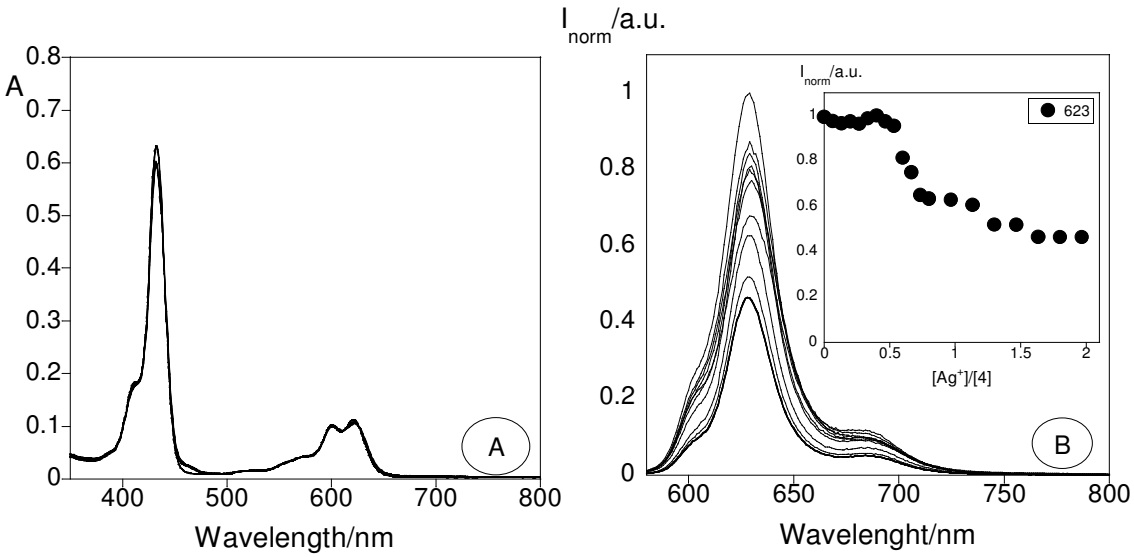

Figure 15– Spectrophotometric (A) and spectrofluorimetric (B) titration of **4** with the addition of Ag^+ in toluene. The inset represents the emission intensity at 626 nm (B) as a function of $[Ag^+]/[\mathbf{4}]$. ($[\mathbf{4}] = 5 \times 10^{-6}$ M, $\lambda_{exc} = 565$ nm, T = 298 k.

The profiles of the absorption and emission spectra of the derivatized nanoparticles were very similar to the ones of the ligand **4**. This result is expected since those silica nanoparticles are totally transparent to the visible light and inert to electron-transfer processes[43] TEM measurements of the new-coated material revealed diameter of 80 ± 30 nm (98%) demonstrating that the derivatization of Ludox with silane derivative **5** induced nanoparticle growth *via* aggregation. Moreover, a smaller sample of bigger nanostructures with 2% of population was observed with sizes of about 600 ± 200 nm.

The interaction of the silica nanoparticles coated with the new silane **5** (SiNPs@**5**) were also explored in the presence of Ag^+, Cu^{2+} and Hg^{2+} metal ions.

The SiNPs@**5** nanoparticles did not show any spectral changes in the presence of Cu^{2+} and Hg^{2+} metal ions, whereas, upon addition of Ag^+ a new satellite AgNPs were formed around the silica nanoparticle. Figure 16 shows the silica nanoparticles coated with silane derivative **5** (SiNPs@**5**) and with AgNPs (AgSiNPs@**5**); the TEM images, the spectrophotometric and spectrofluorimetric titrations of SiNPs@**5** with the increasing addition of Ag^+ resulted on the SiNPs@**5** with a layer of AgNPs inducing a strong aggregation.

As can be seen in the absorption spectra of SiNPs@**5,** the increase of Ag^+ amount induced the formation of satellite AgNPs around the silica nanoparticles coated with compound **5**. Its formation is proven by a change of colour from green to yellow, as well

as, by the appearance of a resonance plasmon band centered at 410 nm. Through TEM images it is possible to visualize the formation of the satellite AgNPs around the SiNPs@**5**, affording AgSiNPs@**5** with sizes around 600 ± 200 nm and a small population between 2 and 5% of bigger nanostructures was detected.

The polydispersed distribution of AgSiNPs@**5** can be due to the stepwise addition of Ag^+. The decrease observed in the emission intensity in the fluorescent spectra, is probably due to the proximity between silver and the nanoparticle monolayer increasing the accessibility to nonradiative processes.

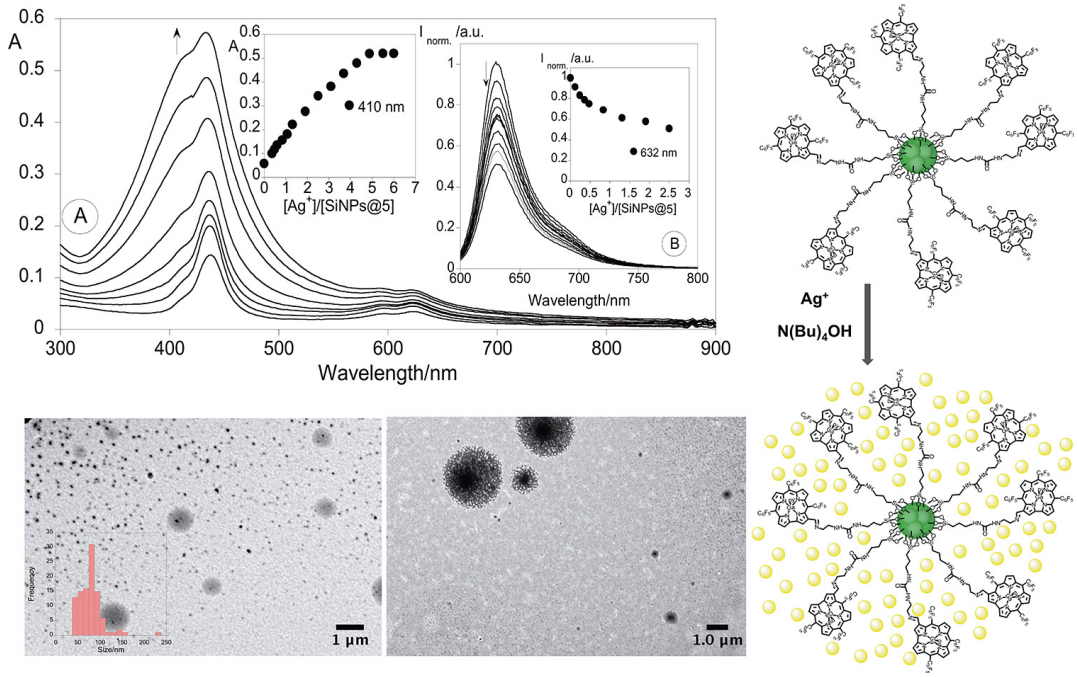

Figure 16- Above: Absorption (A) and emission spectra (B) of SiNPs@5) with the increasing amount of Ag^+ in dichloromethane; and picture of colour change of the nanoparticles formation. The inset B represents the emission at 632 nm as function of $[Ag^+]/[SiNPs@5]$. ([SiNPs@5]=ca. 5.86 x10^{-6} M, λ_{exc}= 410 nm, T = 298K). Bottom: silica nanoparticles coated with silane derivative 5 (SiNPs@5) and with Ag^+ (AgSiNPs@5). TEM image of SiNPs@5 and AgSiNPs@5.

5.3. Conclusions

Corrole **1** was successfully studied in the presence Ag^{+}, Na^{+}, Ca^{2+}, Zn^{2+}, Cd^{2+}, Cu^{2+}, Pb^{2+}, Hg^{2+}, Zn^{2+}, Ni^{2+}, Cr^{3+}, Ga^{3+}, Fe^{3+} and Al^{3+} metal ions in toluene and acetonitrile. Metal complexes with formula L_2M, were obtained in the interaction of $\mathbf{1}^{-}$ with Cd^{2+}, Pb^{2+}, Hg^{2+}, Ag^{+}, Cr^{3+} and Al^{3+}, while LM species were identified with Cu^{2+}, Ga^{3+} and Fe^{3+}, in toluene. The higher association constants were observed for Ag^{+}, Cr^{3+} and Al^{3+}. In toluene, the species corrole $\mathbf{1}^{-}$ shows to be a naked eye sensor in the presence of Hg^{2+}; a change of colour from dark green to *pale* green was vizualized. Also, corrole **1** reveals to be selective for Hg^{2+} in acetonitrile, where a change of colour from purple to green-blue was observed.

A new sophisticated material based on silica nanoparticles coated with compound **5** was successfully synthesized and studied in the presence Cu^{2+}, Hg^{2+} and Ag^{+} metal ions. Upon addition of Ag^{+} new satellite AgNPs were formed around the silica nanoparticles, followed by a change of colour from green to yellow.

All these promising results support the use of chemosensors derivatives based on corroles in environmental control, biology, chemistry or medicine. It is also important to point out the efficiency of species $\mathbf{1}^{-}$ against the heavy, pollutants and toxic Pb^{2+}, Hg^{2+} and Ag^{+} metal ions, whereas a strong and very effective quenching was observed only with the addition of 0.5 equivalents of metal ion.

5.4. Experimental Section

5.4.1 Chemicals and starting materials

$AgCH_3SO_3$, $NaCH_3SO_3$, $Ca(CH_3SO_3)_2$ $Cd(CH_3SO_3)_2$, $Cu(BF_4)_2.6H_2O$, $Pb(BF_4)_2.6H_2O$, $Hg(CH_3SO_3)_2$, $Zn(CH_3SO_3)_2$, $Ni(CH_3SO_3)_2$,$Ga(NO_3)_3.XH_2O$, $Cr(NO_3)_3.9H_2O$, $FeCl_3.{}_6H_2O$ and $Al(NO_3)_3.9H_2O$ salts, and $(CH_3)_4NOH$ (tetramethylammonium hydroxide), have been purchased from Strem Chemicals, Sigma Aldrich and TCI. Ethylenediamine, triethylamine, anhydrous sodium sulphate acetic acid and silica gel for thin layer chromatography (TLC) were purchase from Merck. Ludox AS-30 silica nanoparticles by Sigma-Aldrich. Water was always used purified and deionized (MilliQ grade, Millipore).

All chemicals were used without further purification with exception of triethylamine which was dried under standard procedures. The solvents were obtained from Panreac and Riedel-de-Häen with HPLC grade. Absolute ethanol, dichloromethane and pentane were distilled and dried under standard procedures.

5.4.2 - Spectrophotometric and spectrofluorimetric measurements

Absorption spectra were recorded on a JASCO V-650 spectrophotometer and the fluorescence emission on a spectrofluorimeter HORIBA-JY Scientific Fluromax-4. The linearity of the fluorescence emission *vs*. the concentration was checked out in the concentration used (10^{-4} – 10^{-6} M). A correction for the absorbed light was performed when necessary. The spectrometric characterizations and titrations were performed as follows: the stock solutions of compounds **1** and **4** (*ca* 10^{-3} M) were prepared by dissolving an appropriated amount of each compound in a 10 mL volumetric flask and diluting it to the mark with toluene or acetonitrile. The solutions were prepared by appropriate dilution of the stock solutions up to 10^{-5} – 10^{-6} M. Titrations of compound **1** and **4** were carried out by adding microliter amounts of standard solutions of the ions in DMSO or acetonitrile, when the ligand was in toluene or acetonitrile, respectively.

The spectrometric characterization of silica nanoparticles functionalized with corrole **5** was performed in dichloromethane. Titrations involving silica nanoparticles were carried

out by the addition of microliter amounts of solutions of metals in DMSO or acetonitrile. All the luminescence measurements were performed at 298 K.

Fluorescence quantum yield of compound **4** was measured using a solution of cresyl violet perchlorate in absolute ethanol as a standard ([ϕ]=0.54)[44] and was corrected for different refraction indexes of solvents. The limit of detection (LOD) and the limit of quantification (LOQ) for the metal ions were performed, having in mind their use for real metal ions detection and for analytical applications. For these measurements, ten different analyses for the selected receptor were performed in order to obtain the LOQ. The LOD was obtained by applying the formula:

$$Y_{dl} = y_{blank} + 3std \text{ where}$$

y_{dl} = signal detection limit and std =standard deviation

5.4.3 - TEM measurements

To perform the transmission electron microscopy (TEM) images of the samples 1 μL of the colloidal suspension was dropped on a copper grid coated with a continuous carbon film and the solvent was allowed to evaporate. TEM images were obtained through a JEOL JEM 1010F transmission electron microscope (TEM) operating at 100 kV. Data for size distribution histograms were made measuring more than 200 particles per sample in several TEM images.[45]

5.4.4 – Spectroscopic characterization of ligands

^{1}H NMR and ^{19}F NMR spectra were recorded on Bruker Avance 300 (at 300 and 282 MHz, respectively) spectrometer. $CDCl_3$ and pyridine-d_5 were used as solvents with tetramethylsilane (TMS) as the internal reference; the chemical shifts are expressed in □ (ppm) and the coupling constants (*J*) in Hertz (Hz).

High resolution mass spectra analysis (HRMS-ESI^+) were performed on a microTOF (focus) mass spectrometer. Ions were generated using an Apollo II (ESI) source. Ionization was achieved by electrospray, using a voltage of 4500 V applied to the needle, and a counter voltage between 100 and 150 V applied to the capillary.

IR spectra were obtained for KBr pellets, in the range 400–4000 cm^{-1}, with a Shimadzu FTIR 8400S instrument.

5.4.5 – Synthesis of ligands

The 5,10,15-tris(pentafluorophenyl)corrole **1** was synthesized by condensation of pentafluorobenzaldehyde with pyrrole at room temperature, according to the literature,[40] and the 5,10,15-tris(pentafluorophenyl)corrolatogallium(III)(pyridine) was obtained by refluxing the free base **1** in pyridine with $GaCl_3$.[41] The gallium complex of 5,10,15-tris(pentafluorophenyl)corrole-3-carbaldehyde **3** was obtained by Vilsmeier–Haack formylation of corrole **2** using $POCl_3$ and DMF.[42] The elimination of pyridine from compound **3** was performed according to the procedure described in chapter II.

5.4.5.1- Synthesis of 3-(2-aminoethyl)imino)methyl)-5,10,15-tris(pentafluorophenyl)corrolatogallium(III) 4.

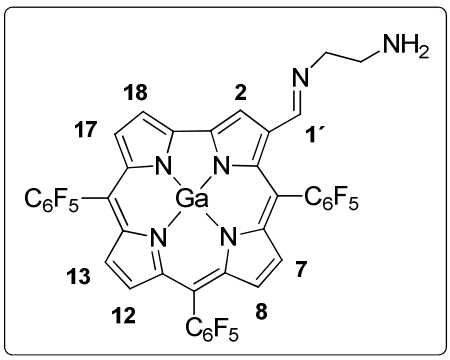

Ethylenediamine (3.4 mg, 0.056 mmol) was added to a solution of **3** (25 mg, 0.028 mmol) in ethanol absolute (5 mL). The resulting solution was gently refluxed with magnetic stirring for *ca*. 4 h. After this period, the solvent was evaporated under reduced pressure and the resultant product crystallized from a mixture of hexane-dichloromethane (18.2 mg, 69% yield).

^{1}H NMR (300.13 Hz, $CDCl_3$, a few drops of pyridine- d_5): 9.27 (s, 1H, H-2), 9.18 (d, 1H, *J* 4.1, H-18), 8.80–8.74 (m, 4H, H-*β*), 8.66 (s, 1H, H-1´), 8.54 (d, 1H, *J* 4.1, H-17), 4.13 (s, 2H, N-H), 3.25-3.23 (m, 2H, CH_2), 3.01-2.97 (m, 2H, CH_2).

^{19}F NMR (282.37, $CDCl_3$, a few drops of pyridine-d_5): δ -185.78 to -185.75 (m; 1 F; F_{meta}); -185.62 to -185.59 (m; 1 F; F_{meta}); -185.51 to -185.35 (m; 1 F; F_{meta}); -185.12 to -185.05 (m; 2 F; F_{meta}); -184.98 to -184.96 (m; 1 F; F_{meta}); -176. 90 (t; 1 F; *J* 21.2 Hz; F_{para}); -176.59 (t; 1 F; *J* 21.2 Hz; F_{para}); -175,19 (t; 1 F; *J* 21.2 Hz; F_{para}), -163.38 (dd; 1 F; *J* 24.0 Hz and *J* 7.1 Hz; F_{ortho}); -160. 94 (dd; 1 F; *J* 25.4 Hz e *J* 8.5 Hz; F_{ortho}), -160.91 to -160.82 (m; 3 F; F_{ortho}), -159.16 (dd; 1 F; *J* 24.0 Hz and *J* 7. 1 Hz; F_{ortho}).

IR (cm^{-1}): 3484 (N-H, Amine), 1657 (C=N, Imine), 1589 and 1492 (C=C, Ar).
HRMS [ESI^+]: *m/z* ([M+H]$^+$) calcd for $C_{40}H_{14}F_{15}GaN_6$: 933.1352, found: 933.1316.
λ_{max} (log ε) CH_2Cl_2 410 (4.61), 432 (5.21), 601 (4.35), 623 (4.48) nm.

5.4.5.2- Synthesis of silane corrole 5

Corrole **4** (16 mg**,** 0.017 mmol) was dissolved in 5 mL of dichloromethane, followed by the addition of triethylamine (3 µL, 0.017 mmol) and of the linker 3-isocyanatopropyltrimethoxysilane (3.6 mg, 0.017 mmol). The reaction mixture was kept under stirring at room temperature for 2 days. After this period the solvent was evaporated and the resulting solid dried was washed with pentane. Compound **5** was used in the subsequent reaction without further purification (12.6 mg, 64% yield).

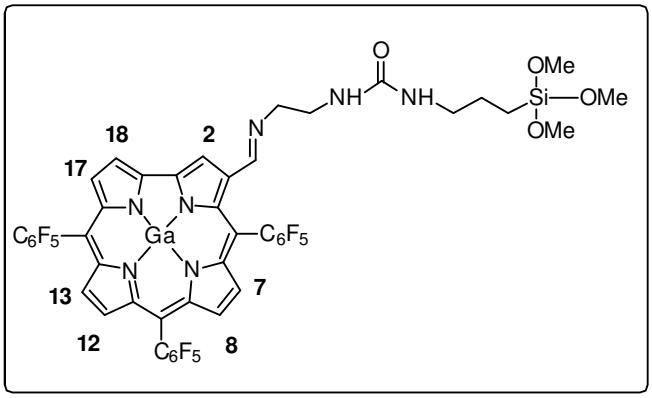

^{1}H NMR (300.13 Hz, $CDCl_3$, a few drops of pyridine- d_5): 9.63 (s, 1H, H-2), 9.10 (d, 1H, *J* 4.0, H-18), 8.76–8.72 (m, 3H, 2H-β + H-1´), 8.67 (d, 1H, *J* 4.9, H-β), 8.51 (d, 1H, *J* 4.7, H-β), 8.47 (d, 1H, *J* 4.5, H-β), 5.52 (bs, 1H, NH), 5.04 (bs, 1H, NH), 3.84-3.74 (3 * CH_3, under solvent), 3.28-3.30 (m, 4H, 2*CH_2), 3.17–3.12 (m, 2H, CH_2), 1.63–1.60 (m, 2H, CH_2), 0.65–0.60 (m, 2H, CH_2).
HRMS [ESI^+]: [M+H]$^+$ calcd for $C_{47}H_{29}F_{15}GaN_7O_4Si$: *m/z* 1138.1048 found: *m/z* 1138.1036.
Elem anal. Calc. for $C_{47}H_{29}F_{15}GaN_7O_4Si$. 2 CH_2Cl_2. 2 C_5H_{12}: C, 48.78; H, 3.95; N, 6.75. Found: C, 48.43; H, 3.81; N, 6.46.
λ_{max} (log ε) CH_2Cl_2 413 (4.53), 430 (5.25), 603 (4.31), 626 (4.47) nm.

5.4.5.3 – Synthesis of silica nanoparticles decorated with compound 5

Compound **5** (12 mg, 0.011 mmol) was dissolved in a mixture of 0.5 mL of ethanol, 0.5 mL water, 0.5 mL of CH_3COOH and 0.680 mL of a water solution of

commercial Ludox AS-30 silica nanoparticles (30nm). The resultant mixture was stirred at 80º C for 2 days, then 200 μL were withdrawn, dissolved in 1 mL of dichloromethane and centrifuged at 6000 rpm, at 21º C, for 10 min. The pellet was washed three times with ethanol (3 x 1mL), and finally dissolved in 0.5 mL of dichloromethane. The commercial silica nanoparticles (LUDOX) were measured by transmission electron microscopy (TEM) and dynamic light scattering (DLS) whereas a diameter of 30 ± 5 nm (TEM) and a hydrodynamic diameter of 40 ± 3 nm (DLS) was determined, respectively. TEM measurements of the new material SiNPs@**5** revealed a diameter of 80 ± 30 nm in 98%. A smaller population of bigger nanoparticles about 2% was observed with 600± 200nm. UV-Vis absorption band (dichloromethane) = 601 nm; Emission band (dichloromethane) = 624 nm; Fluorescent quantum yield = 0.03.

5.4.6. Spectrophotometric and spectrofluorimetric data

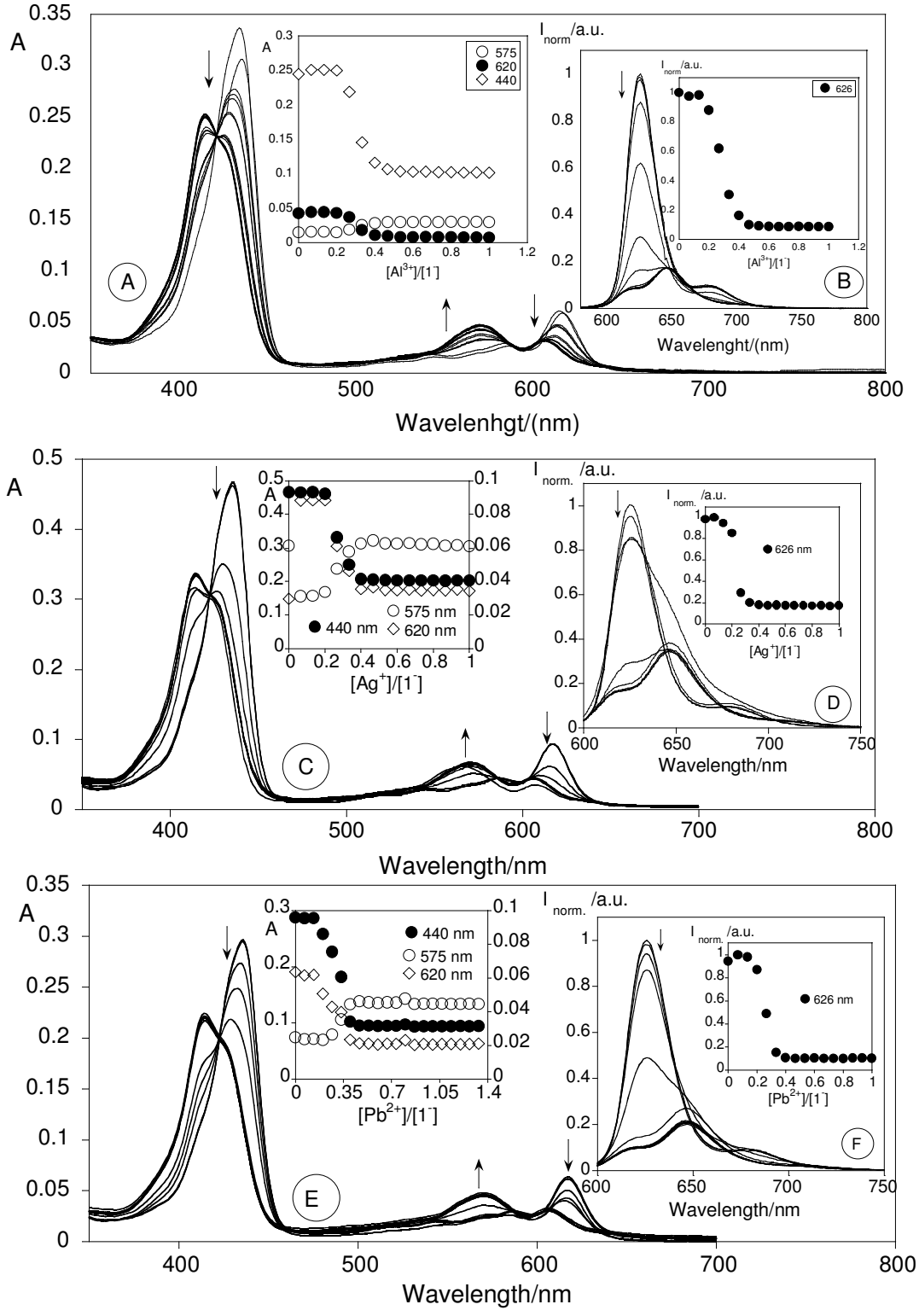

Figure SN1 – Spectrophotometric (A, C, E) and spectrofluorimetric (B, D, F) titration of $\mathbf{1}^-$ with the addition of Al^{3+} (A, B), Ag^+ (C, D) and Pb^{2+} (E, F) in toluene. The inset represents the absorption at 440 nm, 575 nm and 620 nm for A, C and E; and the emission intensity at 626 nm (B, D, F) as a function of $[Al^{3+}]/[\mathbf{1}^-]$, $[Ag^+]/[\mathbf{1}^-]$ and $[Pb^{2+}]/[\mathbf{1}]$, respectively. ($[\mathbf{1}^-] = 1 \times 10^{-5}$ M for $[Al^{3+}]$, $[\mathbf{1}^-] = 1.5 \times 10^{-5}$ M for $[Ag^+]$ and $[\mathbf{1}^-] = 9.5 \times 10^{-6}$ M for $[Cd^{2+}]$ $\lambda_{exc} = 565$ nm, T = 298 K).

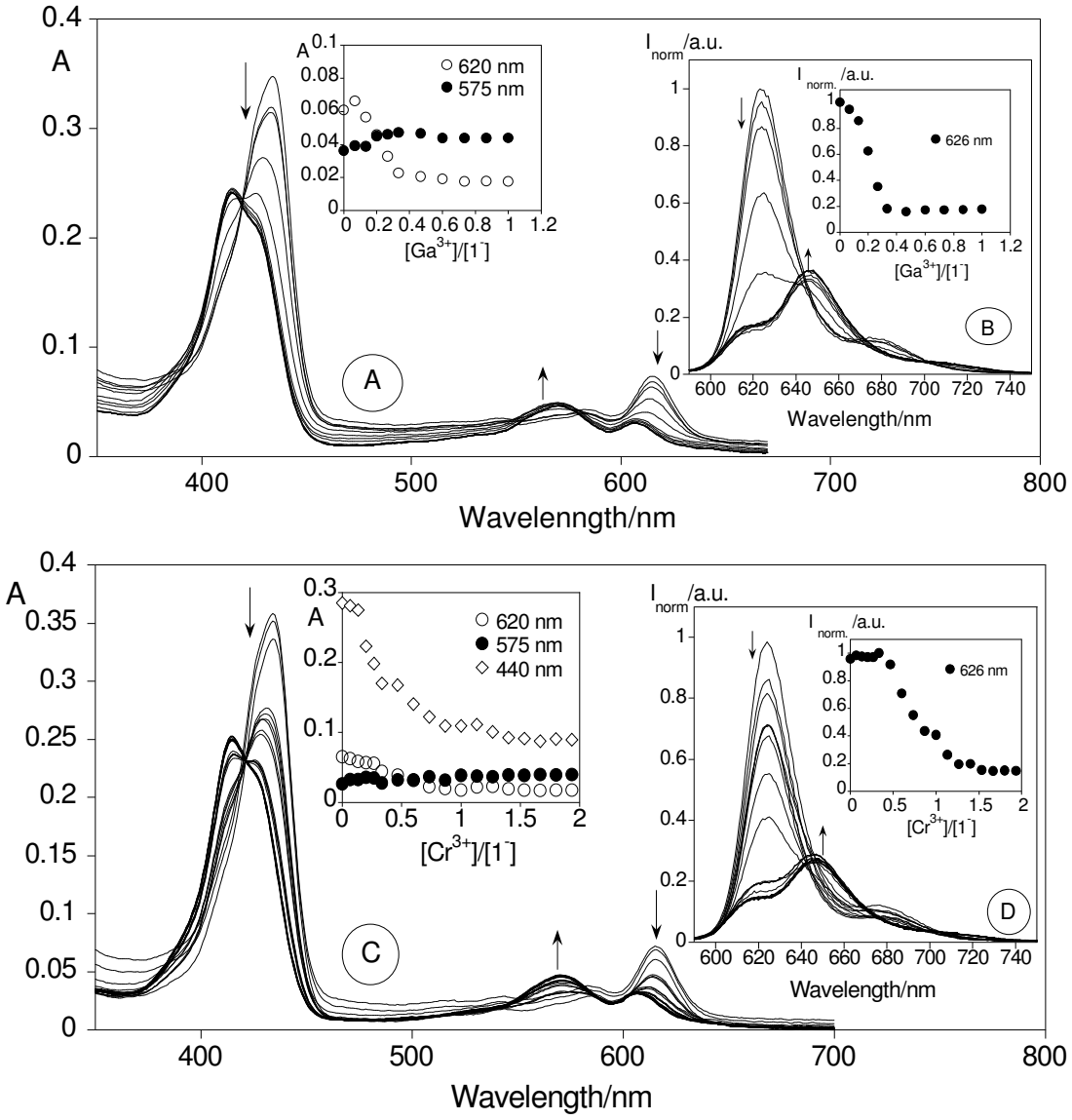

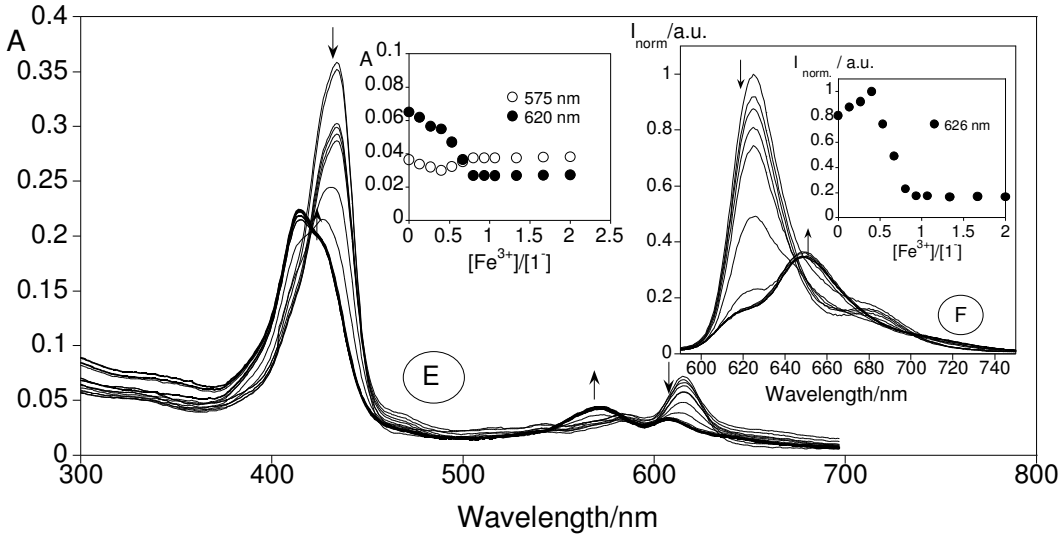

Figure SN2 – Spectrophotometric (A, C, E) and spectrofluorimetric (B, D, F) titration of $\mathbf{1}^-$ with the addition of Ga^{3+} (A, B), Cr^{3+} (C, D) and Fe^{3+} (E, F) in toluene. The inset represents the absorption at 440 nm, 575 nm and 620 nm for C, and 575 nm, 620 nm for A and E; and the emission intensity at 626 nm (B, D, F) as a function of $[Ga^{3+}]/[\mathbf{1}^-]$, $[Cr^{3+}]/[\mathbf{1}^-]$ and $[Fe^{3+}]/[\mathbf{1}^-]$, respectively. ($[\mathbf{1}^-] = 1 \times 10^{-5}$ M, $\lambda_{exc} = 565$ nm, T = 298 K).

5.5 References

[1] Lodeiro, C.; Capelo, J. L.; Mejuto, J.C.; Oliveira, E.; Santos, H.M.; Pedras, B.; Nunez, C. *Chem. Soc. Rev*. **2010**, *39*, 2948-2974.

[2] (a) Chen, P.; He, C. *J. Am. Chem. Soc.* **2004**, *126*, 728-729. (b) Henary, M. M.; Fahrni, C. J. *J. Phys. Chem. A.* **2002**, *106*, 5210. (c) Walkup, G. K.; Imperiali, B. *J. Am. Chem. Soc.* **1996**, *118*, 3053-3054.

[3] Aviv-Harel, I.; Gross, Z. *Chem. Eur. J*. **2009**, *15*, 8382-8394.

[4] Flamigni, L.; Gryko, D. T. *Chem. Soc. Rev.* **2009***, 38*, 1635-1646.

[5] Aviv-Harel, I.; Gross, Z. *Chem. Commun*. **2007**, 1987-1999.

[6] Aviv-Harel, I.; Gross, Z. *Coord. Chem. Rev*. **2011**, *255*, 717-736.

[7] (a) Ventura, B.; Degli Esposti, A.; Koszarna, B.; Gryko, D. T.; Flamigni,L. *New J. Chem.* **2005**, *29*, 1559-1566. (b) Ding, T.; Aleman, E. A.; Mordarelli D. A.; Ziegler, C. J. *J. Phys. Chem. A*. **2005**, *109*, 7411-7417. (c) Paolesse, R. *The Porphyrin Handbook,* ed. Kadish, K. M.; Smith, K. M.; Guilard, R. Academic Press, New York, **2000**, vol. 2, ch. 11, 202.

[8] Pariyar, A.; Bose, S.; Chhetri, S. S; Biswas, A. N.; Bandyopadhyay, P. *Dalton Trans*. **2012**, *41*, 3826-3831.

[9] (a) Santos, C. I. M.; Oliveira, E.; Barata, J. F. B.; Faustino, M. A. F.; Cavaleiro, J. A. S.; Neves, M. G. P. M. S.; Lodeiro, C. *J. Mater. Chem.* **2012**, *22*, 13811-13819. (b) Santos, C.I.M.; Oliveira, E.; Menezes, J.C.J.M.D.S.; Barata, J.F.B.; Faustino, M.A.F: Ferreira, V.F.; Cavaleiro, J.A.S; Neves, M.G.P.M.S.; Lodeiro, C. *Tetrahedron*, **2013**, *in press*.

[10] (a) Vale, L. S. H. P.; Barata, J. F. B; Faustino, M. A. F.; Neves, M. G. P. M. S.; Tomé, A. C.; Silva, A. M. S.; Cavaleiro, J. A. S. *Tetrahedron Lett.* **2007**, *48*, 8904-8908. (b) Vale, L. S. H. P.; Barata, J. F. B.; Santos, C. I. M. ; Neves, M. G. P. M. S.; Faustino, M. A. F.; Tomé, A. C.; Silva, A. M. S.; Paz, F. A. A; Cavaleiro, J. A. S. *J. Porphyrins Phthalocyanines,* **2009**, *13*, 358-368.

[11] (a) Hussain, S. M.; Hess, K. L.; Gearhart, J. M.; Geiss, K. T.; Schlager, J. J.. *Toxicol. In Vitro.* **2005**, *19*, 975-983. (b) Landsdown, A. B. G. *Crit. Rev. Toxicol.* **2007**, *37*, 237-250.

[12] Wygladacz, K.; Radu, A.; Xu, C.; Qin, Y.; Bakker, E. *Anal. Chem.* **2005**, *77,* 4693-4712.

[13] Lione, A. *J. Gen. Pharmacol*., **1985**, *16*, 223-231.

[14] Crisponi, G.; Nurchi, V.M., Bertolas, V.; Remelli, M.; Faa, G. *Coord Chem Rev,* **2012***, 256,* 89-104.

[15] (a) Chen, X.; Nam, S-W.; Jou, M.; Kim, Y.; Kim, S-J.; Park, S.; Yoon, J. *Org. Lett.,* **2008,** *10*, 5235-5238. (b) Nolan, E.M.; Lippard, S. J.; *Chem. Rev.* **2008**, *108*, 3443-3480. (c) Tamayo, A.; Pedras, B.; Lodeiro, C.; Escriche, L.; Casabó, J.; Capelo, J. L.; Covelo, B.; Kivekas, R.; Sillampaa, R. *Inorg. Chem*. **2007,** *46*, 7818-7826. (d) Mameli, M.; Lippolis, V.; Caltagirone, C.; Capelo, J. L.; Nieto-Faza, O.; Lodeiro, C. *Inorg. Chem.* **2010**, *49*, 8276-8286.

[16] (a) Rocha, A.; Marques, M. M. B.; Lodeiro, C. *Tetrahedron Lett*. **2009**, *50*, 4930-4933. (b) Swamy, K. M. K.; Kim, H. N.; Soh, J. H.; Kim, Y.; Kim, S-J.; Yoon, J. *Chem. Commun*. **2009**, 1234-1236. (c) Park, C. S.; Lee, J. Y.; Kang, E-J.; Lee, J-E.; Lee, S. S. *Tetrahedron Lett*. **2009**, *50*, 671-675. (d) Tamayo, A.; Oliveira, E.; Covelo, B.; Casabó, J.; Escriche, Ll.; Lodeiro, C. *Z. Anorg. Allg. Chem*. **2007**, *633*, 1809-1814.

[17] (a) Capelo, J. L.; Maduro, C.; Mota, A. M. *Ultrason. Sonochem*. **2006**, *13*, 98. (b) Nolan, E. M.; Lippard, S. *J. Chem. Rev.* **2008**, *108*, 3443-3480.

[18] Barata, J. F. B.; Daniel-da-Silva, A. L.; Neves, M. G. P. M. S.; Cavaleiro, J. A. S.; Trindade, T. *RSC Advances*, **2013,** *3*, 274-280.

[19] (a) Ding, T.; Aleman, E. A.; Modarelli, D. A.; Ziegler, C. J. *J. Phys. Chem. A* **2005**, *109*,7411-17. (b) Paolesse, R.; Sagnore, F.; Macagnano, A.; Boschi, T.; Prodi, L.; Montalti, M.; Zacchereni, N.; Bolletta, F.; Smith, K. M. *J. Porphyrins Phthalocyanines* **1999**, *3*, 364-370.

[20] Mahammed, A.; Weaver, J. J.; Gray, H. B.; Abdelas, M.; Gross, Z. *Tetrahedron Lett*., **2003**, *44*, 2077-2079.

[21] Shen, J.; Ou, Z.; Shao, J.; Gałęzowski, M.; Gryko, D.T.; Kadish, K.M. *J. Porphyrins Phthalocyanines,* **2007**, *11*, 269-276.

[22] Jensen, W. B. *J. Chem. Ed.* **2003**, *80*, 8, 952-961.

[23] Gans, P.; Sabatini, A.; Vacca, A.; *Talanta.* **1996**, *43*, 1739-1753.

[24] Cotton, F. A; Wilkinson, G. *Advanced Inorganic Chemistry* 5th Ed., Wiley, New York **1988**, 735-738.

[25] Cabbiness, D.K.; Margerum, D.W. *Journal of American Chemical Society.* **1969**, *91*, 6540-6542.

[26] Theoretical calculations were performed using density-functional theory, with Gaussian09. Molecular geometries were optimized using the unrestricted B3LYP

functional with the 6-31G(d,p) basis-set for C, N, F and H and the ECP LanL2DZ mixed basis set for Ag^{+}, Cu^{2+} and Al^{3+}.

[27] Gaussian 09, Revision A.02, Frisch, M. J.; Trucks, G. W.; Schlegel, H. B.; Scuseria, G. E.; Robb, M. A.; Cheeseman, J. R.; Scalmani, G.; Barone, V.; Mennucci, B.; Petersson, G. A.; Nakatsuji, H.; Caricato, M.; Li, X.; Hratchian, H. P.; Izmaylov, A. F.; Bloino, J.; Zheng, G.; Sonnenberg, J. L.; Hada, M.; Ehara, M.; Toyota, K.; Fukuda, R.; Hasegawa, J.; Ishida, M.; Nakajima, T.; Honda, Y.; Kitao, O.; Nakai, H.; Vreven, T.; Montgomery Jr., J. A.; Peralta, J. E.; Ogliaro, F.; Bearpark, M.; Heyd, J. J.; Brothers, E.; Kudin, K. N.; Staroverov, V. N.; Kobayashi, R.; Normand, J.; Raghavachari, K.; Rendell, A.; Burant, J. C.; Iyengar, S. S.; Tomasi, J.; Cossi, M.; Rega, N.; Millam, J. M.; Klene, M.; Knox, J. E.; Cross, J. B.; Bakken, V.; Adamo, C.; Jaramillo, J.; Gomperts, R.; Stratmann, R. E.; Yazyev, O.; Austin, A. J.; Cammi, R.; Pomelli, C.; Ochterski, J. W.; Martin, R. L.; Morokuma, K.; Zakrzewski, V. G.; Voth, G. A.; Salvador, P.; Dannenberg, J. J.; Dapprich, S.; Daniels, A. D.; Farkas, Ö.; Foresman, J. B.; Ortiz, J. V.; Cioslowski, J.; Fox, D. J. Gaussian, Inc., Wallingford CT, **2009**.

[28] (a) Antonietti, M.; Ozin, G. A. *Chem. Eur. J.* **2004**, 10, 28-41. (b) Ajayan, P. M.; Schadler, L. S.; Broun, P. V. *Nanocomposite science and technology*, Wiley-interscience, **2003**.

[29] (a) N. L. Rosi, C. A. Mirkin, *Chem. Rev*. **2005**, 105, 1547 – 1562; (b) E. Katz, I. Willner, *Angew. Chem.* **2004**, 116, 6166 – 6235

[30] (a) Costi, R.; Sanders, A. E.; Banin, U. *Angew. Chem. Int.* **2010**, 49, 4878. (b) Sailor, J. M.; Park, J. H. Adv. Mat. 2012, 24, 3779-3802.

[31] Descalzo, A. B.; Mánez, R. M.; Sancenón, F.; Hoffmann, K.; Rurack, K. Angew. *Chem. Int. Ed*. **2006**, 45, 5924-5948.

[32] (a) Labande, A.; Astruc, D.; *Chem. Commun.* **2000**, 1007 – 1008. (b) Labande, A.; Ruiz, J.; Astruc, D. *J. Am. Chem. Soc.* **2002**, 124, 1782 –1789.

[33] Lin, S.-Y.; Liu, S.-W.; Lin, C.-M. ; Chen, C.-H. *Anal. Chem*. **2002**,74, 330 – 335.

[34] Beck, C.; Härtl, w.; Hempelmann, R. *Angew. Chem. Int. Ed*. **1999**, 38 1297-1300.

[35] (a) Crego-Calama,M.; Reinhoudt, D.N. *Adv. Mater.* **2001**, 13, 1171. (b) Flink, S.; Veggel, F.C.J.M.; Reinhoudt, D. N. *Adv. Mater.* **2000**, 12, 1315-1328.

[36] (a) Arduini, A.; Demuru, D.; Pochini, A.; Secchi, A. *Chem. Commun*. **2005**, 5, 645-647. (b) Tshikhudo, R.; Demuru, D.; Wang, Z.; Brust, M.; Secchi, A.; Anduini, A.; Pochini, A. *Angew. Chem., Int. Ed*. **2005**, 44, 2913-2916. (c) Candel, I.; Calero, P.;

Mánez, R. M.; Sancenón, F.; Marcos, M. D.; Pardo, T.; Soto, J. *Inor. Chim. Acta*. **2012**, 381, 188-194.

[37] Rampazzo, E.; Brasola, E.; Marcuz, S.; Mancin, F.; Tecilla, P.; Tonellato, U. *J. Mater. Chem.* **2005**, 15, 2687 – 2696.

[38] Teolato, P.; Rampazzo, E.; Arduini, M.; Mancin, F.; Tecilla, P.; Tonellato, U. *Chem. Eur. J.* **2007**, 13, 2238-2245.

[39] Seo, S.; Lee, H. Y.; Park, M.; Lim, J. M.; Kang, D.; Yoon, J.; Jung, J. H.*; Eur. J. Inorg. Chem.* **2010**, 6, 843-847.

[40] Gryko, D. T.; Koszarna, B. *Org. Biomol. Chem.* **2003**, *2*, 350-357.

[41] Bendix, J.; Dmochowski, I. J.; Gray, H. B.; Mahammed, A.; Simkhovich, L.; Gross, Z. *Angew. Chem. Int. Ed.* **2000**, *39*, 4048-4051.

[42] Saltsman, I.; Mahammed, A.; Goldberg, I.; Tkachenko, E.; Botoshansky, M.; Gross, Z. *J. Am. Chem. Soc*. **2002**, *124*, 7411-7420.

[43] Cotton, F. A; Wilkinson, G.; Murillo, C. A. Advanced Inorganic Chemistry, 6th Ed., Wiley, New York **1999**.

[44] (a) Berlman, I. B. *Handbook of Fluorescence Spectra of Aromatic Molecules, Academic Press*, New York, 2nd edn, **1971**. (b) Montalti, M.; Credi, A.; Prodi. L.; Gandolfi, M. T. *Handbook of Photochemistry*, Taylor & Francis, Boca Raton, 3rd edn, **2006**.

[45] Sánchez-Iglesias, A.; Pastoriza-Santos, I.; Pérez-Juste, J.; Rodríguez-González, B.; García De Abajo, F.; Liz-Marzán, L. *Adv. Mat.* **2006**, *18*, 2529-2534.

General Conclusions

General Conclusions

The scientific work performed in this thesis allowed to obtain new knowledge on the corrole chemistry. Currently it is known that is possible to introduce a vinyl group in a *β*-pyrrolic position of the corrole core, through a Wittig reaction, and that the resulting *β*-vinylcorrole can participate as diene in Diels-Alder reactions. In terms of sensorial behavior the 5,10,15-trispentafluorophenycorrole showed to be highly sensitive to fluoride anions, and exhibited the highest value of fluorescence quantum yield. It was also observed that the insertion of a substitutent on the position 3 of the corrole unit leads to a decrease of the luminescent quantum yield. This decrease can probably be attributed to conformation issues.

Although the coordination with gallium(III) and the functionalization at 3-position have originated less emissive compounds, these derivatives have found application as colorimetric chemosensors and as solid support sensors. For example, the derivative that contain in their structure a unit of benzoquinone type showed an important enhancement in the emission intensity, when was dopped in an acrylamide gel and submersed in a solution containing nicotine or caffeine. Whereas the benzocorrole, resulting from the Diels-Alder reaction of 3-vinyl-5,10,15-tris(pentafluorophenyl)corrolatogallium(III) (pyridine) with dimethyl acetylenedicarboxilate, showed to be colorimetric in the presence of cyanide anions.

The reactivity of 3-vinyl-5,10,15-tris(pentafluorophenyl)corrolatogallium(III) (pyridine) as dienophile was also evaluated in the presence of reactive *o*-quinone methides generated in situ from Knoevenagel reactions of coumarins with paraformaldehyde. The two adducts obtained showed to be soluble in ethanol and in ethanol: water (50:50) mixtures, and their sensing ability was compared with porphyrin-coumarin analogues. The porphyrinic free-bases showed an unprecedented selectivity for Hg^{2+}, which was accompanied by a colorimetric effect (a change of colour from purple to yellow was observed), whereas all corrole-coumarin conjugates interacted with cyanide anions.

Knowing that the incorporation of organic dyes in silica nanoparticles could improve the affinity, versatility and sensitivity of the chromophores to the guests, in the final study silica nanoparticles were coated with an alkoxisilane corrole with an imine linkage. The sensorial ability of these nanoparticles was evaluated towards Hg^{2+}, Ag^{+} and

the SiNPs. At same time, a change of color from green to yellow was observed. This type of behavior is a result quite innovative and promising. In the future we pretended to perform the condensation of the formyl derivative **I** with primary diamines and subsequent reduction to obtain derivatives of type **III**. The new macrocycles would be used to prepare silica nanoparticles. Subsequently it is expected to evaluate the influence of the expansion of the chain in signal amplification by preorganization of dyes on the nanoparticles surface.

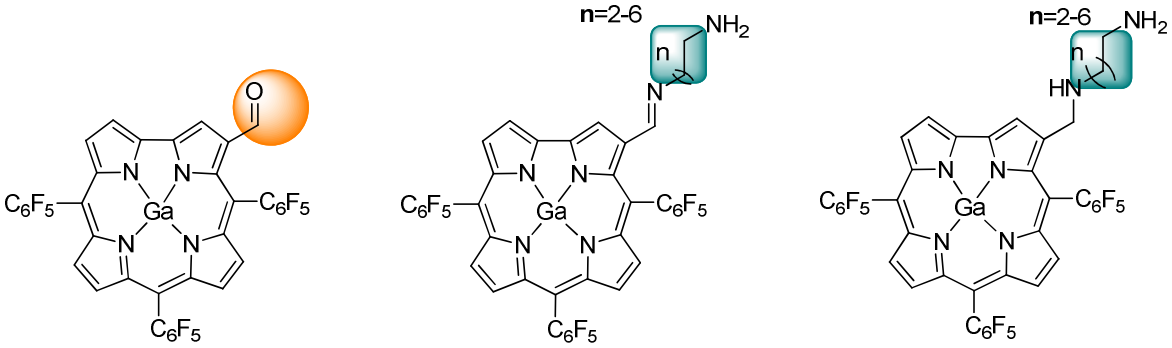

I II III

For all these facts, it is considered that the corroles chemistry has a great potential and it is a new area that deserves further investigation.

Annex

Compounds

Chapter II- Exploiting the fluorescence behavior of a new corrole family as anions chemosensors: From solution to solids-supported devices

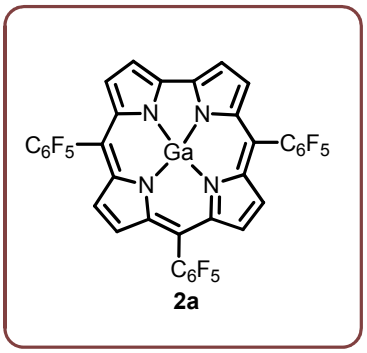

2a

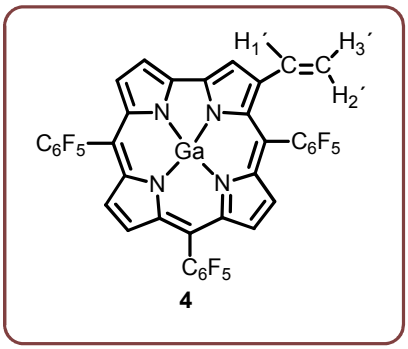

4

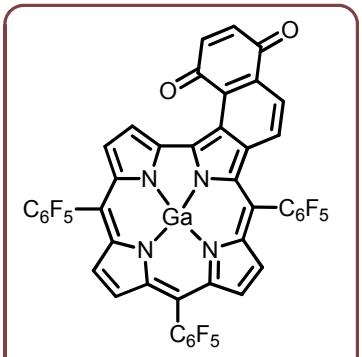

5

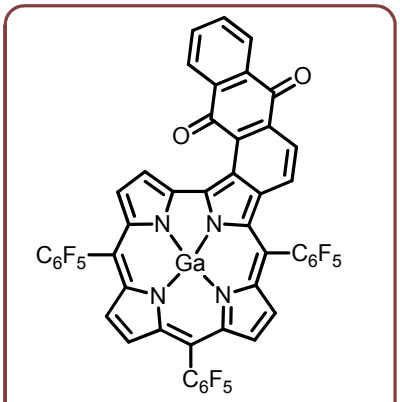

6

Chapter III- New gallium(III) corrole complexes as colorimetric probes for toxic cyanide anion

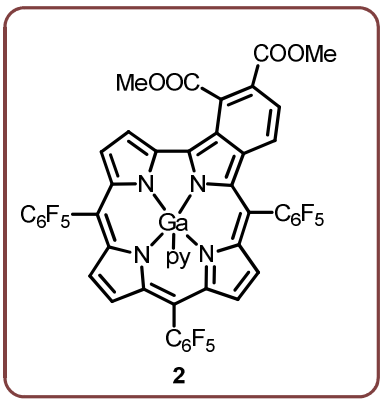

2

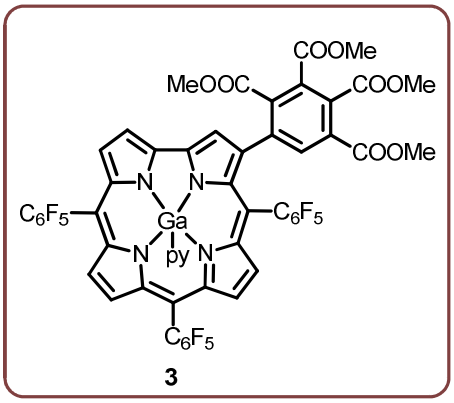

3

Chapter IV- New coumarin-corrole and -porphyrin conjugate as multifunctional probes for anionic or cationic interactions: Synthesis, spectroscopy and solid supported studies

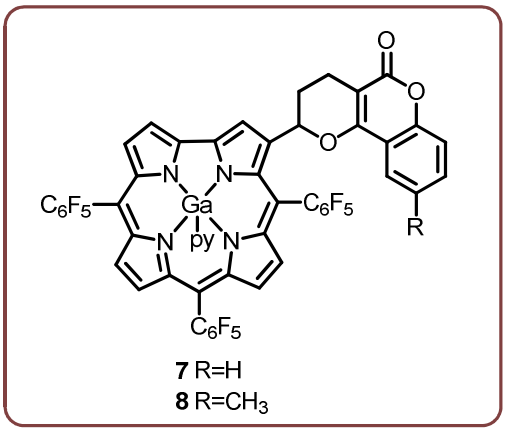

7 R=H
8 R=CH_3

Chapter V- Corrole and corrole functionalized silica nanoparticles as new metal ion chemosensors: A case of silver satellite nanoparticles formation

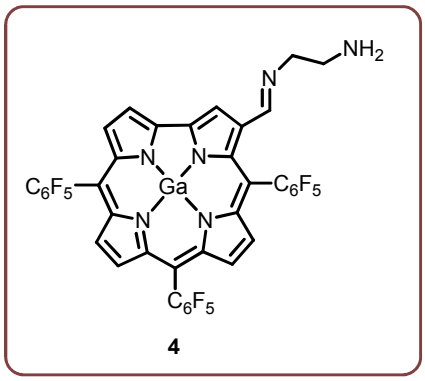

4

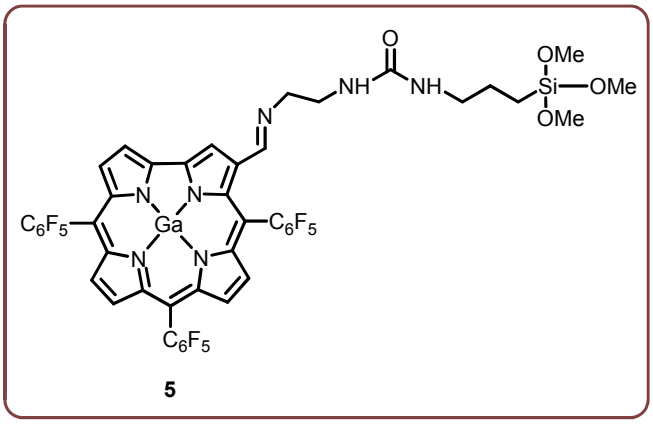

5